The molecular organization of the phagophore assembly site

Ester M. Rieter

The molecular organization of the phagophore assembly site

Ester M. Rieter, 2012
Contact: esterrieter@hotmail.com

Paranimfen: Léon van Gurp
Anke Brouwers

The work described in this thesis was performed at the department of Cell Biology of the University medical Center Utrecht, Faculty of Medicine, Utrecht University, The Netherlands

ISBN: 978-90-6464-584-6
Layout: Ferdinand van Nispen, Citroenvlinder-dtp.nl, Bilthoven
Printing: GVO drukkers & vormgevers B.V. | Ponsen & Looijen, Ede

The molecular organization of the phagophore assembly site

De moleculaire organisatie van de phagophore assemblage plaats
(met een samenvatting in het Nederlands)

Proefschrift

ter verkrijging van de graad van doctor aan de Universiteit Utrecht op gezag van de rector magnificus, prof.dr. G.J. van der Zwaan, ingevolge het besluit van het college voor promoties in het openbaar te verdedigen op dinsdag 23 oktober 2012 des middags te 12.45 uur

door

Ester Mirjam Rieter

geboren op 12 juli 1981 te Roermond

Promotoren: Prof.dr. J. Klumperman
Prof.dr. P.J. Coffer

Co-promotor: Dr. F.M. Reggiori

Printing of this thesis was financially supported by the Stichting tot bevordering van de Electronenmicroscopie in Nederland (SEN) and Roche Diagnostics Nederland.

"Although wherever you are going is always in front of you,
there is no such thing as straight ahead."

- Jeanette Winterson -

CONTENTS

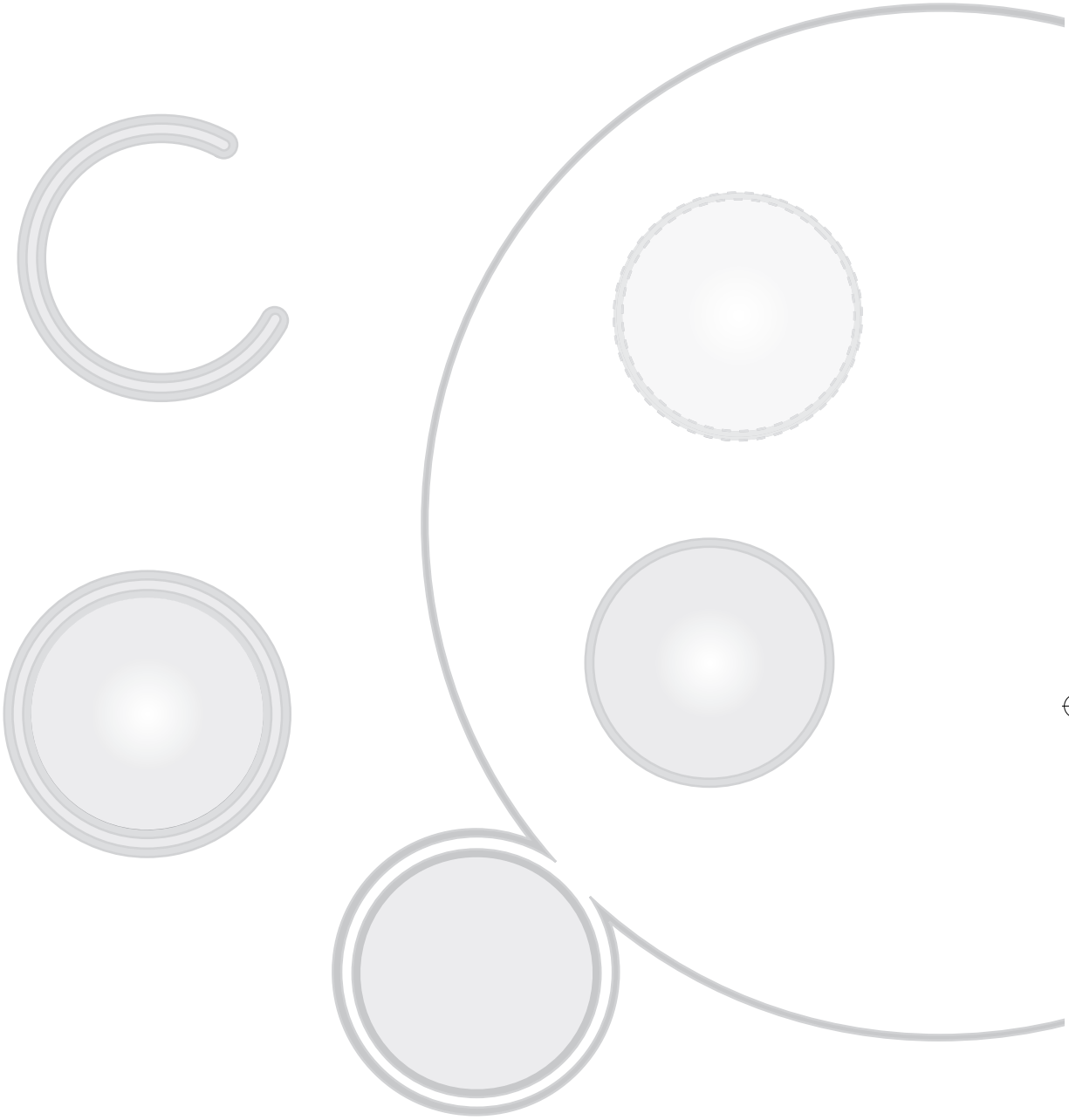

CHAPTER

1

General introduction

AUTOPHAGY

Autophagy (from the Greek, "auto" self, "phagy" to eat) refers to an intracellular degradation pathway that is highly conserved among all eukaryotes. It is a catabolic process crucial for numerous cellular processes and important for maintaining cellular homeostasis and cell survival during stress conditions by recycling cytoplasmic components. Cells have two major intracellular protein degradation pathways: the ubiquitin-proteasome system and autophagy. Whereas the proteasomal system specifically degrades ubiquitinated proteins, autophagy can facilitate the elimination of large portions of the cytoplasm, aberrant protein aggregates, superfluous or damaged organelles and even entire organisms such as invading pathogens in the major lytic compartment of the cell: the lysosome in mammals or the vacuole in plants and yeast.

Autophagy can be divided into three types, depending on the different pathways by which the cargo is delivered to the lysosome: chaperone-mediated autophagy (CMA), microautophagy and macroautophagy (Chen and Klionsky, 2011). The word 'autophagy' is often used as a collective term for these related events. During CMA, a pathway that is only present in higher eukaryotes, cytoplasmic proteins containing a specific targeting motif, e.g. KFERQ, are delivered into the lysosome for degradation (**Figure 1**). In the cytosol these proteins are recognized by a chaperone, the heat shock cognate protein of 70 kDa (Hsc70). This protein/chaperone complex then binds to a receptor on the lysosomal membrane called lysosome-associated membrane protein type 2A (Lamp-2A). This event subsequently leads to the direct translocation of the protein into the lysosome lumen where it is degraded (Cuervo, 2011; Massey et al., 2004). During microautophagy cytoplasmic components are directly delivered into the lysosome/vacuole via invagination and pinching off from the lysosomal/vacuolar limiting membrane (Kunz et al., 2004). In contrast, during macroautophagy targeted cargo such as cytoplasmic components, organelles or large unwanted structures, are sequestered into large double-membrane vesicles called autophagosomes. In yeast, autophagosomes directly fuse with the vacuole, thereby releasing the inner vesicle, called an autophagic body, into the lumen of this organelle. The autophagic body is then degraded together with its content by resident hydrolases into basic cellular components ready to be re-used by the cell (Ravikumar and Rubinsztein, 2006) (**Figure 2**). In mammalian cells autophagosomes first fuse with endosomal vesicles and multivesicular bodies to become amphisomes, which subsequently expose their content to lysosomal hydrolases (Fengsrud et al., 2000).

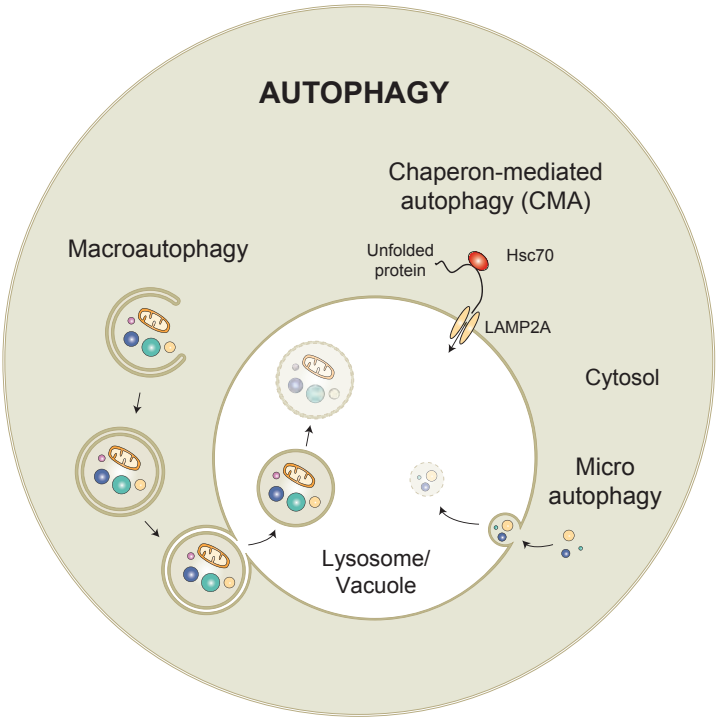

Figure 1. Different types of autophagy. During chaperone-mediated autophagy (CMA) unfolded proteins in the cytosol that contain the targeting motif KFERQ are recognized by the heat shock cognate 70 (Hsc70) chaperone and transported across the lysosomal membrane via the lysosome-associated membrane protein type 2A (LAMP-2A). During microautophagy, the lysosomal/vacuolar membrane engulfs cytoplasmic material by direct invagination of its limiting membrane. During macroautophagy targeted cargo, such as cytoplasmic components, organelles or large unwanted structures, are enwrapped into large double-membrane vesicles called autophagosomes. Adapted and modified from Nakatogawa et al., 2009.

Macroautophagy, hereafter referred to as autophagy, is the most well characterized type of autophagy. Under starvation or during other stress conditions this type of autophagy is quickly induced, leading to the elimination of multiple different cellular components through a mechanism that appears to be random. Historically, for a long period autophagy has been considered a non-selective pathway, governed by extracellular stimuli such as nutrients, hormones, growth factors or cytokines (Shintani and Klionsky, 2004). Under certain circumstances, however, specific cargoes such as damaged mitochondria, protein aggregates or even invading bacteria can be exclusively incorporated into autophagosomes (Levine, 2005; van der Vaart et al., 2008). In these cases, autophagy is defined as

a selective process and seems to be induced by the cargoes and intracellular components rather than extracellular cues. The molecular mechanism by which the cargoes are selectively incorporated into autophagosomes remains largely unknown (**Figure 2**).

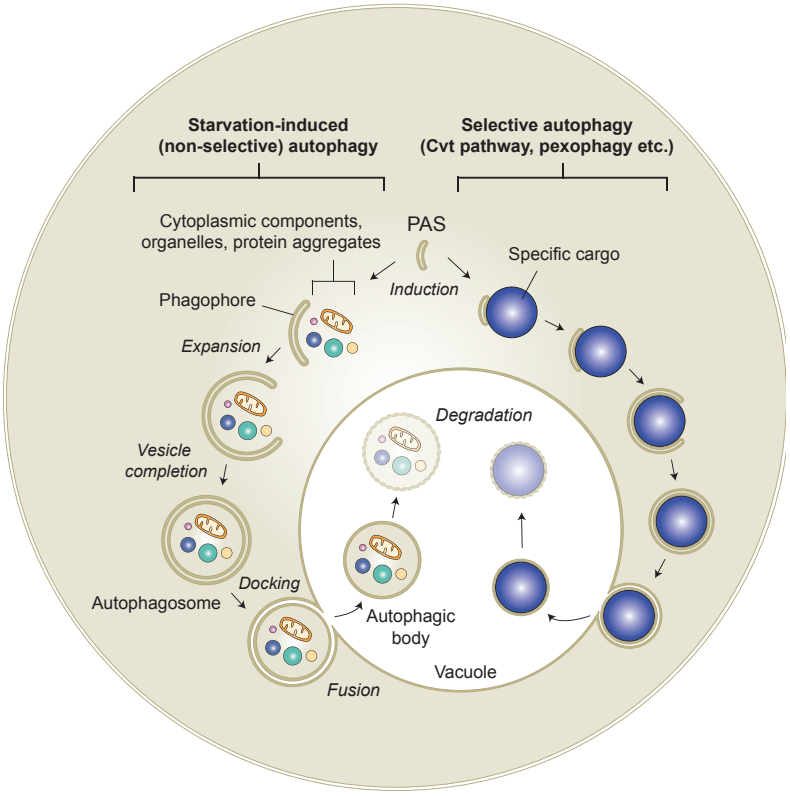

Figure 2. Autophagosome biogenesis and different types of autophagy in yeast. Autophagosome biogenesis starts with the formation of the pre-autophagosomal structure (PAS) close to the vacuole and accordingly can be divided into several stages: induction, expansion, vesicle completion, docking/fusion and degradation. During starvation-induced (on the right) or non-selective autophagy (on the left) large proportions of the cytosol, including organelles, protein aggregates etc., are randomly sequestered into autophagosomes. Subsequent fusion of the autophagosome with the lysosome/vacuole leads to the degradation of the inner autophagosomal membrane, called an autophagic body, and its content in the lumen of this lytic compartment. During selective autophagy (on the right) specific cargoes such as for example damaged or superfluous organelles, or protein structures are specifically and exclusively incorporated into autophagosomes and targeted for degradation in the vacuole/lysosome. Cvt, cytoplasm-to-vacuole targeting. Adapted and modified from Nakatogawa et al., 2009.

AUTOPHAGY IN YEAST

The budding yeast *Saccharomyces cerevisiae* is widely used as model organism to study autophagy and has provided some well-studied examples of selective types of autophagy. Mitophagy, pexophagy and ribophagy, the selective degradation of mitochondria, peroxisomes and ribosomes, respectively, have primarily been characterized in yeast (Dunn et al., 2005; Kanki and Klionsky, 2008; Kim et al., 2007; Kraft et al., 2008). This organism has an additional selective type of autophagy: the biosynthetic cytoplasm-to-vacuole targeting (Cvt) pathway, which is constitutively active under normal growth conditions. Through this process precursors of the resident vacuolar hydrolases aminopeptidase I (prApe1) and α-mannosidase (prAms1) are delivered into the vacuole. In the cytosol prApe1 and prAms1 form oligomers, which assemble in a structure of higher order, the Cvt complex. This complex, together with two other cargos associated to it, namely Ape4 and the Ty1 transposon, gets incorporated into smaller autophagosomes, termed Cvt vesicles and are delivered into the vacuolar lumen (Inoue and Klionsky, 2010; Lynch-Day and Klionsky, 2010; Yuga et al., 2011). In the vacuole both precursors are processed, leading to the activation of the hydrolases.

Autophagosome biogenesis

Although the vesicles formed in the Cvt pathway are much smaller, approximately 140-160 nm, compared to autophagosomes, 300-900 nm, their morphological features are very similar and the process of the formation of Cvt vesicles and autophagosomes is mechanistically very similar except for the cargo selection (Baba et al., 1997; Scott et al., 1996). Both types of vesicles are formed by simultaneous expansion and nucleation of a small cup-shaped cisterna known as the isolation membrane or phagophore. In yeast autophagosome biogenesis occurs at one distinct site close to the vacuole called the phagophore assembly site or pre-autophagosomal structure (PAS) and can be divided into several stages: induction, expansion, vesicle completion, docking/fusion and break down (Klionsky, 2005; Reggiori and Klionsky, 2005) (**Figure 2**). The PAS has an organizational role is assembling the Atg machinery to form the phagophore, and should be considered a highly dynamic structure in constant remodelling where double-membrane vesicle biogenesis occurs. That is the PAS is not simply the phagophore (see below), but reflects different autophagosomal intermediates that are in progression to become an autophagosome (Reggiori, 2006; van der Vaart et al., 2008).

The *ATG* genes required for autophagy

For a long time autophagy has been studied only at a phenomenological level, but genetic studies in *Saccharomyces cerevisiae* have permitted a breakthrough in the field and have led to significant progress in unveiling the mechanism of this pathway. To date 36 autophagy-related (*ATG*) genes have been identified that are required for different/several types of autophagy (Nakatogawa et al., 2009; Thumm et al., 1994; Tsukada and Ohsumi, 1993; van der Vaart et al., 2008) (**Figure 3**).

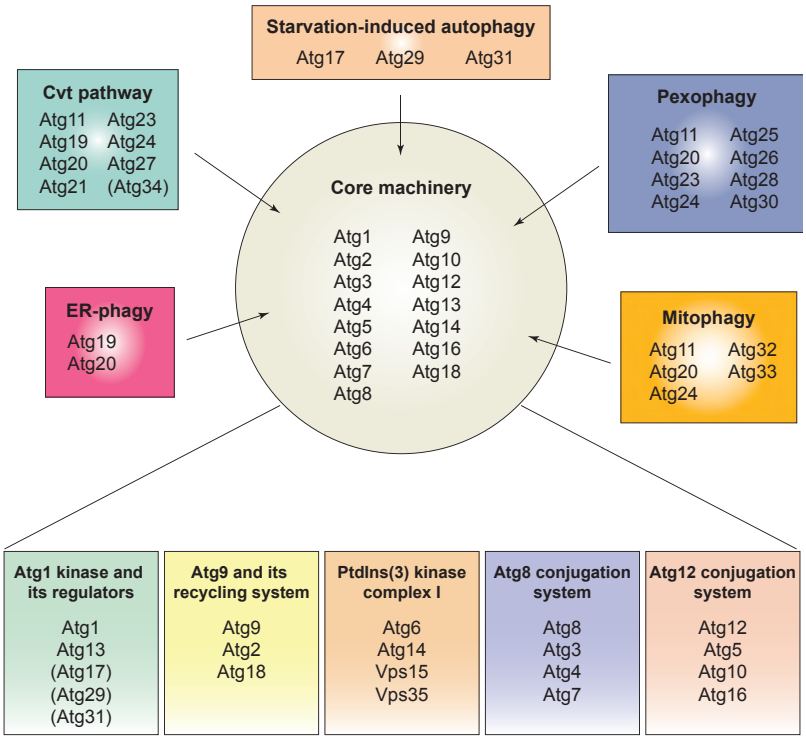

Note: Atg15 is not involved in the formation of the autophagosomes but in the membrane breakdown in the vacuole

Figure 3. Atg protein classification. To date 36 *ATG* genes have been identified, of which 16 are essential for all types of autophagy and form the core machinery that is needed for double-membrane vesicle formation. In addition, selective types of autophagy, such as mitophagy, pexophagy, ER (Endoplasmic Reticulum)-phagy or the cytoplasm-to-vacuole targeting (Cvt) pathway require distinct *ATG* genes while Atg17, Atg29 and Atg31 are specifically required for starvation-induced autophagy. The genes that are considered part of the core machinery can be divided into five functional groups: the Atg1 protein kinase complex and its regulators; the Atg9 recycling system; the autophagy-specific phosphatidylinositol (PtdIns)-3 kinase complex and two ubiquitination-like conjugation systems. Adapted and modified from Nakatogawa et al., 2009.

Genetic analyses of the different yeast *atg* mutants defective in either the Cvt pathway or autophagy have revealed that these two pathways require a

common subset of 16 Atg proteins (Harding et al., 1996; Scott et al., 1996). These proteins, hereafter referred to as the basic core machinery, are required for both selective and non-selective autophagy and catalyze the formation of double-membrane vesicles (Klionsky et al., 2003; Xie and Klionsky, 2007). Almost all of them are peripheral membrane proteins that transiently associate with the PAS. Concerted action of these core Atg proteins in a temporal and spatial order leads the successful formation of the PAS, and eventually first a phagophore and then an autophagosome (**Figure 4**). Their precise function and the relationship between them, however, remain largely unknown (Ishihara et al., 2001; Suzuki et al., 2007). After double-membrane vesicle completion, the majority of these Atg proteins is released back in the cytoplasm and can be reused to form new autophagosomes (Reggiori and Klionsky, 2005). The 16 core Atg proteins can be classified into five major functional groups: the Atg1 protein kinase complex and its regulators; the Atg9 recycling system, the autophagy-specific phosphatidylinositol (PtdIns)-3 kinase complex and two ubiquitination-like conjugation systems (Levine and Kroemer, 2008; Suzuki and Ohsumi, 2007) (**Figure 3**).

Atg1 protein kinase complex and its regulators

Atg1 is a serine/threonine kinase that has an important function during the early stages of autophagosome formation (**Figure 4**). An important regulator of cell growth in response to nutrients is the kinase target of rapamycin (TOR). *Saccharomyces cerevisiae* has two different TOR kinases, Tor1 and Tor2, which exists in two distinct complexes: the TOR complex 1 (TORC1) and TOR complex II (TORC2) (Loewith et al., 2002). The kinase Atg1 is downstream of the rapamycin-sensitive TORC1; rapamycin is an inhibitor of Tor. In growing conditions, TORC1 inhibits autophagy by phosphorylating Atg13 (Kamada et al., 2000). In response to starvation or rapamycin treatment, TORC1 is inactivated and as a result Atg13 is rapidly dephosphorylated. Dephosphorylated Atg13 associates to Atg1 with high affinity resulting in the Atg1-Atg13 complex, which then leads to the upregulation of the kinase activity of Atg1 and thereby stimulating autophagy (Funakoshi et al., 1997; Matsuura et al., 1997).

Together with Atg13, Atg1 plays a major role in determining the magnitude of autophagy, i.e. controlling the size of the double-membrane vesicle to be formed, and the type of autophagy. How the Atg1-Atg13 complex executes this role largely depends on with which other proteins the Atg1-Atg13 complex interacts with, e.g. Atg proteins which are exclusively required for selective or

non-selective types of autophagy (Nakatogawa et al., 2009). For example, the two proteins can exist in a complex together with Atg17, Atg29 and Atg31 (Cheong and Klionsky, 2008b; Cheong et al., 2005; Kabeya et al., 2005). These Atg proteins are not among the core Atg protein required for autophagosome formation, but are specifically required for starvation-induced autophagy (**Figure 3**).

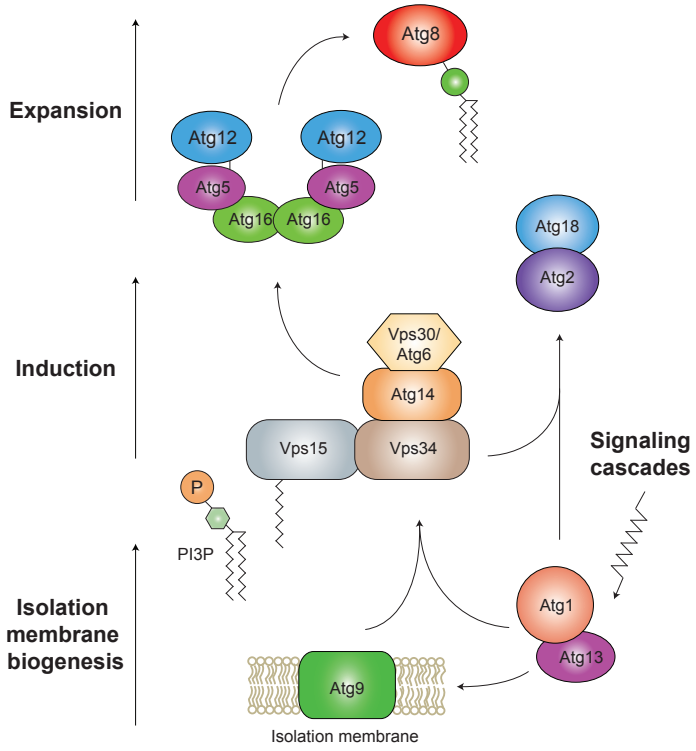

Figure 4. Hierarchical recruitment of the 'core' Atg proteins to the PAS. In both yeast and mammalian cells the Atg proteins/complexes are recruited to the PAS on the basis of this hierarchy diagram. The putative order in which the Atg proteins are recruited as well as the stage of autophagosome biogenesis when this occurs are depicted. The two ubiquitination-like conjugation systems are shown as the Atg5-Atg12-Atg16 complex and ATG8-PE, but also include Atg10 and respectively Atg4 and Atg3. Atg7 is involved in both systems. Adapted and modified from Nakatogawa et al., 2009 and Van der Vaart et al., 2007.

Recent studies in yeast revealed that during starvation conditions Atg1 has two distinct functions (Cheong and Klionsky, 2008b). First of all, Atg1 plays a structural role in the initial step of PAS assembly, independent from its kinase activity. It was shown that the specific interaction with Atg13 and Atg17 through its C-terminus is required for efficient recruitment of other Atg proteins to the PAS. The Atg1 kinase activity, in contrast, was found to be involved in the dynamics

of the Atg proteins at the PAS and necessary for the dissociation of them from the PAS (Cheong et al., 2008; Kawamata et al., 2008). This was concluded from results obtained with cells harbouring an Atg1 kinase-death mutant, in which some Atg proteins abnormally accumulated at the PAS(Cheong et al., 2008).

Atg9 and its recycling system

Atg9 is the only transmembrane protein among the core Atg machinery and it is essential for autophagy (Noda et al., 2000). Upon induction of autophagy, Atg9 is one of the first Atg proteins to localize to the PAS, where it presumably plays a key role in initiating autophagy by recruiting and organizing the rest or at least part of the Atg machinery (Suzuki et al., 2007). The precise molecular function of Atg9, however, is unknown. Because of its association with lipid bilayers, Atg9 is thought to be involved in delivering at least part of the membranes that contribute to the autophagosome biogenesis (Legakis et al., 2007; Reggiori et al., 2005b). This idea is supported by the fact that in yeast, Atg9 cycles between the PAS and several puncta dispersed throughout the cytoplasm some of which are in close proximity of the mitochondria (Mari and Reggiori, 2007; Reggiori et al., 2005b; Reggiori et al., 2004a). The nature of these sites as well as the carriers shuttling Atg9 between the PAS and these locations remain unidentified.

As mentioned, Atg9 is recruited in proximity of the vacuole to form the PAS. This anterograde transport is mediated by Ape1, Atg11, Atg19, Atg23, Atg27 and actin filament during growth conditions when the Cvt pathway is active. In the absence of these factors, the transport of Atg9 to the PAS is blocked (He et al., 2006; Legakis et al., 2007; Monastyrska et al., 2006; Reggiori et al., 2005a; Yen et al., 2007). In contrast, during starvation, when autophagy is active, Atg9 delivery to the PAS becomes independent of these proteins. The factors that take over this function remain largely unknown, with the exception of Atg17. This is the only Atg protein identified so far to be important in the anterograde transport of Atg9 to PAS during starvation (Sekito et al., 2009). Atg9 self-association has also been found to be crucial for anterograde transport but in both nutrient-rich and starvation conditions (He et al., 2008).

No Atg9 is present on mature autophagosomes and this implies that this protein is retrieved from the PAS back to the cytoplasmic pools after autophagosome completion. This retrograde transport requires the Atg1-Atg13 complex, Atg2, Atg18 and the PI-3 kinase complex I (see below) during both the Cvt pathway and autophagy. Absence of any of these factors leads to the accumulation

of Atg9 at the PAS. How they mediate Atg9 retrieval is unknown (Mari and Reggiori, 2007; Reggiori et al., 2005b; Reggiori et al., 2004a). The Atg1-Atg13 complex is thought to determine the size of the double membrane vesicles formed. One way of doing this could be by inducing the retrieval of Atg9 by regulating its association with Atg18 and Atg2 (Reggiori et al., 2004a). Both Atg18 and Atg2 are peripheral membrane proteins that interact with each other and associate with Atg9 at the PAS (Obara et al., 2008b; Reggiori et al., 2004a). It is unknown which is their precise role in autophagosome biogenesis and by which mechanism they mediate Atg9 retrograde transport from the PAS/complete autophagosome. The recruitment and localization of Atg18 and Atg2 to the PAS depends on each other, Atg9 and the Atg1-Atg13 kinase complex, and also on the presence of phosphatidylinositol-3-phosphate (PtdIns3P) generated by the PtdIns-3 kinase complex I (Reggiori et al., 2004a; Shintani et al., 2001; Suzuki et al., 2007; Wang et al., 2001a).

PI-3 kinase complex I

PtdIns3P is a key regulator of autophagy and autophagosomal membranes are highly enriched for this lipid (Kihara et al., 2001; Obara et al., 2008a). The vacuolar protein sorting (Vps) 34 is the sole PtdIns-3 kinase in yeast. This kinase is able to interact with Vps15, Vps30 (also known as Atg6) and either Atg14 or Vps38 to form two distinct large complexes: the PtdIns-3 kinase complex I or complex II, respectively (Kihara et al., 2001). Atg14 and Vps38 are the specific subunits of each complex that determine the localization of the complex by targeting it either to the PAS or the endosomal membranes (Obara et al., 2006). Complex I is involved in autophagy and is required for the early steps of PAS formation (Kihara et al., 2001), whereas complex II plays an important role in the vacuolar protein sorting such as carboxypeptidase Y via endosomes. Both complexes are able to phosphorylate PtdIns into PtdIns3P.

The precise function of PtdIns3P is poorly understood. Presumably it functions at the PAS by recruiting downstream effectors, i.e. PtdIns3P interacting proteins such as Atg18 (Dove et al., 2004), which are needed for autophagy. Another possibility is that PtdIns3P, together with its downstream effectors, is responsible for generating negative curvature at the inner surface of the phagophore, as well as organizing and maintaining the elongating tips of the phagophore (Obara et al., 2008b). In addition, Atg14 might regulate the function of the PtdIns-3 kinase complex I by interacting with other Atg proteins at the PAS. Possible candidates are Atg9, Atg13 and Atg17 (Suzuki et al., 2007).

The two conjugating systems

The core Atg machinery comprises two protein conjugation systems that are responsible for the conjugation of Atg8 and Atg12, two ubiquitin-like proteins. Although Atg8 and Atg12 do not have apparent sequence homology with ubiquitin, each of them contains an ubiquitin fold at the C terminus (Yang and Klionsky, 2009). Atg8 is conjugated to the lipid phosphatidylethanolamine (PE). Atg8-PE localizes to the inner and outer membrane of the autophagosomal structures and is widely used as a marker for the induction and progression of autophagy (Kirisako et al., 1999). The lipidation of Atg8 is initiated by the cleavage of its C-terminal arginine residue by the cysteine protease Atg4, allowing it to interact with Atg7, an E1-like enzyme. Subsequently, Atg8 is transferred to the E2-like enzyme Atg3 and finally to PE, thereby anchoring Atg8 to autophagosomal membranes (**Figure 5**) (Ichimura et al., 2000; Kirisako et al., 2000; Mizushima et al., 1998). The final transfer of Atg8 from Atg3 to PE is facilitated by the Atg12-Atg5 conjugate, the product of the second conjugation system that presumably acts as an E3-like enzyme (Hanada et al., 2007). The conjugation of Atg12 to Atg5 is similar to that of Atg8-PE, and is mediated by the E1- and E2-like enzymes Atg7 and Atg10, respectively (Shintani et al., 1999; Tanida et al., 1999). The Atg12-Atg5 conjugate further forms a multimeric complex with Atg16 (Kuma et al., 2002; Mizushima et al., 1999). Although, the conjugate itself is required for the E3-like activity, Atg16 is crucial for the correct targeting of the whole complex to the PAS thereby specifying the site of Atg8 lipidation, which has been shown is mammalian cells (Fujita et al., 2008b; Hanada et al., 2007).

Upon autophagosome completion, Atg8-PE present on the inner autophagosomal membrane is delivered into the vacuole where it gets degraded, whereas Atg8 that is present on the outer membrane of the autophagosome is cleaved and released in the cytoplasm by Atg4. This protein acts a deconjugating enzyme cleaving the amine bond between Atg8 and the PE anchor. This deconjugating step is crucial for the normal functional organization of the PAS and the phagophore expansion into a complete autophagosome, and thereby affects the number and size of the autophagosomes. Moreover deconjugation of Atg8-PE is thought to be important for the release of some of the Atg proteins from the complete autophagosomes, such as Atg14 (Nair et al., 2012; Nakatogawa et al., 2012).

The precise function of the Atg8-PE conjugate remains unknown. Alterations in the levels of Atg8 expression or the expression of partial functional impaired mutant forms of Atg8 lead to the formation of much smaller

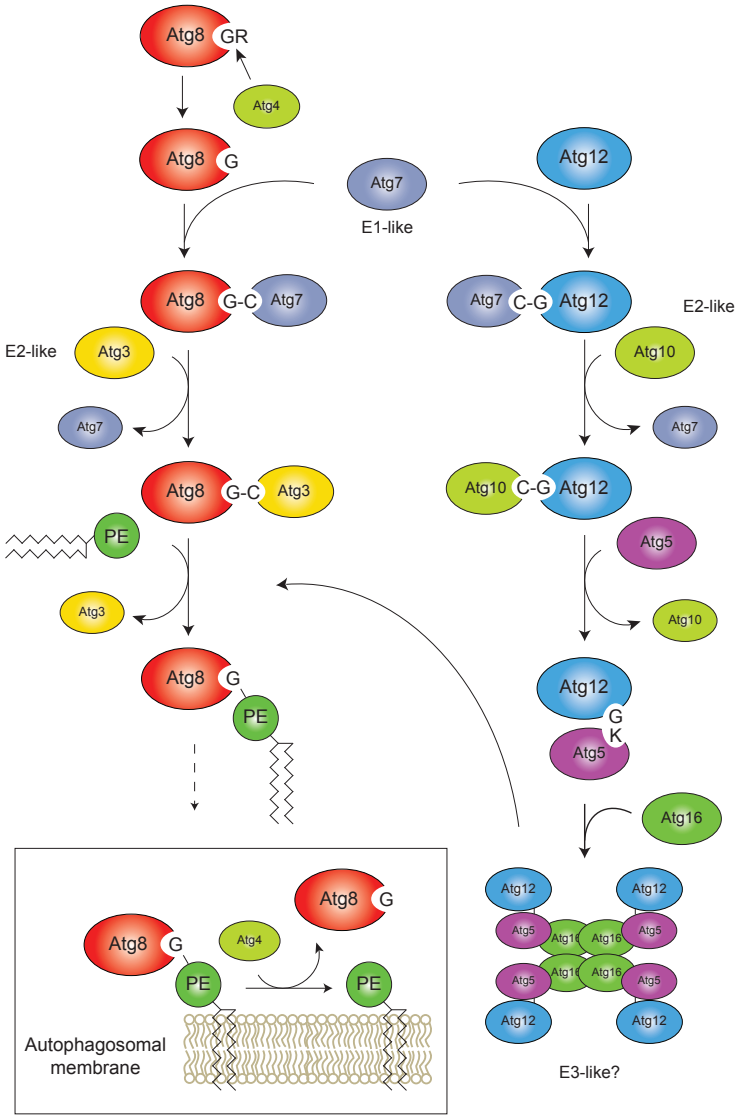

Figure 5. The Atg8 and Atg12 conjugation systems. The conjugation of Atg8 starts with the cleavage of the C-terminal arginine of Atg8 by the protease Atg4. The exposed glycine of Atg8 is then bound to the active site cysteine of the E1-like enzyme, Atg7 and subsequently Atg8 is transferred to the E2-like enzyme Atg3. Finally, Atg3 catalyzes the conjugation of Atg8 to PE. The Atg12-Atg5 conjugate presumably acts an E3-like enzyme and facilitates Atg8-PE conjugation. Once the autophagosome is completed, the Atg8-PE that resides on the outer autophagosomal membrane is released by a second cleavage by Atg4 (box). The conjugation of Atg12 to Atg5 is very similar to that of Atg8-PE. It starts with the formation of a thioester bond between the C-terminal glycine of Atg12 and the active site cysteine of Atg7, which leads to the activation Atg12. Subsequently, the activated Atg12 is transferred to Atg10, also an E2-like enzyme, which catalyzes the conjugation of Atg12 to Atg5 through the formation

of an isopeptide bond between the activated glycine of Atg12 and an internal lysine residue of Atg5. The Atg12-Atg5 conjugate finally assembled with Atg16 to form an Atg12-Atg5-Atg16 multimeric complex that facilitates the final transfer of Atg8 from Atg3 to PE on the target membrane. Adapted and modified from Yorimitsu and Klionsky, 2005.

autophagosomes, suggesting a role for Atg8-PE in membrane expansion during autophagosome formation that determines the autophagosome size (Xie et al., 2008). Further, *in vitro* based studies have shown that multimerization of Atg8-PE causes membrane tethering and hemifusion between liposomes (Nakatogawa et al., 2007). It is expected that Atg8-PE plays a similar role *in vivo*, mediating membrane fusion that may allow expansion of the autophagosomal membrane (Nakatogawa et al., 2007).

Docking and fusion

Based on the current conceptual model of autophagy (**Figure 2**) it is assumed that at the end of vesicle expansion, the two leading edges of the forming autophagosome fuse with each other to close the vesicle. Most of the above described Atg proteins are expected to associate with the PAS at some stage of autophagosome biogenesis based on their function and studies defining the hierarchical order in which they are recruited to this structure (**Figure 4**) (Suzuki et al., 2007). However, the membranes of ready-to-fuse autophagosomes are all most completely devoid from peripheral membrane-associated proteins or transmembrane proteins (Fengsrud et al., 2000), implicating that upon vesicle completion, most of the Atg proteins are released back into the cytosol or in the case of the transmembrane proteins such as Atg9, they are retrieved back (Mari and Reggiori, 2007). This uncoating event is thought to be the trigger for the autophagosomes to dock and fuse with the vacuole. During the fusion step, the outer membrane of the autophagosome becomes part of the vacuolar membrane whereas the autophagic body is released into the interior of this organelle (**Figure 2**).

Genetic screens in yeast have revealed that the machinery used for the heterotypic fusion of the outer membrane of the autophagosome with the vacuole is identical to the one employed for the fusion of vesicles and compartments of the endosomal system with the same organelle. It requires the coordinated action of the Rab GTPase Ypt7, the HOPS (homotypic fusion and vacuole protein sorting) tethering complex and vacuolar SNAREs (soluble *N*-ethylmaleimide-sensitive factor (NSF) attachment receptors). Activation of the Rab GTPase Ypt7 by its guanine nucleotide exchange factor (GEF) the Mon1-Ccz1 complex leads

to its recruitment to membranes (Nordmann et al., 2010; Wang et al., 2002). There it interacts with members of the class C Vps family, which are part of the HOPS tethering complex. After tethering, the SNAREs Vam3, Vam7, Vti1 and Ykt6, which are present on the opposing membranes bring the two bilayers in very close proximity of each other promotingtheir fusion (Brocker et al., 2010; Darsow et al., 1997; Fischer von Mollard and Stevens, 1999; Ishihara et al., 2001; Sato et al., 1998; Sato et al., 2000). Tethering and docking with the vacuole is further regulated by the NSF Sec18 and the SNAP (soluble NSF attachment protein) Sec17, two proteins are required for disassembly of the fusion complex (Klionsky, 2005; Xu et al., 2010).

Breakdown

The main purpose of autophagy is to degrade cytoplasmic components and recycle the resulting macromolecules, such as carbohydrates, lipids and proteins, for the synthesis of essential components needed to maintain cell homeostasis and promote cell survival, or to be a source of energy. Accordingly, the autophagic body that results from fusion of the autophagosome with the vacuole has to be degraded (**Figure 2**). The breakdown depends on proper vacuolar acidification (pH) and the activity of the vacuole resident proteinases A (Pep4) and B (Prb1) (Nakamura et al., 1997; Takeshige et al., 1992). In addition, the putative lipase Atg15 has been directly implicated in breakdown of the vesicle limiting membrane during the degradation process (Epple et al., 2001; Teter et al., 2001).

Recycling

The metabolites resulting from the degradation process are transported back into the cytosol in order to be reused. This occurs through the activity of the membrane permeases such as Atg22, Avt3 (*a*mino acid *v*acuolar *t*ransport) and Avt4. Atg22 is an integral membrane protein located on the vacuolar membrane. Initially it was thought that Atg22 was directly involved in the degradation process, but it turned out that the protein functions as an amino acid effluxer. Although direct evidence is lacking, Atg22 might be a leucine transporter as a loss of viability is observed in yeast cells that are auxotrophic for leucine and lack the *ATG22* gene (Suriapranata et al., 2000; Yang et al., 2006; Yang and Klionsky, 2007). Avt3 and Avt4 seem to be part of the same amino acid transporter family as Atg22, and mediate the efflux of leucine and other amino acids from the vacuole (Russnak et al., 2001; Yang et al., 2006; Yang and Klionsky, 2007).

AUTOPHAGY IN MAMMALIAN CELLS

Although our molecular understanding of autophagy is largely based on studies performed in yeast the mechanism of autophagosome formation or biogenesis in higher eukaryotes, such as worms, insects, plants and mammals, is mechanistically very similar and the mammalian counterparts/homologues of the yeast core Atg proteins have been identified (**Table 1**) (Xie and Klionsky, 2007; Yang and Klionsky, 2010). In contrast to yeast cells, in which only one single PAS at the time is observed and autophagosomes are formed one after the other, in mammalian cells several PAS structures/phagophores can be formed simultaneously at multiple locations giving rise to numerous autophagosomes (Itakura and Mizushima, 2010; Young et al., 2006). In addition, mammalian autophagosomes undergo an additional maturation step that appears to not occur in yeast. Namely, the complete autophagosomes first fuse with endosomal vesicles and multivesicular bodies (MVBs) to become amphisomes (Fengsrud et al., 2000). These structures then successively fuse together or with lysosomes to become autolysosomes.

THE PHAGOPHORE AND THE AUTOPHAGOSMAL MEMBRANES

Despite the increasing insights into the molecular mechanism of autophagy and the growing number of identified *ATG* genes, the fundamental question about the origin of both the phagophore and the membranes required for its expansion into an autophagosome remains largely unanswered.

The origin of the phagophore and the autophagosomal membranes in yeast

Substantial process being made in understanding the molecular mechanism underlying autophagy but the origin the PAS and the source of the membranes required to form the autophagosome is still unknown. It also remains unclear at which stage and how lipids or lipid-bilayers are delivered to the PAS. As mention above, Atg8 and Atg9 are believed to be important for this delivery process because associated with lipid bilayers (Reggiori et al., 2005b; Reggiori et al., 2004a; Yang and Klionsky, 2009).

Table 1. The core Atg proteins in yeast and mammals

Yeast	Mammals	Known or putative function	Reference
Atg1 protein kinase complex and its regulators			
Atg1	ULK1/2/3/4	Target of mTOR that forms a complex with mAtg13 and FIP200.	(Jung et al., 2009; Mizushima, 2010)
Atg13	mAtg13	Binds both UKL1 and UKL2 and mediates their interaction with FIP200.	(Jung et al., 2009)
Atg17	FIP200	Essential for stability and phosphorylation of ULK1	(Jung et al., 2009)
Atg9 and its recycling system			
Atg9	mAtg9	Membrane protein that potentially contributes to delivery of membrane to the forming autophagosome.	(Young et al., 2006)
Atg2	Atg2A/ Atg2B	Both proteins are required for autophagosome formation and interact with Atg18/WIPIs	(Velikkakath et al., 2012)
Atg18	WIPI-1/2/3/4	Operates as a scaffold protein that binds to PtdIns(3)P on the autophagosomal membrane	(Lu et al., 2011; Proikas-Cezanne et al., 2007)
PI-3 kinase complex I			
Atg6/ Vps30	Beclin1	Part of the PtdIns3-Kinase complex composed of Vps34, beclin1/Atg6, Atg14L and p150/Vps15.	(Funderburk et al., 2010; He and Levine, 2010)
Atg14	Atg14L	Directs the PtdIns3-Kinase complex to the autophagosomal membranes	(Yang and Klionsky, 2010), (Funderburk et al., 2010)
Vps38	UVRAG	Enhancer of autophagosome-lysosome fusion and endocytic traffic	(Chen and Klionsky, 2011; Yang and Klionsky, 2010)
Vps34	PIK3C3/ Vps34	PtdIns3-kinase that interacts with Rab5 and Rab7	(Funderburk et al., 2010)
Vps15	PIK3R4/ Vps15	Core activator of the Vps34 PtdIns3-kinase complex	(Chen and Klionsky, 2011; Yang and Klionsky, 2010)
Two conjugating systems			
Atg12	Atg12	Is part of the Atg12-Atg5-Atg16 complex that acts during elongation and expansion of the phagophore	(Geng and Klionsky, 2008; Mizushima, 2010)
Atg5	Atg5	Is conjugated to Atg12	(Yang and Klionsky, 2010), (Geng and Klionsky, 2008)
Atg16	Atg16L	Forms a multimeric complex together with the Atg12-Atg5 conjugate	(Yang and Klionsky, 2010), (Fujita et al., 2008b)
Atg7	Atg7	Acts as an E1-like enzyme for Atg12 and Atg8/LC3 conjugation	{Yang, 2010 #475; Geng, 2008
Atg10	Atg10	Acts as an E2-like enzyme for Atg12 conjugation	(Geng and Klionsky, 2008; Tanida, 2011)
Atg8	LC3A/B/C; GARAPL1.L2/ L3	Is conjugated to PE and acts during elongation and expansion of the phagophore.	(Tanida et al., 2004; Yang and Klionsky, 2010)
Atg3	Atg3	E2-like enzyme for Atg8/LC3 conjugation	(Tanida et al., 2004)
Atg4	Atg4A/B/C/D	Cysteine protease for processing and recycling of Atg8/LC3	(Fujita et al., 2008a)

Various models have been proposed for the formation and expansion of the phagophore of which two are favorable: the maturation model and the assembly model that either involves vesicular expansion or cisternal expansion (Reggiori and Klionsky, 2005; Reggiori et al., 2004b; Tooze and Yoshimori, 2010). In the maturation model, integral membrane proteins involved in autophagosome formation, such as Atg9, are segregated in a compartment derived from the membrane source. This nucleating structure matures into the phagophore and expands to form an autophagosome. At the same time specific organelle marker proteins are retrieved back to the donor compartment. The elongation of the phagophore occurs by a mechanism referred to as vesicular expansion that depends on the delivery of lipid bilayers by vesicular trafficking. In the assembly model, several sets of lipid bilayers are derived from the membrane source by a maturation process similar to the first model. Via cisternal expansion these small compartments/structures are then assembled and ultimately fuse into double-membrane vesicles at the PAS. Another model proposed in the literature implies the *de novo* delivery of lipids by lipid transfer proteins or direct lipid transfer from a donor organelle at sites of membrane contact. Alternatively autophagosomes could be formed by membrane remodelling, extension and curvature of a pre-existing membrane, allowing the phagophore to directly expand from an organelle such as the ER. Similarly to the first two models, autophagosomal membrane proteins would be segregated into a subdomain of this compartment, whereas resident proteins are retained in the donor compartment (Longatti and Tooze, 2009; Tooze and Yoshimori, 2010). It is very well possible that several of these models are applicable and that different mechanisms take place at different stages of autophagosome biogenesis.

Studies in yeast have shown that the Golgi apparatus and correct cycling through the Golgi is essential for autophagy (Geng et al., 2010; Reggiori et al., 2004b; van der Vaart et al., 2010; Yen et al., 2010). Mutations in Sec7, a guanosine exchange factor (GEF) required for trafficking through the Golgi, cause a block in autophagy (Reggiori et al., 2004b). Moreover, a study from our laboratory has shown that Sec7 together with its downstream effectors, the two small GTPases ADP-ribosylation factor (Arf)1 and Arf2, are involved in the expansion of the phagophore. One hypothesis is that Sec7 is involved in the transport of additional Atg9-containing membranes to the PAS that are required for autophagosome completion. This implicates a direct role for the Golgi in providing membranes to the expanding phagophore (van der Vaart et al., 2010). Also subunits of the

conserved oligomeric Golgi (COG) complex were found to be involved in autophagosomes biogenesis (Yen et al., 2010). This complex is important for retrograde trafficking within the Golgi complex and possibly for ER to Golgi and endosome to Golgi transport. Cog2, one of the subunits, localizes to the PAS and both Cog2 and Cog4 interact with particular Atg proteins, e.g. Atg12, Atg17, Atg20, Atg24 and Atg9. It has been postulated that the COG complex is maybe required for the correct sorting of these Atg proteins to the PAS and that possibly it acts as a tethering factor for the fusion of (Atg9-containing) vesicles with the expanding phagophore (Yen et al., 2010). Furthermore, the Rab family GTPase Sec4 and its GEF Sec2, two post-Golgi proteins which are part of the secretion machinery at the *trans*-Golgi network, were also shown to be required for autophagy (Geng et al., 2010). In Sec2 and Sec4 conditional mutants in particular Atg9 movement to the PAS is impaired and fewer autophagosomes are formed. In line with what has been proposed by Van der Vaart *et al.* for Sec7 involvement in autophagy, Sec2 and Sec4 are also thought to be directly or indirectly involved, possibly via Atg9-positive vesicles, in supplying membranes to the expanding phagophore (Geng et al., 2010).

Also the endoplasmic reticulum (ER) and exit from the ER have been shown to be important for autophagy progression. Studies using temperature-sensitive yeast mutants for the early steps secretory pathway revealed that Sec12, a GEF that functions in the formation of coat protein (COP)II vesicles at the ER exit site, as well as some components of the COPII complex itself, i.e. Sec16, Sec23, and Sec24, are essential for autophagy (Ishihara et al., 2001; Reggiori et al., 2004b). The idea that this defect was not indirectly due to an impairment of the transport between the ER and Golgi, which is mediated by COPII-coated vesicles, was based on the fact that components of this protein coat were not required for autophagy. However, it is difficult to exclude that some of the defects observed in autophagosome biogenesis are due to an indirect effect caused by a dysfunctional secretory pathway. One could imagine for example that an impairment of membrane flow through the early compartments of the secretory pathway interferes with the homeostasis of other organelles that are directly involved in providing the membranes to the forming autophagosome.

The origin of the phagophore and the autophagosomal membranes in higher eukaryotes

The origin of the autophagosomal membranes in mammals remains mysterious as in yeast. Freeze-fracture electron microscopy experiments have demonstrated

that autophagosomal membranes isolated from rat liver are predominantly composed of lipids (Fengsrud et al., 2000). The lack of specific organelle protein markers makes it thus extremely difficult to determine the source of the membranes supplied to the expanding autophagosome. In mammalian cells, several intracellular organelles, such as the Golgi, ER, mitochondria and the plasma membrane have been implicated as possible membrane donors for the autophagosome biogenesis (Axe et al., 2008; Hailey et al., 2010; Hayashi-Nishino et al., 2009; Ravikumar et al., 2010).

There is accumulating evidence suggesting that the ER is the source of the autophagosomal membranes, as specific subdomains of the ER that are highly enriched for PtdIns3P were found to be important for the formation of autophagosomes. These subdomains give rise to cup-shaped structures called omegasomes (Axe et al., 2008). Because of the dynamic connection of these omegasomes with the ER, it has been proposed that they represent a platform for autophagosome biogenesis and with lipids needed to create the autophagosome being supplied by the ER. This notion is supported by the observation of a dynamic connection between omegasomes and the forming autophagosomes (Axe et al., 2008). Two recent ultrastructural studies support this view of the ER being the source of the autophagosomal membranes because they reveal a direct connection between the ER and the forming autophagosome by three-dimensional (3D) electron tomography (Hayashi-Nishino et al., 2009; Yla-Anttila et al., 2009). In particular, they show that a subdomain of the ER forms a cradle for the formation of the phagophore, which expands while being surrounded by ER membranes/cisternae to which it is connected. The connections between the ER and the phagophore have been named ER-isolation membrane (IM) complexes (Hayashi-Nishino et al., 2009). Interestingly, the protein double FYVE domain-containing protein 1 (DFCP1), which specifically localizes to omegasomes upon autophagy induction (Axe et al., 2008), also localizes to the ER-IM complexes indicating that these sites are perhaps the omegasomes or at least that these two structures are related (Hayashi-Nishino et al., 2009). Under starvation conditions the mammalian Atg proteins ULK1/Atg1, Atg14, LC3, Atg16L1 and the Atg18 homologues WD40 repeat protein Interacting with PhosphoInositides (WIPI)-1 and WIPI-2, co-localize to a compartment in very close proximity to DFCP1 (Itakura and Mizushima, 2010; Polson et al., 2010). All together, these findings support the idea that a subdomain of the ER is the site for autophagosome formation. It remains, however, to be investigated if omegasomes facilitate

the formation of the phagophore or if the omegasomes represent expanding phagophores.

In addition to the ER also the mitochondria and the plasma membrane have been proposed as source of autophagosomal membranes (Hailey et al., 2010; Ravikumar et al., 2010). One report demonstrates that the outer membrane of the mitochondria participates in autophagosomes biogenesis during starvation. Atg5 and LC3 are found to transiently localize to punctae on the mitochondria, and transfer to autophagosomes of both lipids synthesized in mitochondria and specific outer membrane mitochondrial proteins is also observed (Hailey et al., 2010). The plasma membrane has also been found to contribute to the formation of early autophagosomal precursors (Moreau et al., 2012; Moreau and Rubinsztein, 2012; Ravikumar et al., 2010). Under autophagy inducing conditions, Atg12-Atg5 and Atg16L are found to associate with clathrin-coated vesicles derived from the plasma membrane by endocytosis (Moreau et al., 2012; Ravikumar et al., 2010). These structures could represent early autophagosomal precursors that mature into phagophores and subsequently autophagosomes as they become LC3 positive. Clathrin-independent endocytosis may also contribute to the formation of these precursors via the GPI-Enriched Endocytic Compartments (GEEC) pathway because Atg16L was also found to co-localize with GRAF1, a protein marker for the vesicles of this transport route (Moreau et al., 2012; Moreau and Rubinsztein, 2012).

Studies on transmembrane Atg9 have indicated that the Golgi or a post-Golgi compartment could be involved in providing autophagosomal lipids. In both yeast and mammalian cells, this protein is assumed to supply membranes to the nascent autophagosomes because of its association with lipid bilayers, and potentially can serve as a marker for the membrane source of autophagosomes. (Legakis et al., 2007; Reggiori et al., 2005b; Webber and Tooze, 2010; Webber et al., 2007; Young et al., 2006). In yeast Atg9 cycles between its cytoplasmic pools and the PAS. In mammals, however, the subcellular distribution of this protein appears to be different. Mammalian Atg9 (mAtg9) shuttles between the *trans*-Golgi network (TGN) and peripheral late endosomes under normal growth conditions. Upon starvation there is an increase in the translocation of mAtg9 to the peripheral endosomal membranes, some of which appear to be autophagosomal intermediates or equivalents of the PAS because they are LC3-positive (Webber et al., 2007; Young et al., 2006). This would implicate that via mAtg9-containing vesicles the TGN supplies membranes to the PAS.

All the above mentioned observation do not necessarily have to be mutually exclusive and it may very well be that, indeed, multiple sources contribute to the autophagosomal membranes, possibly providing lipids at different stages of the autophagosome biogenesis.

The lipid composition of autophagosomes

Due to the lack of probes to detect specific lipids and functional assays, very little is known about the lipid composition of autophagosomes, with the exception of PE and PtdIns3P (Ichimura et al., 2000; Kabeya et al., 2000; Obara et al., 2008a). As mentioned, lipidation of Atg8/LC3 with PE is required for the anchoring of this protein onto the autophagosomal membranes (Kirisako et al., 2000; Tanida et al., 2004). As a result, it is assumed that PE is part of the lipid bilayers composing autophagosomes but its concentrations are still unknown. PtdIns3P is also a known component of the autophagosomal membranes. This phosphoinositides is found at the PAS, where it is very likely involved in the recruitment of some of the Atg proteins and it is also found in the interior of complete autophagosomes in both yeast and mammalian cells (Kihara et al., 2001; Obara et al., 2008a).

In agreement with evidences suggesting that the ER is the source of the autophagosomal membranes in mammalian cells, an increase in the synthesis of the major phospholipids forming membranes, e.g. phosphatidylcholine, PE and phosphatidylserine, has been observed upon autophagy induction (Girardi et al., 2011). These newly made phospholipids would allow the ER to provide the massive demand of lipids required for the formation of a large number of double-membrane autophagosomes. In yeast the synthesis of inositol phosphorylceramide (IPC), a sphingolipid, is important for the normal progression of autophagy. In mutant strains that have a block in IPC synthesis, the PAS is formed but the number and size of the autophagosomes is reduced (Yamagata et al., 2011). This would imply that sphingolipids are components of autophagosome membranes or eventually, they could regulate the function of one or more Atg proteins. However, further studies are needed to fully understand the function of this lipid during autophagy because it is also involved in modulating specific signalling cascades.

THE SIGNALING PATHWAYS REGULATING AUTOPHAGY

The TOR pathway and cAMP-dependent protein kinase A (PKA) pathways, two

signaling cascades sensing nutrients, e.g. nitrogen and carbon respectively, are two well-known autophagy regulators (Chen and Klionsky, 2011; Stephan et al., 2009; Stephan et al., 2010). Although, both pathways independently inhibit autophagy in presence of nutrients by phosphorylating Atg13 thereby preventing the formation of the Atg1-Atg13 complex, studies in yeast and mammalian cells have indicated that there is also crosstalk between the two pathways in order to assure an optimal response.

As mentioned, TORC1 is a key regulator of autophagy. In mammalian cells, both the adenosine monophosphate-activated protein kinase (AMPK) and the Akt/protein kinase B (PKB) pathways act upstream of the TORC1 complex (Chen and Klionsky, 2011; He and Klionsky, 2009). AMPK is activated upon reduced cellular energy levels, which are directly correlated with the cellular amount of ATP. Subsequently AMPK activates autophagy by either directly inhibiting TORC1 or via the activation of tuberous sclerosis 2 (TSC2), an upstream effector of TORC1 (Gwinn et al., 2008; Inoki et al., 2003; Yang and Klionsky, 2010). AMPK in turn can be activated by its upstream kinases LKB1, TAK1, and CaMKKβ (Yang and Klionsky, 2010). Sucrose non-fermenting 1 (Snf1), the AMPK homolog in yeast, also positively regulates autophagy through a mechanism that remains unknown and appears to not be conserved in mammals (Wang et al., 2001b). The Akt pathway is also stimulated by insulin and insulin-like growth factors, and negatively regulates autophagy by inhibiting both tuberous sclerosis 1 (TSC1) and TSC2.

The PKA pathway plays an important role in sensing glucose in both yeast and mammals, and can also be regulated by certain growth factors. When mammalian cells are in presence of glucose, PKA negatively regulates autophagy by directly activating TORC1 through the phosphorylation one of the subunits of the PRAS40 complex, which leads to the disassociation of this inhibitory complex from TORC1, and indirectly by phosphorylating and inactivating AMPK, which as mention above inhibits TORC1 directly or via TSC2 (Djouder et al., 2010; Mavrakis et al., 2006). Synergistically to these events, PKA directly phosphorylates LC3, inactivating this molecule and thus leading to the inhibition of autophagy (Cherra et al., 2010). In yeast, PKA also negatively regulates autophagy by phosphorylating both Atg1 and Atg13 (Budovskaya et al., 2004; Stephan et al., 2009; Yorimitsu et al., 2007).

The TORC1 and PKA signaling cascades, however, are not the only pathways controlling autophagy. Depending on the situations, autophagy is positively or negatively modulated by additional signaling cascades, including the unfolded protein response (UPR), the hypoxia-inducible factor 1 (HIF-1) and Toll-

like receptor (TLR) pathways (He and Klionsky, 2009). The exact mechanisms how these signals regulate autophagy wait to be elucidated.

PHYSIOLOGICAL ROLES OF AUTOPHAGY

Under most circumstances autophagy is pro-survival pathway, particularly in response to growth factors, hormones or cellular stress such as nutrient deprivation (Kuma et al., 2004; Pua et al., 2007). In some situations, however, autophagy can cause cell death. Cells are dying as a result of the inability to survive the non-specific degradation of large amounts of cytoplasmic contents or because apoptosis is upregulated, as there is a complex crosstalk between this pathway and autophagy (Maiuri et al., 2007).

Because of its ability to rapidly eliminate large unwanted structures, autophagy is involved in numerous physiological processes including embryonic development, cellular remodelling and differentiation, and it plays a protective role against aging, tumors and invading pathogens. Defective autophagy has been implicated in the pathogenesis of diverse diseases, including cardiovascular and autoimmune diseases, neurodegenerative (e.g. Alzheimer's, Parkinson's and Huntington's diseases) and myodegenerative disorders, cancer and in ageing (Levine and Klionsky, 2004; Mizushima et al., 2008; Rubinsztein et al., 2005; Shintani and Klionsky, 2004).

Development and cell differentiation

Many developmental processes involve growth arrest and the massive elimination of cells via programmed cell death. Autophagy plays an important role in this event, in particular in the removal of cells that have undergone apoptosis. For example, in *Drosophila* larva autophagy is needed for the developmental degradation of salivary glands. Expression of some *ATG* genes in *Drosophila* such as *ATG4*, *ATG5*, *ATG6*/*Beclin1* and *ATG12* is upregulated during salivary glands cell death and consequently the salivary glands are not properly degraded in *atg* mutant larvae (Berry and Baehrecke, 2007; Gorski et al., 2003). During mammalian tissue development, programmed cell death occurs during cavitation of the early embryo when the ectoderm undergoes apoptosis to form the proamniotic cavity. Embryonic stem cells that are cultured in conditions that mimic this process will develop into embryoid bodies, containing an outer layer of endodermal cells

and an inner solid core of ectodermal cells. Eventually, the inner ectodermal cells of these embryoid bodies will undergo apoptosis to form an interior cavity. Embryoid bodies derived from cells lacking Atg5 or Beclin1/Atg6, however, fail to cavitate. The cells from the inner mass of these embryoid bodies undergo programmed cell death, but there is a defect in the clearance of the apoptotic cells, e.g. they are not engulfed by neighboring cells and remain within the lumen of the embryoid body (Qu et al., 2007).

Innate and adaptive immunity

One of the most intriguing systems in which autophagy is involved is the immune system, which can be divided into two categories: innate and adaptive immunity. Because autophagy is modulated by cytokines, such as IFN-γ, TNF-α, IL-4 and IL-13, it can act as an output of both innate and adaptive immunity responses (Deretic, 2009; Inbal et al., 2002; Yap et al., 2007). Autophagy is also part of the innate immune system because it is able to selectively capture and eliminate microorganisms that have invaded the cell. This type of autophagy, termed xenophagy, is able to target bacteria, parasites and viral particles present in the cytoplasm for destruction in the lysosome (Amano et al., 2006; Levine, 2005). Although it remains unclear how the autophagic machinery is able to recognize intracellular pathogens, some progress has been made understanding how autophagy is activated upon infection. Recent studies indicate that pattern recognition receptors (PRRs), such as Toll-like receptors, that get activated by pathogen-associated molecular patterns (PAMPs) of the intracellular microbes, play a role in the activation of autophagy (Delgado et al., 2009; Delgado and Deretic, 2009; Deretic and Levine, 2009; Sanjuan et al., 2007; Xu et al., 2007). In addition, autophagy is triggered by reactive oxygen species (ROS) generated during phagocytosis of intracellular microbes. A large amount of these ROS is generated via the activation of nicotinamide adenine dinucleotide phosphate (NADPH) oxidase upon phagocytosis, but also by some of the invading pathogens to induce damage to their host (Huang et al., 2009; Huang et al., 2011).

Recently it has also become evident that autophagy is involved in the adaptive immune system as well. First of all, the pathway is important for B and T lymphocyte development and homeostasis, the major cells of the adaptive immune system (Deretic, 2009; Miller et al., 2008). Autophagy was shown to be required for the generation of T cells in the thymus and for the survival and proliferation after exiting the thymus (Nedjic et al., 2008; Pua et al., 2007). Moreover, it has

become clear that autophagy contributes to major histocompatibility complex (MHC) class II-antigen presentation of intracellular pathogens by its intrinsic ability of targeting and degrading intracellular molecules, which can subsequently be presented as peptides on MHC class II molecules (Deretic, 2009; Gannage and Munz, 2009; Schmid et al., 2007). A role for autophagy in MHC class I-antigen presentation has also been demonstrated (English et al., 2009). In herpes simplex virus type I-infected macrophages, viral components are targeted by a previously unknown, unique type of autophagy, in which not only double-membrane vesicles are involved but also four layered structures. Both structures are required for antigen processing and presentation on MHC class I molecules to $CD8^+$ T cells, although the mechanism in this process is not well understood (English et al., 2009). Similar to MHC class II-antigen processing and presentation, exogenous antigens targeted by autophagy can be degraded in autolysosomes and the derived peptides can be presented on MHC class I molecules (Deretic, 2009).

During evolution both invading pathogens and host cells have developed adaptations to counter-act upon each other. This is also the case for the autophagy, since it is one of the host defences against intracellular pathogens. Specific pathogens such as *Listeria monocytogenes* and *Shigella flexneri* have developed mechanisms that can effectively hamper the degradation through autophagy by for example blocking the induction of the pathway, inhibiting autophagosomes maturation or by avoiding recognition by autophagosomes (Birmingham et al., 2008; Deretic and Levine, 2009; Ogawa et al., 2005). On the other hand, some microbes have developed ways to utilize parts of the autophagic machinery to their own advantage. For some picornaviruses such as poliovirus, autophagosomes may provide the membranous surfaces for the assembly of viral RNA replication complexes or provide a mechanism for non-lytic viral release (Deretic and Levine, 2009; Taylor and Kirkegaard, 2008).

Ageing and longevity

Caloric restriction or starvation, which induces autophagy, appears to have a positive effect on life-span extension in diverse organisms including yeast, flies, rodents and worms (Levine and Klionsky, 2004). *C. elegans* mutants that have a defect in insulin signaling or in feeding, which were treated with siRNA targeting *ATG* genes such as Bec-1/Atg6 or Ce-Atg7/Atg7, lived less long compared to untreated worms (Jia and Levine, 2007; Melendez et al., 2003). The extension in longevity upon autophagy induction may be the outcome of an increase in protection

against oxidative damage through the removal of dysfunctional mitochondria, as well as by mechanisms involved in the repair and replacement of damaged DNA and organelles (Dai and Rabinovitch, 2011; Huang et al., 2011; Shintani and Klionsky, 2004). Indeed, in ageing cells there is an accumulation of oxidized proteins and damaged organelles. It has been postulated that this accumulation is due to an impairment of autophagy and studies have demonstrated that the rate of autophagy declines with age, which suggests a possible correlation between the two events (Bergamini et al., 2004; Del Roso et al., 2003; Martinez-Vicente and Cuervo, 2007). Whether the decline in autophagy is the cause or the consequence of ageing is still unclear. Interestingly, autophagy is linked to a few specific age-related diseases such as neurodegeneration, cardiomyopathy and cancer.

Neurodegeneration

The accumulation of autophagosomes has been reported in several neurodegenerative disorders such as Huntington's, Alzheimer's and Parkinson's diseases (Levine and Kroemer, 2008; Mizushima et al., 2008; Rubinsztein et al., 2005) and for long it was thought that autophagy contributed to the pathology of the disease. Recent studies, however, have revealed that autophagy in fact protects neurons against degeneration and that the autophagosome accumulation indicates that autophagy is activated in order to eliminate the misfolded protein or aggregates (Martinez-Vicente and Cuervo, 2007). These and other studies have also hypothesized that in diseases caused by prions, the aberrantly folded proteins that aggregate and cause damage, are targeted by autophagosomes rather than the proteasomes (Nassif and Hetz, 2011). The exact mechanisms by which autophagy prevents or reduces neurodegeneration remain unclear. Some studies have revealed that the generation of protein aggregates or inclusion bodies actually has a cytoprotective role and that the cytosolic mutant proteins themselves are neurotoxic (Arrasate et al., 2004; Tanaka et al., 2004). Therefore it is plausible that the primary target of autophagy are the mutant proteins and not the inclusion bodies.

Cancer

Cancer is one of the first diseases that have been linked with autophagy (Levine and Kroemer, 2008). Oncogenes such as Bcl2 have been demonstrated to inhibit autophagy, whereas particular tumor suppressor genes such as those encoding for p53 and PTEN stimulate autophagy (Mathew et al., 2007). Beclin1/

Atg6 is monoallelically deleted in a high percentage of human breast, ovarian, and prostate cancers, and decreased expression of beclin1 has been reported in human breast, ovarian, and brain tumors (Levine and Kroemer, 2008; Liang et al., 1999; Miracco et al., 2007). Therefore, it appears that autophagy functions as a mechanism to suppress tumor growth. It remains largely unclear, however, how autophagy precisely acts as a tumor suppressor pathway (Mizushima et al., 2008). The hypothesis that autophagy suppresses tumor formation is further supported by evidence of the DNA protecting role. It has been demonstrated that the knockout of *ATG5* and *Beclin1/ATG6* results in an increase of DNA damage in epithelial cells (Levine and Kroemer, 2008). In this context, the autophagy defect may prevent mitochondrial turnover. Consequently, the ROS produced by the undigested damaged mitochondria lead to an oxidative stress that, in turn contributes to DNA damage. Based on these observations, it is evident that autophagy plays a protective role in the pathogenesis of cancer.

OUTLINE OF THE THESIS

Autophagy is a degradative pathway crucial for multiple cellular processes and it is implicated in numerous diseases. Despite great efforts being made to understand the fundamental aspects of this pathway, many questions still remain unanswered. For instance, the origin of the PAS is unknown as well as the source of the membranes composing autophagosomes. Moreover, the precise molecular function of many Atg proteins is not well understood. In this thesis I have addressed some of these unresolved questions in order to expand our knowledge about the molecular mechanism underlying the biogenesis of an autophagosome.

Chapter 2 is a review that provides an overview of the roles of the cytoskeleton network in autophagy in both yeast and mammalian cells. In mammalian cells, in particular, this cellular scaffold is critical for the movement of complete autophagosomes towards cellular locations where endosomes and lysosomes concentrate. The mechanism of this transport still needs elucidation and some possible models are described in this part of the thesis.

Chapter 3 focuses on Atg18, a protein essential for autophagy but also for vacuole homeostasis and probably endosomal functions. We investigated how Atg18 recruitment to the PAS is regulated and found that Atg18 via its β-propeller is able to bind both Atg2 and phosphoinositides. In this chapter we propose a

model where the Atg18 β-propeller provides organelle specificity by binding two determinants on the target membrane, thus underlining the potential capacity of specific β-propellers to form protein-lipid complexes.

In **Chapter 4** we characterize the interaction between Atg2 and Atg9. Atg2 is implicated in Atg9 retrieval from the PAS. We have identified the binding motifs in Atg2 and Atg9 and generated a number of Atg9-binding mutants that will allow us to study the function of the Atg2-Atg9 interaction in autophagy and provide a useful tool for studying Atg9 retrieval.

In **Chapter 5** we highlight the contribution of Atg9 to the early stages of autophagosome biogenesis by investigating the role of this protein in the formation of the PAS. We elucidate that in yeast the PAS originates from Atg9-positive clusters of vesicles and tubules that we called Atg9 reservoirs. Translocation of one or more reservoirs in proximity to the vacuole, together with the successive recruitment of other Atg proteins, leads to the generation of the PAS.

The final chapter of this thesis, **Chapter 6**, provides a summarizing discussion in which the findings of chapter 3, 4 and 5 are discussed in a broader perspective.

REFERENCES

1. Amano, A., I. Nakagawa, and T. Yoshimori. 2006. Autophagy in innate immunity against intracellular bacteria. . 140:161-166.
2. Arrasate, M., S. Mitra, E.S. Schweitzer, M.R. Segal, and S. Finkbeiner. 2004. Inclusion body formation reduces levels of mutant huntingtin and the risk of neuronal death. *Nature*. 431:805-810.
3. Axe, E.L., S.A. Walker, M. Manifava, P. Chandra, H.L. Roderick, A. Habermann, G. Griffiths, and N.T. Ktistakis. 2008. Autophagosome formation from membrane compartments enriched in phosphatidylinositol 3-phosphate and dynamically connected to the endoplasmic reticulum. *J Cell Biol*. 182:685-701.
4. Baba, M., M. Osumi, S.V. Scott, D.J. Klionsky, and Y. Ohsumi. 1997. Two distinct pathways for targeting proteins from the cytoplasm to the vacuole/lysosome. *J Cell Biol*. 139:1687-1695.
5. Bergamini, E., G. Cavallini, A. Donati, and Z. Gori. 2004. The role of macroautophagy in the ageing process, anti-ageing intervention and age-associated diseases. *Int J Biochem Cell Bioll*. 36:2392-2404.
6. Berry, D.L., and E.H. Baehrecke. 2007. Growth arrest and autophagy are required for salivary gland cell degradation in *Drosophila*. *Cell*. 131:1137-1148.
7. Birmingham, C.L., D.E. Higgins, and J.H. Brumell. 2008. Avoiding death by autophagy: interactions of *Listeria monocytogenes* with the macrophage autophagy system. *Autophagy*. 4:368-371.
8. Brocker, C., S. Engelbrecht-Vandre, and C. Ungermann. 2010. Multisubunit tethering complexes and their role in membrane fusion. *Curr Biol*. 20:R943-952.
9. Budovskaya, Y.V., J.S. Stephan, F. Reggiori, D.J. Klionsky, and P.K. Herman. 2004. The Ras/cAMP-dependent protein kinase signaling pathway regulates an early step of the autophagy process in *Saccharomyces cerevisiae*. *J Biol Chem*. 279:20663-20671.
10. Chen, Y., and D.J. Klionsky. 2011. The regulation of autophagy - unanswered questions. *J Cell Sci*. 124:161-170.
11. Cheong, H., and D.J. Klionsky. 2008. Dual role of Atg1 in regulation of autophagy-specific PAS assembly in *Saccharomyces cerevisiae*. *Autophagy*. 4:724-726.
12. Cheong, H., U. Nair, J. Geng, and D.J. Klionsky. 2008. The Atg1 kinase complex is involved in the regulation of protein recruitment to initiate sequestering vesicle formation for nonspecific autophagy in Saccharomyces cerevisiae. *Mol Biol Cell*. 19:668-681.
13. Cheong, H., T. Yorimitsu, F. Reggiori, J.E. Legakis, C.W. Wang, and D.J. Klionsky. 2005. Atg17 regulates the magnitude of the autophagic response. *Mol Biol Cell*. 16:3438-3453.
14. Cherra, S.J., 3rd, S.M. Kulich, G. Uechi, M. Balasubramani, J. Mountzouris, B.W. Day, and C.T. Chu. 2010. Regulation of the autophagy protein LC3 by phosphorylation. *J Cell Biol*. 190:533-539.
15. Cuervo, A.M. 2011. Chaperone-mediated autophagy: Dice's 'wild' idea about lysosomal selectivity. *Nat Rev Mol Cell Biol*. 12:535-541.
16. Dai, D.F., and P. Rabinovitch. 2011. Mitochondrial oxidative stress mediates induction of autophagy and hypertrophy in angiotensin-II treated mouse hearts. *Autophagy*. 7:917-918.
17. Darsow, T., S.E. Rieder, and S.D. Emr. 1997. A multispecificity syntaxin homologue, Vam3p, essential for autophagic and biosynthetic protein transport to the vacuole. *J Cell Biol*. 138:517-529.
18. Del Roso, A., S. Vittorini, G. Cavallini, A. Donati, Z. Gori, M. Masini, M. Pollera, and E. Bergamini. 2003. Ageing-related changes in the in vivo function of rat liver macroautophagy and proteolysis. *Exp Gerontol*. 38:519-527.

19. Delgado, M., S. Singh, S. De Haro, S. Master, M. Ponpuak, C. Dinkins, W. Ornatowski, I. Vergne, and V. Deretic. 2009. Autophagy and pattern recognition receptors in innate immunity. *Immunological reviews*. 227:189-202.

20. Delgado, M.A., and V. Deretic. 2009. Toll-like receptors in control of immunological autophagy. *Cell Death Differ*. 16:976-983.

21. Deretic, V. 2009. Multiple regulatory and effector roles of autophagy in immunity. *Current opinion in immunology*. 21:53-62.

22. Deretic, V., and B. Levine. 2009. Autophagy, immunity, and microbial adaptations. *Cell host & microbe*. 5:527-549.

23. Djouder, N., R.D. Tuerk, M. Suter, P. Salvioni, R.F. Thali, R. Scholz, K. Vaahtomeri, Y. Auchli, H. Rechsteiner, R.A. Brunisholz, B. Viollet, T.P. Makela, T. Wallimann, D. Neumann, and W. Krek. 2010. PKA phosphorylates and inactivates AMPKalpha to promote efficient lipolysis. *EMBO J*. 29:469-481.

24. Dove, S.K., R.C. Piper, R.K. McEwen, J.W. Yu, M.C. King, D.C. Hughes, J. Thuring, A.B. Holmes, F.T. Cooke, R.H. Michell, P.J. Parker, and M.A. Lemmon. 2004. Svp1p defines a family of phosphatidylinositol 3,5-bisphosphate effectors. *EMBO J*. 23:1922-1933.

25. Dunn, W.A., Jr., J.M. Cregg, J.A. Kiel, I.J. van der Klei, M. Oku, Y. Sakai, A.A. Sibirny, O.V. Stasyk, and M. Veenhuis. 2005. Pexophagy: the selective autophagy of peroxisomes. *Autophagy*. 1:75-83.

26. English, L., M. Chemali, J. Duron, C. Rondeau, A. Laplante, D. Gingras, D. Alexander, D. Leib, C. Norbury, R. Lippe, and M. Desjardins. 2009. Autophagy enhances the presentation of endogenous viral antigens on MHC class I molecules during HSV-1 infection. *Nature immunology*. 10:480-487.

27. Epple, U.D., I. Suriapranata, E.L. Eskelinen, and M. Thumm. 2001. Aut5/Cvt17p, a putative lipase essential for disintegration of autophagic bodies inside the vacuole. *Journal of bacteriology*. 183:5942-5955.

28. Fengsrud, M., E.S. Erichsen, T.O. Berg, C. Raiborg, and P.O. Seglen. 2000. Ultrastructural characterization of the delimiting membranes of isolated autophagosomes and amphisomes by freeze-fracture electron microscopy. *European journal of cell biology*. 79:871-882.

29. Fischer von Mollard, G., and T.H. Stevens. 1999. The *Saccharomyces cerevisiae* v-SNARE Vti1p is required for multiple membrane transport pathways to the vacuole. *Mol Biol Cell*. 10:1719-1732.

30. Fujita, N., M. Hayashi-Nishino, H. Fukumoto, H. Omori, A. Yamamoto, T. Noda, and T. Yoshimori. 2008a. An Atg4B mutant hampers the lipidation of LC3 paralogues and causes defects in autophagosome closure. *Mol Biol Cell*. 19:4651-4659.

31. Fujita, N., T. Itoh, H. Omori, M. Fukuda, T. Noda, and T. Yoshimori. 2008b. The Atg16L complex specifies the site of LC3 lipidation for membrane biogenesis in autophagy. *Mol Biol Cell*. 19:2092-2100.

32. Funakoshi, T., A. Matsuura, T. Noda, and Y. Ohsumi. 1997. Analyses of APG13 gene involved in autophagy in yeast, *Saccharomyces cerevisiae*. *Gene*. 192:207-213.

33. Funderburk, S.F., Q.J. Wang, and Z. Yue. 2010. The Beclin 1-VPS34 complex--at the crossroads of autophagy and beyond. *Trends in cell biology*. 20:355-362.

34. Gannage, M., and C. Munz. 2009. Autophagy in MHC class II presentation of endogenous antigens. *Current topics in microbiology and immunology*. 335:123-140.

35. Geng, J., and D.J. Klionsky. 2008. The Atg8 and Atg12 ubiquitin-like conjugation systems in macroautophagy. *EMBO Rep*.

36. Geng, J., U. Nair, K. Yasumura-Yorimitsu, and D.J. Klionsky. 2010. Post-golgi sec proteins are required for autophagy in *Saccharomyces cerevisiae*. *Mol Biol Cell*. 21:2257-2269.

37. Girardi, J.P., L. Pereira, and M. Bakovic. 2011. De novo synthesis of phospholipids is coupled with autophagosome formation. *Medical hypotheses*. 77:1083-1087.
38. Gorski, S.M., S. Chittaranjan, E.D. Pleasance, J.D. Freeman, C.L. Anderson, R.J. Varhol, S.M. Coughlin, S.D. Zuyderduyn, S.J. Jones, and M.A. Marra. 2003. A SAGE approach to discovery of genes involved in autophagic cell death. *Curr Biol*. 13:358-363.
39. Gwinn, D.M., D.B. Shackelford, D.F. Egan, M.M. Mihaylova, A. Mery, D.S. Vasquez, B.E. Turk, and R.J. Shaw. 2008. AMPK phosphorylation of raptor mediates a metabolic checkpoint. *Mol Cell*. 30:214-226.
40. Hailey, D.W., A.S. Rambold, P. Satpute-Krishnan, K. Mitra, R. Sougrat, P.K. Kim, and J. Lippincott-Schwartz. 2010. Mitochondria supply membranes for autophagosome biogenesis during starvation. *Cell*. 141:656-667.
41. Hanada, T., N.N. Noda, Y. Satomi, Y. Ichimura, Y. Fujioka, T. Takao, F. Inagaki, and Y. Ohsumi. 2007. The Atg12-Atg5 conjugate has a novel E3-like activity for protein lipidation in autophagy. *J Biol Chem*. 282:37298-37302.
42. Harding, T.M., A. Hefner-Gravink, M. Thumm, and D.J. Klionsky. 1996. Genetic and phenotypic overlap between autophagy and the cytoplasm to vacuole protein targeting pathway. *J Biol Chem*. 271:17621-17624.
43. Hayashi-Nishino, M., N. Fujita, T. Noda, A. Yamaguchi, T. Yoshimori, and A. Yamamoto. 2009. A subdomain of the endoplasmic reticulum forms a cradle for autophagosome formation. *Nat Cell Biol*. 11:1433-1437.
44. He, C., M. Baba, Y. Cao, and D.J. Klionsky. 2008. Self-interaction is critical for Atg9 transport and function at the phagophore assembly site during autophagy. *Mol Biol Cell*. 19:5506-5516.
45. He, C., and D.J. Klionsky. 2009. Regulation mechanisms and signaling pathways of autophagy. *Annual review of genetics*. 43:67-93.
46. He, C., and B. Levine. 2010. The Beclin 1 interactome. *Curr Biol*. 22:140-149.
47. He, C., H. Song, T. Yorimitsu, I. Monastyrska, W.L. Yen, J.E. Legakis, and D.J. Klionsky. 2006. Recruitment of Atg9 to the preautophagosomal structure by Atg11 is essential for selective autophagy in budding yeast. *J Cell Biol*. 175:925-935.
48. Huang, J., V. Canadien, G.Y. Lam, B.E. Steinberg, M.C. Dinauer, M.A. Magalhaes, M. Glogauer, S. Grinstein, and J.H. Brumell. 2009. Activation of antibacterial autophagy by NADPH oxidases. *Proc Natl Acad Sci U S A*. 106:6226-6231.
49. Huang, J., G.Y. Lam, and J.H. Brumell. 2011. Autophagy signaling through reactive oxygen species. *Antioxid Redox Signal*. 14:2215-2231.
50. Ichimura, Y., T. Kirisako, T. Takao, Y. Satomi, Y. Shimonishi, N. Ishihara, N. Mizushima, I. Tanida, E. Kominami, M. Ohsumi, T. Noda, and Y. Ohsumi. 2000. A ubiquitin-like system mediates protein lipidation. *Nature*. 408:488-492.
51. Inbal, B., S. Bialik, I. Sabanay, G. Shani, and A. Kimchi. 2002. DAP kinase and DRP-1 mediate membrane blebbing and the formation of autophagic vesicles during programmed cell death. *J Cell Biol*. 157:455-468.
52. Inoki, K., T. Zhu, and K.L. Guan. 2003. TSC2 mediates cellular energy response to control cell growth and survival. *Cell*. 115:577-590.
53. Inoue, Y., and D.J. Klionsky. 2010. Regulation of macroautophagy in *Saccharomyces cerevisiae*. *Seminars in cell & developmental biology*. 21:664-670.
54. Ishihara, N., M. Hamasaki, S. Yokota, K. Suzuki, Y. Kamada, A. Kihara, T. Yoshimori, T. Noda, and Y. Ohsumi. 2001. Autophagosome requires specific early Sec proteins for its formation and NSF/SNARE for vacuolar fusion. *Mol Biol Cell*. 12:3690-3702.
55. Itakura, E., and N. Mizushima. 2010. Characterization of autophagosome formation site by a hierarchical analysis of mammalian Atg proteins. *Autophagy*. 6:764-776.

56. Jia, K., and B. Levine. 2007. Autophagy is required for dietary restriction-mediated life span extension in *C. elegans*. *Autophagy*. 3:597-599.

57. Jung, C.H., C.B. Jun, S.H. Ro, Y.M. Kim, N.M. Otto, J. Cao, M. Kundu, and D.H. Kim. 2009. ULK-Atg13-FIP200 complexes mediate mTOR signaling to the autophagy machinery. *Mol Biol Cell*. 20:1992-2003.

58. Kabeya, Y., Y. Kamada, M. Baba, H. Takikawa, M. Sasaki, and Y. Ohsumi. 2005. Atg17 functions in cooperation with Atg1 and Atg13 in yeast autophagy. *Mol Biol Cell*. 16:2544-2553.

59. Kabeya, Y., N. Mizushima, T. Ueno, A. Yamamoto, T. Kirisako, T. Noda, E. Kominami, Y. Ohsumi, and T. Yoshimori. 2000. LC3, a mammalian homologue of yeast Apg8p, is localized in autophagosome membranes after processing. *EMBO J*. 19:5720-5728.

60. Kamada, Y., T. Funakoshi, T. Shintani, K. Nagano, M. Ohsumi, and Y. Ohsumi. 2000. Tor-mediated induction of autophagy via an Apg1 protein kinase complex. *J Cell Biol*. 150:1507-1513.

61. Kanki, T., and D.J. Klionsky. 2008. Mitophagy in yeast occurs through a selective mechanism. *J Biol Chem*. 283:32386-32393.

62. Kawamata, T., Y. Kamada, Y. Kabeya, T. Sekito, and Y. Ohsumi. 2008. Organization of the pre-autophagosomal structure responsible for autophagosome formation. *Mol Biol Cell*. 19:2039-2050.

63. Kihara, A., T. Noda, N. Ishihara, and Y. Ohsumi. 2001. Two distinct Vps34 phosphatidylinositol 3-kinase complexes function in autophagy and carboxypeptidase Y sorting in *Saccharomyces cerevisiae*. *J Cell Biol*. 152:519-530.

64. Kim, I., S. Rodriguez-Enriquez, and J.J. Lemasters. 2007. Selective degradation of mitochondria by mitophagy. *Archives of biochemistry and biophysics*. 462:245-253.

65. Kirisako, T., M. Baba, N. Ishihara, K. Miyazawa, M. Ohsumi, T. Yoshimori, T. Noda, and Y. Ohsumi. 1999. Formation process of autophagosome is traced with Apg8/Aut7p in yeast. *J Cell Biol*. 147:435-446.

66. Kirisako, T., Y. Ichimura, H. Okada, Y. Kabeya, N. Mizushima, T. Yoshimori, M. Ohsumi, T. Takao, T. Noda, and Y. Ohsumi. 2000. The reversible modification regulates the membrane-binding state of Apg8/Aut7 essential for autophagy and the cytoplasm to vacuole targeting pathway. *J Cell Biol*. 151:263-276.

67. Klionsky, D.J. 2005. The molecular machinery of autophagy: unanswered questions. *J Cell Sci*. 118:7-18.

68. Klionsky, D.J., J.M. Cregg, W.A. Dunn, Jr., S.D. Emr, Y. Sakai, I.V. Sandoval, A. Sibirny, S. Subramani, M. Thumm, M. Veenhuis, and Y. Ohsumi. 2003. A unified nomenclature for yeast autophagy-related genes. *Dev Cell*. 5:539-545.

69. Kraft, C., A. Deplazes, M. Sohrmann, and M. Peter. 2008. Mature ribosomes are selectively degraded upon starvation by an autophagy pathway requiring the Ubp3p/Bre5p ubiquitin protease. *Nat Cell Biol*. 10:602-610.

70. Kuma, A., M. Hatano, M. Matsui, A. Yamamoto, H. Nakaya, T. Yoshimori, Y. Ohsumi, T. Tokuhisa, and N. Mizushima. 2004. The role of autophagy during the early neonatal starvation period. *Nature*. 432:1032-1036.

71. Kuma, A., N. Mizushima, N. Ishihara, and Y. Ohsumi. 2002. Formation of the approximately 350-kDa Apg12-Apg5.Apg16 multimeric complex, mediated by Apg16 oligomerization, is essential for autophagy in yeast. *J Biol Chem*. 277:18619-18625.

72. Kunz, J.B., H. Schwarz, and A. Mayer. 2004. Determination of four sequential stages during microautophagy in vitro. *J Biol Chem*. 279:9987-9996.

73. Legakis, J.E., W.L. Yen, and D.J. Klionsky. 2007. A cycling protein complex required for selective autophagy. *Autophagy*. 3:422-432.

74. Levine, B. 2005. Eating oneself and uninvited guests: autophagy-related pathways in cellular defense. *Cell*. 120:159-162.

75. Levine, B., and D.J. Klionsky. 2004. Development by self-digestion: molecular mechanisms and biological functions of autophagy. *Dev Cell*. 6:463-477.
76. Levine, B., and G. Kroemer. 2008. Autophagy in the pathogenesis of disease. *Cell*. 132:27-42.
77. Liang, X.H., S. Jackson, M. Seaman, K. Brown, B. Kempkes, H. Hibshoosh, and B. Levine. 1999. Induction of autophagy and inhibition of tumorigenesis by beclin 1. *Nature*. 402:672-676.
78. Loewith, R., E. Jacinto, S. Wullschleger, A. Lorberg, J.L. Crespo, D. Bonenfant, W. Oppliger, P. Jenoe, and M.N. Hall. 2002. Two TOR complexes, only one of which is rapamycin sensitive, have distinct roles in cell growth control. *Mol Cell*. 10:457-468.
79. Longatti, A., and S.A. Tooze. 2009. Vesicular trafficking and autophagosome formation. *Cell Death Differ*. 16:956-965.
80. Lu, Q., P. Yang, X. Huang, W. Hu, B. Guo, F. Wu, L. Lin, A.L. Kovacs, L. Yu, and H. Zhang. 2011. The WD40 repeat PtdIns(3)P-binding protein EPG-6 regulates progression of omegasomes to autophagosomes. *Dev Cell*. 21:343-357.
81. Lynch-Day, M.A., and D.J. Klionsky. 2010. The Cvt pathway as a model for selective autophagy. *FEBS Lett*. 584:1359-1366.
82. Maiuri, M.C., E. Zalckvar, A. Kimchi, and G. Kroemer. 2007. Self-eating and self-killing: crosstalk between autophagy and apoptosis. *Nat Rev Mol Cell Biol*. 8:741-752.
83. Mari, M., and F. Reggiori. 2007. Atg9 trafficking in the yeast *Saccharomyces cerevisiae*. *Autophagy*. 3:145-148.
84. Martinez-Vicente, M., and A.M. Cuervo. 2007. Autophagy and neurodegeneration: when the cleaning crew goes on strike. *Lancet neurology*. 6:352-361.
85. Massey, A., R. Kiffin, and A.M. Cuervo. 2004. Pathophysiology of chaperone-mediated autophagy. *Int J Biochem Cell Bioll*. 36:2420-2434.
86. Mathew, R., V. Karantza-Wadsworth, and E. White. 2007. Role of autophagy in cancer. *Nat Rev Cancer*. 7:961-967.
87. Matsuura, A., M. Tsukada, Y. Wada, and Y. Ohsumi. 1997. Apg1p, a novel protein kinase required for the autophagic process in *Saccharomyces cerevisiae*. *Gene*. 192:245-250.
88. Mavrakis, M., J. Lippincott-Schwartz, C.A. Stratakis, and I. Bossis. 2006. Depletion of type IA regulatory subunit (RIalpha) of protein kinase A (PKA) in mammalian cells and tissues activates mTOR and causes autophagic deficiency. *Human molecular genetics*. 15:2962-2971.
89. Melendez, A., Z. Talloczy, M. Seaman, E.L. Eskelinen, D.H. Hall, and B. Levine. 2003. Autophagy genes are essential for dauer development and life-span extension in *C. elegans*. *Science (New York, N.Y.* 301:1387-1391.
90. Miller, B.C., Z. Zhao, L.M. Stephenson, K. Cadwell, H.H. Pua, H.K. Lee, N.N. Mizushima, A. Iwasaki, Y.W. He, W. Swat, and H.W.t. Virgin. 2008. The autophagy gene ATG5 plays an essential role in B lymphocyte development. *Autophagy*. 4:309-314.
91. Miracco, C., E. Cosci, G. Oliveri, P. Luzi, L. Pacenti, I. Monciatti, S. Mannucci, M.C. De Nisi, M. Toscano, V. Malagnino, S.M. Falzarano, L. Pirtoli, and P. Tosi. 2007. Protein and mRNA expression of autophagy gene Beclin 1 in human brain tumours. *International journal of oncology*. 30:429-436.
92. Mizushima, N. 2010. The role of the Atg1/ULK1 complex in autophagy regulation. *Curr Biol*. 22:132-139.
93. Mizushima, N., B. Levine, A.M. Cuervo, and D.J. Klionsky. 2008. Autophagy fights disease through cellular self-digestion. *Nature*. 451:1069-1075.
94. Mizushima, N., T. Noda, and Y. Ohsumi. 1999. Apg16p is required for the function of the Apg12p-Apg5p conjugate in the yeast autophagy pathway. *EMBO J*. 18:3888-3896.
95. Mizushima, N., T. Noda, T. Yoshimori, Y. Tanaka, T. Ishii, M.D. George, D.J. Klionsky, M. Ohsumi, and Y. Ohsumi. 1998. A protein conjugation system essential for autophagy. *Nature*. 395:395-398.

96. Monastyrska, I., T. Shintani, D.J. Klionsky, and F. Reggiori. 2006. Atg11 directs autophagosome cargoes to the PAS along actin cables. *Autophagy*. 2:119-121.

97. Moreau, K., B. Ravikumar, C. Puri, and D.C. Rubinsztein. 2012. Arf6 promotes autophagosome formation via effects on phosphatidylinositol 4,5-bisphosphate and phospholipase D. *J Cell Biol*. 196:483-496.

98. Moreau, K., and D.C. Rubinsztein. 2012. The plasma membrane as a control center for autophagy. *Autophagy*. 8.

99. Nair, U., W.L. Yen, M. Mari, Y. Cao, Z. Xie, M. Baba, F. Reggiori, and D.J. Klionsky. 2012. A role for Atg8-PE deconjugation in autophagosome biogenesis. *Autophagy*. 8.

100. Nakamura, N., A. Matsuura, Y. Wada, and Y. Ohsumi. 1997. Acidification of vacuoles is required for autophagic degradation in the yeast *Saccharomyces cerevisiae*. *Journal of biochemistry*. 121:338-344.

101. Nakatogawa, H., Y. Ichimura, and Y. Ohsumi. 2007. Atg8, a ubiquitin-like protein required for autophagosome formation, mediates membrane tethering and hemifusion. *Cell*. 130:165-178.

102. Nakatogawa, H., J. Ishii, E. Asai, and Y. Ohsumi. 2012. Atg4 recycles inappropriately lipidated Atg8 to promote autophagosome biogenesis. *Autophagy*. 8:177-186.

103. Nakatogawa, H., K. Suzuki, Y. Kamada, and Y. Ohsumi. 2009. Dynamics and diversity in autophagy mechanisms: lessons from yeast. *Nat Rev Mol Cell Biol*. 10:458-467.

104. Nassif, M., and C. Hetz. 2011. Targeting autophagy in ALS: a complex mission. *Autophagy*. 7:450-453.

105. Nedjic, J., M. Aichinger, J. Emmerich, N. Mizushima, and L. Klein. 2008. Autophagy in thymic epithelium shapes the T-cell repertoire and is essential for tolerance. *Nature*. 455:396-400.

106. Noda, T., J. Kim, W.P. Huang, M. Baba, C. Tokunaga, Y. Ohsumi, and D.J. Klionsky. 2000. Apg9p/Cvt7p is an integral membrane protein required for transport vesicle formation in the Cvt and autophagy pathways. *J Cell Biol*. 148:465-480.

107. Nordmann, M., M. Cabrera, A. Perz, C. Brocker, C. Ostrowicz, S. Engelbrecht-Vandre, and C. Ungermann. 2010. The Mon1-Ccz1 complex is the GEF of the late endosomal Rab7 homolog Ypt7. *Curr Biol*. 20:1654-1659.

108. Obara, K., T. Noda, K. Niimi, and Y. Ohsumi. 2008a. Transport of phosphatidylinositol 3-phosphate into the vacuole via autophagic membranes in *Saccharomyces cerevisiae*. *Genes Cells*. 13:537-547.

109. Obara, K., T. Sekito, K. Niimi, and Y. Ohsumi. 2008b. The Atg18-Atg2 complex is recruited to autophagic membranes via phosphatidylinositol 3-phosphate and exerts an essential function. *J Biol Chem*. 283:23972-23980.

110. Obara, K., T. Sekito, and Y. Ohsumi. 2006. Assortment of phosphatidylinositol 3-kinase complexes-Atg14p directs association of complex I to the pre-autophagosomal structure in *Saccharomyces cerevisiae*. *Mol Biol Cell*. 17:1527-1539.

111. Ogawa, M., T. Yoshimori, T. Suzuki, H. Sagara, N. Mizushima, and C. Sasakawa. 2005. Escape of intracellular *Shigella* from autophagy. *Science (New York, N.Y.* 307:727-731.

112. Polson, H.E., J. de Lartigue, D.J. Rigden, M. Reedijk, S. Urbe, M.J. Clague, and S.A. Tooze. 2010. Mammalian Atg18 (WIPI2) localizes to omegasome-anchored phagophores and positively regulates LC3 lipidation. *Autophagy*. 6:506-522.

113. Proikas-Cezanne, T., S. Ruckerbauer, Y.D. Stierhof, C. Berg, and A. Nordheim. 2007. Human WIPI-1 puncta-formation: a novel assay to assess mammalian autophagy. *FEBS Lett*. 581:3396-3404.

114. Pua, H.H., I. Dzhagalov, M. Chuck, N. Mizushima, and Y.W. He. 2007. A critical role for the autophagy gene Atg5 in T cell survival and proliferation. *The Journal of experimental medicine*. 204:25-31.

115. Qu, X., Z. Zou, Q. Sun, K. Luby-Phelps, P. Cheng, R.N. Hogan, C. Gilpin, and B. Levine. 2007. Autophagy gene-dependent clearance of apoptotic cells during embryonic development. *Cell*. 128:931-946.

116. Ravikumar, B., K. Moreau, L. Jahreiss, C. Puri, and D.C. Rubinsztein. 2010. Plasma membrane contributes to the formation of pre-autophagosomal structures. *Nat Cell Biol*. 12:747-757.

117. Ravikumar, B., and D.C. Rubinsztein. 2006. Role of autophagy in the clearance of mutant huntingtin: a step towards therapy? *Molecular aspects of medicine*. 27:520-527.

118. Reggiori, F. 2006. 1. Membrane origin for autophagy. *Curr Top Dev Biol*. 74:1-30.

119. Reggiori, F., and D.J. Klionsky. 2005. Autophagosomes: biogenesis from scratch? *Curr Biol*. 17:415-422.

120. Reggiori, F., I. Monastyrska, T. Shintani, and D.J. Klionsky. 2005a. The actin cytoskeleton is required for selective types of autophagy, but not nonspecific autophagy, in the yeast *Saccharomyces cerevisiae*. *Mol Biol Cell*. 16:5843-5856.

121. Reggiori, F., T. Shintani, U. Nair, and D.J. Klionsky. 2005b. Atg9 cycles between mitochondria and the pre-autophagosomal structure in yeasts. *Autophagy*. 1:101-109.

122. Reggiori, F., K.A. Tucker, P.E. Stromhaug, and D.J. Klionsky. 2004a. The Atg1-Atg13 complex regulates Atg9 and Atg23 retrieval transport from the pre-autophagosomal structure. *Dev Cell*. 6:79-90.

123. Reggiori, F., C.W. Wang, U. Nair, T. Shintani, H. Abeliovich, and D.J. Klionsky. 2004b. Early stages of the secretory pathway, but not endosomes, are required for Cvt vesicle and autophagosome assembly in *Saccharomyces cerevisiae*. *Mol Biol Cell*. 15:2189-2204.

124. Rubinsztein, D.C., M. DiFiglia, N. Heintz, R.A. Nixon, Z.H. Qin, B. Ravikumar, L. Stefanis, and A. Tolkovsky. 2005. Autophagy and its possible roles in nervous system diseases, damage and repair. *Autophagy*. 1:11-22.

125. Russnak, R., D. Konczal, and S.L. McIntire. 2001. A family of yeast proteins mediating bidirectional vacuolar amino acid transport. *J Biol Chem*. 276:23849-23857.

126. Sanjuan, M.A., C.P. Dillon, S.W. Tait, S. Moshiach, F. Dorsey, S. Connell, M. Komatsu, K. Tanaka, J.L. Cleveland, S. Withoff, and D.R. Green. 2007. Toll-like receptor signalling in macrophages links the autophagy pathway to phagocytosis. *Nature*. 450:1253-1257.

127. Sato, T.K., T. Darsow, and S.D. Emr. 1998. Vam7p, a SNAP-25-like molecule, and Vam3p, a syntaxin homolog, function together in yeast vacuolar protein trafficking. *Mol Cell Biol*. 18:5308-5319.

128. Sato, T.K., P. Rehling, M.R. Peterson, and S.D. Emr. 2000. Class C Vps protein complex regulates vacuolar SNARE pairing and is required for vesicle docking/fusion. *Mol Cell*. 6:661-671.

129. Schmid, D., M. Pypaert, and C. Munz. 2007. Antigen-loading compartments for major histocompatibility complex class II molecules continuously receive input from autophagosomes. *Immunity*. 26:79-92.

130. Scott, S.V., A. Hefner-Gravink, K.A. Morano, T. Noda, Y. Ohsumi, and D.J. Klionsky. 1996. Cytoplasm-to-vacuole targeting and autophagy employ the same machinery to deliver proteins to the yeast vacuole. *Proc Natl Acad Sci U S A*. 93:12304-12308.

131. Sekito, T., T. Kawamata, R. Ichikawa, K. Suzuki, and Y. Ohsumi. 2009. Atg17 recruits Atg9 to organize the pre-autophagosomal structure. *Genes Cells*. 14:525-538.

132. Shintani, T., and D.J. Klionsky. 2004. Autophagy in health and disease: a double-edged sword. *Science (New York, N.Y.*. 306:990-995.

133. Shintani, T., N. Mizushima, Y. Ogawa, A. Matsuura, T. Noda, and Y. Ohsumi. 1999. Apg10p, a novel protein-conjugating enzyme essential for autophagy in yeast. *EMBO J*. 18:5234-5241.

134. Shintani, T., K. Suzuki, Y. Kamada, T. Noda, and Y. Ohsumi. 2001. Apg2p functions in autophagosome formation on the perivacuolar structure. *J Biol Chem*. 276:30452-30460.

135. Stephan, J.S., Y.Y. Yeh, V. Ramachandran, S.J. Deminoff, and P.K. Herman. 2009. The Tor and PKA signaling pathways independently target the Atg1/Atg13 protein kinase complex to control autophagy. *Proc Natl Acad Sci U S A*. 106:17049-17054.

136. Stephan, J.S., Y.Y. Yeh, V. Ramachandran, S.J. Deminoff, and P.K. Herman. 2010. The Tor and cAMP-dependent protein kinase signaling pathways coordinately control autophagy in *Saccharomyces cerevisiae*. *Autophagy*. 6:294-295.

137. Suriapranata, I., U.D. Epple, D. Bernreuther, M. Bredschneider, K. Sovarasteanu, and M. Thumm. 2000. The breakdown of autophagic vesicles inside the vacuole depends on Aut4p. *J Cell Sci*. 113 (Pt 22):4025-4033.

138. Suzuki, K., Y. Kubota, T. Sekito, and Y. Ohsumi. 2007. Hierarchy of Atg proteins in pre-autophagosomal structure organization. *Genes Cells*. 12:209-218.

139. Suzuki, K., and Y. Ohsumi. 2007. Molecular machinery of autophagosome formation in yeast, *Saccharomyces cerevisiae*. *FEBS Lett*. 581:2156-2161.

140. Takeshige, K., M. Baba, S. Tsuboi, T. Noda, and Y. Ohsumi. 1992. Autophagy in yeast demonstrated with proteinase-deficient mutants and conditions for its induction. *J Cell Biol*. 119:301-311.

141. Tanaka, M., Y.M. Kim, G. Lee, E. Junn, T. Iwatsubo, and M.M. Mouradian. 2004. Aggresomes formed by alpha-synuclein and synphilin-1 are cytoprotective. *J Biol Chem*. 279:4625-4631.

142. Tanida, I. 2011. Autophagosome formation and molecular mechanism of autophagy. *Antioxid Redox Signal*. 14:2201-2214.

143. Tanida, I., N. Mizushima, M. Kiyooka, M. Ohsumi, T. Ueno, Y. Ohsumi, and E. Kominami. 1999. Apg7p/Cvt2p: A novel protein-activating enzyme essential for autophagy. *Mol Biol Cell*. 10:1367-1379.

144. Tanida, I., T. Ueno, and E. Kominami. 2004. LC3 conjugation system in mammalian autophagy. *Int J Biochem Cell Biol*. 36:2503-2518.

145. Taylor, M.P., and K. Kirkegaard. 2008. Potential subversion of autophagosomal pathway by picornaviruses. *Autophagy*. 4:286-289.

146. Teter, S.A., K.P. Eggerton, S.V. Scott, J. Kim, A.M. Fischer, and D.J. Klionsky. 2001. Degradation of lipid vesicles in the yeast vacuole requires function of Cvt17, a putative lipase. *J Biol Chem*. 276:2083-2087.

147. Thumm, M., R. Egner, B. Koch, M. Schlumpberger, M. Straub, M. Veenhuis, and D.H. Wolf. 1994. Isolation of autophagocytosis mutants of *Saccharomyces cerevisiae*. *FEBS Lett*. 349:275-280.

148. Tooze, S.A., and T. Yoshimori. 2010. The origin of the autophagosomal membrane. *Nat Cell Biol*. 12:831-835.

149. Tsukada, M., and Y. Ohsumi. 1993. Isolation and characterization of autophagy-defective mutants of *Saccharomyces cerevisiae*. *FEBS Lett*. 333:169-174.

150. van der Vaart, A., J. Griffith, and F. Reggiori. 2010. Exit from the Golgi is required for the expansion of the autophagosomal phagophore in yeast *Saccharomyces cerevisiae*. *Mol Biol Cell*. 21:2270-2284.

151. van der Vaart, A., M. Mari, and F. Reggiori. 2008. A picky eater: exploring the mechanisms of selective autophagy in human pathologies. *Traffic*. 9:281-289.

152. Velikkakath, A.K., T. Nishimura, E. Oita, N. Ishihara, and N. Mizushima. 2012. Mammalian Atg2 proteins are essential for autophagosome formation and important for regulation of size and distribution of lipid droplets. *Mol Biol Cell*. 23:896-909.

153. Wang, C.W., J. Kim, W.P. Huang, H. Abeliovich, P.E. Stromhaug, W.A. Dunn, Jr., and D.J. Klionsky. 2001a. Apg2 is a novel protein required for the cytoplasm to vacuole targeting, autophagy, and pexophagy pathways. *J Biol Chem*. 276:30442-30451.

154. Wang, C.W., P.E. Stromhaug, J. Shima, and D.J. Klionsky. 2002. The Ccz1-Mon1 protein complex is required for the late step of multiple vacuole delivery pathways. *J Biol Chem*. 277:47917-47927.

155. Wang, Z., W.A. Wilson, M.A. Fujino, and P.J. Roach. 2001b. Antagonistic controls of autophagy and glycogen accumulation by Snf1p, the yeast homolog of AMP-activated protein kinase, and the cyclin-dependent kinase Pho85p. *Mol Cell Biol*. 21:5742-5752.

156. Webber, J.L., and S.A. Tooze. 2010. New insights into the function of Atg9. *FEBS Lett*. 584:1319-1326.

157. Webber, J.L., A.R. Young, and S.A. Tooze. 2007. Atg9 trafficking in Mammalian cells. *Autophagy*. 3:54-56.

158. Xie, Z., and D.J. Klionsky. 2007. Autophagosome formation: core machinery and adaptations. *Nat Cell Biol*. 9:1102-1109.

159. Xie, Z., U. Nair, and D.J. Klionsky. 2008. Atg8 controls phagophore expansion during autophagosome formation. *Mol Biol Cell*. 19:3290-3298.

160. Xu, H., Y. Jun, J. Thompson, J. Yates, and W. Wickner. 2010. HOPS prevents the disassembly of trans-SNARE complexes by Sec17p/Sec18p during membrane fusion. *EMBO J* . 29:1948-1960.

161. Xu, Y., C. Jagannath, X.D. Liu, A. Sharafkhaneh, K.E. Kolodziejska, and N.T. Eissa. 2007. Toll-like receptor 4 is a sensor for autophagy associated with innate immunity. *Immunity*. 27:135-144.

162. Yamagata, M., K. Obara, and A. Kihara. 2011. Sphingolipid synthesis is involved in autophagy in *Saccharomyces cerevisiae*. *Biochem Biophys Res Commun*. 410:786-791.

163. Yang, Z., J. Huang, J. Geng, U. Nair, and D.J. Klionsky. 2006. Atg22 recycles amino acids to link the degradative and recycling functions of autophagy. *Mol Biol Cell*. 17:5094-5104.

164. Yang, Z., and D.J. Klionsky. 2007. Permeases recycle amino acids resulting from autophagy. *Autophagy*. 3:149-150.

165. Yang, Z., and D.J. Klionsky. 2009. An overview of the molecular mechanism of autophagy. *Curr Top Microbiol Immunol*. 335:1-32.

166. Yang, Z., and D.J. Klionsky. 2010. Mammalian autophagy: core molecular machinery and signaling regulation. *Curr Biol*. 22:124-131.

167. Yap, G.S., Y. Ling, and Y. Zhao. 2007. Autophagic elimination of intracellular parasites: convergent induction by IFN-Y and CD40 ligation? *Autophagy*. 3:163-165.

168. Yen, W.L., J.E. Legakis, U. Nair, and D.J. Klionsky. 2007. Atg27 is required for autophagy-dependent cycling of Atg9. *Mol Biol Cell*. 18:581-593.

169. Yen, W.L., T. Shintani, U. Nair, Y. Cao, B.C. Richardson, Z. Li, F.M. Hughson, M. Baba, and D.J. Klionsky. 2010. The conserved oligomeric Golgi complex is involved in double-membrane vesicle formation during autophagy. *J Cell Biol*. 188:101-114.

170. Yla-Anttila, P., H. Vihinen, E. Jokitalo, and E.L. Eskelinen. 2009. 3D tomography reveals connections between the phagophore and endoplasmic reticulum. *Autophagy*. 5:1180-1185.

171. Yorimitsu, T., S. Zaman, J.R. Broach, and D.J. Klionsky. 2007. Protein kinase A and Sch9 cooperatively regulate induction of autophagy in *Saccharomyces cerevisiae*. *Mol Biol Cell*. 18:4180-4189.

172. Young, A.R.J., E.Y.W. Chan, X.W. Hu, R. Köchl, S.G. Crawshaw, S. High, D.W. Hailey, J. Lippincott-Schwartz, and S.A. Tooze. 2006. Starvation and ULK1-dependent cycling of mammalian Atg9 between the TGN and endosomes. *J Cell Sci*. 119:3888-3900.

173. Yuga, M., K. Gomi, D.J. Klionsky, and T. Shintani. 2011. Aspartyl aminopeptidase is imported from the cytoplasm to the vacuole by selective autophagy in *Saccharomyces cerevisiae*. *J Biol Chem*. 286:13704-13713.

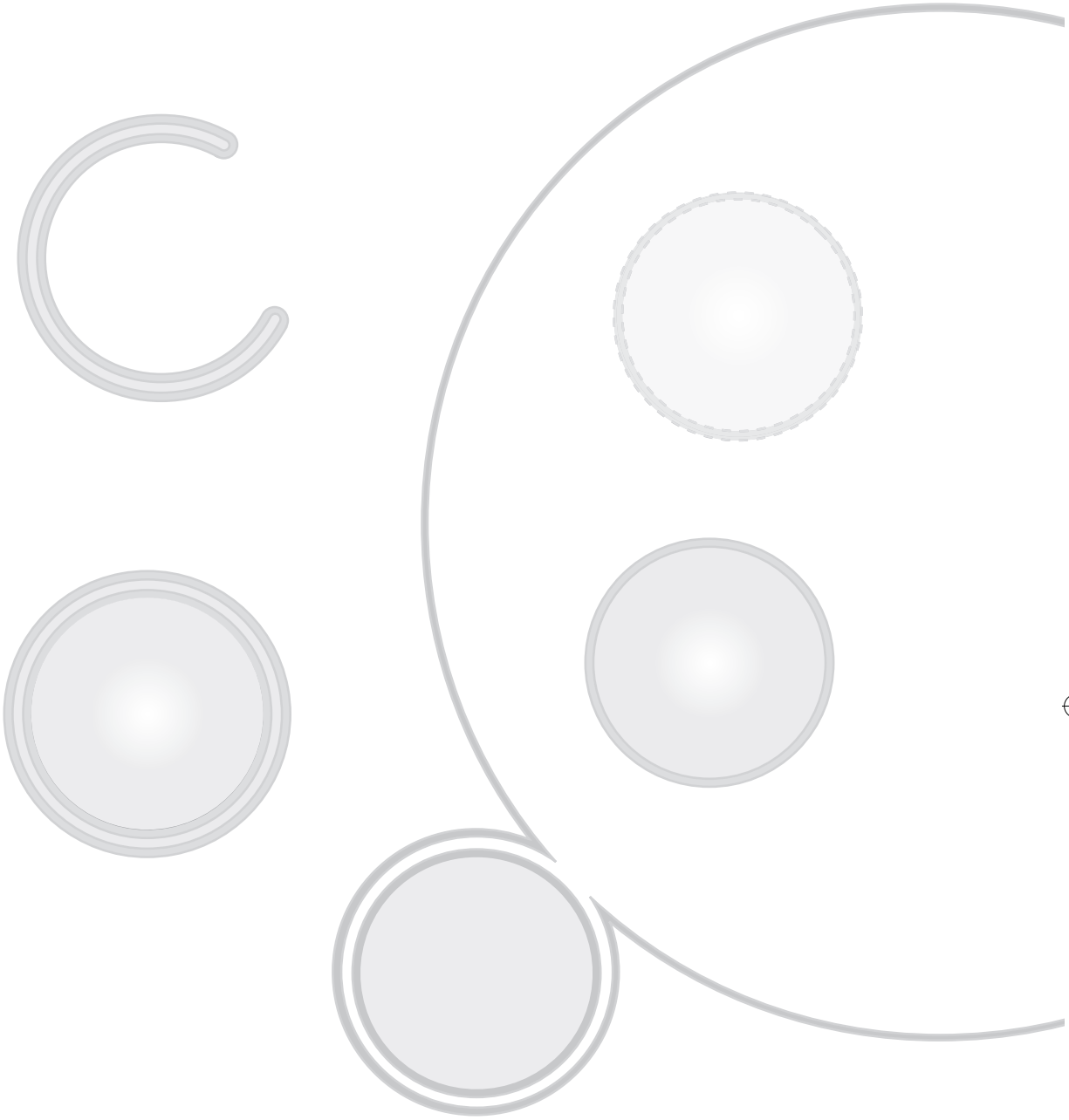

CHAPTER

2

Multiple roles of the Cytoskeleton in autophagy

Ester Rieter[1*], Iryna Monastyrska[1*], Daniel J. Klionsky[2], and Fulvio Reggiori[1]

[1]Department of Cell Biology and Institute of Biomembranes, University Medical Centre Utrecht, 3584 CX Utrecht, The Netherlands; [2]Life science Institute, and Departments of Molecular, Cellular and Developmental Biology and Biochemical Chemistry, University of Michigan, Ann Arbor, Michigan

[*]These authors contributed equally to this work

Biological reviews of the Cambridge Philosophical Society 2009 84:431-448

ABSTRACT

Autophagy is involved in a wide range of physiological processes including cellular remodeling during development, immuno-protection against heterologous invaders and elimination of aberrant or obsolete cellular structures. This conserved degradation pathway also plays a key role in maintaining intracellular nutritional homeostasis and during starvation, for example, it is involved in the recycling of unnecessary cellular components to compensate for the limitation of nutrients. Autophagy is characterized by specific membrane rearrangements that culminate with the formation of large cytosolic double-membrane vesicles called autophagosomes. Autophagosomes sequester cytoplasmic material that is destined for degradation. Once completed, these vesicles dock and fuse with endosomes and/or lysosomes to deliver their contents into the hydrolytically active lumen of the latter organelle where, together with their cargoes, they are broken down into their basic components. Specific structures destined for degradation via autophagy are in many cases selectively targeted and sequestered into autophagosomes.

A number of factors required for autophagy have been identified, but numerous questions about the molecular mechanism of this pathway remain unanswered. For instance, it is unclear how membranes are recruited and assembled into autophagosomes. In addition, once completed, these vesicles are transported to cellular locations where endosomes and lysosomes are concentrated. The mechanism employed for this directed movement is not well understood. The cellular cytoskeleton is a large, highly dynamic cellular scaffold that has a crucial role in multiple processes, several of which involve membrane rearrangements and vesicle-mediated events. Relatively little is known about the roles of the cytoskeleton network in autophagy. Nevertheless, some recent studies have revealed the importance of cytoskeletal elements such as actin microfilaments and microtubules in specific aspects of autophagy. In this review, we will highlight the results of this work and discuss their implications, providing possible working models. In particular, we will first describe the findings obtained with the yeast *Saccharomyces cerevisiae*, for long the leading organism for the study of autophagy, and, successively, those attained in mammalian cells, to emphasize possible differences between eukaryotic organisms.

Keywords: autophagy, autophagosome, Cvt pathway, actin, microtubules, cytoskeleton

CONTENTS

I. INTRODUCTION

Macroautophagy, here referred to simply as autophagy, is a degradative pathway mostly implicated in the recycling of portions of cytosol and in the removal of superfluous or damaged organelles. In addition to proteins, this transport route is uniquely able to catabolize other cellular constituents such as lipids, carbohydrates and nucleic acids. This process occurs at a basal level in most tissues and contributes to the routine turnover of cytoplasmic components. However, it can also be massively induced by a change in the environmental conditions or by cytokines and other signaling molecules to adapt and/or cope with various physiological and pathological situations (**Table 1**). As a result, autophagy is important for cellular remodeling and development, and is involved in preventing ageing and controlling cell growth (Levine & Klionsky, 2004).

Moreover, it plays a protective role in several human diseases such as cancer, neurodegeneration (Huntington's, Parkinson's and Alzheimer's diseases) and muscular disorders (Huang & Klionsky, 2007; Levine, 2007; Levine & Kroemer, 2008; Mizushima *et al*., 2008; Shintani & Klionsky, 2004*a*). Autophagy also defends cells from invasion by certain pathogenic bacteria such as *Mycobacterium tuberculosis*, group A *Streptococcus* and *Staphylococcus aureus*, viruses such as the herpes simplex virus and the tobacco mosaic virus, and intracellular parasites like *Toxoplasma gondii* (Amano, Nakagawa & Yoshimori, 2006; Gutierrez *et al*., 2004; Huang & Klionsky, 2007; Kirkegaard, Taylor & Jackson, 2004; Levine & Deretic, 2007; Levine & Kroemer, 2008; Nakagawa *et al*., 2004; Yap, Ling & Zhao, 2007). In opposition to these cytoprotective roles, autophagy can also be detrimental in specific circumstances. For example, some cancer cells use this pathway to recover from radiation therapy (Levine, 2007; Paglin *et al*., 2005) and various bacteria and viruses such as *Listeria monocytogenes*, *Shigella flexneri* and the poliovirus have evolved mechanisms to subvert autophagy for their own purposes (Birmingham, Higgins & Brumell, 2008; Mizushima *et al*., 2008; Ogawa *et al*., 2005; Taylor & Kirkegaard, 2008). Finally, autophagy may be the central player of type II programmed cell death and in some cases appears to be regulated in conjunction with apoptosis (Gorski et al., 2003; Maiuri *et al*., 2007).

Autophagy is conserved among all eukaryotes. Although this process was described at the morphological level in mammalian cells in the 1950s, researchers only recently have begun to gain insight into its molecular mechanism. The intracellular endomembrane system, including the endoplasmic reticulum (ER), Golgi complex, endosomes, lysosomes/vacuoles and plasma membrane, is maintained by dynamic membrane flow among various compartments. In general, these transport events involve vesicular budding from an existing donor organelle followed by fusion with an acceptor compartment. By contrast, autophagy employs unique membrane rearrangements distinct from any other intracellular processes (Reggiori, 2006). Nevertheless, similar to other intracellular trafficking events, autophagosome movement in mammalian cells employs microtubule-dependent machinery (Fass *et al*., 2006; Jahreiss, Menzies & Rubinsztein, 2008; Köchl *et al*., 2006).

A unique feature of autophagy that has lately emerged is that this pathway is able to specifically eliminate unwanted structures. This has led to sub-grouping autophagy into selective and nonselective types (Reggiori & Klionsky, 2005; van der Vaart, Mari & Reggiori, 2008). This process is defined as selective when a precise structure is specifically and exclusively eliminated, whereas it

is considered nonselective when multiple different components are eliminated through a mechanism that appears to be random. Interestingly, actin filaments have been implicated in selective types of autophagy in the yeast *S. cerevisiae*, but they are dispensable for the bulk process in the same organism (Hamasaki *et al.*, 2005; He *et al.*, 2006; Monastyrska *et al.*, 2006; Reggiori *et al.*, 2005*a*).

These recent observations have provided evidence for the relevance of the cytoskeleton to specific aspects of autophagy. Herein, we review the body of experimental work that has led to these findings and to the discovery of possible molecular connections between the machinery involved in autophagy and cytoskeletal elements.

Table 1. Some of the roles of autophagy in health and disease

Cellular process	Positive roles	Negative roles
Cell homeostasis	Viability and adaptation to stress conditions (starvation, high population density and elevated temperatures)	
Anti-aging	Turnover of damaged mitochondria and consequent decrease in the cellular damage caused by free radicals leads to life-span extension	
Development and cell differentiation	Mediates cellular architectural changes by controlling cell growth and type II programmed cell death	
Innate and adaptive immunity	Cellular defence against intracellular bacteria and viruses, and antigen cross-presentation	Subversion of the autophagy machinery to establish a replicative niche
Cancer	Tumour suppressor by controlling cell growth and type II programmed cell death	Permits tumours to survive nutrient-limiting and low-oxygen conditions; protects some cancer cells against ionizing radiation
Neurodegenerative disorders	Facilitates the removal of toxic neuropeptides and micro-aggregates	
Cardiomyopathy	Protects during ischemia and pressure overload	Harmful during reperfusion
Liver diseases	Allows removal of misfolded proteins accumulated in the Endoplasmic reticulum	Increased mortality due to excessive mitochondrial autophagy

II. THE MOLECULAR MECHANISM OF AUTOPHAGY

(1) Autophagosome biogenesis

Autophagy is induced when eukaryotic cells are starved or, for example, when mammalian cells bind glucagon or cytokines such as the interferon-γ (IFN-γ and

the tumor necrosis factor-α (TNFα) (Kondomerkos *et al*., 2005; Yap *et al*., 2007). The result is the simultaneous nucleation and expansion of cytoplasmic cisternae of unknown origin, termed phagophores or isolation membranes (Reggiori, 2006; Reggiori & Klionsky, 2005) (**Figure 1**). The expansion is probably mediated through the acquisition of lipid bilayers by fusion with vesicles, whereas the molecular basis of the nucleation is still almost completely mysterious (Reggiori, 2006; Reggiori & Klionsky, 2005). In yeast, autophagosome biogenesis occurs at the phagophore assembly site or pre-autophagosomal structure (PAS). This site probably includes all the autophagosomal intermediates that first lead to the formation of the phagophore and successively to that of the autophagosome. Therefore, the PAS may be the actual vesicle precursor but it cannot be excluded that it may just organize and donate membranes to the expanding vesicle. The growing phagophore ultimately closes to become a double-membrane autophagosome (**Figure 1**), which is different from the conventional, single-membrane transport vesicles that bud from a pre-existing organelle. In yeast, the mature autophagosome directly docks and fuses with the vacuole, allowing the release of its inner vesicle, the autophagic body, into the lumen of this organelle where it is degraded together with its cargo material (**Figure 1**). Finally, the components resulting from the degradation of the autophagic bodies and their contents, e.g. amino acids, lipids and sugars, are transported back into the cytosol for re-use. The nature of the sequestration process is another unique characteristic of autophagy: the sequestered material is removed from the cytosol to the equivalent of the extracellular space, the lysosome/vacuole lumen. By contrast with most vesicle transport pathways that specifically preserve the topology of the cargo, autophagy results in its degradation.

In mammalian cells, there is sometimes an additional maturation step before these events; complete autophagosomes may first fuse with endosome- and *trans*-Golgi-network (TGN)-derived vesicles but also endosomes, to become amphisomes (Reggiori, 2006). The process of degradation then begins in the amphisomes and is completed in the lysosomes. Another difference from yeast is that the smaller size of the lysosome relative to the vacuole prevents the release of the autophagic body into the lysosome lumen.

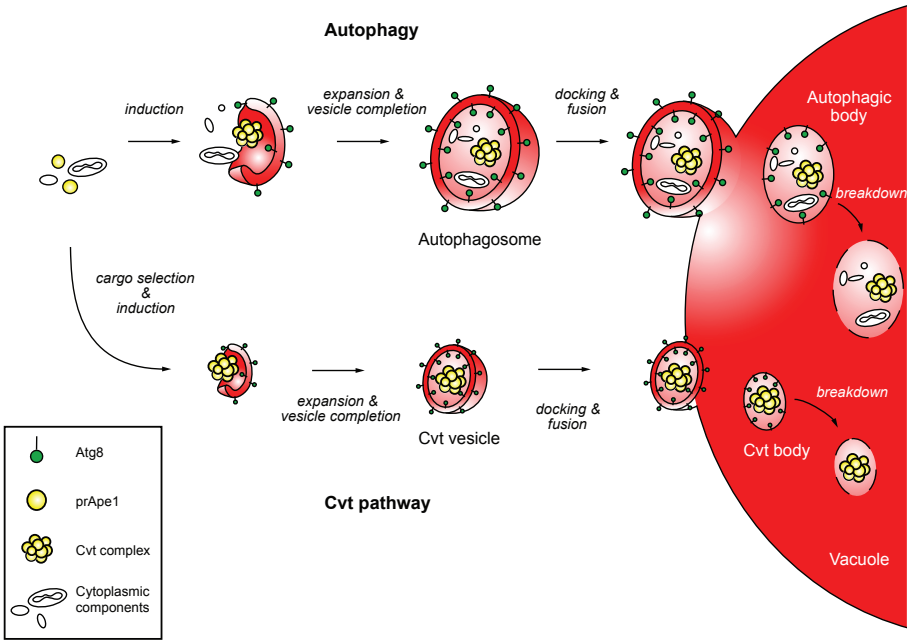

Figure 1. The cytoplasm to vacuole targeting (Cvt) pathway and autophagy in yeast. Autophagy is induced upon starvation, and cytosolic components are randomly sequestered into autophagosomes. By contrast, the Cvt pathway, a selective type of autophagy, operates under vegetative conditions and is involved in delivering prApe1 oligomers into the vacuole using small double-membrane vesicles called Cvt vesicle. During starvation, the prApe1 oligomers are also selectively incorporated into autophagosomes. The biogenesis and subsequent clearance of the double-membrane vesicles can be divided into at least five discrete steps: induction, expansion, vesicle completion, docking and fusion, and breakdown. After fusion with the vacuole, the inner membrane vesicles referred to as an autophagic body or Cvt body, are released into the vacuole lumen where, together with their contents, they are degraded or processed by resident hydrolases.

(2) Selective types of autophagy

Autophagy has long been considered a bulk process with cytoplasmic structures being randomly sequestered into autophagosomes. However, there is an increasing number of examples of selective types of autophagy where a specific cargo destined for destruction is exclusively incorporated into an autophagosome. (Reggiori & Klionsky, 2005; van der Vaart *et al*., 2008) (**Table 2**). For example, superfluous organelles such as peroxisomes or mitochondria can be specifically targeted for degradation, and the autophagic elimination of invasive bacteria appears to involve a selective mechanism. There may even be mechanisms for selecting particular cytosolic proteins during bulk autophagy

(Ohshiro *et al*., 2008; Onodera & Ohsumi, 2004). Although different cargos for selective types of autophagy have been described (**Table 2**), remains unknown how they are accurately recognized by autophagosomes (**Table 2**). One of the best-characterized examples is the cytoplasm to vacuole targeting (Cvt) pathway in yeast *S. cerevisiae* (**Figure 1**). The principal cargo of the Cvt pathway is the precursor form of the resident vacuolar hydrolase aminopeptidase I (prApe1). Following delivery via an autophagosome-like vesicle, prApe1 is processed in the vacuole lumen into the active enzyme Ape1. This transport process can be divided into several steps similar to those occurring during autophagosome biogenesis (**Figure 1**). After synthesis, prApe1 forms an oligomer in the cytosol, which then binds to the Atg19 receptor to form the Cvt complex. Subsequently, this complex associates with Atg11, and the latter protein mediates recruitment of the complex to the PAS. As a result, the Cvt complex is packed into double-membrane vesicles that are smaller than nonspecific autophagosomes and are termed Cvt vesicles. Cvt vesicles appear to exclude bulk cytoplasm, and instead are tightly apposed to the cargo. These vesicles then fuse with the vacuole and release prApe1 into the interior of this organelle where the zymogen is proteolytically processed into the mature active form of the enzyme (Yorimitsu & Klionsky, 2005*b*). The Cvt pathway seems to be present only in fungi and so far is the only reported example of a biosynthetic autophagy-related process. Nonetheless, the Cvt pathway shares most of the machinery utilized for bulk autophagy (see **Section II.3**), and morphologically and topologically these pathways also show great similarity (Shintani *et al*., 2002; Shintani & Klionsky, 2004*b*). Another well-described example of a selective type of autophagy is pexophagy, the selective degradation of peroxisomes (**Table 2**). This process occurs in many organisms, ranging from unicellular eukaryotes to mammals, but it has been studied in most detail in methylotrophic yeasts such as *Pichia pastoris* and *Hansenula polymorpha* (Farre & Subramani, 2004). In these yeasts, peroxisome biogenesis is induced when cells are grown in the presence of methanol as a sole carbon source. When the cells are shifted to media containing preferred carbon sources such as glucose, peroxisomes become superfluous and are rapidly degraded via pexophagy (Farre *et al*., 2008). Again, the machinery utilized by pexophagy overlaps to a great extent with that used for bulk autophagy (Dunn *et al*., 2005; Hutchins, Veenhuis & Klionsky, 1999).

Importantly, and in contrast to the bulk process, selective types of autophagy possess an extra step during the formation of the double-membrane vesicle that allows the high fidelity selection of the cargo that has to be eliminated

(Reggiori & Klionsky, 2005; van der Vaart *et al*., 2008). This allows the exclusion of bulk cytosol from the interior of the double-membrane vesicles. For example, the selective import of the prApe1 oligomer via the Cvt pathway requires Atg19, which serves as a receptor. The binding of Atg19 to prApe1 targets the Cvt complex to the PAS via its interaction with Atg11; the latter elicits the signal that triggers the PAS and Cvt vesicle formation (Shintani *et al*., 2002; Shintani & Klionsky, 2004*b*). Recent studies in *Pichia pastoris* have unveiled a similar mechanism for pexophagy where Atg30 plays an equivalent role to Atg19 and, together with Atg11, mediates the recognition and selection of peroxisomes for elimination (Farre *et al*., 2008). Another example of selective cargo recognition is in the disposal of cytoplasmic proteinacious aggregates by autophagosomes during aggrephagy. In several situations, this process involves p62, a protein that specifically interacts with ubiquitin and polyubiquitin chains attached to physiological and pathological aggregates and also to the pool of Atg8/microtubule-associated protein light chain 3 (LC3) present on the interior face of the forming autophagosome (Komatsu *et al*., 2007; Pankiv *et al*., 2007) (**Section II.3**). This dual binding capacity of p62 allows this protein to dictate specificity by effectively presenting ubiquitinated aggregates to double-membrane vesicles. Relatively little is known about the mechanism(s) involved in the recognition of invasive pathogens, but the overall process is presumably similar in nature, involving a surface epitope on the pathogen and one or more components of the autophagic machinery. For example, the VirG surface protein of *Shigella flexneri* appears to be recognized by Atg5 as a prelude to sequestration into autophagosomes (Ogawa *et al*., 2005).

Table 2. Different types of selective autophagy

Name	Cargo	Organism	Reference
Cvt pathway	prApe1 and prAms1	yeast	Shintani *et al.* (2002)
pexophagy	peroxisomes	yeast and mammals	Farre *et al.* (2008)
mitophagy	mitochondria	yeast and mammals	Kim *et al.* (2007)
reticulophagy	ER	yeast and mammals	Bernales *et al.* (2006); Klionsky *et al.* (2007)
ribophagy	ribosomes	yeast	Kraft *et al.* (2008)
xenophagy	bacteria and viruses	mammals and plants	Levine (2005)
aggrephagy	protein aggregates	yeast, *D. melanogaster*, *C. elegans* and mammals	Overbye *et al.* (2007)

Cvt, cytoplasm to vacuole targeting; ER, endoplasmic reticulum; prApe1, precursor aminopeptidase 1; prAms1, precursor α-mannosidase

(3) The *AUTOPHAGY* genes

Genetic screens in *S. cerevisiae* and other fungi have led to the identification of a number of molecular factors essential for autophagy. There are currently over 30 genes that are primarily involved in bulk and selective types of autophagy, and they have been named autophagy-related genes (*ATG*) (Klionsky *et al*., 2003). Fifteen of them compose the basic machinery required for the formation of double-membrane vesicles in all eukaryotes (Levine & Klionsky, 2004; Reggiori, 2006) (**Table 3**). The proteins they encode are recruited to the PAS in a temporal order and are involved in the formation and expansion of the PAS/phagophore (Cheong & Klionsky, 2008; Suzuki *et al*., 2007). However, their specific function and the exact relationships among them are largely unknown. Here we will only very briefly mention what is known about the role of these fifteen key Atg proteins in double-membrane vesicle formation because numerous reviews are already available (Geng & Klionsky, 2008; Reggiori, 2006; Suzuki & Ohsumi, 2007; van der Vaart *et al*., 2008; Xie & Klionsky, 2007; Yorimitsu & Klionsky, 2005*b*).

Some of the first Atg components to be found at the yeast PAS under autophagy-inducing conditions are the serine/threonine protein kinase Atg1 and its binding partners Atg13 and Atg17 (Cheong & Klionsky, 2008; Suzuki *et al*., 2007). The Atg1-Atg13-Atg17 complex interacts with several proteins that are required exclusively for selective or nonselective types of autophagy, and therefore it is proposed that this complex governs the switch between the different modes of autophagy (Cheong & Klionsky, 2008; Kamada *et al*., 2000; Reggiori *et al*., 2004). A similar complex apparently exists in mammalian cells (Hara *et al*., 2008). Atg9, the only transmembrane protein among the conserved basic machinery, is also one of the first factors localizing to the PAS (Suzuki *et al*., 2007). In contrast to the rest of the Atg proteins that transiently localize to the forming autophagosomes, Atg9 shuttles between the PAS and several peripheral sites, some of which are in close proximity to the mitochondria (Reggiori *et al*., 2005*b*). The Atg1-Atg13-Atg17 complex together with Atg18 and Atg2, are involved in the retrograde transport of Atg9 from the yeast PAS (Mari & Reggiori, 2007; Reggiori *et al*., 2004). In mammals, Atg9 also cycles, but in this case between the TGN and endosomes; nonetheless this trafficking is regulated by the Atg1 orthologue unc-51-like kinase 1 (ULK1) (Young *et al*., 2006). One of the functions of Atg9 appears to be the recruitment of the autophagy-specific phosphatidylinositol 3-kinase (AS-PI3K) complex to the PAS, which is composed of Atg14, Atg6, vacuolar protein sorting 15 (Vps15) and Vps34. The AS-PI3K complex generates the phosphatidylinositol 3-phosphate

(PtdIns-3-P) crucial for the recruitment of additional Atg proteins to the PAS (Suzuki *et al*., 2007). In yeast, PtdIns-3-P is also necessary for retrograde transport of Atg9 (Mari & Reggiori, 2007; Reggiori *et al*., 2004). Because of the trafficking characteristics of Atg9 and its association with lipid bilayers, it is proposed that, in addition to initiating double-membrane vesicle biogenesis, Atg9 participates in the delivery of lipids necessary for the extension of the phagophore (Reggiori *et al*., 2005*b*, 2004).

The two ubiquitin-like molecules Atg12 and Atg8 also seem to be involved in the recruitment of additional membranes to the PAS. Two highly conserved conjugation systems are important in this process (Geng & Klionsky, 2008; Ohsumi & Mizushima, 2004). In both yeast and mammals, Atg12 is covalently conjugated to Atg5 in a ubiquitin-like manner, which is mediated by the E1-like activating enzyme Atg7 and the E2-like conjugating enzyme Atg10. The newly formed Atg12–Atg5 conjugate then associates with Atg16 and this event appears crucial to trigger the expansion of the autophagosomal membrane and finally its fusion with the vacuole/lysosome (Mizushima *et al*., 2001). Activation of the Atg12 conjugation system triggers the Atg8 conjugation system that directs the association of Atg8 to the PAS, after being conjugated to phosphatidylethanolamine (PE); Atg12–Atg5-Atg16 may function as an E3 ubiquitin ligase, and Atg16 appears to target the site of Atg8–PE formation (Fujita *et al*., 2008; Hanada *et al*., 2007). After synthesis, the C-terminus of Atg8 is cleaved by Atg4, a cysteine protease, exposing a C-terminal glycine residue. This cleaved form is conjugated to PE, mediated by the E1-like activating enzyme Atg7, and the E2-like conjugating enzyme Atg3. After double-membrane vesicle completion, the majority of the Atg proteins is released back into the cytoplasm and can be reused for additional rounds of vesicle formation. This includes the dissociation of the Atg8 bound to the external side of autophagosomes through a second cleavage by the Atg8-processing enzyme Atg4, which cleaves the lipid anchor, and the retrieval of Atg9. This uncoating event seems to be a prerequisite for fusion between autophagosomes and lysosomes/vacuoles. Importantly, a pool of Atg8 remains attached to the inner membrane of the autophagosome and is delivered into the lumen of the lysosome/vacuole, which makes it a reliable autophagic protein marker (**Figure 1**). These two conjugation systems are highly conserved and are present in mammals (see **Section IV**).

Table 3. The 15 conserved autophagy-related gene (Atg) proteins involved in double-membrane vesicle formation (adapted from Reggiori, 2006)

Protein	Role	Interactions
Atg1	Serine/threonine protein kinase	Atg13, Atg11, Atg17
Atg2	Atg9 recycling	Atg9, Atg18
Atg3	Atg8 conjugation system (E2)	Atg7, Atg8, Atg12
Atg4	Cysteine protease	Atg8
Atg5	Atg12 conjugation system	Atg12, Atg16
Atg6	PtdIns-3-P synthesis	Atg14, Vps15, Vps34
Atg7	Atg8 and Atg12 conjugation systems (E1)	Atg3, Atg8, Atg10, Atg12
Atg8	Ubiquitin-like protein	Atg3, Atg4, Atg7, Atg19
Atg9	Transmembrane protein	Atg2, Atg18, Atg23, Atg27
Atg10	Atg12 conjugation system (E2)	Atg12
Atg12	Ubiquitin-like protein	Atg3, Atg5, Atg7, Atg10, Atg16
Atg13	Modulates Atg1 activity	Atg1, Atg17, Vac8
Atg14	PtsIns-3-P synthesis	Atg6, Vps15, Vps34
Atg16	Associates with the Atg12–Atg5 conjugate	Atg5, Atg12, Atg16
Atg18	PtdIns-3-P binding protein	Atg2, Atg9

PtdIns-3-P, phosphatidylinositol 3-phosphate; Vps, vacuolar protein sorting

III. THE CYTOSKELETON

The cytoskeleton is a network of elongated protein polymer fibres that support cell shape, compartmentalization and intracellular trafficking or even whole-cell movement. Microfilaments and microtubules are the two basic components that constitute the cytoskeletal system. Both are protein polymers that are constantly restructured in a tightly regulated manner in order to facilitate a dynamic spatial organization and rapid remodelling of the cytoskeleton (Pollard, 2003; Shih & Rothfield, 2006). Although there is a third distinct type of polymer fibres present in the cell known as intermediate filaments that are composed of many different cytoskeletal or nucleoskeletal proteins they are essentially static in structure and do not associate with molecular motors (Helfand, Chang & Goldman, 2004); in this review we focus mainly on microtubules and microfilaments.

(1) The microtubule network

Microtubules are a crucial cellular component because they are involved in cell division and differentiation, in the determination of cell shape, in chromosome segregation, in cytoplasm organization and in the positioning of organelles, and they are a structural element of flagella and cilia (Desai & Mitchison, 1997). Microtubules are tube-like structures composed of self-assembling αβ-tubulin heterodimers. To generate a microtubule, α- and β-tubulin monomers first heterodimerize and then assemble into protofilaments. Then, 12 to 15 of these linear protofilaments are joined to form a hollow cylinder structure with an approximate diameter of 25-30 nm (**Figure 2A**). Successive polymerization of additional heterodimers onto this initial template structure leads to the assembling of the microtubule (Nogales, 1999). Because of the arrangement of the tubulin dimers within the microtubule, α-tubulins are exposed at one end while β-tubulins are exposed at the other. This ordered rearrangement gives the microtubule a structural polarity. The terminus exposing α-tubulins is termed the minus end and is anchored near the centre of a cell, whereas the edge exposing β-tubulins is the plus end and extends towards the cell surface (**Figure 2**). Microtubule growth and disassembly occur at both ends. However, the plus end is the most dynamic extremity and therefore polymerizes and depolymerizes faster than the minus end.

Microtubules interconvert between periods of slow growth and fast shrinkage. In general though, a population of microtubules exhibits an overall bulk steady state, even if some of these structures are growing while others are shrinking. A single microtubule never reaches a steady-state length, but persists in prolonged states of polymerization and depolymerization that interconvert infrequently. This phenomenon is referred to as dynamic instability and allows microtubules to adopt spatial arrangements that can change rapidly in response to cellular cues. The principal factor governing the rate of microtubule growth is the concentration of free GTP- and GDP-bound tubulin dimers floating in the surroundings of the microtubule extremities. Because GTP-tubulin dimers are more favorably incorporated, the newly formed microtubules initially consist of GTP-tubulin. The incorporation of GTP-tubulin dimers at the end of microtubules stimulates the GTPase activity of β-tubulin to hydrolyze the GTP bound to β-tubulin into GDP (Weisenberg & Deery, 1976). The α-tubulin also binds GTP, but it is bound in a non-exchangeable manner and is not hydrolyzed during polymerization. The conversion of GTP into GDP leads to a microtubule lattice that is predominantly composed of GDP-bound tubulin dimers (**Figure 2A**). Importantly, the hydrolysis of GTP drives

the conformational change of 'straight' GTP-bound tubulin dimers into 'curved' GDP-bound tubulin dimers. Because the GDP-bound tubulins are prevented from adopting the fully curved conformation while in the lattice, the energy generated from GTP hydrolysis is stored in the lattice as a mechanical strain. This strain is released only when GDP-tubulin is exposed at the microtubule ends and provides the driving force for rapid depolymerization or shrinkage of this structure (Amos, 2004; Muller-Reichert *et al*., 1998) (**Figure 2A**).

Cells possess a large variety of proteins that can modulate microtubule dynamics and they can be sub-grouped into microtubule-associated proteins (MAPs), destabilizing factors and nucleating factors (Amos & Schlieper, 2005). MAPs are proteins that bind, stabilize and promote the assembly of microtubules. Most MAPs are negatively regulated by kinases. Phosphorylation reduces their affinity for the microtubule lattice inhibiting their ability to stabilize them. Microtubule destabilizing factors, by contrast, have an opposite function; they destabilize microtubules by simultaneously reducing their assembly rate and accelerating their turnover. The precise mechanism by which these factors accomplish these results poorly understood. Nucleating factors are a third class of proteins that play a role in microtubule dynamics. In most eukaryotic cells, microtubules primarily nucleate in close proximity to the centrosome, whereas in fungi they do this adjacent to the spindle poles. The centrosome consists of a pair of centrioles surrounded by a complex collection of proteins known as the pericentriolar material (PCM). In higher eukaryotes, γ-tubulin, a third type of tubulin, localizes to the PCM and is part of a ring-shaped structure containing several other proteins known as the γ-Tubulin Ring Complex (γ-TuRC) (Goldstein & Philp, 1999). This complex is a nucleating factor that serves as a template for the microtubule lattice and stimulates microtubule nucleation (Amos, 2004; Desai & Mitchison, 1997).

Microtubules form a complex, interconnected network, which often serves as tracks for intracellular movement powered by specific motor proteins that are part of either the kinesin or dynein protein families (Brown, 1999). Most utilize the energy generated by ATP hydrolysis to translocate in a stepwise manner along the surface of the microtubules. In general, kinesins move cargo towards the plus end of microtubules, whereas dyneins are involved in movement towards the minus end (Gross, Vershinin & Shubeita, 2007; Wang, Khan & Sheetz, 1995) (**Figure 2B**).

Kinesins moving along microtubules convey from the centre of the cell to its periphery a variety of cargos including vesicles, organelles and RNA. They

also play an important role in the movement of chromosomes during mitosis and meiosis. Next to their role in transport, some types of kinesins control microtubule polymerization and stability, whereas others are important for organizing the microtubular network by zippering, cross-linking and moving microtubules (Goldstein & Philp, 1999; Hunter & Wordeman, 2000). Most kinesins contain an N-terminal catalytic motor domain or head that directly interacts with the microtubule and hydrolyzes ATP, and a globular tail domain that provides the binding specificity for different cargoes, adaptor proteins and other motor proteins (**Figure 2B**). The tail domain sometimes is also non-covalently associated with so-called kinesin light chains. The head and the tail are connected by a coiled-coil stalk or neck domain important for movement and control of direction (**Figure 2B**). Kinesins often form dimeric units that are connected by the stalk region (**Figure 2B**). It remains poorly understood how kinesins recognize the correct cargo and how this is delivered to the correct destination (Brown, 1999; Goldstein & Philp, 1999; Vale, 2003).

Dyneins, are structurally unrelated to kinesins and belong to the class of AAA (ATPase associated with diverse cellular activities) proteins. They can be classified into two subfamilies: cytoplasmic and axonemal dyneins (Mallik & Gross, 2004). In addition to the transport of intracellular cargos, cytoplasmic dyneins display a diverse range of functions: they play a key role in the orientation of the cell spindle during mitosis, nuclear migration and neuronal transport (Gibbons, 1996; Wang *et al*., 1995). By contrast, axonemal dyneins are immobilized. They are not required to be progressive since they function as a large linear array of motors. In cilia and flagella, for example, adjacent microtubules slide over each other by the acting of opposite rows of axonemal dyneins positioned on their surface (Mallik & Gross, 2004). This movement generates the bending motion of cilia and flagella. Despite the difference in their cellular functions, cytoplasmic and axonemal dyneins have quite similar structures. They are multisubunit complexes composed of heavy, intermediate, light intermediate and light chains, and therefore are much larger than kinesins (Cross, 2004; Mallik & Gross, 2004). The dynein heavy chains possess motor domains that are much more complex than those of kinesins and consist of six or seven structurally related sub-domains, called the AAA domains, which are arranged in a ring (**Figure 2B**). Two lever arms protrude from this ring-shaped head. One is called the 'stem' and in addition to engaging the cargo, it provides most of the force for the movement, while the other arm interacts with the microtubule track through a long microtubule-binding stalk

(Gee, Heuser & Vallee, 1997) (**Figure 2B**). The dynein motor domain contains multiple ATP binding sites that hydrolyze this nucleotide to generate the energy necessary for movement. Like kinesins, dyneins form homodimers (**Figure 2B**) and multiple dynein homodimers can act together in the transport of a single cargo (McGrath, 2005).

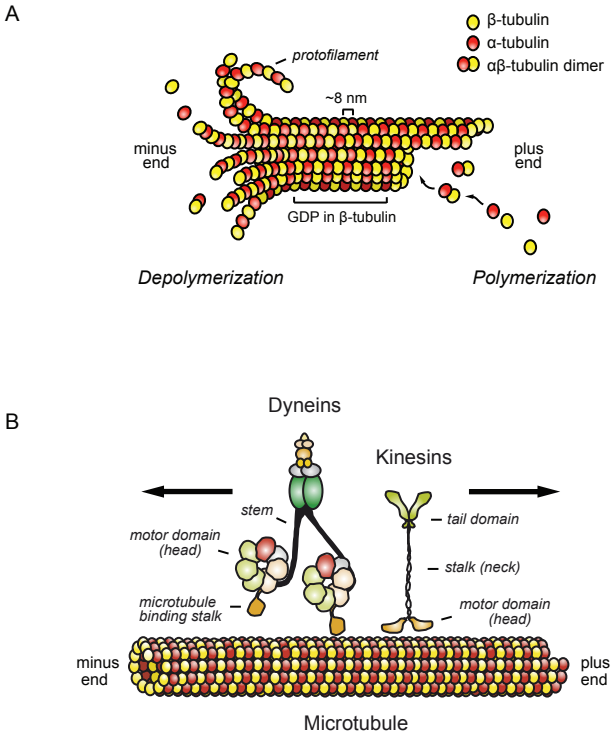

Figure 2. Structure of microtubules, kinesins and dyneins. (A) Microtubules are tube-like structures composed of α- and β-tubulin heterodimers that are assembled into long protofilaments, which are assembled together to form a microtubule. One extremity of the microtubule is termed the minus end, the other is the plus end. During polymerization or growth, GTP-tubulin dimers are incorporated preferentially at the plus end. Subsequently, the GTP bound to β-tubulin is hydrolyzed into GDP, leading to a microtubule lattice that is principally composed of GDP-tubulin dimers. When GDP-tubulin becomes exposed at one of the microtubule extremities, the mechanical strain stored in the lattice is released and this triggers rapid depolymerization. (B) Kinesins and dyneins mediate movement along microtubules and both often form homodimers. In general, kinesins move the cargo toward the plus end whereas dyneins transport the cargo in the opposite direction. Kinesin and dynein are structurally very different. Kinesins contain a motor and a tail domain linked by a stalk region. Cytoplasmic dyneins are multi-subunit complexes with a motor domain consisting of six or seven AAA (ATPase associated with diverse cellular activities) domains arranged in a ring. Two lever arms protrude from this ring-shaped head; the cargo-engaging stem and the microtubule-binding stalk (modified from Mallik & Gross, 2004).

(2) Actin filaments

Microfilaments, also known as actin filaments or filamentous actin (F-actin), are tube-like structures composed of long filamentous polymers. They consist of two coiled strands of chains of actin subunits also called globular actin (G-actin) (Winder & Ayscough, 2005) (**Figure 3A**). The diameter of actin filaments at approximately 5 nm is much smaller than that of microtubules. In addition, they are significantly shorter than microtubules and their orientation throughout the cell is more random. Like microtubules, actin filaments are polar structures with two different extremities termed the barbed end and the pointed end (Winder & Ayscough, 2005). In general, microfilaments form *de novo* either from the side or the severing end of an existing filament. Under appropriate conditions, however, actin filaments can self-assemble. This event starts with a nucleation process consisting of three actin monomers assembling into an initial core. Further elongation of this nucleus by the addition of a multitude of actin subunits gives rise to a new microfilament.

Although actin filaments do not exhibit dynamic instability like microtubules, they are assembled and disassembled in a highly dynamic manner as well and the regulation of their rearrangements is important for processes such as intracellular trafficking, contractility, cell locomotion and cell division (Winder & Ayscough, 2005). Microfilament assembly and disassembly involves the addition and loss of actin subunits at both ends. Actin monomers can either bind ATP or ADP, but the ATP-bound monomers are preferentially added to the growing end of actin filaments (**Figure 3A**). Incorporation into the microfilaments stimulates rapid hydrolysis of ATP, and the resulting ADP and phosphate (Pi) remain bound to the actin unit generating an ADP-Pi-actin intermediate form. In a second event, Pi is released resulting in long filaments primarily composed of ADP-actin with cap-regions composed of ATP- and ADP-Pi-actin (**Figure 3A**). The hydrolysis of ATP is not required for actin assembly but it is a pre-requisite for actin dissociation from filaments and consequently it is important for the disassembly of these structures. Not much is known about the mechanism of Pi dissociation except that it causes a conformational change in the actin subunits that causes destabilization of the filament (Belmont *et al*., 1999).

Polymerization mostly occurs at the barbed ends of the microfilaments, whereas disassembly principally takes place at the pointed ends (Winder & Ayscough, 2005) (**Figure 3A**). The assembly of actin filaments depends on a critical concentration of free ATP-actin. The level of this critical concentration at

the fast-growing barbed ends differs from that at the slow-growing pointed ends due to the difference in the ATP-actin and ADP-Pi-actin composition of the cap regions at these two extremities (Stukalin & Kolomeisky, 2006; Vavylonis, Yang & O'Shaughnessy, 2005) (**Figure 3A**). Control of filament growth is necessary for polymerization to occur at specific times and places.

A wide range of actin binding and remodelling proteins including nucleation factors, monomer binding proteins, capping proteins, and stabilizing and destabilizing factors, govern the balance between assembly and disassembly that determines the filament growth rate (Cooper & Schafer, 2000; Winder & Ayscough, 2005). Nucleation factors such as formins and the actin-related protein 2/3 (Arp2/3) complex are crucial to initiate the formation of new filaments, which is otherwise energetically unfavorable. The Arp2/3 complex consists of seven subunits: Arp2, Arp3, Arc15/p15, Arc18/p18/p21, Arc19/p19, Arc35/p35 and Arc40/p40, which are all highly conserved among eukaryotes (Mahaffy & Pollard, 2006; Mullins & Pollard, 1999). This complex has multiple roles in the regulation of the actin cytoskeleton. It branches existing actin filaments by binding to their side and thus initiating the outgrowth of new filaments. In addition, it interacts with the barbed ends of microfilaments to initiate branching at this location and it is involved in the cross-linking of actin filaments. As mentioned above, the concentration of free actin monomers is crucial for filaments assembly. Certain monomer-binding proteins inhibit polymerization by sequestering away free actin subunits, whereas others stimulate the same process by facilitating the exchange of ADP for ATP. Capping proteins can modulate the assembly and disassembly of microfilaments as well. These factors, such as gelsolin, that bind to the barbed ends can stop filament growth by blocking the addition of new monomers, whereas those associating with the pointed ends reduce the loss of subunits and consequently control the rapid extension of filaments. Actin depolymerizing factors such as cofilin, actophorin, depactin and destrin mediate depolymerization in two ways. First, they can create more ends that disassemble by severing the microfilaments. Second, they can increase the rate of subunit loss from the filament termini by inducing the dissociation of the capping proteins present at pointed ends (Maciver & Hussey, 2002). Finally, actin stabilizing proteins carry out their function by binding along the side of actin filaments and protect them against spontaneous depolymerization and severing (Winder & Ayscough, 2005). In addition to all these regulatory factors, there are actin-bundling and cross-linking proteins that participate in the organization of the actin network

but also proteins that are involved in interconnections between actin filaments and either membranes, membrane proteins or other cytoskeletal elements.

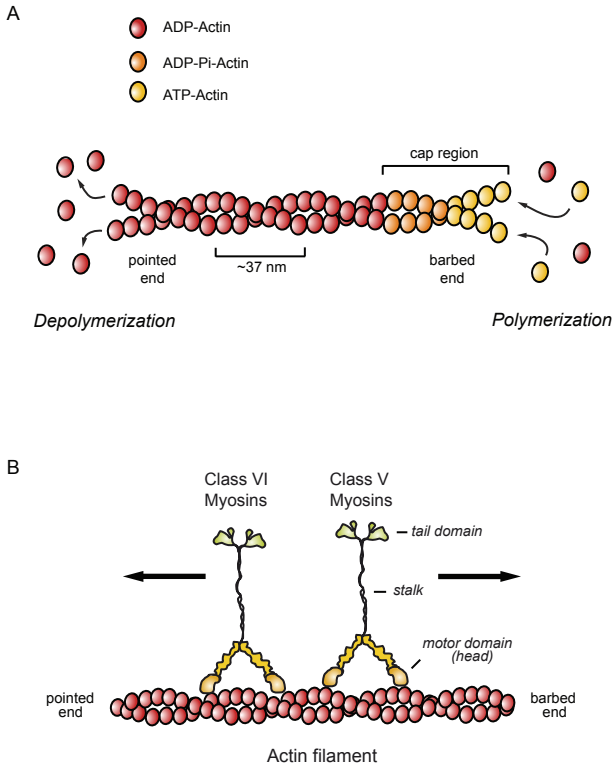

Figure 3. The structure of actin filaments and myosins. (A) Actin filaments or microfilaments are composed of two coiled chains of actin monomers; one end is called the barbed or plus end, and the other is the pointed or minus end. Microfilament polymerization or growth mostly takes place at the barbed end by the addition of ATP- actin subunits. Hydrolysis of ATP bound to these monomers and the subsequent release of phosphate (Pi), results in actin filaments primarily composed of ADP-actin with a cap-region enriched in ATP-actin and ADP-Pi-actin. Disassembly or depolymerization of actin filaments primarily occurs at the pointed ends and releases ADP-actin subunits. (B) Motor proteins of the myosin superfamily mediate movement along microfilaments. Class V and VI myosins are the most well-studied members of this protein superfamily; they form homodimers and play a central role in vesicular transport. Class V myosins move towards the barbed end whereas class VI myosins traffic in the opposite direction. Myosins possess a motor domain important for displacement along microfilaments and a tail domain involved in cargo recognition. These two domains are connected by a coiled-coil stalk region (modified from Mallik & Gross, 2004).

Microfilaments can serve as tracks for directed intracellular movement of various cargos and also entire organelles (Winder & Ayscough, 2005). Motor proteins of the myosin superfamily travel along microfilaments (**Figure 3B**). All the members of this superfamily share a similar motor domain and a tail

portion involved in cargo binding, which are connected to each other by a coiled-coil stalk region (**Figure 3B**). Myosins are sub-grouped into approximately 15 classes based on the amino acid sequence of their motor domains. This domain is considerably larger than that of kinesins and it can contain one or more ATP-binding sites. Myosins are structurally related to kinesins and similarly, they also often form homodimers (Brown, 1999; Krendel & Mooseker, 2005) (**Figure 3B**). Class V and VI myosins are among the most well-characterized classes and they have been shown to play a central role in vesicular transport along actin filaments. Class V myosins are responsible for movement towards the plus or barbed ends whereas class VI myosins transport cargos in the opposite direction (Brown, 1999; De La Cruz *et al*., 1999; Wells *et al*., 1999). Besides cargo transport, myosins can also have other cellular functions. For example, class II myosins and actin are the key components responsible for the contraction of muscles. Class I myosins, on the other hand, participate in motility functions such as endocytosis, polarized morphogenesis and cell migration. The class I myosin Myo5 for instance, facilitates the pinching of endocytic vesicles off the plasma membrane (Evangelista *et al*., 2000; Girao, Geli & Idrissi, 2008).

IV. THE ROLE OF MICROTUBULES IN AUTOPHAGY

(1) Microtubules are unnecessary for yeast autophagy

The first possible connection between autophagy and microtubules emerged with the discovery that one of the genes specifically involved in autophagy and isolated through genetic screens in yeast, *ATG8*, is homologous to the mammalian microtubule-associated protein 1 light chain 3, MAP1-LC3 or simply LC3 (28% identity to rat MAP1-LC3) (Lang *et al*., 1998; Reggiori & Klionsky, 2002). MAP1-LC3 belongs to the protein family of MAPs and interacts with MAP1A or 1B to form a complex that binds and modulates the shape of microtubules (Mann & Hammarback, 1994; Pedrotti *et al*., 1996). It has now been shown that identically to yeast Atg8 (see **Section II.3**), LC3 is immediately cleaved after synthesis by an Atg4 cysteine protease. This cleaved cytosolic LC3-I form is then conjugated to PE to form LC3-PE through the actions of E1- and E2-like enzymes. The lipidated form of LC3, called LC3-II, is tightly associated with the autophagosomal membrane and is involved in the expansion of the phagophore. Therefore, LC3 functions as an Atg8 orthologue. In humans, in addition to three LC3 isoforms

(LC3A, LC3B, and LC3C), four additional Atg8 homologues have been identified: GABARAP, GEC1/GABARAPL1, GATE16/GABARAPL2, and GABARAPL3. It is unclear if these GABARAP proteins have a completely redundant function with the LC3 isoforms or a peculiar role in autophagy, but at least the lipidated forms of GABARAP and GATE16, co-localize with autophagosomes (Kabeya *et al*., 2000, 2004; Tanida, Ueno & Kominami, 2004).

The first published work about *ATG8* showed that this gene is essential for autophagy because in its absence, cells are unable to accumulate autophagic bodies in the vacuole when starved in the presence of protease inhibitors (Lang *et al*., 1998). Instead the same mutant amassed structures in the cytosol that were proposed to be autophagosome-like. Together with impaired maturation of prApe1, this observation suggested that the *atg8*Δ deletant is unable to deliver autophagosomes and prApe1 to the vacuole (Lang *et al*., 1998). Based on these results and the fact that Atg8 interacts *in vitro* and by yeast two-hybrid assay with the tubulins Tub1 and Tub2 via Atg4, Lang *et al*. (1998) proposed that Atg8 and Atg4 form a complex that binds to microtubules. Moreover, they also hypothesized that this complex could function in the attachment of autophagosomes to microtubules mediating their targeting to the vacuole.

Successive reports have challenged the initial idea about the molecular function of Atg8 (Huang *et al*., 2000; Kirisako *et al*., 1999). In particular, *atg8*Δ strains are severely impaired in autophagy but they do not accumulate complete autophagosomes in the cytoplasm (Kirisako *et al*., 1999). Instead, these cells are blocked in autophagosome formation. This finding is in agreement with a recent report showing that Atg8 is required for autophagosome formation because it is involved in membrane tethering and hemifusion (Nakatogawa, Ichimura & Ohsumi, 2007) and/or in phagophore expansion (Xie, Nair & Klionsky, 2008). Crucially, Kirisako *et al*. (1999) also revealed that treatment of cells with nocodazole, a chemical that disrupts microtubules, does not affect autophagy, demonstrating that microtubules are not required for bulk autophagy in yeast. This result is also supported by evidence that autophagy proceeds normally in the *tub*2Δ mutant (Kirisako *et al*., 1999). The reason for this difference between the results described in the early report and the more recent ones is unclear but it cannot be excluded *a priori* that Atg8 could also have functions connected with microtubules that are distinct from its role in autophagy (Cali *et al*., 2008; Sagiv *et al*., 2000).

(2) Microtubule-dependent movement of autophagosomes in mammalian cells

More than a decade ago, pioneering studies indicated that in rat hepatocytes and kidney epithelial cells, disruption of the microtubule network using agents such as nocodazole and vinblastine that interfere with microtubule polymerization, blocks fusion of autophagosomes with late endosomes and lysosomes but not the biogenesis of these double-membrane vesicles (Aplin *et al*., 1992; Seglen *et al*., 1996). However, a number of more recent investigations have shown that in mammalian cells, the disruption of the microtubule network provokes a delay in autophagy rather than a complete block in this process (Fass *et al*., 2006; Jahreiss *et al*., 2008; Köchl *et al*., 2006).

Data from two of these recent publications have made it evident that in addition to a role in fusion, microtubules also regulate and facilitate autophagosome formation (Fass *et al*., 2006; Köchl *et al*., 2006). In one of these studies, primary rat hepatocytes expressing green fluorescent protein (GFP)-LC3 were pre-treated with nocodazole and vinblastine before inducing autophagy by nitrogen starvation (Köchl *et al*., 2006). The rate and magnitude of autophagosome biogenesis was quantified by measuring the lipidation of GFP-LC3 but also by the translocation of this fluorescent chimera into punctate structures representing autophagosomes. The results indicated that the formation of autophagosomes is facilitated by microtubules, but does not require them. Moreover, analysis of LC3-II turnover and of the overlap of GFP-LC3-positive vesicles with LysoTracker Red-positive late endosomes/lysosomes confirmed that intact microtubules contribute to the fusion of autophagosomes with late endosomes/lysosomes (Köchl *et al*., 2006).

Fass et al. (2006) proposed that once completed, autophagosomes are linked to and transported along microtubules. They established a Chinese hamster ovary (CHO) cell line stably expressing GFP-LC3, and newly formed autophagosomes labeled with this fluorescent probe were imaged in living cells in the presence or absence of nocodazole. GFP-LC3-positive autophagosomes were concentrated at the minus ends of microtubules in a microtubule-dependent manner under all growth conditions. In addition, time-lapse video microscopy revealed that only mature autophagosomes but not phagophores associate with microtubules and move along these tracks (Fass *et al*., 2006). These authors also investigated the dynamics of autophagosome formation and degradation in the same cells in the absence of intact microtubules. In contrast to the data published by Köchl *et al*. (2006), they showed that this component of the cytoskeleton is not

essential for the targeting and fusion of autophagosomes with late endosomes/lysosomes. The discrepancy in these results could be due to the different cell lines used in the two studies. Nevertheless, Fass et al. (2006) also found that microtubules facilitate autophagosome biogenesis because the formation of these large vesicles occurs to a significantly lower extent in the absence of intact microtubules.

A further study on the same issue concluded that microtubule dissolution simply delays the arrival of autophagosomes in the proximity of late endosomes and lysosomes preventing their efficient fusion with these organelles (Jahreiss *et al*., 2008). Using fluorescence microscopy and live-cell imaging they found that in mammalian normal rat kidney (NRK) cells, the majority of late endosomes/lysosomes are concentrated at the perinuclear region around the microtubule-organizing centre (MTOC), while the autophagosomes are formed randomly at the periphery of the cell (Jahreiss *et al*., 2008). Obviously, to be able to fuse with late endosomes/lysosomes, autophagosomes must be transported into their proximity. Jahreiss *et al*. (2006) determined that newly formed autophagosomes move bidirectionally along microtubules in live NRK cells but they finally concentrate in a similar way as late endosomes/lysosomes. The MTOC-directed movement of autophagosomes depends on microtubules; the disruption of the latter using nocodazole abolishes this centripetal conveyance (Jahreiss *et al*., 2008). Similar results obtained using time-lapse microscopy, showed that autophagosomes are formed throughout the cytoplasm in cervical cancer HeLa cells and move to the cell centre in a microtubule-dependent manner (Kimura, Noda & Yoshimori, 2008).

Despite the different hypotheses about the exact role(s) of microtubules in autophagy, all the published studies agree that microtubules facilitate autophagosome trafficking. An obvious question, however, is how are microtubules connected to autophagosomes? An interesting hint comes from another study that revealed that autophagosomes are moved by dyneins along microtubule tracks *en route* to the lysosomes located near the MTOC (Ravikumar *et al*., 2005). Interestingly, the functional loss of dynein has been linked to certain neurodegenerative disorders. *In vitro* studies have demonstrated that the loss of dynein leads to an impairment of the clearance of aggregate-prone proteins by autophagy and to increased levels of LC3-II, reflecting a defect in the fusion between autophagosomes and lysosomes (Ravikumar *et al*., 2005). These data perfectly complement a previous investigation showing that although microtubule

disruption by nocodazole inhibits aggregate formation, this treatment leads to an overall increase in aggregate formation due to an impairment of autophagosome-late endosome/lysosome fusion (Webb, Ravikumar & Rubinsztein, 2004).

These data have recently also been confirmed using live-cell imaging analyses that revealed that dynein is required for autophagosome trafficking along microtubules and this centripetal movement discontinues once the autophagosome reaches the microtubule-organizing centre (Jahreiss *et al*., 2008). In particular, treatment of GFP-LC3-expressing NRK cells with the dynein ATPase adenosine deaminase inhibitor or with RNAi targeting the same molecule, caused an impairment of the trafficking of GFP-LC3-positive vesicles and decreased the fusion of these structures with late endosomes/lysosomes (Jahreiss *et al*., 2008). The latter phenomenon is almost certainly a consequence of the role of dynein on the centripetal movement of autophagosomes as this event is probably the rate-limiting factor for the eventual fusion with perinuclearly located lysosomes (Jahreiss *et al*., 2008). Kimura *et al*. (2008) analyzed the involvement of dynein in autophagosome trafficking using a different approach. HeLa cells stably expressing GFP-LC3 were microinjected with anti-dynein intermediate chain antibodies, which are known to impair dynein activity, before monitoring autophagosome trafficking using time-lapse microscopy. The rapid movements of GFP-LC3-positive autophagosomes were almost completely blocked (Kimura *et al*., 2008).

How dynein interacts with autophagosomes is still unknown. One attractive possibility is that this protein directly or indirectly binds to LC3 (**Figure 4A**). This hypothesis is supported by the observation that the trafficking of autophagosomes was abolished when HeLa cells were microinjected with antibodies against the LC3 N-terminus (Kimura *et al*., 2008). In addition to an indirect interaction with microtubules via dynein (**Figure 4A**), LC3 could bind to these structures in other ways, tightening the association of autophagosomes to them and resulting in facilitated movement. LC3 could directly associate with microtubules through its N-terminal domain or indirectly via MAP1A and MAP1B (Kouno *et al*., 2005; Mann & Hammarback, 1994) (**Figure 4B**). All these scenarios are not mutually exclusive. As suggested by Kimura *et al*. (2008), for example, the N-terminus of LC3 could play a dual role by both recruiting dynein to the autophagosomes and by acting as an adaptor protein between microtubules and these double-membrane vesicles (**Figure 4B**).

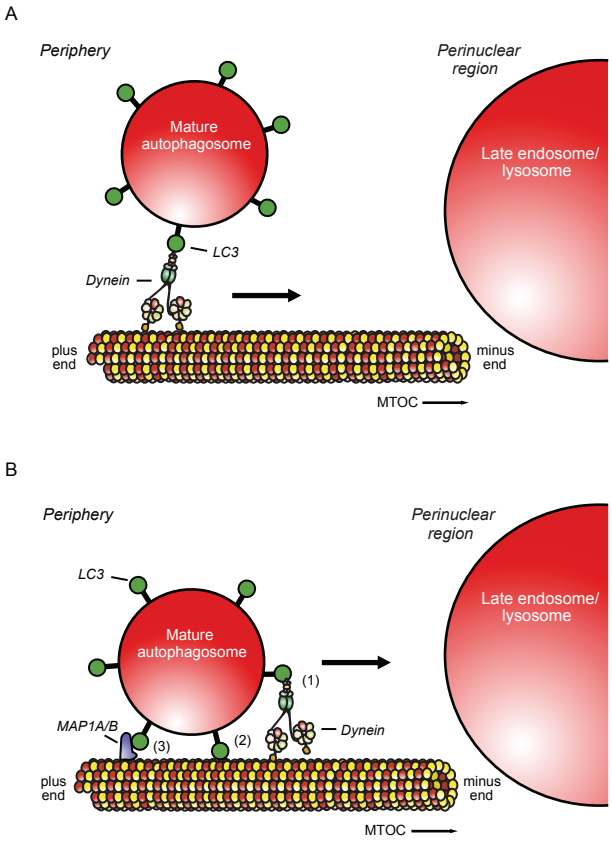

Figure 4. Models for dynein–mediated trafficking of mammalian autophagosomes along microtubules. Microtubules and dynein play a crucial role in the centripetal movement of autophagosomes from peripheral locations in the cell to the microtubule-organizing centre (MTOC) where lysosomes are concentrated. (A) Microtubule-associated protein 1 light chain 3 (LC3) could provide the direct or indirect structural link that anchors autophagosomes to dynein, which then will carry these large vesicles along the microtubule tracks. (B) LC3 could bind directly to microtubules. Therefore, in addition to its function in binding dynein (1), the protein could also play a role as a direct (2) or indirect (3) adaptor between microtubules and autophagosomes, and, by increasing the affinity between these two structures, it could facilitate autophagosome trafficking. MAP, microtubule-associated protein.

V. THE ACTIN CYTOSKELETON AND AUTOPHAGY

(1) Actin is required for cargo selection during selective types of autophagy in yeast

Two different studies have revealed that actin filaments are not necessary for bulk autophagy in yeast. In particular, treatment of cells with latrunculin A (LatA), a

chemical that blocks actin polymerization, does not affect the autophagy-mediated delivery into the vacuole of either the cytosolic protein marker Pho8Δ60 nor GFP-Atg8 (Hamasaki *et al*., 2005; Reggiori *et al*., 2005*a*). Analysis of the same process in *act1* mutants (*ACT1* is the gene that encodes for actin) has led to the same conclusion (Reggiori *et al*., 2005*a*).

By contrast, accumulating evidence suggests that microfilaments are essential for selective types of autophagy in this unicellular eukaryote (Hamasaki *et al*., 2005; He *et al*., 2006; Monastyrska *et al*., 2006; Reggiori *et al*., 2005*a*). A substantial amount of progress has been made by studying the molecular mechanisms of the Cvt pathway (Yorimitsu & Klionsky, 2005*a*). As discussed previously (**Section II**, **Figure 1**), by this transport route oligomers formed by prApe1 are delivered into the vacuole by Cvt vesicles. In addition to Atg19 and Atg11, actin filaments appear to be a crucial component of the machinery that guarantees that the prApe1 oligomers are specifically recognized and selectively packed into Cvt vesicles. Analyses of prApe1 processing by pulse-chase radiolabeling experiments in yeast cells grown in the presence of LatA or in mutant strains such as *act1-159* carrying specific point mutations in *ACT1*, showed a severe impairment in the Cvt pathway (Reggiori *et al*., 2005*a*). This defect is caused by an inability to recruit the Cvt complex to the PAS in the absence of actin cables as revealed by either co-localization studies between cyan fluorescent protein (CFP)-Ape1 and yellow fluorescent protein (YFP)-Atg8 in LatA-treated cells, or protease-protection assays in the *act1-159* mutant (Reggiori *et al*., 2005*a*). Importantly, this block is identical to that observed in the *atg11*Δ knockout (Kim *et al*., 2001*b*). In the absence of Atg11, most of the Atg proteins fail to be recruited to the PAS, suggesting that this factor plays a crucial role in the organization of this specialized site under vegetative conditions (Shintani & Klionsky, 2004*a*). Atg8 is also not recruited to the PAS in the *act1-159* strain emphasizing further that microfilaments and Atg11 mediate the same step of the Cvt pathway (Reggiori *et al*., 2005*a*).

Atg11 is a coiled-coil domain protein that interacts with several other Atg proteins, including Atg1, Atg9 and Atg19. Thus, it appears that Atg11 acts in part as a scaffold that dictates the recruitment of Atg proteins at the PAS, possibly coordinating the cargo with the vesicle-forming machinery (He *et al*., 2006; Kim *et al*., 2001*b*; Shintani *et al*., 2002; Yorimitsu & Klionsky, 2005*a*). As noted in **Section II**, Atg9 is an integral membrane protein required for autophagy. Atg9 binds to Atg11 independently from Atg19 (He *et al*., 2006). Atg9 has a quite distinctive

intracellular distribution; unlike most Atg proteins that, when associated with membranes, localize primarily at the PAS, this protein localizes to this site plus several other cytoplasmic punctate structures. Atg9 shuttles between these peripheral sites and the PAS (Reggiori *et al*., 2005*b*) (**Section II**). Interestingly, Atg9 delivery to the PAS is blocked in the absence of Atg11 as well as in the presence of LatA or the *act1-159* mutation (Reggiori *et al*., 2005*a*) indicating that transport of Atg9 and the Cvt complex to the PAS is coordinated.

An interesting question is how Atg11 and actin filaments interact at a molecular level in order to mediate this coordinated movement. What is known is that in the *act1-159* mutant Atg11 is no longer detected on the PAS, underlying a possible connection between the movement of this protein and actin filaments (He *et al*., 2006). An intriguing speculation arising from a structural comparison between Atg11 and Myo2, one of the two yeast myosin V proteins, highlighted that the third coiled-coil domain of Atg11 displays some similarity with that of Myo2 (Monastyrska *et al*., 2006). It is still unknown, however, if Atg11 can bind actin filaments. This protein does not possess a motor domain and consequently it cannot move the Cvt complex along the actin cable by itself. One possibility could be that it associates with myosins or an unknown protein that possesses a similar motor activity. An alternative hypothesis emerged from a recent study in which it was shown that the Arp2/3 complex also plays an essential role in the Cvt pathway (Monastyrska *et al*., 2008). Strains carrying temperature-sensitive mutations in genes encoding for Arp2/3 complex subunits display a strong defect in prApe1 transport (Monastyrska *et al*., 2008). This study also revealed that Atg9 transport to the PAS is defective in the *arp2-1* mutant and that Arp2 briefly co-localizes with Atg9 at the peripheral sites. Importantly, using the yeast two-hybrid-based assay and co-immunoprecipitation experiments, they demonstrated that Atg9 interacts with the Arp2/3 complex via Atg11. This result provides a possible molecular link between actin filaments, Atg11, Atg9 and the Cvt complex, but also suggests potential models for the microfilament-dependent movement of these factors.

One attractive hypothesis could be that binding of the Arp2/3 complex to the Cvt complex and/or Atg9-containing structures induces actin nucleation leading to the synthesis of new actin filaments (**Figure 5A**). The adjacent growth of these actin filaments could provide the force required for the directional transport of the Cvt complex and Atg9 to the PAS. This model has already been proposed for the Arp2/3 complex- and actin-dependent motility of yeast

mitochondria or certain intracellular pathogens (Boldogh *et al*., 2001; Gouin, Welch & Cossart, 2005). In this model, in addition to assembling all the different travelling partners, Atg11 could play a role in their stable association with actin cables (**Figure 5A**). It cannot be excluded, however, that the Arp2/3 complex has a different function in the Cvt pathway. Its presence at the peripheral sites could initiate the formation of Atg9-containing carriers from an unknown membrane source by inducing actin polymerization, before Atg11 takes over and transports the Atg9 carriers together with the Cvt complex to the PAS along the actin cables (**Figure 5B**). A similar function has been assigned to actin and to the Arp2/3 complex during membrane invagination occurring at the plasma membrane, which is required for the formation of endocytic vesicles (Kaksonen, Sun & Drubin, 2003). In this model, another unknown factor would then be required to act as a motor to push the Cvt complex and Atg9 toward the PAS. It is also possible that aspects of the two models coexist (**Figure 5**) and the Arp2/3 complex mediates both the biogenesis of the Atg9 carriers and transport along microfilaments.

Importantly, actin filaments also seem to play a crucial role in other selective types of autophagy in yeast, in particular during the specific removal of superfluous organelles such as peroxisomes and ER. When yeast cells are grown in conditions that require peroxisome functions, these organelles proliferate. Once peroxisomes become unnecessary, they are selectively eliminated via a process called pexophagy (Hutchins *et al*., 1999) (**Section II** and **Table 2**). In analogy to the Cvt pathway, when pexophagy is induced, peroxisomes presumably have to be specifically recruited to the PAS in order to be efficiently and selectively enwrapped by the emerging double-membrane vesicles. Importantly, after disruption of actin with LatA or in the actin point mutant *act1-159*, peroxisome degradation is blocked, possibly due to an inability to target it specifically to the PAS. It is important to note that both Atg11 and the Arp2/3 complex are also essential for pexophagy (Kim, Huang & Klionsky, 2001*a*; Monastyrska *et al*., 2008).

Interestingly and in contrast to delivery of prApe1 to the vacuole, the selective uptake of peroxisomes required intact actin filaments even in starvation conditions when autophagy is active (Reggiori *et al*., 2005*a*). This observation could indicate that if specific structures are preferentially degraded during bulk autophagy, their selective elimination would also need the presence of actin cables. This hypothesis is sustained by an investigation that has shown that the uptake of ER fragments into autophagosomes during starvation is microfilament-dependent (Hamasaki *et al*., 2005). When autophagy is induced in yeast cells by

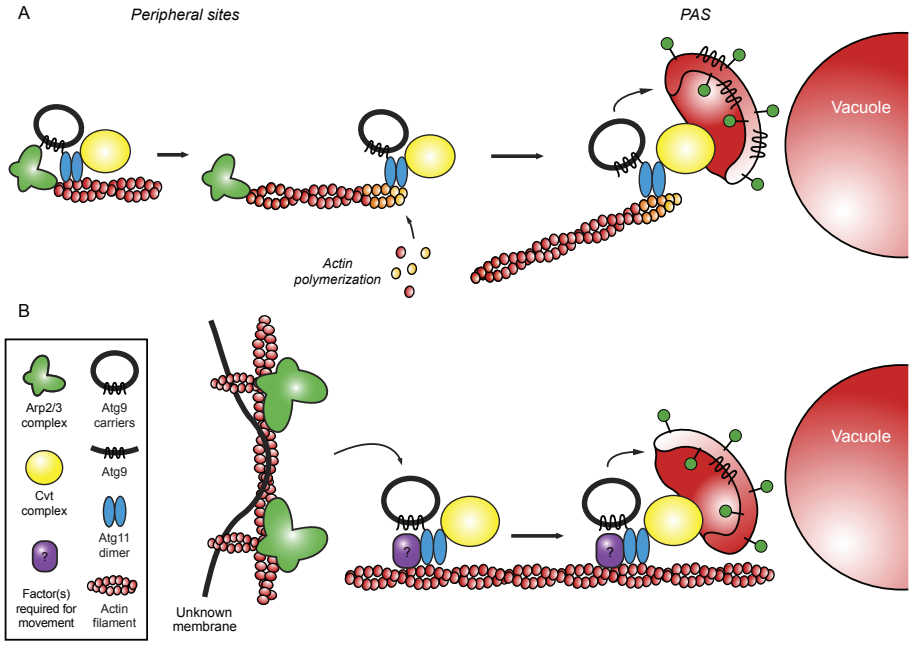

Figure 5. Models for the role of actin filaments and the actin-related protein 2/3 (Arp2/3) complex in the cytoplasm to vacuole (Cvt) pathway. (A) Atg11 recruits and brings together the Cvt complex, Atg9 carriers and the Arp2/3 complex at a peripheral site in the cells. This event activates the Arp2/3 complex, which in turn induces actin nucleation. The polymerization of several actin cables and the consequent formation of new adjacent microfilaments drive the movement of Atg9 and the Cvt complex to the phagophore assembly site (PAS). In this model, Atg11 could also be involved in binding to the actin cable. (B) The Arp2/3 complex and actin filaments are essential for the formation of Atg9-containing carriers from a yet unknown membrane source. Next, Atg11 together with some unknown factor(s) takes over and transports these Atg9-containing structures and the Cvt complex to the PAS along the actin microfilaments. The models illustrated in A and B could co-exist in which case, the Arp2/3 complex would mediate the biogenesis of Atg9 carriers and their delivery plus that of the Cvt complex to the PAS.

rapamycin or upon starvation, part of the ER fragments and the resulting mini-cisternae are transported together with other cytoplasmic components into the vacuole lumen by autophagosomes. When autophagy is triggered in cells pre-treated with LatA, however, delivery of ER fragments into the vacuole is perturbed, whereas that of the autophagosomal protein marker GFP-Atg8 is not. Consequently, this result confirms that bulk autophagy is not blocked upon disruption of the actin cytoskeleton but ER fragments escape engulfment by autophagosomes. An attractive hypothesis then is that disruption of the actin network interferes directly with the recognition and/or the sequestration of ER

fragments by autophagosomes. Although the morphology of the ER network was almost the same in LatA-treated cells as in untreated cells, a possibility that cannot be excluded yet is that LatA affects the proper dynamics of this organelle and thus alters the fragmentation of this compartment essential for its incorporation into double-membrane vesicles (Hamasaki *et al*., 2005; Prinz *et al*., 2000).

(2) The role of the actin cytoskeleton in mammalian cells

Very little is known about the relationship between the actin cytoskeleton and autophagy in higher eukaryotes. In contrast to the findings that have shown that actin cables are dispensable for bulk autophagy in yeast (Reggiori *et al*., 2005*a*), an electron microscopy study performed almost 20 years ago in rat kidney epithelial cells has shown that microfilament depolymerizing agents such as cytochalasins B and D block the formation of autophagosomes (Aplin *et al*., 1992). Their data, however, have to be carefully interpreted. Rat kidney cells were incubated for 5 h in the presence of cytochalasins which provoked dramatic morphological changes as well as other effects. Therefore, it cannot be excluded that the detected block in autophagy is caused indirectly by the impairment of one or more other pathways.

VI. CONCLUSIONS

(1) The involvement of microtubules in the formation and fusion of autophagosomes with late endosomes/lysosomes in mammals has been under considerable debate. Microtubules appeared to be required for the fusion of autophagosomes with late endosomes/lysosomes, but not for the biogenesis of these double-membrane vesicles. However, some recent studies suggest that these cytoskeletal structures also play a role in autophagosome biogenesis while another report showed that microtubules are not essential for targeting and fusion events in CHO cells. Such discrepancies could be due to the use of different cell lines; autophagy could proceed at least partially in a tissue-specific way or perhaps microtubule-dependent biogenesis and trafficking of autophagosomes is more critical in some cell types. Another explanation for the reported differences could be variation in experimental conditions.

(2) Despite the different hypotheses about the exact role of microtubules in autophagy, it is clear that they facilitate autophagosome trafficking. Autophagosomes are formed at the periphery of the cell and move along

microtubule tracks toward the lysosomes concentrated near the MTOC. Dynein is involved in this movement, and although the precise mechanism is not known, LC3 could form a link between these two structures; this protein is also important for the trafficking of autophagosomes (**Fig. 4A**). In addition, LC3 could increase the affinity of autophagosomes for microtubules via its ability to bind directly or indirectly to them (**Fig. 4B**).

(3) In contrast to mammalian cells, in yeast microtubules appear to be unnecessary for both the formation of autophagosomes and their fusion with the vacuole. The yeast PAS is adjacent to the vacuole and therefore, once complete, an autophagosome does not need to travel far to reach and fuse with this large hydrolytic compartment. A difference in the function or properties of Atg8 and LC3 could also underlie this distinction between eukaryotes. Even though Atg8 shows 28% homology to the mammalian MAP1-LC3A, Atg8 does not interact directly with tubulin, whereas LC3 can bind directly to microtubules. Therefore, LC3 may have additional functions in mammalian autophagy that are absent for Atg8 in yeast. Surprisingly, the role of microtubules in selective types of yeast autophagy has not been investigated.

(4) Studies in yeast have revealed that microfilaments are not required for bulk autophagy but are essential for selective types of autophagy such as the Cvt pathway, pexophagy and possibly reticulophagy. Actin filaments and the Arp2/3 complex together with Atg11 are crucial for the coordinated movement of the Cvt complex and Atg9-containing membranes to the PAS, an event essential to trigger autophagosome biogenesis. It is largely unknown how these three factors interact at a molecular level, but it is possible that Atg11 binds both the Cvt complex and Atg9, and also the Arp2/3 complex, which in turn is able to associate with microfilaments. How this putative complex move toward the PAS is a complete mystery due to the apparent lack of involvement of a motor protein.

(5) Little is known about the relationship between the actin cytoskeleton and autophagy in mammalian cells. Actin filaments have been considered essential for the initial formation of autophagosomes in starved cells. However, more recent works reported no association of GFP-LC3-labeled autophagosomes with actin filaments. To date, there are no published studies investigating the role of actin filaments or microtubules in selective types of autophagy in mammals, due to the fact that simple assays to measure quantitatively selective types of autophagy in mammalian cells do not exist.

VII. ACKNOWLEDGEMENTS

The authors thank René Scriwanek for the generation of the figures. F.R. is supported by the Netherlands Organization for Health Research and Development (ZonMW-VIDI-917.76.329) and the Utrecht University (High Potential grant). D.J.K. is supported by the NIH grant GM53396.

VIII. REFERENCES

1. Amano, A., Nakagawa, I. & Yoshimori, T. (2006). Autophagy in innate immunity against intracellular bacteria. *J Biochem* 140, 161-6.
2. Amos, L. A. (2004). Microtubule structure and its stabilisation. *Org Biomol Chem* 2, 2153-60.
3. Amos, L. A. & Schlieper, D. (2005). Microtubules and maps. *Adv Protein Chem* 71, 257-98.
4. Aplin, A., Jasionowski, T., Tuttle, D. L., Lenk, S. E. & Dunn, W. A., Jr. (1992). Cytoskeletal elements are required for the formation and maturation of autophagic vacuoles. *J Cell Physiol* 152, 458-66.
5. Belmont, L. D., Orlova, A., Drubin, D. G. & Egelman, E. H. (1999). A change in actin conformation associated with filament instability after Pi release. *Proc Natl Acad Sci USA* 96, 29-34.
6. Bernales, S., McDonald, K. L. & Walter, P. (2006). Autophagy counterbalances endoplasmic reticulum expansion during the unfolded protein response. *PLoS Biol* 4, e423.
7. Birmingham, C. L., Higgins, D. E. & Brumell, J. H. (2008). Avoiding death by autophagy: interactions of *Listeria monocytogenes* with the macrophage autophagy system. *Autophagy* 4, 368-71.
8. Boldogh, I. R., Yang, H. C., Nowakowski, W. D., Karmon, S. L., Hays, L. G., Yates, J. R., 3rd & Pon, L. A. (2001). Arp2/3 complex and actin dynamics are required for actin-based mitochondrial motility in yeast. *Proc Natl Acad Sci USA* 98, 3162-7.
9. Brown, S. S. (1999). Cooperation between microtubule- and actin-based motor proteins. *Annu Rev Cell Dev Biol* 15, 63-80.
10. Cali, T., Galli, C., Olivari, S. & Molinari, M. (2008). Segregation and rapid turnover of EDEM1 by an autophagy-like mechanism modulates standard ERAD and folding activities. *Biochem Biophys Res Commun* 371, 405-10.
11. Cheong, H. & Klionsky, D. J. (2008). Dual role of Atg1 in regulation of autophagy-specific PAS assembly in *Saccharomyces cerevisiae*. *Autophagy* 4, 724-6.
12. Cooper, J. A. & Schafer, D. A. (2000). Control of actin assembly and disassembly at filament ends. *Curr Opin Cell Biol* 12, 97-103.
13. Cross, R. A. (2004). Molecular motors: Dynein's gearbox. *Curr Biol* 14, R355-6.
14. De La Cruz, E. M., Wells, A. L., Rosenfeld, S. S., Ostap, E. M. & Sweeney, H. L. (1999). The kinetic mechanism of myosin V. *Proc Natl Acad Sci USA* 96, 13726-31.
15. Desai, A. & Mitchison, T. J. (1997). Microtubule polymerization dynamics. *Annu Rev Cell Dev Biol* 13, 83-117.
16. Dunn, W. A., Jr., Cregg, J. M., Kiel, J. A., van der Klei, I. J., Oku, M., Sakai, Y., Sibirny, A. A., Stasyk, O. V. & Veenhuis, M. (2005). Pexophagy: the selective autophagy of peroxisomes. *Autophagy* 1, 75-83.
17. Evangelista, M., Klebl, B. M., Tong, A. H., Webb, B. A., Leeuw, T., Leberer, E., Whiteway, M., Thomas, D. Y. & Boone, C. (2000). A role for myosin-I in actin assembly through interactions with Vrp1p, Bee1p, and the Arp2/3 complex. *J Cell Biol* 148, 353-62.
18. Farre, J. C., Manjithaya, R., Mathewson, R. D. & Subramani, S. (2008). PpAtg30 tags peroxisomes for turnover by selective autophagy. *Dev Cell* 14, 365-76.
19. Farre, J. C. & Subramani, S. (2004). Peroxisome turnover by micropexophagy: an autophagy-related process. *Trends Cell Biol* 14, 515-23.
20. Fass, E., Shvets, E., Degani, I., Hirschberg, K. & Elazar, Z. (2006). Microtubules support production of starvation-induced autophagosomes but not their targeting and fusion with lysosomes. *J Biol Chem* 281, 36303-16.

21. Fujita, N., Itoh, T., Omori, H., Fukuda, M., Noda, T. & Yoshimori, T. (2008). The Atg16L complex specifies the site of LC3 lipidation for membrane biogenesis in autophagy. *Mol Biol Cell* 19, 2092-2100.
22. Gee, M. A., Heuser, J. E. & Vallee, R. B. (1997). An extended microtubule-binding structure within the dynein motor domain. *Nature* 390, 636-9.
23. Geng, J. & Klionsky, D. J. (2008). The Atg8 and Atg12 ubiquitin-like conjugation systems in macroautophagy. *EMBO Rep* 9, 859-64.
24. Gibbons, I. R. (1996). The role of dynein in microtubule-based motility. *Cell Struct Funct* 21, 331-42.
25. Girao, H., Geli, M. I. & Idrissi, F. Z. (2008). Actin in the endocytic pathway: from yeast to mammals. *FEBS Lett* 582, 2112-9.
26. Goldstein, L. S. & Philp, A. V. (1999). The road less traveled: emerging principles of kinesin motor utilization. *Annu Rev Cell Dev Biol* 15, 141-83.
27. Gorski, S. M., Chittaranjan, S., Pleasance, E. D., Freeman, J. D., Anderson, C. L., Varhol, R. J., Coughlin, S. M., Zuyderduyn, S. D., Jones, S. J. & Marra, M. A. (2003). A SAGE approach to discovery of genes involved in autophagic cell death. *Curr Biol* 13, 358-63.
28. Gouin, E., Welch, M. D., Cossart, P. (2005). Actin-based motility of intracellular pathogens. *Curr Opin Microbiol* 8, 35-45.
29. Gross, S. P., Vershinin, M. & Shubeita, G. T. (2007). Cargo transport: two motors are sometimes better than one. *Curr Biol* 17, R478-86.
30. Gutierrez, M. G., Master, S. S., Singh, S. B., Taylor, G. A., Colombo, M. I. & Deretic, V. (2004). Autophagy is a defense mechanism inhibiting BCG and *Mycobacterium tuberculosis* survival in infected macrophages. *Cell* 119, 753-66.
31. Hamasaki, M., Noda, T., Baba, M. & Ohsumi, Y. (2005). Starvation triggers the delivery of the endoplasmic reticulum to the vacuole via autophagy in yeast. *Traffic* 6, 56-65.
32. Hanada, T., Noda, N. N., Satomi, Y., Ichimura, Y., Fujioka, Y., Takao, T., Inagaki, F. & Ohsumi, Y. (2007). The Atg12-Atg5 conjugate has a novel E3-like activity for protein lipidation in autophagy. *J Biol Chem* 282, 37298-302.
33. Hara, T., Takamura, A., Kishi, C., Iemura, S., Natsume, T., Guan, J. L. & Mizushima, N. (2008). FIP200, a ULK-interacting protein, is required for autophagosome formation in mammalian cells. *J Cell Biol* 181, 497-510.
34. He, C., Song, H., Yorimitsu, T., Monastyrska, I., Yen, W. L., Legakis, J. E. & Klionsky, D. J. (2006). Recruitment of Atg9 to the preautophagosomal structure by Atg11 is essential for selective autophagy in budding yeast. *J Cell Biol* 175, 925-35.
35. Helfand, B. T., Chang, L. & Goldman, R. D. (2004). Intermediate filaments are dynamic and motile elements of cellular architecture. *J Cell Sci* 117, 133-41.
36. Huang, J. & Klionsky, D. J. (2007). Autophagy and human disease. *Cell Cycle* 6, 1837-49.
37. Huang, W. P., Scott, S. V., Kim, J. & Klionsky, D. J. (2000). The itinerary of a vesicle component, Aut7p/Cvt5p, terminates in the yeast vacuole via the autophagy/Cvt pathways. *J Biol Chem* 275, 5845-51.
38. Hunter, A. W. & Wordeman, L. (2000). How motor proteins influence microtubule polymerization dynamics. *J Cell Sci* 113, 4379-89.
39. Hutchins, M. U., Veenhuis, M. & Klionsky, D. J. (1999). Peroxisome degradation in *Saccharomyces cerevisiae* is dependent on machinery of macroautophagy and the Cvt pathway. *J Cell Sci* 112, 4079-87.
40. Jahreiss, L., Menzies, F. M. & Rubinsztein, D. C. (2008). The itinerary of autophagosomes: from peripheral formation to kiss-and-run fusion with lysosomes. *Traffic* 9, 574-87.

41. Kabeya, Y., Mizushima, N., Ueno, T., Yamamoto, A., Kirisako, T., Noda, T., Kominami, E., Ohsumi, Y. & Yoshimori, T. (2000). LC3, a mammalian homologue of yeast Apg8p, is localized in autophagosome membranes after processing. *EMBO J* 19, 5720-8.

42. Kabeya, Y., Mizushima, N., Yamamoto, A., Oshitani-Okamoto, S., Ohsumi, Y. & Yoshimori, T. (2004). LC3, GABARAP and GATE16 localize to autophagosomal membrane depending on form-II formation. *J Cell Sci* 117, 2805-12.

43. Kaksonen, M., Sun, Y. & Drubin, D. G. (2003). A pathway for association of receptors, adaptors, and actin during endocytic internalization. *Cell* 115, 475-87.

44. Kamada, Y., Funakoshi, T., Shintani, T., Nagano, K., Ohsumi, M. & Ohsumi, Y. (2000). Tor-mediated induction of autophagy via an Apg1 protein kinase complex. *J Cell Biol* 150, 1507-13.

45. Kim, I., Rodriguez-Enriquez, S. & Lemasters, J. J. (2007). Selective degradation of mitochondria by mitophagy. *Arch Biochem Biophys* 462, 245-53.

46. Kim, J., Huang, W. P. & Klionsky, D. J. (2001a). Membrane recruitment of Aut7p in the autophagy and cytoplasm to vacuole targeting pathways requires Aut1p, Aut2p, and the autophagy conjugation complex. *J Cell Biol* 152, 51-64.

47. Kim, J., Kamada, Y., Stromhaug, P. E., Guan, J., Hefner-Gravink, A., Baba, M., Scott, S. V., Ohsumi, Y., Dunn, W. A., Jr. & Klionsky, D. J. (2001b). Cvt9/Gsa9 functions in sequestering selective cytosolic cargo destined for the vacuole. *J Cell Biol* 153, 381-96.

48. Kimura, S., Noda, T. & Yoshimori, T. (2008). Dynein-dependent movement of autophagosomes mediates efficient encounters with lysosomes. *Cell Struct Funct* 33, 109-22.

49. Kirisako, T., Baba, M., Ishihara, N., Miyazawa, K., Ohsumi, M., Yoshimori, T., Noda, T. & Ohsumi, Y. (1999). Formation process of autophagosome is traced with Apg8/Aut7p in yeast. *J Cell Biol* 147, 435-46.

50. Kirkegaard, K., Taylor, M. P. & Jackson, W. T. (2004). Cellular autophagy: surrender, avoidance and subversion by microorganisms. *Nat Rev Microbiol* 2, 301-14.

51. Klionsky, D. J., Cregg, J. M., Dunn, W. A., Jr., Emr, S. D., Sakai, Y., Sandoval, I. V., Sibirny, A., Subramani, S., Thumm, M., Veenhuis, M. & Ohsumi, Y. (2003). A unified nomenclature for yeast autophagy-related genes. *Dev Cell* 5, 539-45.

52. Klionsky, D. J., Cuervo, A. M., Dunn, W. A., Jr., Levine, B., van der Klei, I. & Seglen, P. O. (2007). How shall I eat thee? *Autophagy* 3, 413-6.

53. Köchl, R., Hu, X. W., Chan, E. Y. & Tooze, S. A. (2006). Microtubules facilitate autophagosome formation and fusion of autophagosomes with endosomes. *Traffic* 7, 129-45.

54. Komatsu, M., Waguri, S., Koike, M., Sou, Y. S., Ueno, T., Hara, T., Mizushima, N., Iwata, J., Ezaki, J., Murata, S., Hamazaki, J., Nishito, Y., Iemura, S., Natsume, T., Yanagawa, T., Uwayama, J., Warabi, E., Yoshida, H., Ishii, T., Kobayashi, A., Yamamoto, M., Yue, Z., Uchiyama, Y., Kominami, E. & Tanaka, K. (2007). Homeostatic levels of p62 control cytoplasmic inclusion body formation in autophagy-deficient mice. *Cell* 131, 1149-63.

55. Kondomerkos, D. J., Kalamidas, S. A., Kotoulas, O. B. & Hann, A. C. (2005). Glycogen autophagy in the liver and heart of newborn rats. The effects of glucagon, adrenalin or rapamycin. *Histol Histopathol* 20, 689-96.

56. Kouno, T., Mizuguchi, M., Tanida, I., Ueno, T., Kanematsu, T., Mori, Y., Shinoda, H., Hirata, M., Kominami, E. & Kawano, K. (2005). Solution structure of microtubule-associated protein light chain 3 and identification of its functional subdomains. *J Biol Chem* 280, 24610-7.

57. Kraft, C., Deplazes, A., Sohrmann, M. & Peter, M. (2008). Mature ribosomes are selectively degraded upon starvation by an autophagy pathway requiring the Ubp3p/Bre5p ubiquitin protease. *Nat Cell Biol* 10, 602-10.

58. Krendel, M. & Mooseker, M. S. (2005). Myosins: tails (and heads) of functional diversity. *Physiology* 20, 239-51.

59. Lang, T., Schaeffeler, E., Bernreuther, D., Bredschneider, M., Wolf, D. H. & Thumm, M. (1998). Aut2p and Aut7p, two novel microtubule-associated proteins are essential for delivery of autophagic vesicles to the vacuole. *EMBO J* 17, 3597-607.
60. Levine, B. (2005). Eating oneself and uninvited guests: autophagy-related pathways in cellular defense. *Cell* 120, 159-62.
61. Levine, B. (2007). Cell biology: autophagy and cancer. *Nature* 446, 745-7.
62. Levine, B. & Deretic, V. (2007). Unveiling the roles of autophagy in innate and adaptive immunity. *Nat Rev Immunol* 7, 767-77.
63. Levine, B. & Klionsky, D. J. (2004). Development by self-digestion: molecular mechanisms and biological functions of autophagy. *Dev Cell* 6, 463-77.
64. Levine, B. & Kroemer, G. (2008). Autophagy in the pathogenesis of disease. *Cell* 132, 27-42.
65. Maciver, S. K. & Hussey, P. J. (2002). The ADF/cofilin family: actin-remodeling proteins. *Genome Biol* 3, reviews3007.
66. Mahaffy, R. E. & Pollard, T. D. (2006). Kinetics of the formation and dissociation of actin filament branches mediated by Arp2/3 complex. *Biophys J* 91, 3519-28.
67. Maiuri, M. C., Zalckvar, E., Kimchi, A. & Kroemer, G. (2007). Self-eating and self-killing: crosstalk between autophagy and apoptosis. *Nat Rev Mol Cell Biol* 8, 741-52.
68. Mallik, R. & Gross, S. P. (2004). Molecular motors: strategies to get along. *Curr Biol* 14, R971-82.
69. Mann, S. S. & Hammarback, J. A. (1994). Molecular characterization of light chain 3. A microtubule binding subunit of MAP1A and MAP1B. *J Biol Chem* 269, 11492-7.
70. Mari, M. & Reggiori, F. (2007). Atg9 trafficking in the yeast *Saccharomyces cerevisiae*. *Autophagy* 3, 145-8.
71. McGrath, J. L. (2005). Dynein motility: four heads are better than two. *Curr Biol* 15, R970-2.
72. Mizushima, N., Levine, B., Cuervo, A. M. & Klionsky, D. J. (2008). Autophagy fights disease through cellular self-digestion. *Nature* 451, 1069-75.
73. Mizushima, N., Yamamoto, A., Hatano, M., Kobayashi, Y., Kabeya, Y., Suzuki, K., Tokuhisa, T., Ohsumi, Y. & Yoshimori, T. (2001). Dissection of autophagosome formation using Apg5-deficient mouse embryonic stem cells. *J Cell Biol* 152, 657-68.
74. Monastyrska, I., He, C., Geng, J., Hoppe, A. D., Li, Z. & Klionsky, D. J. (2008). Arp2 links autophagic machinery with the actin cytoskeleton. *Mol Biol Cell* 19, 1962-75.
75. Monastyrska, I., Shintani, T., Klionsky, D. J. & Reggiori, F. (2006). Atg11 directs autophagosome cargoes to the PAS along actin cables. *Autophagy* 2, 119-21.
76. Muller-Reichert, T., Chretien, D., Severin, F. & Hyman, A. A. (1998). Structural changes at microtubule ends accompanying GTP hydrolysis: information from a slowly hydrolyzable analogue of GTP, guanylyl (α,β) methylenediphosphonate. *Proc Natl Acad Sci USA* 95, 3661-6.
77. Mullins, R. D. & Pollard, T. D. (1999). Structure and function of the Arp2/3 complex. *Curr Opin Struct Biol* 9, 244-9.
78. Nakagawa, I., Amano, A., Mizushima, N., Yamamoto, A., Yamaguchi, H., Kamimoto, T., Nara, A., Funao, J., Nakata, M., Tsuda, K., Hamada, S. & Yoshimori, T. (2004). Autophagy defends cells against invading group A *Streptococcus*. *Science* 306, 1037-40.
79. Nakatogawa, H., Ichimura, Y. & Ohsumi, Y. (2007). Atg8, a ubiquitin-like protein required for autophagosome formation, mediates membrane tethering and hemifusion. *Cell* 130, 165-78.
80. Nogales, E. (1999). A structural view of microtubule dynamics. *Cell Mol Life Sci* 56, 133-42.
81. Ogawa, M., Yoshimori, T., Suzuki, T., Sagara, H., Mizushima, N. & Sasakawa, C. (2005). Escape of intracellular *Shigella* from autophagy. *Science* 307, 727-31.

82. Ohshiro, K., Rayala, S. K., El-Naggar, A. K. & Kumar, R. (2008). Delivery of cytoplasmic proteins to autophagosomes. *Autophagy* 4, 104-6.

83. Ohsumi, Y. & Mizushima, N. (2004). Two ubiquitin-like conjugation systems essential for autophagy. *Semin Cell Dev Biol* 15, 231-6.

84. Onodera, J. & Ohsumi, Y. (2004). Ald6p is a preferred target for autophagy in yeast, Saccharomyces cerevisiae. *J Biol Chem* 279, 16071-6.

85. Overbye, A., Fengsrud, M. & Seglen, P. O. (2007). Proteomic analysis of membrane-associated proteins from rat liver autophagosomes. *Autophagy* 3, 300-22.

86. Paglin, S., Lee, N. Y., Nakar, C., Fitzgerald, M., Plotkin, J., Deuel, B., Hackett, N., McMahill, M., Sphicas, E., Lampen, N. & Yahalom, J. (2005). Rapamycin-sensitive pathway regulates mitochondrial membrane potential, autophagy, and survival in irradiated MCF-7 cells. *Cancer Res* 65, 11061-70.

87. Pankiv, S., Clausen, T. H., Lamark, T., Brech, A., Bruun, J. A., Outzen, H., Overvatn, A., Bjorkoy, G. & Johansen, T. (2007). p62/SQSTM1 binds directly to Atg8/LC3 to facilitate degradation of ubiquitinated protein aggregates by autophagy. *J Biol Chem* 282, 24131-45.

88. Pedrotti, B., Ulloa, L., Avila, J. & Islam, K. (1996). Characterization of microtubule-associated protein MAP1B: phosphorylation state, light chains, and binding to microtubules. *Biochemistry* 35, 3016-23.

89. Pollard, T. D. (2003). The cytoskeleton, cellular motility and the reductionist agenda. *Nature* 422, 741-5.

90. Prinz, W. A., Grzyb, L., Veenhuis, M., Kahana, J. A., Silver, P. A. & Rapoport, T. A. (2000). Mutants affecting the structure of the cortical endoplasmic reticulum in *Saccharomyces cerevisiae*. *J Cell Biol* 150, 461-74.

91. Ravikumar, B., Acevedo-Arozena, A., Imarisio, S., Berger, Z., Vacher, C., O'Kane, C. J., Brown, S. D. & Rubinsztein, D. C. (2005). Dynein mutations impair autophagic clearance of aggregate-prone proteins. *Nat Genet* 37, 771-6.

92. Reggiori, F. (2006). 1. Membrane origin for autophagy. *Curr Top Dev Biol* 74, 1-30.

93. Reggiori, F. & Klionsky, D. J. (2002). Autophagy in the eukaryotic cell. *Eukaryot Cell* 1, 11-21.

94. Reggiori, F. & Klionsky, D. J. (2005). Autophagosomes: biogenesis from scratch? *Curr Opin Cell Biol* 17, 415-22.

95. Reggiori, F., Monastyrska, I., Shintani, T. & Klionsky, D. J. (2005a). The actin cytoskeleton is required for selective types of autophagy, but not nonspecific autophagy, in the yeast *Saccharomyces cerevisiae*. *Mol Biol Cell* 16, 5843-56.

96. Reggiori, F., Shintani, T., Nair, U. & Klionsky, D. J. (2005b). Atg9 cycles between mitochondria and the pre-autophagosomal structure in yeasts. *Autophagy* 1, 101-9.

97. Reggiori, F., Tucker, K. A., Stromhaug, P. E. & Klionsky, D. J. (2004). The Atg1-Atg13 complex regulates Atg9 and Atg23 retrieval transport from the pre-autophagosomal structure. *Dev Cell* 6, 79-90.

98. Rubinsztein, D. C., Ravikumar, B., Acevedo-Arozena, A., Imarisio, S., O'Kane, C. J. & Brown, S. D. (2005). Dyneins, autophagy, aggregation and neurodegeneration. *Autophagy* 1, 177-8.

99. Sagiv, Y., Legesse-Miller, A., Porat, A. & Elazar, Z. (2000). GATE-16, a membrane transport modulator, interacts with NSF and the Golgi v-SNARE GOS-28. *EMBO J* 19, 1494-504.

100. Seglen, P. O., Berg, T. O., Blankson, H., Fengsrud, M., Holen, I. & Stromhaug, P. E. (1996). Structural aspects of autophagy. *Adv Exp Med Biol* 389, 103-11.

101. Shih, Y. L. & Rothfield, L. (2006). The bacterial cytoskeleton. *Microbiol Mol Biol Rev* 70, 729-54.

102. Shintani, T., Huang, W. P., Stromhaug, P. E. & Klionsky, D. J. (2002). Mechanism of cargo selection in the cytoplasm to vacuole targeting pathway. *Dev Cell* 3, 825-37.

103. Shintani, T. & Klionsky, D. J. (2004a). Autophagy in health and disease: a double-edged sword. *Science* 306, 990-5.

104. Shintani, T. & Klionsky, D. J. (2004b). Cargo proteins facilitate the formation of transport vesicles in the cytoplasm to vacuole targeting pathway. *J Biol Chem* 279, 29889-94.

105. Stukalin, E. B. & Kolomeisky, A. B. (2006). ATP hydrolysis stimulates large length fluctuations in single actin filaments. *Biophys J* 90, 2673-85.

106. Suzuki, K., Kubota, Y., Sekito, T. & Ohsumi, Y. (2007). Hierarchy of Atg proteins in pre-autophagosomal structure organization. *Genes Cells* 12, 209-18.

107. Suzuki, K. & Ohsumi, Y. (2007). Molecular machinery of autophagosome formation in yeast, *Saccharomyces cerevisiae*. *FEBS Lett* 581, 2156-61.

108. Tanida, I., Ueno, T. & Kominami, E. (2004). LC3 conjugation system in mammalian autophagy. *Int J Biochem Cell Biol* 36, 2503-18.

109. Taylor, M. P. & Kirkegaard, K. (2008). Potential subversion of autophagosomal pathway by picornaviruses. *Autophagy* 4, 286-9.

110. Vale, R. D. (2003). The molecular motor toolbox for intracellular transport. *Cell* 112, 467-80.

111. van der Vaart, A., Mari, M. & Reggiori, F. (2008). A picky eater: exploring the mechanisms of selective autophagy in human pathologies. *Traffic* 9, 281-9.

112. Vavylonis, D., Yang, Q. & O'Shaughnessy, B. (2005). Actin polymerization kinetics, cap structure, and fluctuations. *Proc Natl Acad Sci USA* 102, 8543-8.

113. Wang, Z., Khan, S. & Sheetz, M. P. (1995). Single cytoplasmic dynein molecule movements: characterization and comparison with kinesin. *Biophys J* 69, 2011-23.

114. Webb, J. L., Ravikumar, B. & Rubinsztein, D. C. (2004). Microtubule disruption inhibits autophagosome-lysosome fusion: implications for studying the roles of aggresomes in polyglutamine diseases. *Int J Biochem Cell Biol* 36, 2541-50.

115. Weisenberg, R. C. & Deery, W. J. (1976). Role of nucleotide hydrolysis in microtubule assembly. *Nature* 263, 792-3.

116. Wells, A. L., Lin, A. W., Chen, L. Q., Safer, D., Cain, S. M., Hasson, T., Carragher, B. O., Milligan, R. A. & Sweeney, H. L. (1999). Myosin VI is an actin-based motor that moves backwards. *Nature* 401, 505-8.

117. Winder, S. J. & Ayscough, K. R. (2005). Actin-binding proteins. *J Cell Sci* 118, 651-4.

118. Xie, Z. & Klionsky, D. J. (2007). Autophagosome formation: core machinery and adaptations. *Nat Cell Biol* 9, 1102-9.

119. Xie, Z., Nair, U. & Klionsky, D. J. (2008). Atg8 controls phagophore expansion during autophagosome formation. *Mol Biol Cell* 19, 3290-8.

120. Yap, G. S., Ling, Y. & Zhao, Y. (2007). Autophagic elimination of intracellular parasites: convergent induction by IFN-Y and CD40 ligation? *Autophagy* 3, 163-5.

121. Yorimitsu, T. & Klionsky, D. J. (2005a). Atg11 links cargo to the vesicle-forming machinery in the cytoplasm to vacuole targeting pathway. *Mol Biol Cell* 16, 1593-605.

122. Yorimitsu, T. & Klionsky, D. J. (2005b). Autophagy: molecular machinery for self-eating. *Cell Death Differ* 12 Suppl 2, 1542-52.

123. Young, A. R. J., Chan, E. Y. W., Hu, X. W., Köchl, R., Crawshaw, S. G., High, S., Hailey, D. W., Lippincott-Schwartz, J. & Tooze, S. A. (2006). Starvation and ULK1-dependent cycling of mammalian Atg9 between the TGN and endosomes. *J Cell Sci* 119, 3888-900.

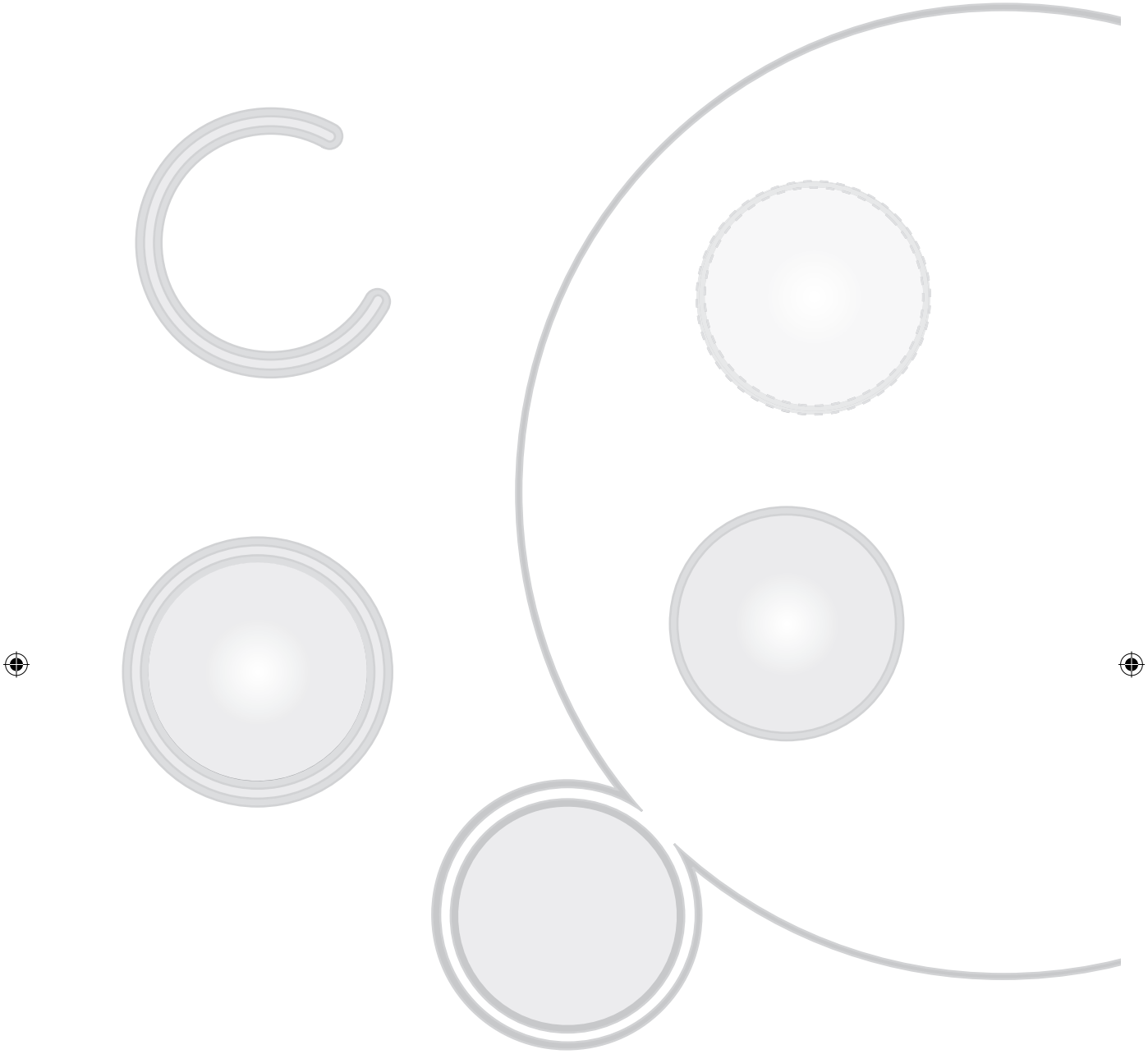

CHAPTER

3

Atg18 function in autophagy is regulated by specific sites within its ß-propeller

Ester Rieter[1], Fabian Vinke[1], Daniela Bakula[2], Eduardo Cebollero[1], Christian Ungermann[3], Tassula Proikas-Cezanne[2] and Fulvio Reggiori[1]

[1]Department of Cell Biology and Institute of Biomembranes, University Medical Centre Utrecht, Heidelberglaan 100, Utrecht, The Netherlands; [2]Autophagy Laboratory, Interfaculty Institute for Cell Biology, Eberhard Karls University Tuebingen, Auf der Morgenstelle 15, Tuebingen, Germany; [3]Department of Biology/Chemistry, University of Osnabrück, Barbarastrasse 13, Osnabrück, Germany

In revision

ABSTRACT

Autophagy is a conserved degradative transport pathway. It is characterized by the formation of double-membrane autophagosomes at the phagophore assembly site (PAS). Atg18 is essential for autophagy but also for vacuole homeostasis and probably endosomal functions. This protein has a N-terminal β-propeller formed by 7 WD40 repeats, which contains a conserved FRRG motif that binds phosphoinositides and promotes Atg18 recruitment to the PAS, endosomes and vacuoles. It is unknown, however, how Atg18 association with these organelles is regulated as the specific phosphoinositides are on all membranes. We have investigated Atg18 recruitment to the PAS and found that Atg18 binds Atg2 through a specific stretch of amino acids in the β-propeller on the opposite surface from the FRRG motif. As in absence of the FRRG sequence, the inability of Atg18 to interact with Atg2 impairs its association with the PAS, causing an autophagy block. Our data provide a model, where the Atg18 β-propeller provides organelle specificity by binding two determinants on the target membrane and underline the potential capacity of specific β-propellers to form protein-lipid complexes.

Key words: Atg2/Atg18/autophagy/phagophore assembly site/phosphoinositides

INTRODUCTION

Eukaryotes utilize two catabolic pathways to dispose unwanted cellular components: The ubiquitin-proteasome pathway and autophagy. The proteasome is exclusively involved in the degradation of proteins while autophagy permits the elimination of large protein complexes and even entire organelles or microorganisms, thus allowing the turnover of all cellular components (Nakatogawa et al., 2009; Ravid and Hochstrasser, 2008). Autophagy is characterized by the formation of double-membrane vesicles called autophagosomes, which sequester and deliver cytoplasmic structures into the mammalian lysosomes or the yeast and plant vacuoles mainly for degradation (Klionsky, 2007). The resulting degradation products are transported back in the cytoplasm and used for either the synthesis of new macromolecules or as a source of energy. Induction of autophagy often occurs during stress conditions such as starvation but this pathway also plays a key role in numerous physiological and pathological situations including development and tissue remodelling, ageing, immunity, neurodegeneration and cancer (Mizushima et al., 2008).

Although the molecular mechanism of autophagosome biogenesis remains largely unknown, genetic studies in yeast have led to the identification of 36 autophagy-related genes (*ATG*) that play a role in autophagy and/or autophagy-related pathways. Among them, 16 Atg proteins compose the conserved core machinery essential for double-membranes vesicle formation. In yeast, these Atg proteins are recruited to a single perivacuolar site, called the phagophore assembly site or pre-autophagosomal structure (PAS) (Suzuki et al., 2007), which appears to be present in mammals as well (Itakura and Mizushima, 2010). According to the current model, Atg proteins first mediate the biogenesis of a small cup-shaped cisterna known as the phagophore or isolation membrane, and then its expansion into an autophagosome through the acquisition of additional lipid bilayers (Nakatogawa et al., 2009). An important event during autophagosome biogenesis is the generation of phosphatidylionositol-3-phosphate (PtdIns3P) at the PAS by the autophagy-specific phosphatidylinositol-3 kinase complex I (Kihara et al., 2001). Although it has been shown that PtdIns3P is a key regulator of autophagy, the precise function of this lipid is poorly understood (Kihara et al., 2001). One hypothesis is that the PtdIns3P on autophagosomal membranes is necessary for the recruitment of a subset of the Atg proteins.

One of these proteins is yeast Atg18, which is part of the core machinery

and is essential for autophagy (Barth et al., 2001; Guan et al., 2001). The main structural feature of Atg18 is that its 7 WD40 repeats, which are stretches of approximately 40 amino acids ending with the residues tryptophan and aspartate, fold into a 7-bladed β-propeller (Barth et al., 2001; Dove et al., 2004). WD40 domain-containing proteins often act as scaffolds, which promote and/or coordinate the assembly of protein complexes by creating a stable platform for simultaneous and reversible protein-protein interactions (Chen et al., 2004; Paoli, 2001; Smith et al., 1999). Atg18 is in addition also able to bind both PtdIns3P and phosphatidylinositol-3,5-biphosphate [PtdIns(3,5)P_2] through a conserved phenylalanine-arginine-arginine-glycine (FRRG) motif within its β-propeller (Dove et al., 2004; Krick et al., 2006). Interaction of Atg18 with these phosphoinostides is essential for its localization to the PAS, endosomes and vacuole (Krick et al., 2008; Krick et al., 2006; Nair et al., 2010; Obara et al., 2008b; Stromhaug et al., 2004). While very little is known about the role of Atg18 at the endosomes, this protein is part of a large complex at the vacuolar membrane that regulates PtdIns(3,5)P_2 levels on this organelle (Efe et al., 2007; Jin et al., 2008; Michell and Dove, 2009). The localization of Atg18 to the PAS also depends upon Atg2 and *vice versa* (Guan et al., 2001; Obara et al., 2008b; Suzuki et al., 2007), and it has been proposed that these two proteins constitutively form a cytosolic complex (Obara et al., 2008b; Suzuki et al., 2007). The Atg18 ability to interact with Atg2 does not depend on its PtdIns3P-binding capacity, whereas the binding of Atg18 to PtdIns3P seems necessary for the appropriate targeting of the Atg18-Atg2 complex to the PAS (Obara et al., 2008b). The presence of Atg18 on three different localizations probably requires a tight control of Atg18 recruitment and function. The molecular principles of this regulation are unknown.

In order to understand Atg18 regulation in autophagy and gain insights into the principles controlling the different cellular functions of this protein, we have studied how Atg18 is recruited to the PAS. We have identified the Atg2-binding site of Atg18 and discovered that this sequence, termed loop 2 here, is located in a stretch of amino acids connecting beta-sheets between WD-repeat 2 and 3 of the β-propeller. This result indicates a role of this structural domain as a scaffold for the assembly of proteins-lipids complexes. We have also found that PtdIns3P and Atg2 are the two determinants that mediate the specific recruitment of Atg18 to the PAS. In absence of one of these interactions, Atg18 remains cytosolic and autophagosome biogenesis is blocked at an early stage, thus causing a severe impairment in autophagy.

MATERIALS AND METHODS

Strains and media

The *S. cerevisiae* strains used in this study are listed in **Supplementary Table S1**. For gene disruptions, coding regions were replaced with genes expressing auxothrophic markers using PCR primers containing ~60 bases of identity to the regions flanking the open reading frame generated from the pUG27, pUG72, pUG73 or pFA6a-TRP1 template plasmids (Gueldener et al., 2002; Longtine et al., 1998). Gene knockouts were verified by examining prApe1 processing by western blot using a polyclonal antibody against Ape1 (Mari et al., 2010) and/or PCR analysis of the deleted gene locus.

Chromosomal tagging of the *ATG2* gene at the 3` end was done by PCR-based integration of the PA or the GFP tag using pFA6a-PA-TRP1 and pFa6a-GFP(S65T)-TRP1 as template plasmids, respectively (Longtine et al., 1998). For construction of the strain expressing Atg2 under the control of the *GAL1* promoter, the *ATG2* gene was chromosomally tagged at the 5` end with the *GAL1* promoter and the HA tag by PCR-based integration using the pFA6a-HIS3MX6-PGAL1-3HA plasmid as a template (Longtine et al., 1998). Chromosomal taggings were verified by western blot using antibodies against goat IgG for the detection of PA (Invitrogen Life Science, Carlsbad, CA), or monoclonal antibodies recognizing either GFP (Roche, Basel, Switzerland) and HA (Covance, Princeton, NJ).

For the BiFC assay, the *ATG2* and *ATG18* genes were chromosomally tagged at the 3` end by PCR-based integration of the N- (VN) or C-terminal fragment (VC) of Venus using pFA6a-VN-HIS3MX6 or pFa6a-VC-TRP1 as template plasmids (Sung and Huh, 2007). Correct integration of the tags was verified by PCR.

Yeast cells were grown in rich (YPD; 1% yeast extract, 2% peptone, 2% glucose) or synthetic minimal media (SM; 0.67% yeast nitrogen base, amino acids and vitamins as needed) containing 2% glucose. Starvation experiments were conducted in synthetic media lacking nitrogen (SD-N; 0.17% yeast nitrogen base without amino acids, 2% glucose). For galactose-induced overexpression of proteins, cells were grown overnight in SM medium containing 2% glucose, diluted and re-grown to an exponential phase in SM medium containing 2% raffinose. Protein overexpression was then induced by transferring cells in SM medium containing 2% galactose overnight.

Plasmids

For the construction of the Y2H plasmids, DNA fragments encoding *ATG2* and *ATG18* were generated by PCR using *S. cerevisiae* genomic DNA as a template and cloned as a *Xma*I-*Sal*I and *Eco*RI-*Sal*I fragment, respectively, into both pGAD-C1 and pGBDU-C1 vectors (James et al., 1996). The C-terminal truncation of *ATG18* (1-377) was generated by PCR using the same 5` primer as for the cloning of the full-length gene and a 3` primer for the specific site of truncation, which introduced a stop codon followed by a *Sal*I restriction site. The point mutations in *ATG18* designed to create the loop mutants were introduced by PCR using unique restriction sites in close proximity of the nucleotide stretch coding for each loop. Combinations of Atg18 loop mutants were made by PCR by combining primers used to create the different loop mutants and already constructed Atg18 loop mutant plasmids as templates. The correct introduction of the point mutations was verified by DNA sequencing.

Plasmids expressing untagged Atg18 loop mutants under the control of the endogenous promoter of Atg18 were constructed by PCR using the Y2H plasmids of the different loop mutants as templates and cloned as *Nhe*I-*Nde*I fragments into the pCvt18(415) plasmid, which carries the wild type *ATG18* gene (Guan et al., 2001).

The promAtg18GFP416 plasmid was generated by amplifying the promoter (700 bp) and the *ATG18* gene from genomic DNA by PCR and cloning it as a *Xho*I-*Bcl*I fragment in a pRS416 vector (Sikorski and Hieter, 1989) digested with *Xho*I-*Bam*HI and containing a $(gly\text{-}Ala)_3$-linker and *GFP*, which were inserted as a *Bam*HI-*Sac*II fragment at the 3' end of the gene. Similar to the untagged constructs, the GFP-fusion proteins of the Atg18 loop mutants were then generated by PCR using the Y2H plasmids of the different loop mutants as templates and cloned as *Tth*111I-*Bsi*WI fragments into the Atg18-GFP plasmid. To generate the plasmids expressing the different *ATG18* mutants tagged with 13xmyc, the *GFP* gene was replaced with the sequence coding for the 13xmyc tag followed by the *ADH1* terminator obtained by PCR from the pFA6a-13xmyc plasmid (Longtine et al., 1998). To create the vectors integrating the various Atg18-GFP and Atg18-13xmyc constructs into the genome, the backbone of the expression plasmids was replaced with that of the pRS405 vector (Sikorski and Hieter, 1989) using *Xho*I and *Sac*I. Correct integration of the different constructs was verified by western blot analysis using polyclonal antibodies against myc (Santa Cruz Biotechnology, Santa Cruz, CA) or monoclonal antibodies against

GFP. Plasmids expressing the different *ATG18* loop mutants under the control of the *GAL1* promoter were generated by PCR amplification of the sequences coding for the different *Atg18* loop mutants, plus the 13xmyc tag and the *ADH1* terminator from the plasmids described above. The PCR fragments were cloned into the pRS416 vector (Sikorski and Hieter, 1989) using *Hind*III and *Kpn*I before inserting the *GAL1* promoter using *Xho*I and *Hind*III.

The pCuGFPATG8414 and pCuGFPATG8416 plasmids expressing GFP-Atg8 under the control of the *CUP1* promoter have been described elsewhere (Kim et al., 2002). To create the integrative pCFPATG8406 plasmid that leads to the expression of the CFP-Atg8 fusion protein from the authentic *ATG8* promoter, the backbone of the pRS314 ECFP-AUT7 plasmid (Suzuki et al., 2001) was exchanged for that of the pRS406 vector (Sikorski and Hieter, 1989) using *Xho*I and *Sac*II. The integrative pCumCheV5ATG8406 plasmid, which expresses mCherry-V5-Atg8 from the *CUP1* promoter, was generated by replacing the vector backbone of the pCumCheV5ATG8415 plasmid (Mari and Reggiori, 2010) with that of the pRS406 vector using *Kpn*I and *Sac*I.

Yeast two-hybrid assay

The plasmids pGAD-C1 and pGBDU-C1 containing *ATG2* and *ATG18* or its mutated and truncated forms were transformed into the PJ69-4A test strain and grown on 2% glucose-containing SM medium lacking leucine and uracil (James et al., 1996). Colonies were then spotted on 2% glucose-containing SM medium lacking histidine, leucine and uracil. When both proteins interact, the test strain grows on plates lacking histidine.

Protein A affinity purifications

Cells were grown to 1 OD_{600} in 50 ml of YPD, collected by centrifugation and resuspended in 1 ml of lysis buffer [20 mM Tris-HCl, pH 8.0, 150 mM KCl, 5 mM $MgCl_2$, 1% Triton X-100, supplemented with 1 mM phenylmethylsulfonyl fluoride and a cocktail of protease inhibitors (Roche)]. Cells were broken using glass beads and vortexing, and centrifuged at 13'000 rpm for 10 min at 4°C. After centrifugation, 75 µl of the supernatant was collected and kept to represent the input (total lysate). The rest of the supernatant was incubated with 50 µl IgG-Sepharose beads (GE Healthcare, Waukesha, WI) on a rotating wheel for 1 h at 4°C. The beads were washed once with 1 ml of lysis buffer, once with lysis buffer containing 300 mM KCl, once with lysis buffer containing 500 mM KCl, then

once again with lysis buffer containing 300 mM KCl, and finally one more time with the lysis buffer (Reggiori et al., 2003). Bound proteins were eluted by boiling the beads for 5 min in 75 µl SDS-PAGE sample buffer and eluates were resolved by SDS-PAGE and immunoblotted using antibodies against myc or goat IgG (to detect PA).

Fluorescence microscopy

Cells were grown in YPD medium to an early log phase or nitrogen starved in SD-N medium for 3 h. Fluorescence signals were captured with a DeltaVision RT fluorescence microscope (Applied Precision, Issaquah, WA) equipped with a CoolSNAP HQ camera (Photometrix, Tucson, AZ). Images were generated by collecting a stack of 18 pictures with focal planes 0.20 µm apart, and by successively deconvolving and analyzing them with the SoftWoRx software (Applied Precision). A single focal plane is shown at each time. The percentage of cells positive for a CFP-Atg8, Atg2-GFP or BiFC-positive puncta was determined by analysing at least 100 cells from 2 independent experiments. To determine the degree of colocalization between the fusion proteins Atg18-GFP and mCheV5-Atg8, the number of mCheV5-Atg8 puncta positive for the Atg18-GFP signal was counted in at least 100 cells from 2 independent experiments.

Phospholipid binding assay

Phospholipid binding assays with native cell extracts has previously been described (Proikas-Cezanne et al., 2007) and adapted to yeast as follows. Native yeast cell extracts were generated from 200 OD_{600} equivalents of frozen yeast cells by vortexing them 3 times for 30 s in the binding buffer [750 mM aminocraproic acid, 50 mM Bis-Tris, 0.5 mM EDTA, pH 7.0, supplemented with protease and phosphatase inhibitor cocktails (Roche)] in presence of glass beads. The soluble fraction was obtained by removing the glass beads and cell debris through centrifugation at 14'000 rpm at 4°C for 15 min. Before use, the membrane-immobilized phospholipids (Echelon Biosciences, Salt-Lake City, UT) were rinsed first in TBS buffer (Tris-buffered saline, 20 mM Tris-HC1, 0.15 M sodium chloride, pH 7.5) and then in 0.1 % Tween 20 in TBS buffer before blocking them in 0.1% Tween 20 /3 % BSA in TBS buffer for 1 h at room temperature. Membranes were subsequently incubated with cell extracts at 4°C for 2 days before detecting bound proteins by western blot using anti-myc antibodies.

Miscellaneous procedures

The protein extraction, western blot analyses and the GFP-Atg8 processing assay were carried out as previously described (Cheong and Klionsky, 2008a; Reggiori et al., 2003). Detection and quantification of the western blot were done using an Odyssey system (Li-cor Biosciences, Lincoln, NE). Processing of the electron microscopy samples and the counting of autophagic bodies has already been illustrated (van der Vaart et al., 2010).

RESULTS

Identification of the Atg2-binding site of Atg18

Atg18 is a 500 amino acids protein with uncharacterized linear motifs in its C-terminal part (**Figure 1A**). Its N-terminus, however, contains seven WD40 repeats predicted to fold into a 7-bladed β-propeller (Dove et al., 2004). Previous studies have indicated that Atg18 requires Atg2 for its recruitment to the PAS, and that these two proteins are able to form a large complex of approximately 500 kDa (Suzuki et al., 2007; Obara et al., 2008). To study how the function of Atg18 is regulated at the PAS, we decided to identify the Atg2-binding region in Atg18. We thus generated a truncated form of Atg18, i.e. Atg18(1-377), lacking the last 123 C-terminal amino acids and leaving the first 377 amino acids forming the β-propeller. The ability of this protein fragment to interact with Atg2 was tested by tyeast two-hybrid (Y2H) assay. As shown in **Figure 1A**, no growth was observed in cells harboring an empty vector or exclusively expressing Atg2. In contrast, cells carrying Atg2 and full-length Atg18 were able to grow, confirming that Atg18 interacts with Atg2 (**Figure 1A**). Binding was also detected between Atg2 and Atg18(1-377) revealing that the β-propeller probably mediates the association of Atg18 with Atg2.

Crystallographic studies of other WD40 domain-containing proteins have previously shown that the amino acids from the loops that interconnect the blades of the β-propeller are often at the interacting face between the protein and its binding partners (Paoli, 2001). To determine whether the loops within the Atg18 β-propeller mediate the interaction to Atg2, we decided to create point mutant versions of Atg18 modifying the 6 loops and tested them by Y2H. We opted to not sequentially deleting the WD40 domains because this approach is likely to disrupt the overall structure of the β-propeller. Since protein-protein interactions often occur via charged or polar amino acids, all these types of

amino acids present in the 6 loops were replaced by alanines (**Figure 1B**). When the 6 loops were individually mutated, the association between Atg18 and Atg2 was not affected (**Figure 1C**). Importantly, the mutation of the two arginines in loop 5 that play a critical role in the binding of Atg18 to specific phosphoinositides (Dove et al., 2004) also did not interfere with the Atg18-Atg2 interaction (**Figure 1C**). There are numerous documented cases, where WD40 domain-containing proteins associate with their binding partners through amino acid residues present in different parts of the β-propeller (Chen et al., 2004; Cheng et al., 2004; Paoli, 2001; Pashkova et al., 2010). Accordingly, we constructed a number of Atg18 mutants that combine several loop mutants and tested their ability to bind Atg2. We found that the binding of Atg18 to Atg2 was perturbed when loop 1 and 2 were simultaneously mutated (**Figure 1D**), indicating that that the charged amino acids in these sequences could mediate the interaction between the two proteins.

Loop 2 of the Atg18 ß-propeller is essential for the in vivo interaction between Atg2 and Atg18, but not for phosphoinositide binding

To verify the results obtained with the Y2H assay in the appropriate physiological context, we performed a protein A (PA) affinity isolation experiment. For this purpose, we first generated a plasmid expressing a functional 13xmyc-tagged Atg18 fusion protein under the control of the endogenous promoter (**Supplementary Figure S1**), before inserting the different loop mutations. To test the binding capacity of the resulting chimera, the plasmids were transformed into either the *atg18Δ* strain, in which Atg2 was endogenously tagged with PA or just the *atg18Δ* knockout, which served as negative control. Analysis of the cell extracts confirmed that all the Atg18 point mutants have similar expression levels than the wild-type protein, suggesting that the mutant proteins are not degraded due to a potential misfolding (**Figure 2A**). Mutations in loop 1 led to the appearance of an additional lower molecular weight Atg18 band and the cause of this phenotype is currently under investigation. In accordance with the Y2H results and previous work (Obara et al., 2008b), we were able to co-isolate wild-type Atg18 and Atg2-PA confirming the interaction between these two proteins (**Figure 2A**, lane 2). No wild type Atg18-13xmyc was detected in the affinity eluate, when the pull-down was performed using the negative control (**Figure 2A**, lane 7). Atg18(L1) and Atg18(L5) were also co-isolated with Atg2-PA in comparable amounts to wild type Atg18. Crucially, almost no Atg18(L2) and Atg18(L1,2) were detected

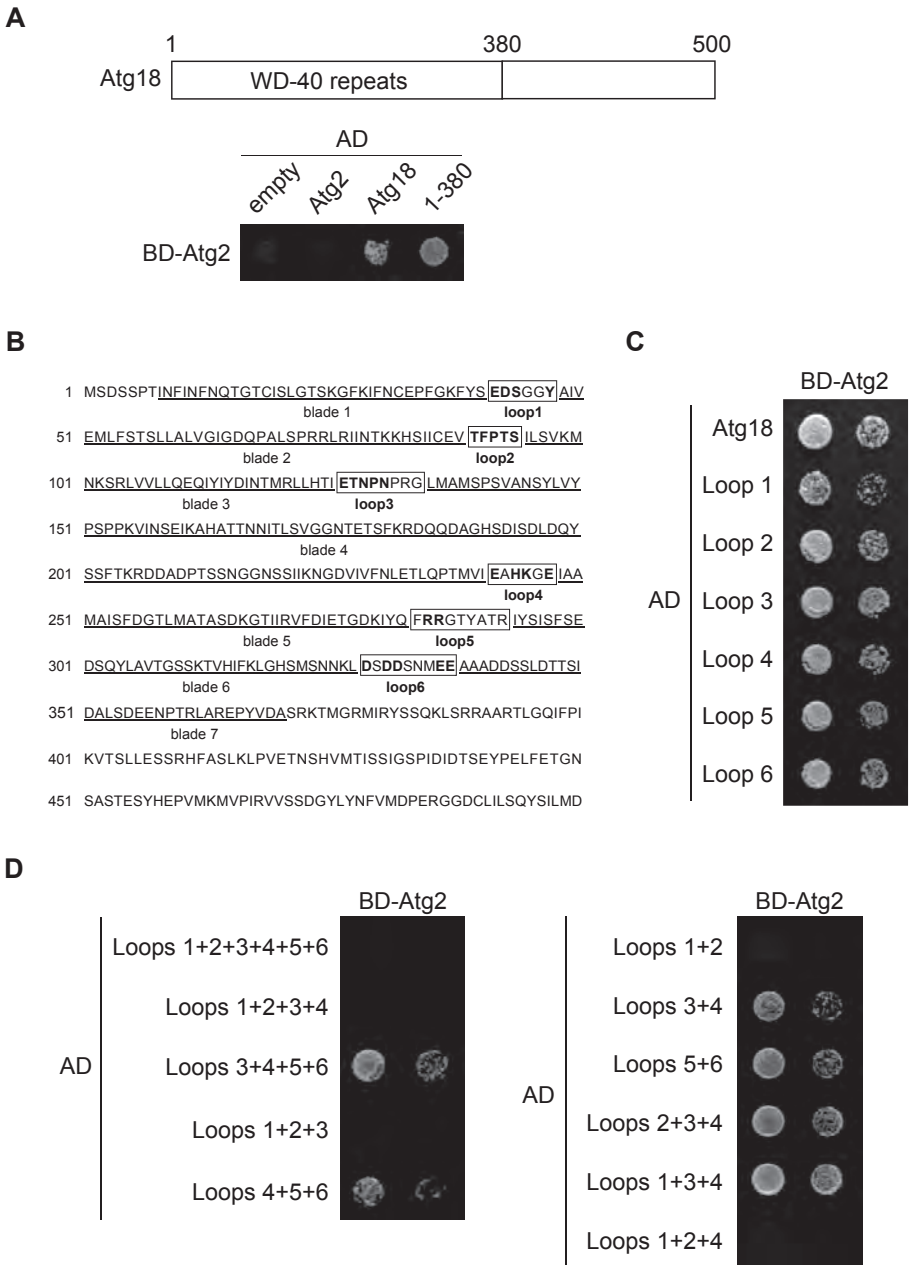

Figure 1. Identification of the Atg2-interaction region in Atg18. A. The first 377 amino acids of Atg18 coding for the β-propeller are essential for Atg18 interaction with Atg2. Atg2, Atg18 and the Atg18 (1-377) truncation were fused to the activation domain (AD) and/or the DNA binding domain (BD) of the transcription factor Gal4. Plasmids were transformed into the PJ69-4A strain and colonies were spotted on medium lacking uracil, tryptophan

and histidine. Growth on these plates indicates that the tested proteins interact. The empty pGAD-C1 plasmid was used as a control. B. Overview of the amino acid sequence of Atg18. The 7 β-sheets forming the blades of Atg18 β-propeller are underlined and the loops connecting them are highlighted with boxes. Charged and polar amino acids present in each loop that were substituted with alanines are indicated in bold. C. Mutations in a single loop do not disrupt the binding between Atg2 and Atg18. AD-fusions of the different Atg18 mutants were tested for their ability to interact with the BD-Atg2 chimera using the Y2H assay as in panel A. D. Loop 1 and 2 of Atg18 are essential for binding with Atg2. Combinations of several mutated Atg18 loops were cloned in the pGAD-C1 vector and tested for interaction with BD-Atg2 as in panel A.

after pull-down with Atg2-PA, showing that these two mutant proteins are no longer able to interact with Atg2. These data show the key role played by the amino acids in loop 2 of the Atg18 β-propeller in binding Atg2.

To show that the mutated amino acids in loops 1 and 2 do not affect the folding of the Atg18 β-propeller, we determined the lipid-binding capacity of each Atg18 loop mutant by conducting a phospholipid-binding assay. Native cell extracts from strains overexpressing the myc-tagged *ATG18* loop mutants were incubated on phospholipid strips and proteins detected as described in *Materials and methods*. We found that the Atg18(L1), Atg18(L2) and Atg18(L1,2) mutants were able to specifically bind PtdIns(3,5)P_2 to the same extent as wild type Atg18 (**Figure 2B**). As expected and consistently with previous data (Dove et al., 2004; Krick et al., 2006), the Atg18(L5) mutant carrying the mutated FRRG motif did not bind phosphoinositides (**Figure 2B**). Dove and co-workers have reported that recombinant Atg18 predominately binds PtdIns(3,5)P_2 but also PtdIns3P with a much lower affinity (Dove et al., 2004). In agreement with this observation, we also found that in our experimental set-up, the binding of the Atg18 variants to PtdIns(3,5)P_2 is favored while what associated to PtdIns3P is below detection levels. These data show that mutations in the Atg2-binding domain do not affect the phosphoinositide binding capacity of Atg18 and consequently the β-propeller is correctly folded.

Atg2 binding to Atg18 is essential for bulk and selective types of autophagy

To investigate the relevance of the interaction between Atg18 and Atg2 in autophagy, we generated plasmids expressing the untagged Atg18(L1), Atg18(L2), Atg18(L1,2) and Atg18(L5) mutants under the control of the authentic *ATG18* promoter. These constructs were then co-transformed with a plasmid carrying the GFP-Atg8 fusion protein into *atg18Δ* mutant cells to perform the GFP-Atg8 processing assay. This is a well-established method to monitor bulk autophagy in yeast by measuring the accumulation of free GFP in the vacuole over time

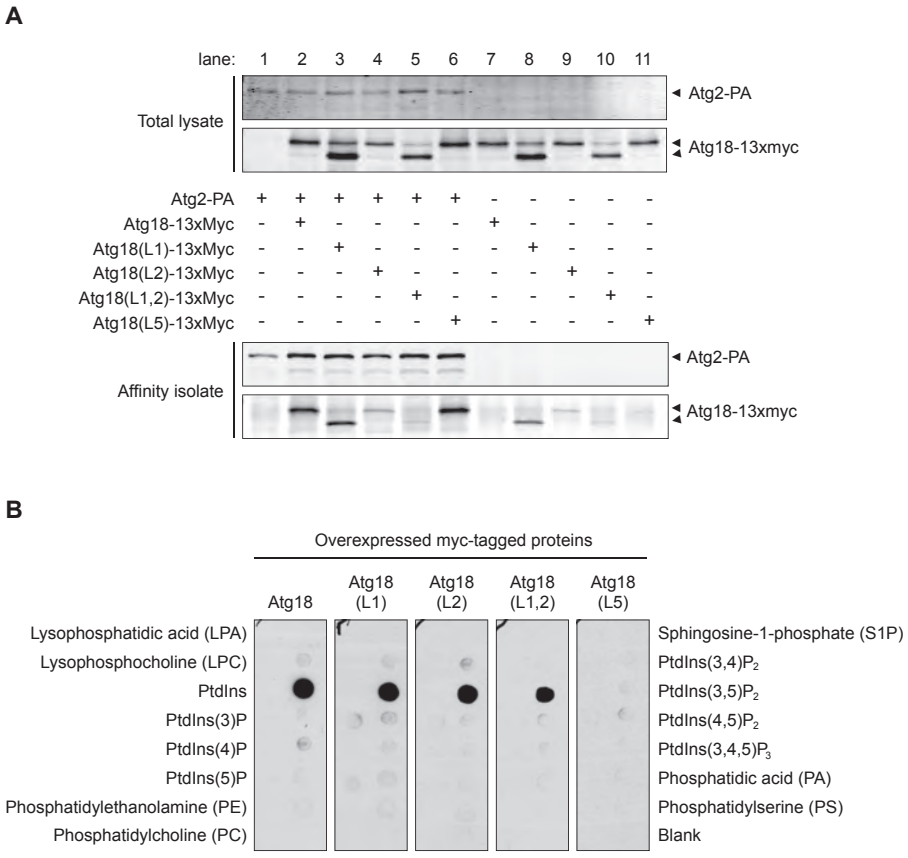

Figure 2. Amino acids in loop2 of the Atg18 ß-propeller are essential for the interaction between Atg2 and Atg18 *in vivo*. A. The identified Atg18 loop 2 and 1,2 mutants do not interact with Atg2 *in vivo*. Cell lysates from the *atg18*Δ (JGY3) and *atg18*Δ *ATG2-PA* (FRY387) strains transformed with plasmids expressing the *ATG18* loop mutants tagged with 13xmyc were subjected to pull-down experiments as described in *Materials and Methods*. Affinity isolates were resolved by SDS-PAGE and analyzed by western blot. On each lane of the SDS-PAGE gel, 1% of cell lysate or 20% of affinity isolate was loaded. Although there is a small amount of Atg18(L1) in the affinity eluate of the negative control (lane 8), this fusion protein is highly enriched in the sample containing Atg2-PA (lane 3), indicating that it still binds to Atg2-PA. B. Atg2-binding mutants of Atg18 still bind phosphoinositides. To determine the phosphoinositide binding capacity of the various Atg18 constructs, native cell extracts from the *atg18*Δ strain transformed with plasmids expressing the 13xmyc-tagged Atg18 loop mutants under the control of *GAL1* promoter. Cell were then grown on galactose overnight to induce the protein overexpression (approximately 70 fold, not shown), were incubated on phospholipid strips before western blot analysis. The lipids present on the membranes are indicated next to the panels.

(Cheong and Klionsky, 2008a). When this assay was performed in wild type cells, a band of 25 kDa corresponding to free GFP appeared under starvation conditions

indicating normal autophagy (**Figure 3A**). In contrast, no GFP-Atg8 cleavage was observed in the *atg18Δ* mutant due to the complete block of autophagy (Barth et al., 2001; Guan et al., 2001). As shown in **Figure 3A**, wild type Atg18 and Atg18(L1) were able to complement this defect indicating that loop1 is not required for bulk autophagy. In contrast, a complete block of the pathway was observed when this mutation was combined with that in loop 2. The relevance of loop 2 in autophagy was also underscored by the analysis of Atg18(L2), which showed a severe defect in the progression of autophagy, which was even more pronounced than the one for cells expressing Atg18(L5) (**Figure 3A**) and already reported (Krick et al., 2006; Nair et al., 2010).

Next, we examined the effects of the loop mutations on a selective type of autophagy, the biosynthetic cytosol-to-vacuole targeting (Cvt) pathway, which delivers a large cytoplasmic oligomer mostly composed of aminopeptidase I (Ape1) into the vacuole (Lynch-Day and Klionsky, 2010). Ape1 is present in the cytoplasm as an inactive precursor (prApe1) that is proteolytically cleaved into its mature active form (mApe1) once it reaches the vacuolar lumen. As expected, the majority of Ape1 was present in the mature form in wild type cells while the *atg18*Δ mutant accumulated prApe1 as consequence of its block in the Cvt pathway (**Figure 3B**) (Barth et al., 2001; Guan et al., 2001). A severe impairment of this transport route was also observed in the *atg18*Δ knockout carrying the Atg18(L2), Atg18(L1,2) and Atg18(L5) mutants. In contrast, cells expressing Atg18 or Atg18(L1) processed prApe1 into mApe1 to an almost identical extent as the wild type strain (**Figure 3B**). Based on this result and the one obtained with the pull-down experiment (**Figure 2A**), we decided to focus on the Atg18(L2) mutant rather than on Atg18(L1,2) to study the role of the interaction between Atg18 and Atg2 in autophagy because it appears to be specific for this interaction.

The interaction between Atg2 and Atg18 is essential for autophagosome biogenesis

Cells expressing the Atg18(L2) or the Atg18(L5) mutant were then analyzed at the ultrastructural level by electron microscopy (EM) to gain insights into the autophagy step that was impaired. Autophagic bodies, the vesicles resulting from the fusion of the autophagosomes with the vacuole, are rapidly degraded in the interior of this organelle (Takeshige et al., 1992). By deleting *PEP4*, the gene encoding for the main vacuolar protease, however, autophagic bodies accumulate in the vacuolar lumen over time upon autophagy induction. This type of examination also provides an alternative way to quantify autophagy and also allows determining whether the

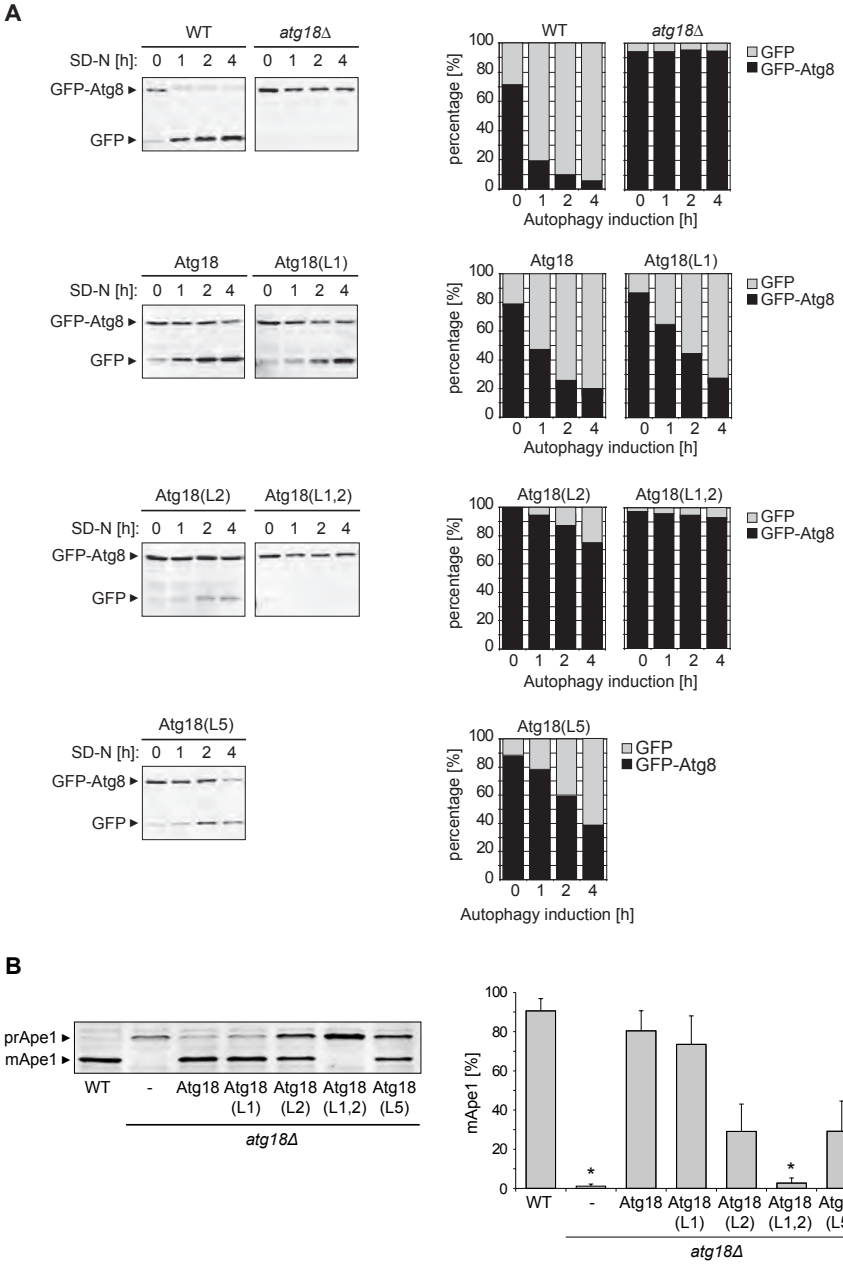

Figure 3. Atg18-Atg2 interaction is essential for the Cvt pathway and autophagy. A. Mutations in the Atg18 loops 1, 2 and 5 lead to an impairment of autophagy. Wild type (SEY6210) and *atg18*Δ (JGY3) cells carrying both the pCuGFPATG8414 construct and, one of the plasmids expressing the untagged Atg18 loop mutants were grown in rich medium and transferred to starvation medium (SD-N) to induce autophagy. Cell aliquots were taken at

0, 1, 2 and 4 h, before analyzing the cell extracts by western blot. The detected bands were quantified using the Odyssey software and the percentages of GFP-Atg8 (black) and free GFP (grey) were plotted. Data represent the average of three experiments. B. Mutations in the Atg18 loops 1, 2 and 5 severely affect the Cvt pathway. Wild-type (SEY6210) and *atg18*Δ (JGY3) cells transformed with plasmids expressing the untagged Atg18 loop mutants were grown in rich mediumand cell extracts analysed by western blot using anti-Ape1 antibodies. The detected bands were quantified as in panel A and the percentages of mApe1 were plotted. The graphs represent the average of 3 experiments ± SEM and asterisks indicate a significant difference with the WT (two-tailed *t*-test: $P < 0.05$).

fusion between autophagosomes and the vacuole occurs normally (Darsow et al., 1997). The *atg18*Δ strain expressing wild type Atg18 or the different Atg18 loop mutants were grown in rich medium before being nitrogen starved for 3 h and processed for EM. An average of eight autophagic bodies per vacuole section was found in cells expressing wild type Atg18 (**Figure 4**). As expected, no autophagic bodies were detected in the *atg18*Δ strain. In agreement with the data obtained with the GFP-Atg8 processing assay (**Figure 3A**), the number of autophagic bodies was dramatically decreased in *atg18*Δ cells carrying the Atg18(L2) or the Atg18(L5) construct, indicating a severe impairment in autophagy (**Figure 4**). In addition, the absence of autophagosomes in the cytoplasm of the *atg18*Δ strain expressing Atg18(L2) indicated that this Atg2-binding mutant blocks autophagy at an early stage during the biogenesis of autophagosomes rather than interfering with the fusion of these vesicles with the vacuole.

To unveil the step of autophagosome biogenesis in which the interaction between Atg18 and Atg2 is required, we scrutinized the formation of the PAS by fluorescence microscopy using CFP-tagged Atg8 as a marker protein for this structure (Suzuki et al., 2001). The *atg18*Δ strains carrying both genomically integrated CFP-Atg8 and 13xmyc-tagged wild type Atg18, Atg18(L2) or Atg18(L5) were assessed in both growing and starvation conditions to determine whether the PAS is formed. In accordance with the literature (Suzuki et al., 2007), the recruitment of CFP-Atg8 to this structure seen as a perivacuolar puncta was not affected by the deletion of *ATG18* in the presence or absence of nutrients (**Figure 5A**). CFP-Atg8 also localized to the PAS in cells expressing wild type Atg18 or the loop mutants in all growing conditions (**Figure 5A**). In nutrient-rich conditions no significant differences were detected between the different strains upon quantification of the number of cells displaying a CFP-Atg8-positive punctate structure (**Figure 5B**). Under autophagy conditions, in contrast, expression of the loop mutants led to a clear increase in the number of CFP-Atg8-positive cells compared to wild type Atg18 (**Figure 5B**). A similar result was also obtained in

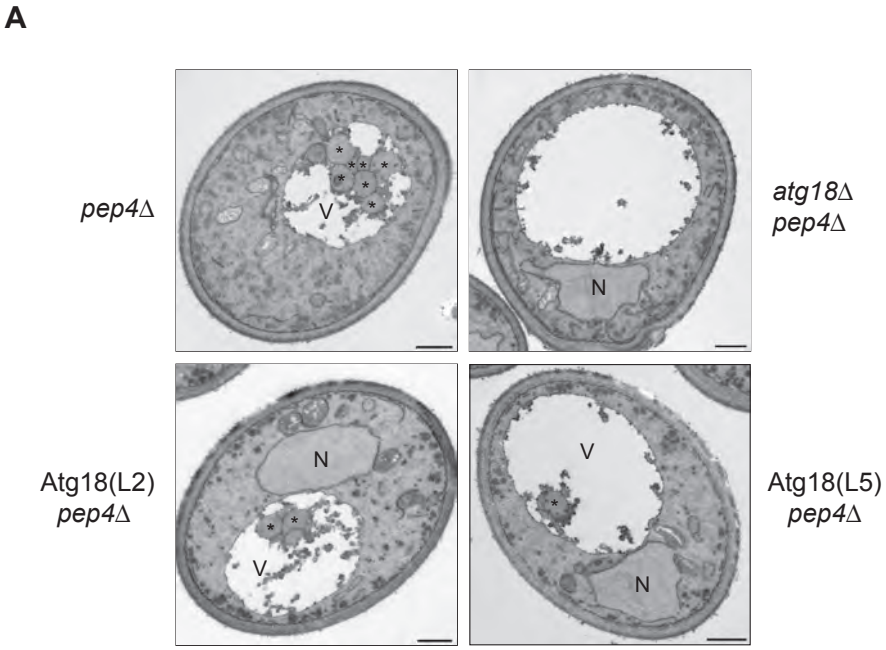

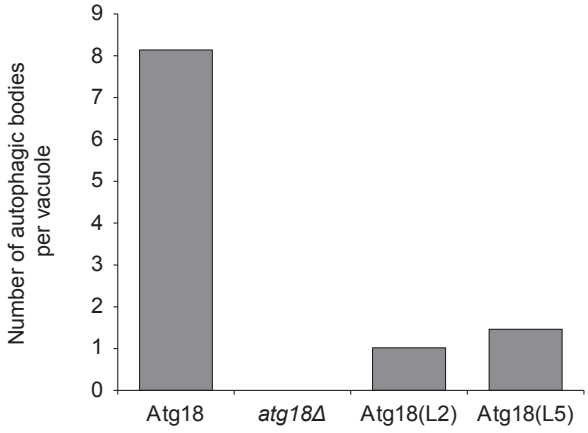

Figure 4. Atg2-binding mutants of Atg18 have a defect in autophagosome biogenesis. A. The Atg2-binding mutant of Atg18 blocks autophagosome biogenesis at an early stage. The *atg18*Δ *pep4*Δ (ERY060) cells carrying one of the plasmids expressing the untagged Atg18 loop mutants 2 or 5 were grown in rich medium and then transferred to SD-N medium for 3 h before processing them for EM. B. Quantification of the autophagic bodies present in the vacuoles. The experiment shown in panel A was quantified as described in *Materials and Methods*, and the results are expressed as the average number of autophagic bodies per vacuole. N, nucleus; V, vacuole; autophagic body: *. Scale bar, 500 nm.

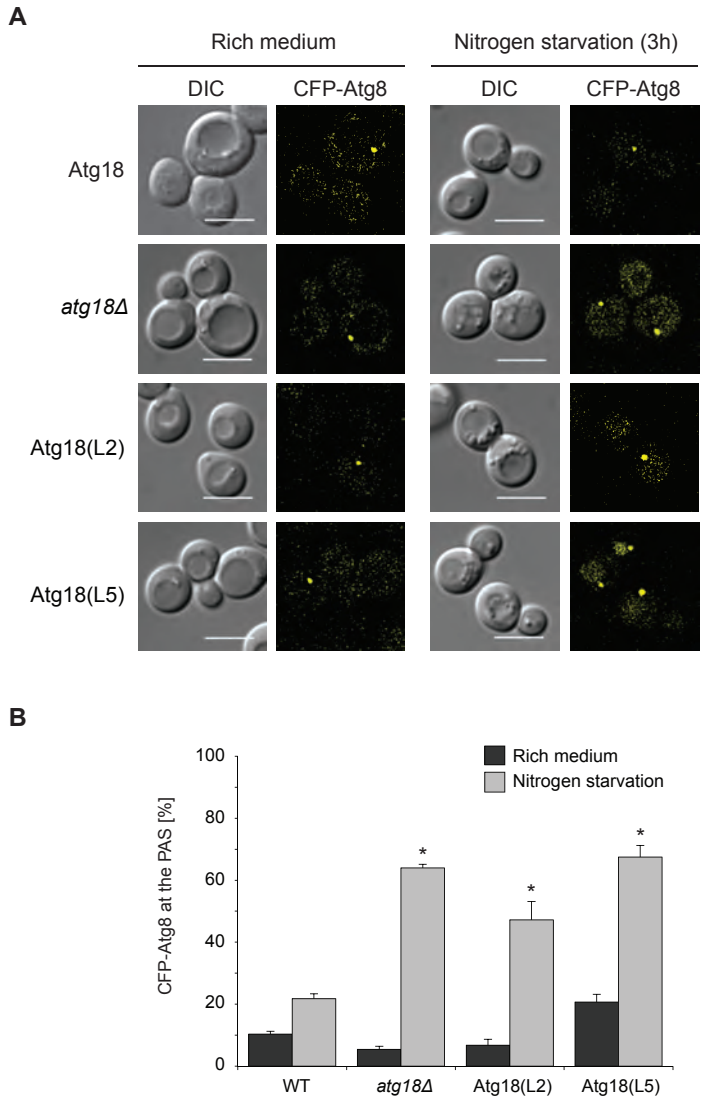

Figure 5. The Atg2-Atg18 interaction is not necessary for PAS formation. A. PAS formation was assessed using CFP-tagged Atg8 as the marker protein. The *atg18*Δ strain with the integrated CFP-Atg8 fusion and carrying no construct (ERY068), 13xmyc-tagged *ATG18* (ERY070) or one of the 13xmyc-tagged *ATG18* loop mutants (ERY072 and ERY074) were grown to an early log phase before being nitrogen starved for 3 h to induce autophagy. Cells were imaged by fluorescence microscopy before and after nitrogen starvation. For clarity the cyan-blue fluorescence signal was converted into yellow. DIC, differential interference contrast. Scale bar, 5 μm. B. Quantification of the percentage of cells with a single CFP-Atg8-positive punctum presented in panel A. Data represent the average of two independent experiments ± SEM and asterisks indicate a significant difference with the WT (two-tailed *t*-test: $P < 0.05$).

the *atg18*Δ knockout. These data show that the interaction between Atg18 and Atg2 is not required for the induction of the PAS formation but rather for the proper organization and function of this structure.

Atg2 is recruited to the PAS independently from Atg18

Next, we asked whether the interaction between Atg2 and Atg18 is required for the recruitment of Atg2 to the PAS as proposed (Obara et al., 2008b; Suzuki et al., 2007). We examined the subcellular distribution of Atg2-GFP in presence of wild type Atg18 or the different loop mutants. As shown in **Figure 6** and as expected (Shintani et al., 2001; Suzuki et al., 2007), Atg2-GFP localized to a single perivacuolar puncta representing the PAS in cells expressing wild type Atg18 in both presence and absence of nitrogen. It has been shown that this distribution depends on Atg18 (Obara et al., 2008b; Suzuki et al., 2007). Unexpectedly, we detected Atg2-GFP at the PAS in both the *atg18*Δ knockout and the *atg18*Δ strain expressing Atg18(L2) (**Figure 6**), suggesting that the recruitment of Atg2 to this site can also occur independently from its interaction with Atg18. While a minor decrease in the number of Atg2-GFP positive structures was observed in cells expressing Atg18(L5), a substantial amount of protein was still found at the PAS.

Atg18 and Atg21 share a high degree of sequence homology and it has been shown that these two proteins are partially redundant in nutrient-rich conditions (Nair et al., 2010). Although Atg21 has a function in Atg8 association with the PAS rather than recruiting Atg2 to the same location (Meiling-Wesse et al., 2004; Stromhaug et al., 2004), we examined whether the Atg2-GFP localization observed in our *atg18*Δ background was due to the presence of Atg21. As shown in **Figure 6**, Atg2-GFP localization was not altered upon deletion of *ATG21* in the *atg18*Δ knockout strain in both nutrient-rich and starvation conditions, indicating that Atg2 recruitment to the PAS can also occur in absence of Atg18 and Atg21.

The Atg2-binding site of Atg18 is essential for Atg18 recruitment to the PAS

We subsequently explored whether Atg18 binding to Atg2 is required for its association to the PAS. As Atg18 localizes to the PAS, endosomes and the vacuole, we labeled the PAS with the mCherry-V5 (mCheV5)-Atg8 chimera to specifically investigate the subpopulation of this protein at this structure. The *atg18*Δ strains carrying both genomically integrated mCheV5-Atg8 and GFP-tagged versions of Atg18 or the different loop mutants were imaged before and after 3 h of nitrogen starvation (**Figure 7** and **Supplementary Figure S2**). Consistent

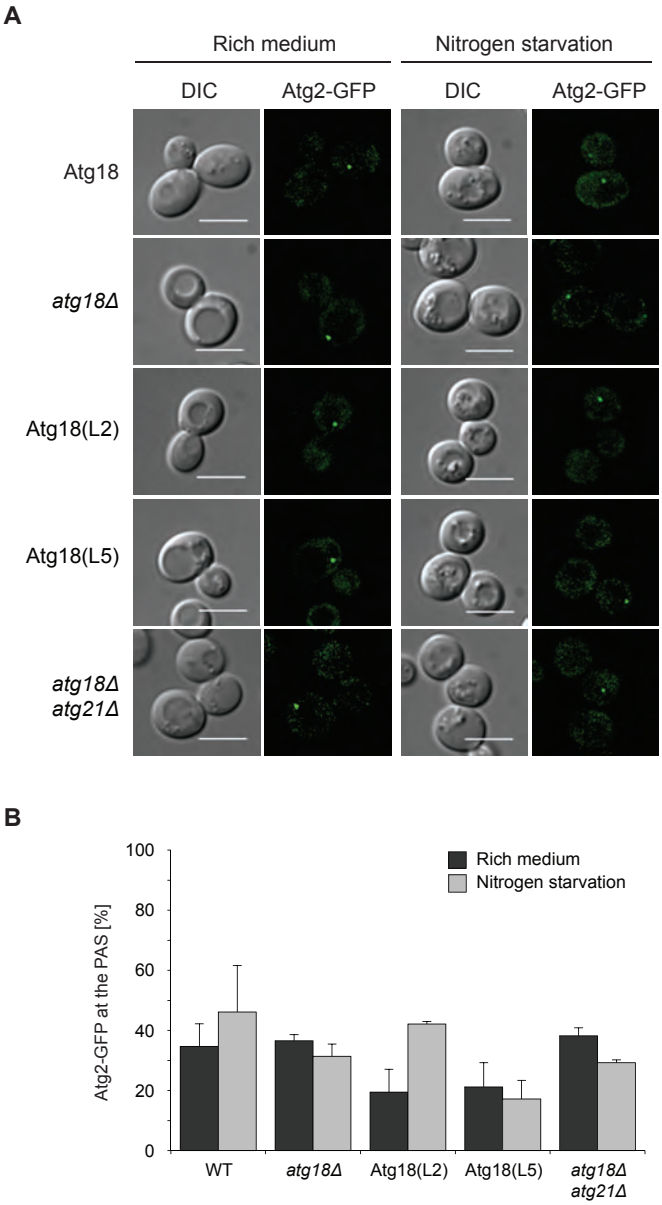

Figure 6. Atg2 association with the PAS does not require Atg18 and/or Atg21. A. Atg2 is recruited in an Atg18- and Atg21-independent manner to the PAS. The atg18D strain expressing endogenous Atg2-GFP and carrying either no other constructs (ERY087), integrated 13xmyc-tagged ATG18 (ERY094) or a 13xmyc-tagged ATG18 loop mutant (ERY095 and ERY097), or the atg18D atg21D strain expressing only endogenous Atg2-GFP (ERY103), were grown to an early log phase before being nitrogen starved for 3 h. Cells were imaged by fluorescence microscopy before and after nitrogen starvation. DIC, differential interference

contrast. Scale bar, 5 µm. B. Quantification of the percentage of cells with a single Atg2-GFP-positive dot presented in panel A. The graph represents the average of two experiments ± SEM and asterisks indicate a significant difference with the WT (two-tailed t-test: $P < 0.05$).

with previous results (Guan et al., 2001; Krick et al., 2008; Obara et al., 2008b), Atg18-GFP was found at the vacuolar membrane and punctuate structures, one of them colocalizing with mCheV5-Atg8 (**Figure 7A**). Wild type Atg18-GFP and mCheV5-Atg8 were colocalizing in 50-60% of the cells in both growing and starvation conditions (**Figure 7B**). This colocalization was almost completely abolished in cells expressing Atg18(L2)-GFP or Atg18 (L5)-GFP to the same extent as in the *atg2*Δ mutant (**Figure 7B**). These data show that the interaction between Atg18 and Atg2 is required for the recruitment of Atg18 to the PAS. They also confirm that Atg18 binding to the PtdIns3P is also crucial for Atg18 association with this structure (Krick et al., 2006; Nair et al., 2010; Obara et al., 2008b).

To determine whether Atg18 binding to Atg2 and phosphoinositides is required for the specific formation of the Atg2-Atg18 complex on the PAS membranes, we turn to the bimolecular fluorescence complementation (BiFC) approach (Sung and Huh, 2007). This assay allows studying *in vivo* protein-protein interactions and it is based on the formation of a fluorescent complex by the C- and N-terminal fragments of Venus, a variant of the yellow fluorescent protein, which are fused to two proteins of interest. An interaction between the two proteins of interest brings them together leading to the reconstitution of the fluorescent protein Venus, which can be visualized by fluorescence microscopy. We created strains expressing solely or in combination Atg2 that was endogenously tagged with the N-terminal fragment of Venus (VN), and Atg18, which was tagged with the C-terminal fragment of Venus (VC). After confirming that the fusion proteins are functional (**Supplementary Figure S3**), cells were imaged before and after 3 h of nitrogen starvation. In both the wild type strain and cells expressing only one of the fusion proteins, no fluorescence signal was detected (**Figure 8A** and not shown). In the strain carrying both Atg2-VN and Atg18-VC, in contrast, a strong BiFC signal concentrating to a single perivacuolar punctuate structure was observed in presence and absence of nitrogen. Atg2 accumulates at the PAS in *atg3*Δ cells but not in *atg13*Δ mutant (Suzuki et al., 2007). When we repeated the experiment in these strains, we observed an increase in the percentage of cells positive for the perivacuolar punctuate BiFC signal in *atg3*Δ cells, and a complete

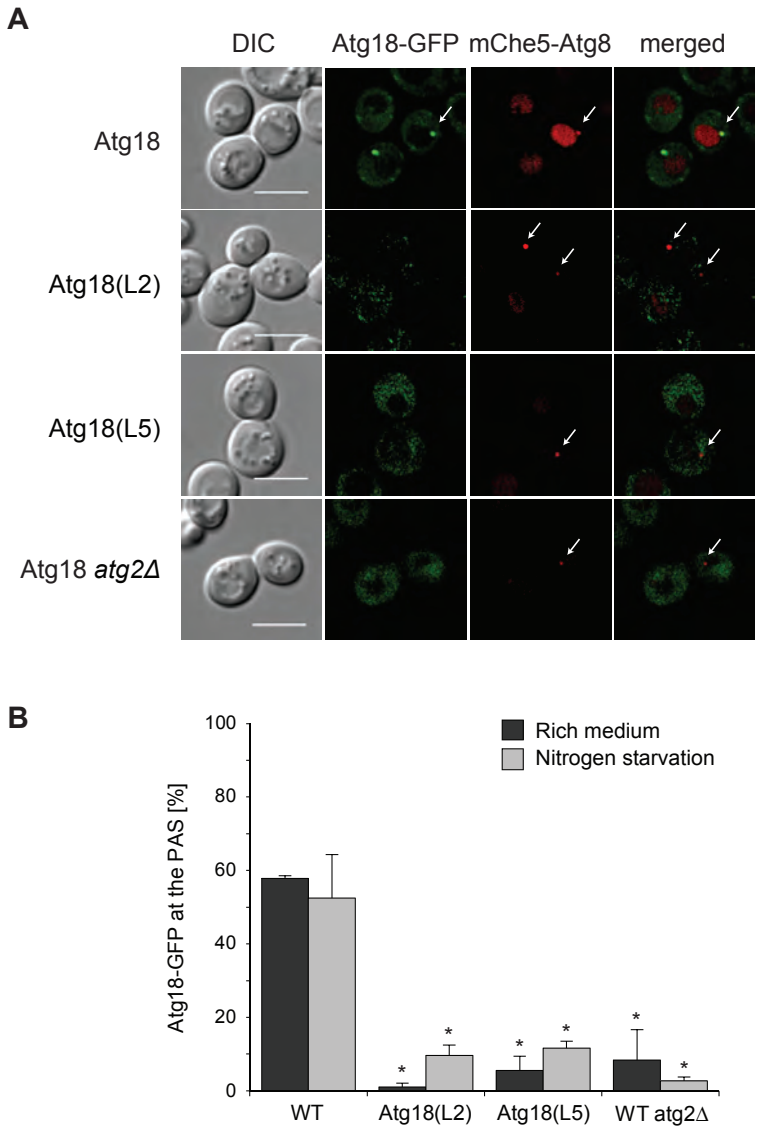

Figure 7. Atg18 binding to Atg2 is essential for its recruitment to the PAS. A. Atg2-binding mutants of Atg18 do not localize to the PAS. The *atg18*Δ strain carrying the mCheV5-Atg8 fusion and genomically integrated GFP-tagged *ATG18* (ERY090) or the GFP-tagged *ATG18* loop mutants 2 or 5 (ERY091 and ERY093), and the *atg18*Δ *atg2*Δ strain carrying GFP-tagged *ATG18* (ERY102) were grown to an early log phase before being nitrogen starved for 3 h to induce autophagy and imaged by fluorescence microscopy. White arrows highlight colocalization of the fluorescence signals. DIC, differential interference contrast. Scale bar, 5 µm. B. Quantification of the percentage of cells with colocalizing puncta presented in panel A and Supplementary Figure S2. All data represent the average of 2 independent experiments ± SEM. Asterisks indicate a significant difference with the WT (two-tailed *t*-test: $P < 0.05$).

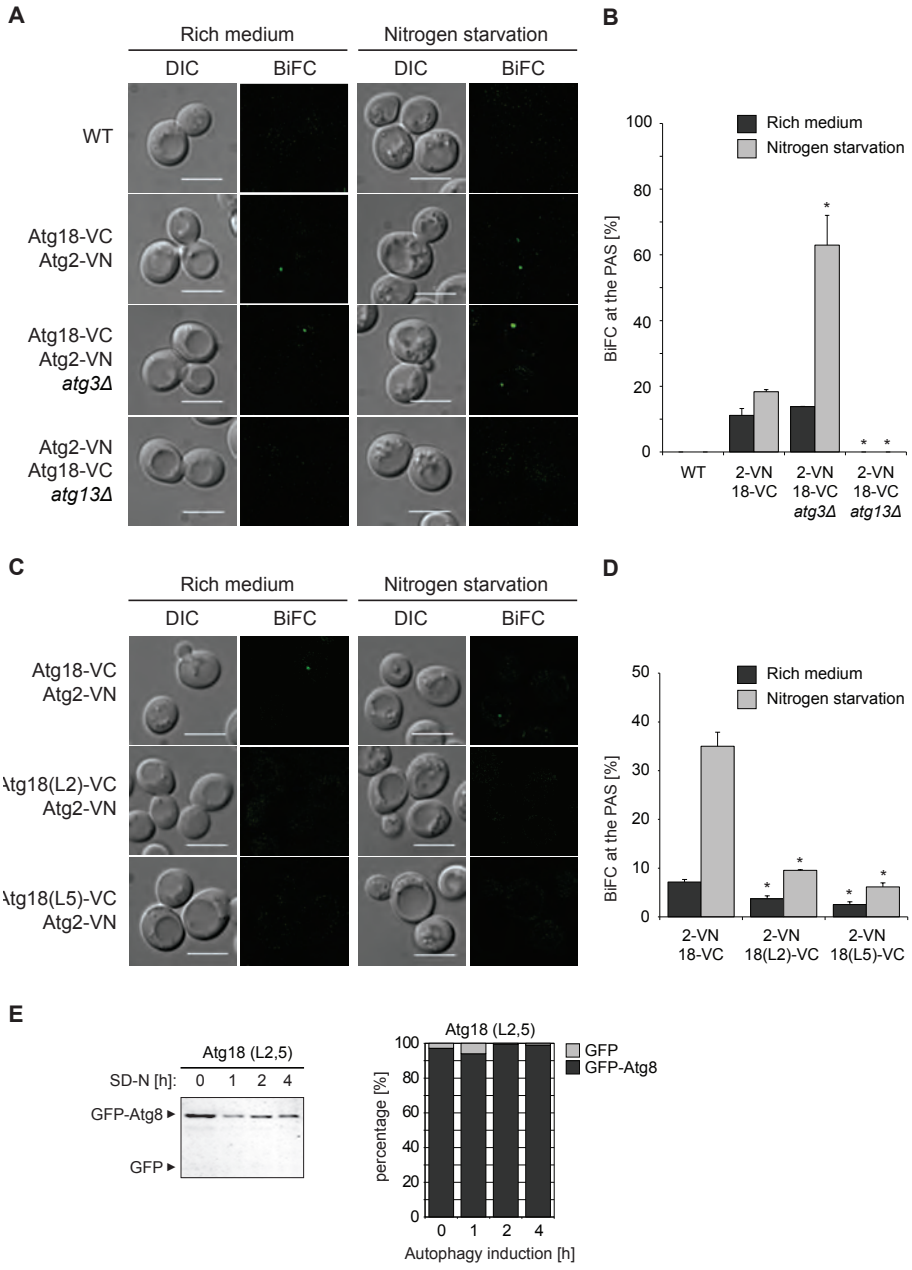

Figure 8. Atg2-Atg18 association at the PAS depends on both the Atg2- and phosphoinositide-binding motifs of Atg18. A. Atg2-Atg18 interaction at the PAS was visualized using the BiFC system. Wild type, *atg3*Δ or *atg13*Δ cells expressing endogenous Atg2-VN and/or Atg18-VC (ERY117, ERY118 and ERY119) were grown in rich medium before being nitrogen starved for 3 h. Fluorescence images were taken before and after nitrogen starvation. DIC, differential interference contrast. Scale bar, 5 µm. B. Quantification of the percentage

of cells analyzed in panel A that are positive for a perivacuolar BiFC punctum. The graph represents the average of 2 experiments ± SEM and asterisks indicate a significant difference with the WT (two-tailed *t*-test: $P < 0.05$). C. Wild type cells expressing endogenous Atg2-VN and Atg18-VC, Atg18(L2)-VC or Atg18(L5)-VC (ERY132, ERY133 and ERY137) were as in panel A. D. Quantification of the percentage of cells positive for a single perivacuolar BiFC punctum analyzed in panel C, and carried out as in panel B. E. Simultaneous defect of Atg18 binding to Atg2 and PtdIns3P completely blocks autophagy. The *atg18*Δ (JGY3) strain transformed with the pCuGFPATG8414 construct and the plasmid expressing untagged Atg18(L2,5) was grown in rich medium and transferred to SD-N medium to induce autophagy. Cell aliquots were taken at 0, 1, 2 and 4 h, before analyzing the cell extracts by western blot. The detected bands were quantified as mentioned earlier and the percentages of GFP-Atg8 (black) and free GFP (grey) were plotted. Data represent the average of two experiments.

loss in *atg13*Δ cells demonstrating that the visualized puncta are PAS (**Figures 8A** and **B**). The same experiment was also performed with both the Atg2-binding mutants Atg18(L2) and Atg18(L5) fused to the VC tag. The frequency of cells displaying the BiFC signal was dramatically reduced in cells expressing Atg2-VN and these two chimeras (**Figures 8C** and **D**). This result shows that the interaction between Atg2 and Atg18 at the PAS requires the specific targeting of Atg18 to this site, which is mediated through the dual recognition of Atg2 and PtdIns3P.

Cells expressing either Atg18(L2) or Atg18(L5) are still able to sustain minimal levels of autophagy (**Figure 4**) and based on our data this could be due to the fact that these two Atg18 mutants are still capable of binding one of the determinants present at the PAS. To prove this hypothesis, we combined the mutations in loop 2 with those of loop 5, creating an Atg18 mutant unable to bind both Atg2 and PtdIns3P, and assessed autophagy in *atg18*Δ cells expressing this construct. As shown in **Figure 8E**, this strain displayed a complete autophagy block. We conclude that the β-propeller plays a key role in mediating the specific association of Atg18 to the PAS by binding two determinants on this structure, namely PtsIns3P and Atg2.

DISCUSSION

The main conclusion of our work is that the β-propeller of Atg18 has a phosphoinositide-binding site that is combined with an organelle-specific binding site, which results in a multiplied affinity and allows the specific recruitment of Atg18 to either the PAS and possibly endosomes and the vacuole. Our findings thus highlight a novel way for localizing multi-purpose adaptor proteins onto different membranes by utilizing the versatile nature of the β-propeller as a platform. In

addition they also suggest a possible mechanism, i.e. dual determinants, assuring that peripheral membrane-associated proteins interacting with lipids, bind to the correct target compartment.

The ß-propeller of Atg18 mediates its interaction with Atg2

Atg18 localizes to the PAS, vacuole and endosomes (Dove et al., 2004; Guan et al., 2001; Krick et al., 2008) and consequently the recruitment of this protein to these organelles has to be tightly regulated to correctly carry out its function. Atg18 association to membranes depends on the presence of either PtdIns3P and/or PtdIns(3,5)P_2. These phosphoinositides are enriched at the PAS, vacuole and endosomes (Gillooly et al., 2000; Obara et al., 2008a), implying that the temporal and spatial regulation of Atg18 localization must depend at least on one other organelle-specific factor. To shed light on the molecular bases underlying Atg18 association to specific membranes, we have investigated its recruitment to the PAS because it is known that this localization also requires its interaction with Atg2 (Obara et al., 2008b).

The computational prediction of the Atg18 structure indicates that this protein folds into a 7-bladed β-propeller, each propeller unit composed of 4-stranded antiparallel β-sheets, which are interconnected via 6 loops (**Figure 9A**). During the preparation of this manuscript, a report describing the structure of Hsv2, a yeast homologue of Atg18 (see below), has been published and confirms this prediction (Baskaran et al., 2012). Loop 5 contains the FRRG motif that based on the Hsv2 model participates most probably in two different binding pockets that bind the phosphorylated lipid headgroups on the target membrane (Baskaran et al., 2012; Dove et al., 2004; Krick et al., 2006). Our data now reveal that one or more amino acids situated in loop 2 mediate Atg18 interaction with Atg2. Both loop 2 and 5 are positioned on the top of the β-propeller and protrude from its surface but they are on opposite sides of the barrel (**Figure 9A**; (Baskaran et al., 2012)). With loop 5 docking the barrel on membrane horizontally, loop 2 will be exposed towards the cytoplasm (Baskaran et al., 2012). As results, it is thus very well possible that the Atg18 β-propeller has the ability to simultaneously bind a phosphoinositide and Atg2, supporting the notion that it could act as a scaffold for the assembly of protein-lipid complexes. While to the best of our knowledge this is the first report of a β-propeller mediating the formation of protein-lipid complexes, other WD40 domain-containing proteins use the loops exposed on the top surface of their β-propeller to interact with multiple binding partners at

the same time. For example, Ski8 plays an essential role in the assembly of a multi-protein complex, which also comprises Ski2 and Ski3, involved in the exosome-dependent mRNA decay, but also in the meiotic recombination by interacting with Spo11. The residues presents in the loops exposed on the top surface of Ski8 β-propeller were found to be important for all these different interactions (Cheng et al., 2004).

Our pull-down experiments show that the residues in loop 2 are predominantly mediating the binding of Atg18 to Atg2. A couple of evidences, however, indicate that specific residues in loop 1 could also be involved in the association between these two proteins. First, the interaction between Atg18 and Atg2 detected using the Y2H assay, where proteins are highly overexpressed, could only be abolished when the mutations in loops 1 and 2 were combined. Second, while the Atg18(L2) mutant is still able to sustain minimal levels of autophagy, the Atg18(L1,2) mutant displays a complete block of this pathway. Loop 1, however, appears to have no major roles in Atg18 binding to both Atg2 and phosphoinositides. Because of its proximity to loop 2 (**Figure 9A**), we cannot exclude that few of the amino acids in loop 1 participate in the binding to Atg2 even if not being essential. Alternatively, loop 1 could be used to regulate the Atg18-Atg2 interaction or other functions of Atg18. This hypothesis is evoked by the observation that the mutations in this stretch of amino acids lead to the appearance of a lower molecular form of Atg18 (**Figure 3A**), indicating that this protein undergoes a post-translational modification. The nature of this post-translational modification is currently under investigation.

Comparison of the amino acid sequence of loop 2 of Atg18 β-propeller with the same region of Atg21 and Hsv2, two yeast proteins highly homologous to Atg18 that also bind phosphoinositides (Krick et al., 2006; Stromhaug et al., 2004), shows almost no conservation (**Figure 9B**). In agreement with this observation, we have not been able to detect an interaction between Atg2 and Atg21 or Hsv2 (not shown). Atg18 is evolutionary related to the mammalian WD40 repeat protein Interacting with PhosphoInositides (WIPI) protein family, which compromises four proteins: WIPI1, WIPI2, WIPI3 and WIPI4 (Jeffries et al., 2004; Proikas-Cezanne et al., 2004). All WIPI proteins are suggested to fold into a 7-bladed β-propeller with an open-velcro configuration, harbouring critical arginine residues for specific phosphoinositide binding (Proikas-Cezanne et al., 2007; Proikas-Cezanne et al., 2004). WIPI1, WIPI2 and WIPI4 have been implicated in autophagy (Lu et al., 2011; Polson et al., 2010; Proikas-Cezanne and Robenek,

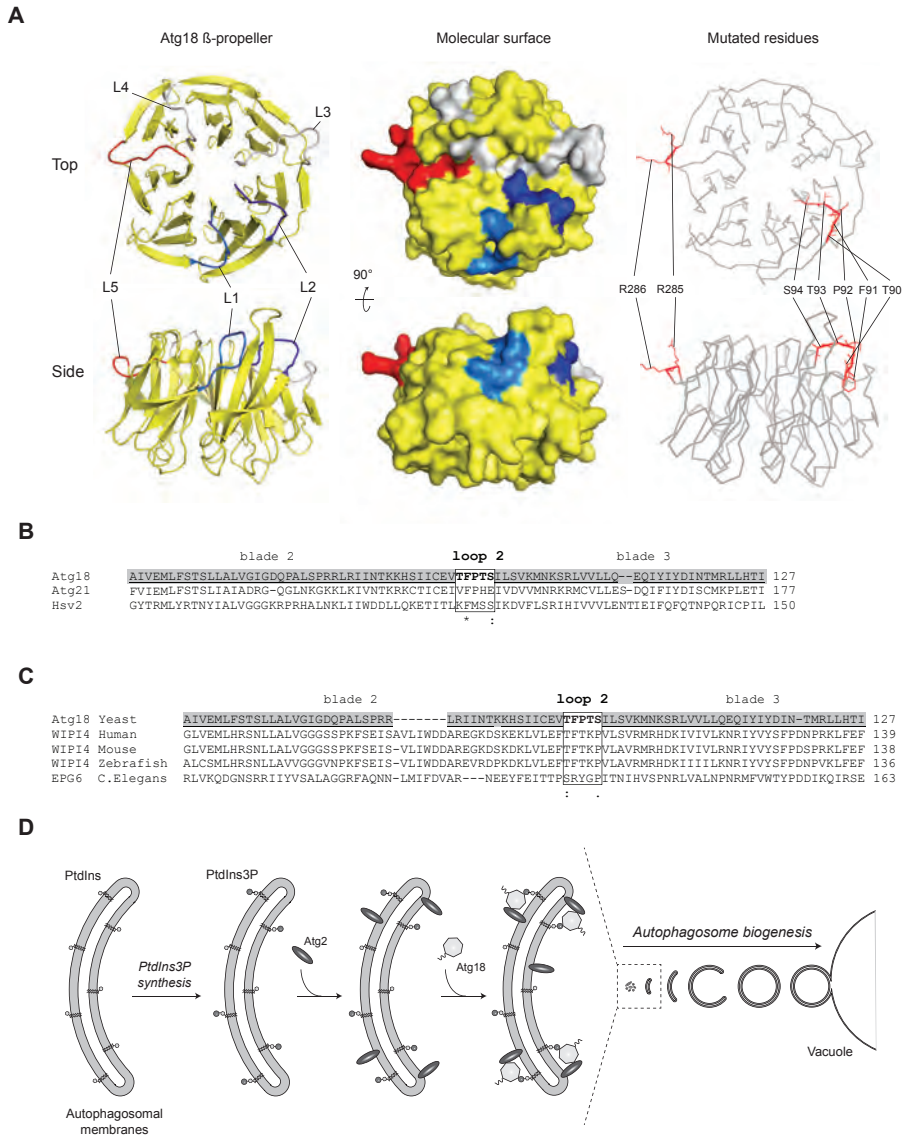

Early stages of the PAS formation

Figure 9. Model for Atg18 ß-propeller function in autophagy. A. Putative structure of the Atg18 β-propeller. On the left, a cartoon view of the predicted structure of the Atg18 β-propeller from the top and side is shown. The blades are colored in yellow, loop 1 in marine blue, loop 2 in dark blue and loop 5 in red. In the middle, the molecular surface of the Atg18 β-propeller is presented with the same colors. On the right, the β-propeller is displayed in line view with the mutated residues in loop 2 and 5 highlighted in red. The FRRG sequence is located in loop 5, whereas the residues important for Atg2-binding are situated in loop 2. The PyMol software (www.pymol.org) was used to generate all the structural projections. B. Alignment of

the amino acid sequence around loop 2 of the β-propeller of Atg18, Atg21 and Hsv2. Part of the amino acid sequences of Atg18, Atg21 and Hsv2 from *S. cerevisiae* were aligned using the ClustalW2 software. Blades 2 and 3 of Atg18 β-propeller are underlined and highlighted in grey. Loop 2 is bordered by a box and the mutated residues are highlighted in bold. C. Alignment of the amino acid sequence around loop 2 of the β-propeller of Atg18 and WIPI4 from various organisms. The amino acid sequences of Atg18, EPG-6 from *C. elegans*, and WIPI4 from *H. sapiens*, *M. musculus*, and *D. rerio*, have been aligned and presented as in Panel B. D. Model for Atg18 recruitment to the PAS. At an early stage of the PAS formation, PtdIns is converted into PtdIns3P by the PtdIns 3-kinase complex I. This lipid is essential for the subsequent association of Atg2 to this structure. Presence of PtdIns3P and Atg2 on the autophagosomal membrane triggers the recruitment of Atg18 through its β-propeller. It is presently unclear whether these events occur on the phagophore or on another precursor membrane.

2011; Proikas-Cezanne et al., 2004), inciting a debate about which one of them is the functional Atg18 orthologue. Recently, two mammalian Atg2 homologs, Atg2A and Atg2B, have been identified and both are required for autophagy (Velikkakath et al., 2012). Interestingly, human WIPI4 interacts with Atg2A and Atg2B as well as *C. elegans* EPG-6/WIPI4 with ATG-2 (Behrends et al., 2010; Lu et al., 2011). These observations suggest that WIPI4/EPG-6 and yeast Atg18 overlap in their role in autophagy by carrying out the functional interconnections with Atg2. The amino acid sequence alignment of loop 2 of the Atg18 β-propeller with that of various WIPI4 proteins from different species supports this idea, because several amino acids are well conserved except for *C. elegans* EPG-6 (**Figure 9C**). The ATG-2 binding site of EPG-6 has been mapped to the fifth and sixth blades of the EPG-6 β-propeller, and this could explain the lack of amino acid conservation in loop 2 of EPG-6 β-propeller (Lu et al., 2011). This binding region was identified by sequential deletion of the blades and therefore it cannot be excluded that this type of approach leads to a complete disruption of the β-propeller structure making the interpretation of this result difficult. Additional experiments are necessary to address the bases of this divergence.

The mechanism of Atg18 recruitment to the PAS

Similarly to the mutant form of Atg18 that is unable to bind phosphoinositides, the one blocking the interaction between Atg18 and Atg2, i.e. Atg18(L2), severely impairs the progression of non-selective and selective autophagy by affecting an early stage of autophagosome biogenesis. In both situations, this defect is caused by the inability these two mutant proteins to be recruited to the PAS. The two binding capacities of Atg18 β-propeller, however, appear to not be reciprocally regulated but rather independent. That is, mutation of the FRRG motif within loop 5 does not affect the interaction between Atg18 and Atg2, and conversely

the Atg2-binding mutant of Atg18 is capable of binding phosphoinositides. The fact that cells expressing either Atg18(L2) or Atg18(L5) are still able to sustain minimal levels of autophagy supports this notion as Atg18 is still capable of binding one of the determinants present at the PAS via either loop 5 or 2, respectively. Indeed, when we combined the two sets of mutations, creating an Atg18 mutant unable to bind both Atg2 and PtdIns3P, we observed a complete autophagy block.

Based on our observations, we propose the following mechanistic model for Atg18 recruitment to the PAS (**Figure 9D**). Upon induction of the formation of a double-membrane vesicle, one of the first events during the organisation of this specialized site is the association of the phosphatidylinositol-3 kinase complex I to it (Suzuki et al., 2007), which presumably starts synthesizing PtdIns3P. As reported (Shintani et al., 2001; Suzuki et al., 2007), the phosphatidylinositol-3 kinase complex I and/or PtdIns3P are required for the recruitment of Atg2 to the PAS. So far, we have not been able to determine whether Atg2 binds PtdIns3P. Therefore, we do not known whether this protein directly, or indirectly through another factor, interacts with this lipid to associate with the PAS. Nevertheless, the simultaneous presence of PtdIns3P and Atg2 at this location allows the Atg18 β-propeller to bind to this structure with high affinity, and subsequently forms the Atg18-Atg2 complex. Our fluorescence microscopy data support this model, because they show that Atg2 is recruited to the PAS independently from Atg18. Furthermore, the BiFC experiments indicate that the Atg2-Atg18 interaction occurs at this site.

Our results are in part contradictory with the published literature, which indicate that Atg18 and Atg2 form a cytoplasmic complex that is recruited as a unit to the PAS and Atg2 fails to associate with this structure in absence of *ATG18* (Obara et al., 2008b; Suzuki et al., 2007). The assumption that Atg2 and Atg18 form a cytoplasmic complex is based on data showing that upon gel filtration of solubilized cell extracts,Atg2 is not detected as a monomer but rather in a complex of approximately 500 kDa, and part of Atg18 is in the same fraction (Obara et al., 2008b). We fractionated proteins and protein complexes present in solubilized cell extracts from a wild type strain expressing endogenously PA-tagged Atg2 on a continuous 10-50 % glycerol gradient (**Supplementary Figures S4A** and **S4B**). We did not observe an evident difference in the distribution of Atg2 over the gradient in presence or absence of Atg18. To substantiate this observation, we also overexpressed Atg2 with or without Atg18. Overexpression of both proteins resulted in very similar fractionation profiles as with the endogenous

proteins (**Supplementary Figures S4C** and **S4D**). The absence of Atg18 did not influence the fractionation profile of overexpressed Atg2, indicating that the apparent high molecular weight of Atg2 is due to some structural characteristics of this protein and/or self-interaction. While we cannot exclude that Atg2 and Atg18 can also form a cytoplasmic complex under certain circumstances, we currently ascribe the observed differences to a more sensitive strain background or experimental conditions. Alternatively, a yet unidentified factor, which depends on Atg18, mediates the functional Atg2-Atg18 interaction and this is at least in some circumstances reflected by our experimental setup.

Alternative models or variations of the proposed one describing the Atg18 recruitment to the PAS can also be contemplated. Therefore, additional studies are necessary to fully understand the regulation of this event and the unique property of the Atg18 β-propeller to form lipid-protein complexes. This information will also be crucial to understand the function of Atg18 in autophagy.

ACKNOWLEDGMENTS

The authors thank Daniel Klionsky for reagents and Janice Griffith for technical assistance. F.R. is supported by the ZonMW-VIDI (917.76.329), ECHO (700.59.003), ALW Open Program (821.02.017) and DFG-NWO cooperation (DN82-303/UN111/7-1, together with C.U.) grants. T.P.-C. is supported by the DFG SFB 773 (A3).

REFERENCES

1. Barth, H., K. Meiling-Wesse, U.D. Epple, and M. Thumm. 2001. Autophagy and the cytoplasm to vacuole targeting pathway both require Aut10p. *FEBS Lett.* 508:23-28.
2. Baskaran, S., M.J. Ragusa, E. Boura, and J.H. Hurley. 2012. Two-Site Recognition of Phosphatidylinositol 3-Phosphate by PROPPINs in Autophagy. *Mol Cell*.
3. Behrends, C., M.E. Sowa, S.P. Gygi, and J.W. Harper. 2010. Network organization of the human autophagy system. *Nature*. 466:68-76.
4. Chen, S., B.D. Spiegelberg, F. Lin, E.J. Dell, and H.E. Hamm. 2004. Interaction of GβY with RACK1 and other WD40 repeat proteins. *J Mol Cell Cardiol*. 37:399-406.
5. Cheng, Z., Y. Liu, C. Wang, R. Parker, and H. Song. 2004. Crystal structure of Ski8p, a WD-repeat protein with dual roles in mRNA metabolism and meiotic recombination. *Protein Sci.* 13:2673-2684.
6. Cheong, H., and D.J. Klionsky. 2008. Biochemical methods to monitor autophagy-related processes in yeast. *Methods Enzymol.* 451:1-26.
7. Darsow, T., S.E. Rieder, and S.D. Emr. 1997. A multispecificity syntaxin homologue, Vam3p, essential for autophagic and biosynthetic protein transport to the vacuole. *J Cell Biol.* 138:517-529.
8. Dove, S.K., R.C. Piper, R.K. McEwen, J.W. Yu, M.C. King, D.C. Hughes, J. Thuring, A.B. Holmes, F.T. Cooke, R.H. Michell, P.J. Parker, and M.A. Lemmon. 2004. Svp1p defines a family of phosphatidylinositol 3,5-bisphosphate effectors. *EMBO J.* 23:1922-1933.
9. Efe, J.A., R.J. Botelho, and S.D. Emr. 2007. Atg18 regulates organelle morphology and Fab1 kinase activity independent of its membrane recruitment by phosphatidylinositol 3,5-bisphosphate. *Mol Biol Cell.* 18:4232-4244.
10. Gillooly, D.J., I.C. Morrow, M. Lindsay, R. Gould, N.J. Bryant, J.M. Gaullier, R.G. Parton, and H. Stenmark. 2000. Localization of phosphatidylinositol 3-phosphate in yeast and mammalian cells. *EMBO J.* 19:4577-4588.
11. Guan, J., P.E. Stromhaug, M.D. George, P. Habibzadegah-Tari, A. Bevan, W.A. Dunn, Jr., and D.J. Klionsky. 2001. Cvt18/Gsa12 is required for cytoplasm-to-vacuole transport, pexophagy, and autophagy in *Saccharomyces cerevisiae* and *Pichia pastoris*. *Mol Biol Cell.* 12:3821-3838.
12. Gueldener, U., J. Heinisch, G.J. Koehler, D. Voss, and J.H. Hegemann. 2002. A second set of loxP marker cassettes for Cre-mediated multiple gene knockouts in budding yeast. *Nucleic Acids Res.* 30:e23.
13. Itakura, E., and N. Mizushima. 2010. Characterization of autophagosome formation site by a hierarchical analysis of mammalian Atg proteins. *Autophagy*. 6:764-776.
14. James, P., J. Halladay, and E.A. Craig. 1996. Genomic libraries and a host strain designed for highly efficient two-hybrid selection in yeast. *Genetics*. 144:1425-1436.
15. Jeffries, T.R., S.K. Dove, R.H. Michell, and P.J. Parker. 2004. PtdIns-specific MPR pathway association of a novel WD40 repeat protein, WIPI49. *Mol Biol Cell.* 15:2652-2663.
16. Jin, N., C.Y. Chow, L. Liu, S.N. Zolov, R. Bronson, M. Davisson, J.L. Petersen, Y. Zhang, S. Park, J.E. Duex, D. Goldowitz, M.H. Meisler, and L.S. Weisman. 2008. Vac14 nucleates a protein complex essential for the acute interconversion of PI3P and PI(3,5)P(2) in yeast and mouse. *EMBO J.* 27:3221-3234.
17. Kihara, A., T. Noda, N. Ishihara, and Y. Ohsumi. 2001. Two distinct Vps34 phosphatidylinositol 3-kinase complexes function in autophagy and carboxypeptidase Y sorting in Saccharomyces cerevisiae. *J Cell Biol.* 152:519-530.

18. Kim, J., W.P. Huang, P.E. Stromhaug, and D.J. Klionsky. 2002. Convergence of multiple autophagy and cytoplasm to vacuole targeting components to a perivacuolar membrane compartment prior to de novo vesicle formation. *J Biol Chem*. 277:763-773.

19. Klionsky, D.J. 2007. Autophagy: from phenomenology to molecular understanding in less than a decade. *Nat Rev Mol Cell Biol*. 8:931-937.

20. Krick, R., S. Henke, J. Tolstrup, and M. Thumm. 2008. Dissecting the localization and function of Atg18, Atg21 and Ygr223c. *Autophagy*. 4:896-910.

21. Krick, R., J. Tolstrup, A. Appelles, S. Henke, and M. Thumm. 2006. The relevance of the phosphatidylinositolphosphat-binding motif FRRGT of Atg18 and Atg21 for the Cvt pathway and autophagy. *FEBS Lett*. 580:4632-4638.

22. Longtine, M.S., A. McKenzie, 3rd, D.J. Demarini, N.G. Shah, A. Wach, A. Brachat, P. Philippsen, and J.R. Pringle. 1998. Additional modules for versatile and economical PCR-based gene deletion and modification in *Saccharomyces cerevisiae*. *Yeast*. 14:953-961.

23. Lu, Q., P. Yang, X. Huang, W. Hu, B. Guo, F. Wu, L. Lin, A.L. Kovacs, L. Yu, and H. Zhang. 2011. The WD40 repeat PtdIns(3)P-binding protein EPG-6 regulates progression of omegasomes to autophagosomes. *Dev Cell*. 21:343-357.

24. Lynch-Day, M.A., and D.J. Klionsky. 2010. The Cvt pathway as a model for selective autophagy. *FEBS Lett*. 584:1359-1366.

25. Mari, M., J. Griffith, E. Rieter, L. Krishnappa, D.J. Klionsky, and F. Reggiori. 2010. An Atg9-containing compartment that functions in the early steps of autophagosome biogenesis. *J Cell Biol*. 190:1005-1022.

26. Mari, M., and F. Reggiori. 2010. Atg9 reservoirs, a new organelle of the yeast endomembrane system? *Autophagy*. 6:1221-1223.

27. Meiling-Wesse, K., H. Barth, C. Voss, E.L. Eskelinen, U.D. Epple, and M. Thumm. 2004. Atg21 is required for effective recruitment of Atg8 to the preautophagosomal structure during the Cvt pathway. *J Biol Chem*. 279:37741-37750.

28. Michell, R.H., and S.K. Dove. 2009. A protein complex that regulates PtdIns(3,5)P2 levels. *EMBO J*. 28:86-87.

29. Mizushima, N., B. Levine, A.M. Cuervo, and D.J. Klionsky. 2008. Autophagy fights disease through cellular self-digestion. *Nature*. 451:1069-1075.

30. Nair, U., Y. Cao, Z. Xie, and D.J. Klionsky. 2010. Roles of the lipid-binding motifs of Atg18 and Atg21 in the cytoplasm to vacuole targeting pathway and autophagy. *J Biol Chem*. 285:11476-11488.

31. Nakatogawa, H., K. Suzuki, Y. Kamada, and Y. Ohsumi. 2009. Dynamics and diversity in autophagy mechanisms: lessons from yeast. *Nat Rev Mol Cell Biol*. 10:458-467.

32. Obara, K., T. Noda, K. Niimi, and Y. Ohsumi. 2008a. Transport of phosphatidylinositol 3-phosphate into the vacuole via autophagic membranes in *Saccharomyces cerevisiae*. *Genes Cells*. 13:537-547.

33. Obara, K., T. Sekito, K. Niimi, and Y. Ohsumi. 2008b. The Atg18-Atg2 complex is recruited to autophagic membranes via phosphatidylinositol 3-phosphate and exerts an essential function. *J Biol Chem*. 283:23972-23980.

34. Paoli, M. 2001. Protein folds propelled by diversity. *Prog Biophys Mol Biol*. 76:103-130.

35. Pashkova, N., L. Gakhar, S.C. Winistorfer, L. Yu, S. Ramaswamy, and R.C. Piper. 2010. WD40 repeat propellers define a ubiquitin-binding domain that regulates turnover of F box proteins. *Mol Cell*. 40:433-443.

36. Polson, H.E., J. de Lartigue, D.J. Rigden, M. Reedijk, S. Urbe, M.J. Clague, and S.A. Tooze. 2010. Mammalian Atg18 (WIPI2) localizes to omegasome-anchored phagophores and positively regulates LC3 lipidation. *Autophagy*. 6:506-522.

37. Proikas-Cezanne, T., and H. Robenek. 2011. Freeze-fracture replica immunolabelling reveals human WIPI-1 and WIPI-2 as membrane proteins of autophagosomes. *Journal of cellular and molecular medicine*. 15:2007-2010.

38. Proikas-Cezanne, T., S. Ruckerbauer, Y.D. Stierhof, C. Berg, and A. Nordheim. 2007. Human WIPI-1 puncta-formation: a novel assay to assess mammalian autophagy. *FEBS Lett*. 581:3396-3404.

39. Proikas-Cezanne, T., S. Waddell, A. Gaugel, T. Frickey, A. Lupas, and A. Nordheim. 2004. WIPI-1alpha (WIPI49), a member of the novel 7-bladed WIPI protein family, is aberrantly expressed in human cancer and is linked to starvation-induced autophagy. *Oncogene*. 23:9314-9325.

40. Ravid, T., and M. Hochstrasser. 2008. Diversity of degradation signals in the ubiquitin-proteasome system. *Nat Rev Mol Cell Biol*. 9:679-690.

41. Reggiori, F., C.W. Wang, P.E. Stromhaug, T. Shintani, and D.J. Klionsky. 2003. Vps51 is part of the yeast Vps fifty-three tethering complex essential for retrograde traffic from the early endosome and Cvt vesicle completion. *J Biol Chem*. 278:5009-5020.

42. Shintani, T., K. Suzuki, Y. Kamada, T. Noda, and Y. Ohsumi. 2001. Apg2p functions in autophagosome formation on the perivacuolar structure. *J Biol Chem*. 276:30452-30460.

43. Sikorski, R.S., and P. Hieter. 1989. A system of shuttle vectors and yeast host strains designed for efficient manipulation of DNA in *Saccharomyces cerevisiae*. *Genetics*. 122:19-27.

44. Smith, T.F., C. Gaitatzes, K. Saxena, and E.J. Neer. 1999. The WD repeat: a common architecture for diverse functions. *Trends Biochem Sci*. 24:181-185.

45. Stromhaug, P.E., F. Reggiori, J. Guan, C.W. Wang, and D.J. Klionsky. 2004. Atg21 is a phosphoinositide binding protein required for efficient lipidation and localization of Atg8 during uptake of aminopeptidase I by selective autophagy. *Mol Biol Cell*. 15:3553-3566.

46. Sung, M.K., and W.K. Huh. 2007. Bimolecular fluorescence complementation analysis system for in vivo detection of protein-protein interaction in *Saccharomyces cerevisiae*. *Yeast*. 24:767-775.

47. Suzuki, K., T. Kirisako, Y. Kamada, N. Mizushima, T. Noda, and Y. Ohsumi. 2001. The pre-autophagosomal structure organized by concerted functions of *APG* genes is essential for autophagosome formation. *EMBO J*. 20:5971-5981.

48. Suzuki, K., Y. Kubota, T. Sekito, and Y. Ohsumi. 2007. Hierarchy of Atg proteins in pre-autophagosomal structure organization. *Genes Cells*. 12:209-218.

49. Takeshige, K., M. Baba, S. Tsuboi, T. Noda, and Y. Ohsumi. 1992. Autophagy in yeast demonstrated with proteinase-deficient mutants and conditions for its induction. *J Cell Biol*. 119:301-311.

50. van der Vaart, A., J. Griffith, and F. Reggiori. 2010. Exit from the Golgi is required for the expansion of the autophagosomal phagophore in yeast *Saccharomyces cerevisiae*. *Mol Biol Cell*. 21:2270-2284.

51. Velikkakath, A.K., T. Nishimura, E. Oita, N. Ishihara, and N. Mizushima. 2012. Mammalian Atg2 proteins are essential for autophagosome formation and important for regulation of size and distribution of lipid droplets. *Mol Biol Cell*. 23:896-909.

SUPPLEMENTARY FIGURES

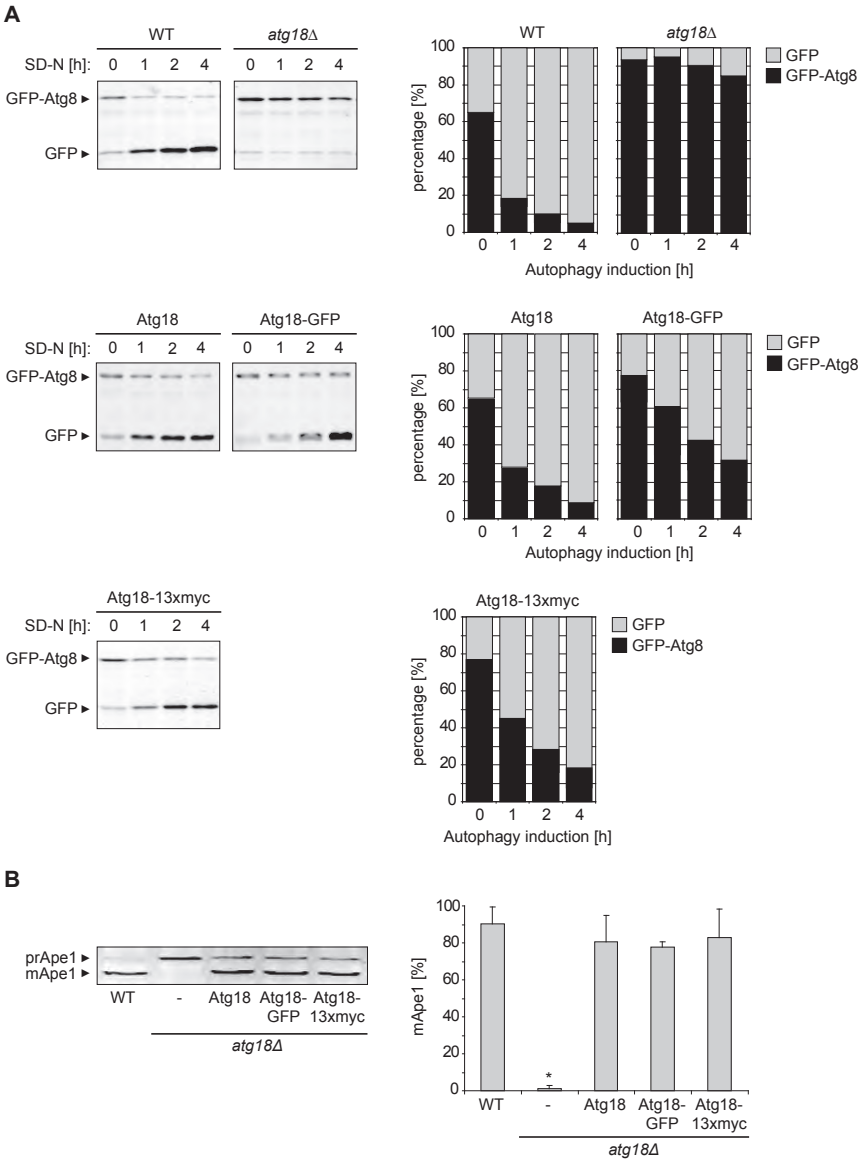

Supplementary Figure 1. GFP- and myc-tagged wild type Atg18 is functional. A. Wild type (SEY6210) and *atg18*Δ (JGY3) cells carrying both the pCuGFPATG8414 construct and either the plasmid expressing untagged, myc-tagged or GFP-tagged wild type Atg18 under the control of the endogenous promoter were grown in rich medium to an early log phase and transferred to starvation SD-N medium to induce autophagy. Cell aliquots were taken at 0, 1, 2 and 4 h, before analyzing the cell extracts by western blot using an antibody against GFP. The detected bands were quantified using the Odyssey software and the percentages of

GFP-Atg8 (black) and free GFP (grey) were plotted. B. Wild-type (SEY6210) and *atg18*Δ (JGY3) cells transformed with plasmids expressing the untagged, myc-tagged or GFP-tagged wild type Atg18 were grown in rich medium to an early log phase. Cell aliquots were collected and cell extracts analysed by western-blot using anti-Ape1 antibodies. The detected bands were quantified as in panel A and the percentages of mApe1 were plotted. The graphs represent the average of 2 experiments ± SEM and asterisks indicate a significant difference with the WT (*$P < 0.05$).

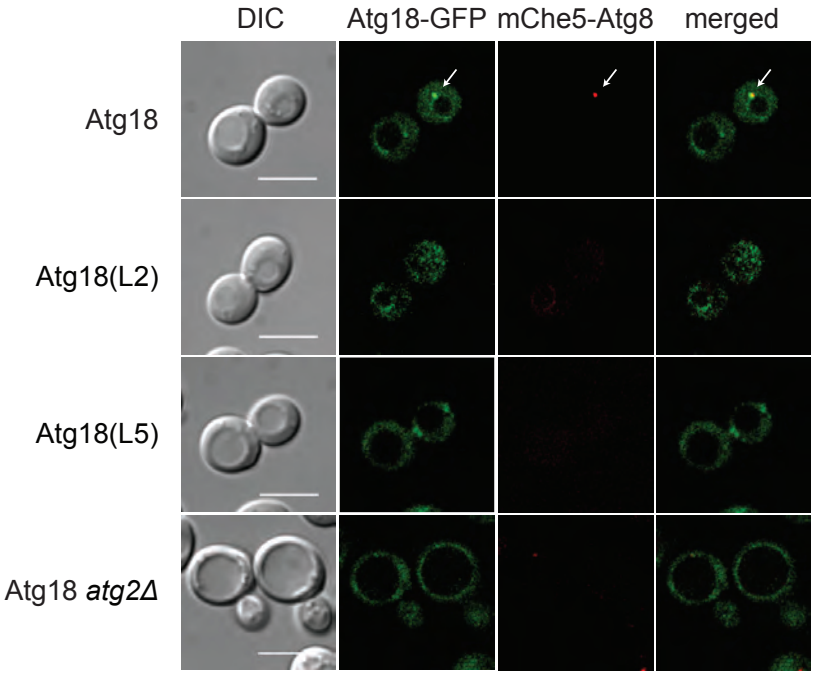

Supplementary Figure 2. Atg2-binding mutants of Atg18 do not localize to the PAS in growing conditions. The *atg18*Δ strain carrying the mCheV5-Atg8 fusion and genomically integrated GFP-tagged *ATG18* (ERY090) or the different GFP-tagged *ATG18* loop mutants (ERY091 and ERY093) and the *atg18*Δ *atg2*Δ strain carrying GFP-tagged *ATG18* (ERY102) were grown to an early log phase and imaged by fluorescence microscopy. White arrows highlight colocalization of the fluorescence signals. DIC, differential interference contrast. Scale bar, 5 µm. The quantification of the percentage of cells with colocalizing puncta is presented in Figure 6B.

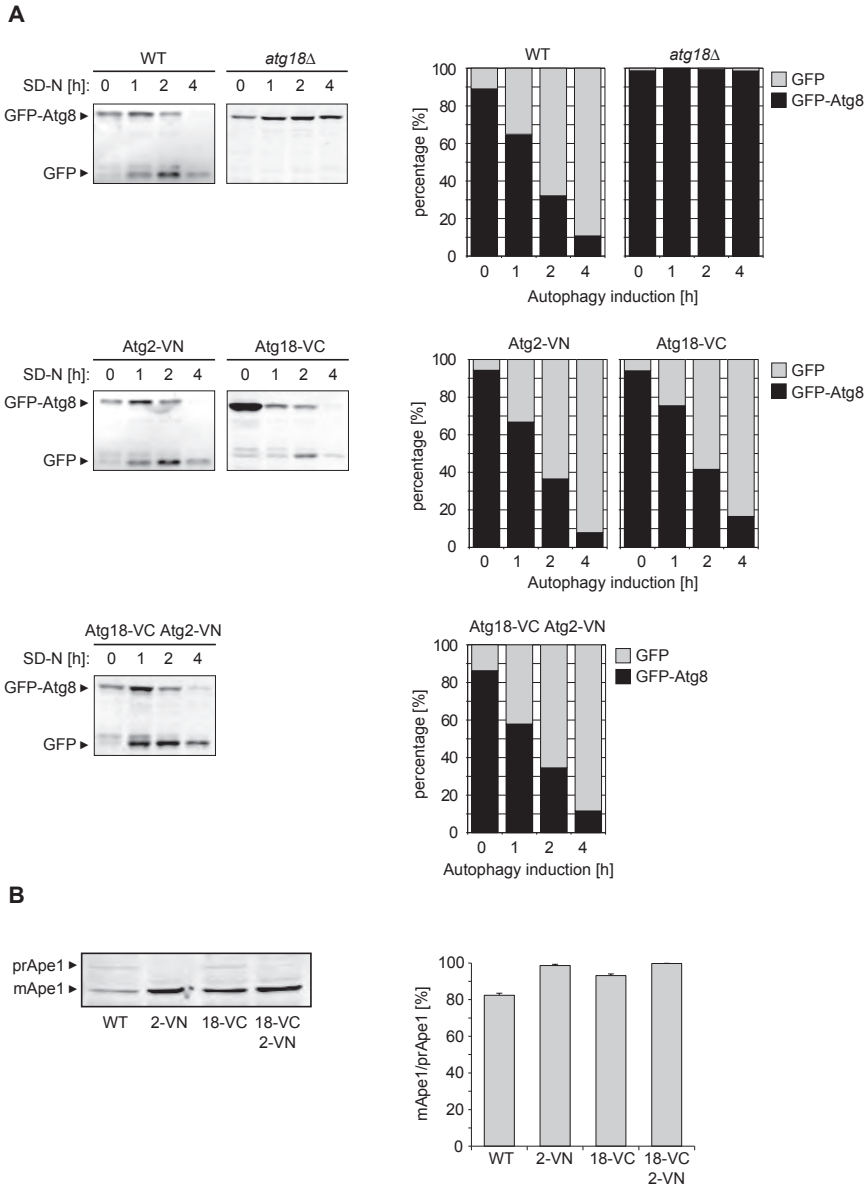

Supplementary Figure 3. VN-tagged Atg2 and VC-tagged Atg18 fusion proteins are functional for the Cvt pathway and autophagy. A. Wild type cells and cells expressing endogenous Atg2-VN and/or Atg18-VC (ERY115, ERY116, and ERY117) carrying the pCuGFPATG8414 construct were grown in rich medium to an early log phase and transferred into SD-N medium to induce autophagy. Cell aliquots were taken at 0, 1, 2 and 4 h, before analyzing the cell extracts by western blot using an antibody against GFP. The detected bands were quantified using the Odyssey software and the percentages of GFP-Atg8 (black) and free

GFP (grey) were plotted. B. Wild type cells expressing endogenous Atg2-VN and/or Atg18-VC (ERY115, ERY116 and ERY117) were grown in rich medium to an early log phase. Cell aliquots were collected and cell extracts analysed by western blot using anti-Ape1 antibodies. The detected bands were quantified as in panel A and the percentage of mApe1 was plotted. The graphs represent the average of 2 experiments ± SEM and asterisks indicate a significant difference with the WT (*$P < 0.05$).

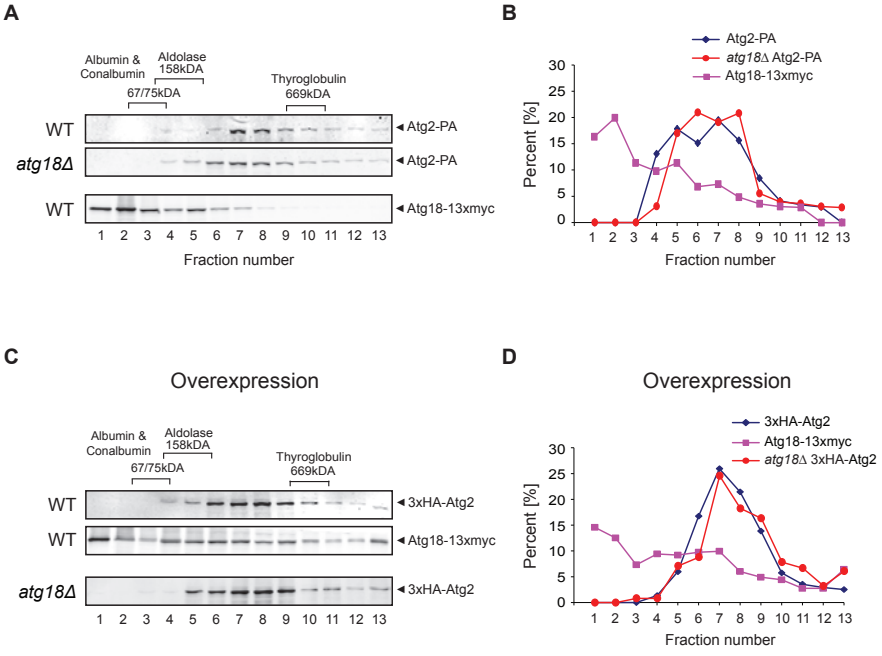

Supplementary Figure 4. Analysis of endogenous and overexpressed Atg2 and Atg18 on continuous glycerol gradients. A. Analysis of Atg2 and Atg18 on continuous glycerol gradients. Cell lysates from Atg2-PA-expressing *atg18*Δ strain (ERY086) carrying endogenously 13xmyc-tagged Atg18 were fractionated on 10-15% glycerol gradients as described in *Materials and methods*. For each gradient 13 fractions were collected, resolved by SDS-PAGE and analyzed by western blot using antibodies against myc and PA. B. Quantification of the immunoblots presented in panel A. The graphs represent the average of 2 experiments. C. The *atg18*Δ strain overexpressing 3xHA-Atg2 (ERY052), and either untransformed or transformed with a plasmid expressing wild type *ATG18* tagged with 13xmyc under the control of the *GAL1* promoter, was grown on galactose for 3 h to induce protein overexpression. Cell lysates were fractionated on 10-15% glycerol gradients and analyzed using antibodies against HA and myc. D. Quantification of the immunoblots presented in panel C. The graphs represent the average of two experiments.

Supplementary Table S1. Strains used in this study

Name	Genotype	Reference / Origin
atg18Δ	BY4742 *atg18Δ::kanMX4*	Euroscarf
BY4742	*MATa his3Δ1 leu2Δ0 lys2Δ0 ura3Δ0*	Euroscarf
ERY052	BY4247 *atg18Δ::kanMX4 HIS3MX6::pGAL1-3HA-ATG2*	This study
ERY060	SEY6210 *atg18Δ::HIS5 S.p. pep4Δ::LEU2*	This study
ERY068	SEY6210 *atg18Δ::HIS5 S.p. CFP-ATG8::URA3*	This study
ERY070	SEY6210 *atg18Δ::HIS5 S.p. CFP-ATG8::URA3 ATG18-13xmyc::LEU2*	This study
ERY072	SEY6210 *atg18Δ::HIS5 S.p CFP-ATG8::URA3 ATG18(L2)-13xmyc::LEU2*	This study
ERY074	SEY6210 *atg18Δ::HIS5 S.p. CFP-ATG8::URA3 ATG18(L5)-13xmyc::LEU2*	This study
ERY086	SEY6210 *atg2Δ::TRP1 atg18Δ::HIS5 S.p.*	This study
ERY087	SEY6210 *ATG2-GFP::HIS5 S.p. atg18Δ::TRP1*	This study
ERY090	SEY6210 *atg18Δ::HIS5 S.p. pCUP1-mCheV5-ATG8::URA3 ATG18-GFP::LEU2*	This study
ERY091	SEY6210 *atg18Δ::HIS5 S.p. pCUP1- mCheV5-ATG8::URA3 ATG18(L2)-GFP::LEU2*	This study
ERY093	SEY6210 *atg18Δ::HIS5 S.p. pCUP1- mCheV5-ATG8::URA3 ATG18(L5)-GFP::LEU2*	This study
ERY094	SEY6210 *ATG2-GFP::HIS5 S.p. atg18Δ::TRP1 ATG18-13xmyc::LEU2*	This study
ERY095	SEY6210 *ATG2-GFP::HIS5 S.p. atg18Δ::TRP1 ATG18(L2)-13xmyc::LEU2*	This study
ERY097	SEY6210 *ATG2-GFP::HIS5 S.p. atg18Δ::TRP1 ATG18(L5)-13xmyc::LEU2*	This study
ERY102	SEY6210 *atg18Δ::HIS5 S.p. pCUP1- mCheV5-ATG8::URA3 ATG18-GFP::LEU2 atg2Δ::TRP1*	This study
ERY103	SEY6210 *ATG2-GFP::HIS5 S.p. atg18Δ::TRP1 atg21Δ::URA3 K.l.*	This study
ERY117	SEY6210 *ATG2-VN::HIS5 S.p.ATG18-VC::TRP1*	This study
ERY118	SEY6210 *ATG2-VN::HIS5 S.p.ATG18-VC::TRP1 atg3Δ::URA*	This study
ERY119	SEY6210 *ATG2-VN::HIS5 S.p.ATG18-VC::TRP1 atg13Δ::URA*	This study
ERY132	SEY6210 *ATG2-VN::HIS5 S.p. atg18Δ::TRP1 ATG18-VC::LEU2*	This study
ERY133	SEY6210 *ATG2-VN::HIS5 S.p. atg18Δ::TRP1 ATG18(L2)-VC::LEU2*	This study
ERY137	SEY6210 *ATG2-VN::HIS5 S.p. atg18Δ::TRP1 ATG18(L5)-VC::LEU2*	This study
FRY387	SEY6210 *ATG2-PA::TRP1 atg18Δ::HIS5 S.p.*	This study
JGY3	SEY6210 *atg18Δ::HIS5 S.p.*	(Guan et al, 2001)
PJ69-4A	*MATa leu2-3,112 trp1-Δ901ura3-52 his3-Δ 200 gal Δ4 gal80Δ LYS::GAL1-HIS3 GAL2-ADE2 met2::GAL7-lacZ*	(James et al, 1996)
PSY102	SEY6210 *ATG2-GFP::HIS5 S.p.*	Reggiori lab collection
SEY6210	*MATa ura3-52 leu2-3,112 his3-Δ200 trp1-Δ901 lys2-801 suc2-Δ9 mel GAL*	(Robinson et al, 1988)

SUPPLEMENTARY MATERIALS AND METHODS

Plasmids

To create the promAtg18VC405, promAtg18(L2)VC405 and promAtg18(L5) VC405 plasmids, the VC fragment was amplified by PCR using the pFa6a-VC-TRP1 plasmid as a template and used to replace the myc tag coding sequence in the integrative plasmids expressing wild type Atg18-13xmyc, Atg18(L2)-13xmyc

and Atg18(L5)-13xmyc using *Pac*I and *Sac*I. Correct integration of the constructs into yeast was then verified by PCR analysis.

The plasmid expressing untagged Atg18 loop mutant 2,5 under the control of the endogenous promoter of Atg18 was constructed by PCR using the Y2H plasmid of Atg18 (L2) as a template and cloned as *Nhe*I-*Nco*I fragment into the pCvt18(415) plasmid, already carrying the L5 mutation in the *ATG18* gene.

Continuous 10-15% glycerol gradients

Overnight grown cells were diluted, grown to an exponential phase and 100 OD_{600} equivalent of cells were either immediately collected or starved for 3 h. Cells were subsequently resuspended in 300 µl of ice-cold lysis buffer before adding 300 µl of glass beads and breaking the cells by vortexing twice for 10 min at maximum speed at 4°C with 5 min intervals on ice. After removal of the cell debris and part of the membranes by centrifugation at 13'000 rpm for 10 min at 4°C, the supernatant was subjected to high-speed centrifugation at 45'000 rpm for 1 h at 4°C. Subsequently, 100 µl of the supernatant (S100) was loaded on the top of a continuous 10-15% glycerol gradient (w/v) in lysis buffer. After centrifugation at 33'000 rpm for 18 h at 4°C in a SW41Ti rotor (Beckman Coulter, Brea, CA), 13 fractions of 861 µl were collected from the top of the gradient. After precipitation by addition of 95 µl of tri-chloroacetic acid (final concentration 10%), proteins were resolved by SDS-PAGE and analyzed by western blot using antibodies against myc and goat IgG. Thyroglobulin (669 kDa), aldolase (158 kDa), conalbumin (75 kDa) and albumin (67 kDa) molecular weight protein standards were used to calibrate the gradient (GE Healthcare).

SUPPLEMENTARY REFERENCES

1. Guan J, Stromhaug PE, George MD, Habibzadegah-Tari P, Bevan A, Dunn WA, Jr., Klionsky DJ (2001) Cvt18/Gsa12 is required for cytoplasm-to-vacuole transport, pexophagy, and autophagy in *Saccharomyces cerevisiae* and *Pichia pastoris*. *Mol Biol Cell* 12: 3821-3838
2. James P, Halladay J, Craig EA (1996) Genomic libraries and a host strain designed for highly efficient two-hybrid selection in yeast. *Genetics* 144: 1425-1436
3. Robinson JS, Klionsky DJ, Banta LM, Emr SD (1988) Protein sorting in *Saccharomyces cerevisiae*: isolation of mutants defective in the delivery and processing of multiple vacuolar hydrolases. *Mol Cell Biol* 8: 4936-4948

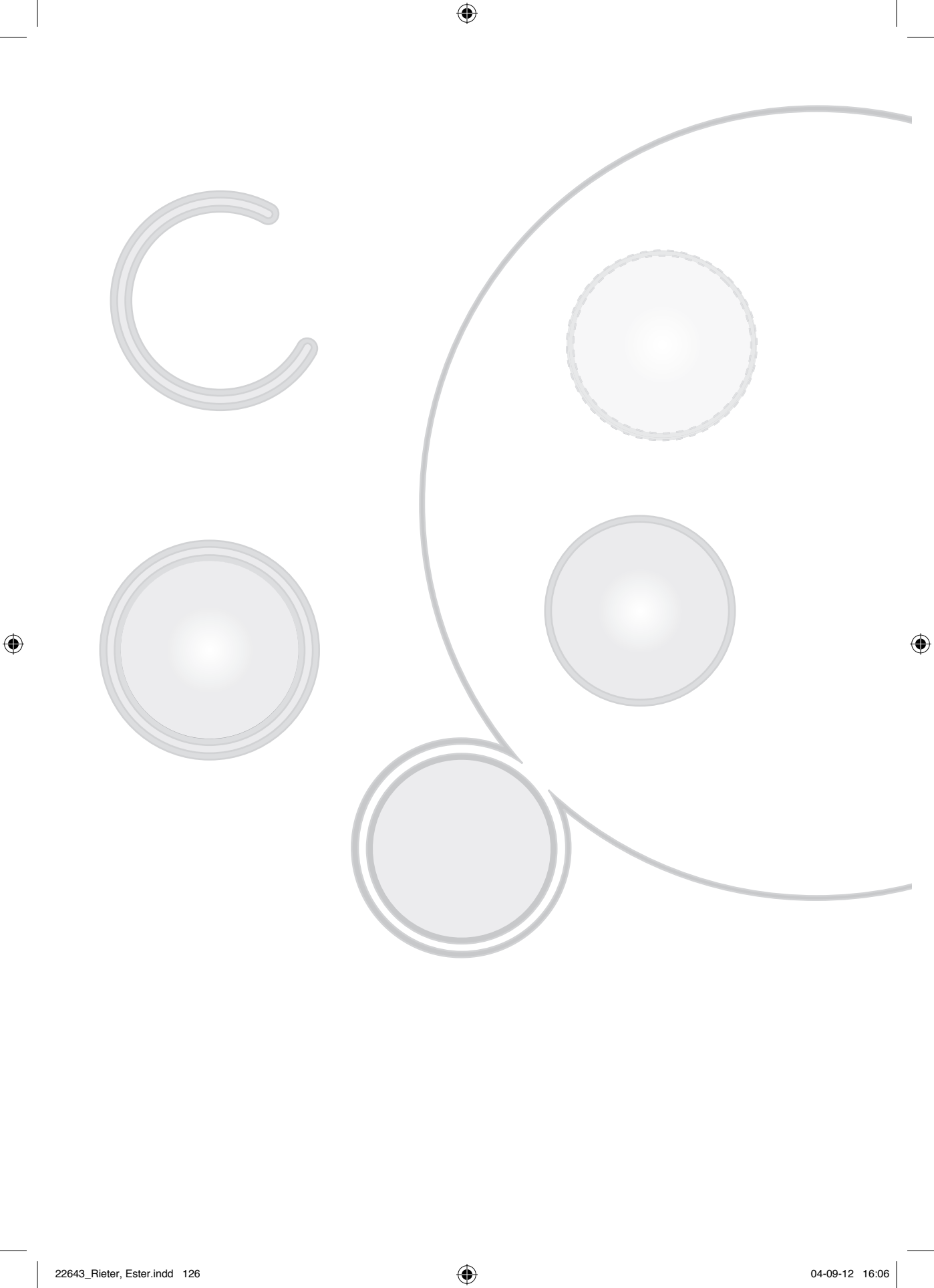

CHAPTER

4

Molecular basis of the interaction between Atg2 and Atg9

Ester Rieter[1], Aniek van der Vaart[1], Ana Maria Guzman Prieto[1], Elena Iskandarani[1], Tessa Hoogenhuijzen[1], Remko Goossens[1] and Fulvio Reggiori[1]

[1]Department of Cell Biology and Institute of Biomembranes, University Medical Centre Utrecht, Heidelberglaan 100, Utrecht, The Netherlands

Manuscript in preparation

ABSTRACT

Autophagy is a conserved catabolic pathway allowing cells to rapidly degrade and recycle cellular components. Structures targeted for degradation are sequestered into large double-membrane vesicles called autophagosomes. Autophagosomes biogenesis occurs at the phagophore assembly site (PAS) and the transmembrane protein Atg9 is a key autophagy regulator because playing a central role in the formation of this specialized site. After autophagosome completion, Atg9 is retrieved from the PAS by a yet unknown mechanism. Atg2 has been implicated in this event but what its exact molecular role is, remains elusive. Previous studies have shown that Atg2 probably interacts with Atg9. In this work we have characterized the principles of this interaction by identifying a sequence of 34 amino acids residing in the C-terminus of Atg2 important for binding to Atg9. We show that mutating several conserved residues within the identified binding region abolishes the interaction with Atg9 and causes a block in autophagy. Finally, we have found that a stretch of approximately 60 amino acids within the C-terminus of Atg9 is responsible for the binding to Atg2. The point mutants generated in this work will provide the basis for future studies aimed to explore the role of the Atg2-Atg9 interaction *in vivo* and provide a useful tool to study Atg9 retrieval from autophagosomal membranes.

Key words: Atg2/Atg9/autophagy/PAS

INTRODUCTION

Autophagy is a highly conserved transport pathway that allows cells to rapidly dispose unwanted cellular components, such as large protein-aggregates and damaged organelles (Nakatogawa et al., 2009). Autophagosomes are the hallmark of this pathway and targeted structures are sequestered into these large double-membrane vesicles, which subsequently deliver them into the yeast/plant vacuoles or mammalian lysosomes for degradation (Klionsky, 2007). The resulting metabolites are re-used either for the synthesis of new macromolecules or as a source of energy. Because of its ability to rapidly turnover intracellular components, autophagy allows cells to survive severe environmental conditions such as starvation, and multiple internal cellular stress conditions. Autophagy also plays a crucial role in numerous cellular processes such as type II programmed cell death, development and differentiation, and has a protective role against invading pathogens, cancer and aging. Defective autophagy is correlated with a variety of pathological conditions, including cardiovascular, autoimmune, neurodegenerative and myodegenerative disorders, and malignancies (Levine and Klionsky, 2004; Mizushima et al., 2008).

Studies in yeast have been pivotal for the progress in unveiling the mechanism of autophagy by leading to the identification of 36 autophagy-related genes (*ATG*) to date, many of which are conserved among higher eukaryotes. Sixteen of them form the core Atg machinery that mediates the generation of autophagosomes in all eukaryotes (Xie and Klionsky, 2007; Yang and Klionsky, 2010). The process of autophagosome biogenesis is initiated by the formation of the phagophore, a cup-shaped double-layered membrane, at the phagophore assembly site (PAS) (Itakura and Mizushima, 2010; Reggiori, 2006; Suzuki et al., 2001; Suzuki et al., 2007). The phagophore subsequently expands and elongates thereby sequestering the cargo that has to be degraded. Finally, in yeast complete autophagosomes directly dock and fuse with the vacuole releasing their internal vesicle in the lumen of this organelle, whereas in mammals they first fuse with endosomal vesicles and multivesicular bodies to form amphisomes, which subsequently expose their content to lysosomal hydrolases (Fengsrud et al., 2000). The molecules generated by the hydrolysis of the autophagosome content are finally transported back into the cytoplasm for reuse.

The precise origin of the phagophore and the source of the membranes used to generate an autophagosome remain unknown. Advances have been made

by studying Atg9, the only transmembrane protein among the core Atg machinery and a key regulator of autophagy induction (Noda et al., 2000; Wang et al., 2001). It is one of the first factors to be recruited to the PAS, where it presumably plays an important role in initiating autophagy by recruiting and organizing the rest or at least part of the Atg machinery (Suzuki et al., 2007). Because of its association with lipid bilayers, Atg9 is also thought to bring at least part of the membranes that contribute to the autophagosome biogenesis (Legakis et al., 2007; Reggiori et al., 2005). Immuno-electron microscopy studies from our laboratory have shown that in yeast Atg9 localizes to several cytoplasmic pools, called the Atg9 reservoirs (Mari et al., 2010; Mari and Reggiori, 2010). A similar structure appears to exist in mammalian cells as well (Orsi et al., 2012). The movement of one of these reservoirs from the periphery of the cell close to the vacuole and the subsequent recruitment of additional Atg proteins leads to the formation of the PAS. Atg9 is not present on the complete autophagosome, but instead is retrieved from the autophagosomal membranes and transported back to the reservoirs prior to the fusion of the autophagosome with the vacuole (Mari and Reggiori, 2007; Reggiori et al., 2004). The exact molecular mechanism of Atg9 retrieval remains to be elucidated, but it has been shown that it depends on the Atg1-Atg13 complex, Atg2, Atg18 and the presence of phosphatidylionositol-3-phosphate (PtdIns3P) (Reggiori et al., 2004). In absence of any one of these factors Atg9 recycling from the PAS is blocked.

In yeast, there is good evidence suggesting that Atg9 interacts with Atg2, another key Atg protein essential for autophagy (Barth and Thumm, 2001; Reggiori et al., 2004; Shintani et al., 2001; Wang et al., 2001). The molecular function of Atg2 in autophagy is unknown and this protein does not possess any known functional and structural domains. Atg2 is not essential for the localization of most of the other Atg proteins to the PAS, with the exception of Atg18 (Suzuki et al., 2007)(Rieter *et al*, in preparation). This suggests that Atg2 is one of the most downstream factors during the autophagic process and that it might act prior to autophagosome completion, presumably in recycling components such as Atg9 back from the PAS (Reggiori et al., 2004). Interestingly, some of the factors that are essential for Atg9 retrieval are also required for the localization of Atg2 to the PAS, i.e. the Atg1-Atg13 complex and PtdIns3P. Moreover, Atg2 localization to the PAS depends on Atg9 itself (Shintani et al., 2001; Suzuki et al., 2007; Wang et al., 2001).

To gain more insights into both the mechanism of Atg9 retrieval and the

molecular role of Atg2 in this event, we decided to characterize the interaction between Atg2 and Atg9. The identification of the motifs mediating the binding between Atg2 and Atg9 will allow us to generate specific mutant versions of both Atg2 and Atg9 that are no longer able to interact, and thus specifically investigate the role of Atg2 in Atg9 recycling. This approach is preferred over knocking out the genes, since interactions with other proteins will still able to occur and presumably other functions of Atg2 and Atg9 remain unaltered. We have thus identified the binding motifs of Atg2 and Atg9 required for their interaction and found that the Atg9-binding sequence of Atg2 resides in its C-terminus, while Atg9 interacts with Atg2 via a stretch of amino acids just after the last transmembrane domain. Subsequently, we have created a number of Atg9-binding mutants of Atg2 and perform an initial characterization. These mutant versions of Atg2 will allow us to study *in vivo* the relevance of the Atg2-Atg9 interaction in autophagy and possibly provide a unique tool for studying Atg9 retrieval from the PAS.

MATERIALS AND METHODS

Strains and media

The *S. cerevisiae* strains used in this study are listed in **Table 1**. For gene disruptions, the entire *ATG2* or *ATG18* coding region were replaced with the *Schizosaccharomyces pombe HIS5, S. cerevisiae LEU2* or the *S. cerevisiae TRP1* gene using PCR primers containing ~60 bases of identity to the regions flanking the open reading frame generated from the pUG27, pUG73 or pFA6a-TRP1 template plasmids (Gueldener et al., 2002; Longtine et al., 1998). Gene knockouts were verified by examining prApe1 processing by western blot using a polyclonal antibody against Ape1 (Mari et al., 2010) and/or PCR analysis of the gene locus.

Yeast cells were grown in rich (YPD; 1% yeast extract, 2% peptone, 2% glucose) or synthetic minimal media (SMD; 0.67% yeast nitrogen base, 2% glucose, amino acids and vitamins as needed). Starvation experiments were conducted in synthetic media lacking nitrogen (SD-N; 0.17% yeast nitrogen base without amino acids, 2% glucose).

Table 1. Strains used in this study

Name	Genotype	Reference / Origin
FRY375	SEY6210 *atg2Δ::HIS5 S.p.*	This study
FRY382	PJ69-4A *atg18Δ::TRP1*	This study
FRY383	SEY6210 *atg2Δ::LEU2*	This study
PJ69-4A	*MATa leu2-3,112 trp1-Δ901ura3-52 his3-Δ 200 gal Δ4 gal80Δ LYS::GAL1-HIS3 GAL2-ADE2 met2::GAL7-lacZ*	(James et al., 1996)
SEY6210	*MATa ura3-52 leu2-3,112 his3-Δ200 trp1-Δ901 lys2-801 suc2-Δ9 mel GAL*	(Robinson et al., 1988)

Plasmids

The plasmids for the split-ubiquitin assay were constructed as follows. DNA fragments encoding *ATG2, ATG9* and *ATG18* were generated by PCR using *S. cerevisiae* genomic DNA as a template. *ATG9* was cloned as a *Cla*I-*Sal*I fragment into the pCub_RURA3_Met313 vector to generate the pAtg9_Cub_RURA3_Met313 plasmid (Wittke et al., 1999). *ATG9*, *ATG2 and ATG18* plus 300bp of their terminator sequences were cloned as *Bcl*I-*Kpn*I fragments into the pNui_CUP_314 plasmid.

For the construction of the Y2H plasmids, a DNA fragment encoding *ATG2* was generated by PCR using *S. cerevisiae* genomic DNA as a template and cloned as a *Xma*I-*Sal*I fragment into the pGBDU-C1 vector (James et al., 1996). The pGAD-Atg9 plasmid was a gift from Prof. D.J. Klionsky (He et al., 2006).

C-terminal truncations of *ATG9* were generated by PCR exploiting the unique *Age*I restriction site inside the *ATG9* gene, and using a 5` primer containing the *Age*I restriction site and a 3` primer specific for each truncation, which introduces a stop codon followed by a *Sal*I restriction site. The *ATG9* truncations were then cloned as *Age*I-*Sal*I fragments into the pGAD-Atg9 plasmid.

The C-terminal truncations of *ATG2* were generated by PCR using a 5` primer that introduces a *Xma*I restriction site just before the start codon of the gene and a 3` primer specific for each truncation, which introduces a stop codon followed by a *Sal*I restriction site. These truncations were cloned as *Xma*I-*Sal*I fragments into the pGBDU-C1 plasmid. The point mutations in *ATG2* were introduced by PCR exploiting the unique *Pml*I restriction site in the sequence of *ATG2*, which is in close proximity of the stretch of nucleotides of interest. For each point mutant a specific 5` primer was used that contains the *Pml*I restriction site and introduces the point mutations and a 3` primer that introduces a *Sal*I restriction site after the stop codon of the full-length *ATG2*. The PCR fragments were then cloned into the pGBDU-Atg2 plasmid using *Pml*I and *Sal*I.

Using *Blp*I and *Bsi*WI, fragments containing the Atg2 point mutants were sub-cloned into the pYCG_YNL242w (Euroscarf, Frankfurt, Germany) plasmid, which carries the *ATG2* gene (Barth and Thumm, 2001).

The pCuGFPATG8414 plasmid expressing GFP-Atg8 under the control of the *CUP1* promoter has been described elsewhere (Kim et al., 2002).

All plasmids were transformed into yeast according a standard procedure that employs lithium acetate (Gietz and Schiestl, 2007).

Yeast two-hybrid assay

The plasmids pGAD-C1 and pGBDU-C1 containing *ATG2* and *ATG9* or the mutated and truncated forms were transformed into the different Y2H strains and grown on SMD medium lacking leucine and uracil (James et al., 1996). Colonies, which contain both vectors, were then spotted on SMD medium lacking histidine, leucine and uracil. When both proteins interact the reporter gene *HIS3* is transcribed and the test strain grows on plates lacking histidine.

Split-ubiquitin assay

The pAtg9_Cub_RURA3_Met313 and pNui_CUP_314 plasmids harboring the *ATG2*, *ATG9* or *ATG18* gene were transformed into wild-type or *atg2Δ* cells and grown on SMD medium lacking tryptophane and histidine. Colonies carrying both plasmids were restricted on SMD medium plates lacking tryptophan, histidine and uracil, and supplemented with 250μM methionine (Wittke et al., 1999). The modified *URA3* gene in the pCub_RURA3_Met313 vector was used as reporter for the interaction. Reconstitution of ubiquitin upon interaction between the two proteins of interest leads to the degradation of Ura3 by ubiquitin specific proteases. As a result the transformed cells are not able to grow on the test plates.

Miscellaneous procedures

The protein extraction, western blot analyses and the GFP-Atg8 processing assay were carried out as previously described (Cheong and Klionsky, 2008; Reggiori et al., 2003). Detection and quantification of the western blot results were done using an Odyssey infrared imaging system (Li-cor Biosciences, Lincoln, NE).

RESULTS

The interaction between Atg2 and Atg9

Atg2 is a large protein of 1592 amino acids without any known functional or structural domains, which does not appear to be post-translationally modified (Wang et al., 2001). In yeast, the majority of the protein localizes to the PAS and is no longer present on complete autophagosomes (Shintani et al., 2001; Suzuki et al., 2007; Wang et al., 2001). There are evidences suggesting that Atg2 interacts with Atg9 (Reggiori et al., 2004; Shintani et al., 2001). To determine whether this interaction indeed exists, we exploited the split-ubiquitin system. This technique is frequently used to study interactions between transmembrane proteins (Wittke et al., 1999). To this end, the *ATG9, ATG2* and *ATG18* genes were cloned into the split-ubiquitin vectors pCub_RURA3_Met313 and pNui_CUP_314, resulting in *ATG9* being fused to C-terminal part of ubiquitin (Cub), and *ATG2*, *ATG18* or *ATG9* being fused to the N-terminal part of ubiquitin (Nui). The plasmids harboring the different genes were co-transformed into either a wild type or *atg2Δ* strain to test protein interaction. The empty Nui_CUP_314 and pCub_Atg9_RURA3_Met313 plasmids were used as the negative control and as expected, cells carrying these constructs were able to grow on the test plate (**Figure 1A**). As a positive control, we used the self-interaction of Atg9 (He et al., 2008; Reggiori et al., 2004) and as predicted, the *atg2Δ* strain transformed with the two plasmids expressing Atg9 did not grow. Importantly, cells expressing Atg9-C_{ub}-RUra3 and N_{ui}-Atg2 were also not able to grow indicating that Atg9 interacts with Atg2 (**Figure 1A**). Furthermore, to show that the previously described interaction between Atg9 and Atg18 depends on the presence of Atg2, we co-expressed Atg9-C_{ub}-RUra3 and N_{ui}-Atg18 in both wild type and *atg2Δ* cells (Reggiori et al., 2004). As shown in **Figure 1A**, an interaction between Atg9 and Atg18 was observed in the wild type but not in the *atg2Δ* mutant showing that Atg18 interacts with Atg9 through Atg2.

To recapitulate the Atg2-Atg9 interaction we turned to yeast two-hybrid (Y2H) system, which also provides an experimental advantage for identification of the binding domains. The *ATG9* and *ATG2* genes were cloned into the Y2H vectors pGAD-C1 and pGBDU-C1, respectively, resulting in fusion proteins that are N-terminally tagged with either the activation domain (AD) or DNA binding domain (BD). Both plasmids were co-transformed into the Y2H strain to test their

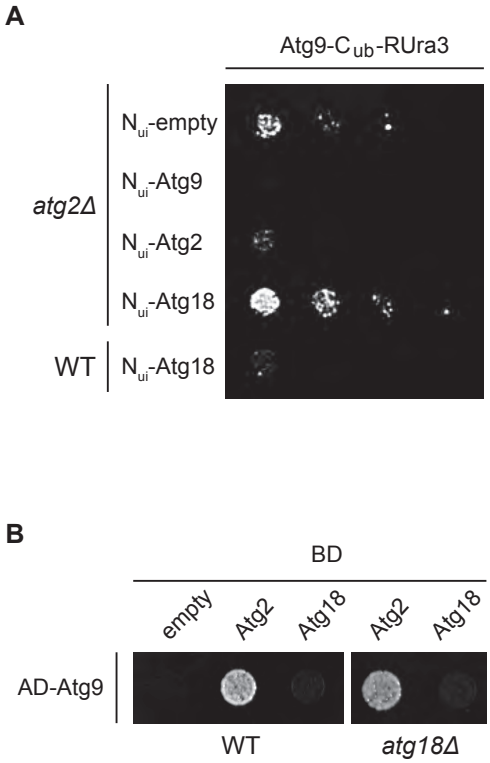

Figure 1. The binding between Atg2 and Atg9. A. Confirmation of the Atg2-Atg9 interaction using the split-ubiquitin assay. The different split-ubiquitin constructs pAtg9_Cub_RURA3_Met313, pAtg9_Nui_CUP_314, pAtg18_Nui_CUP_314 and pAtg2_Nui_CUP_314, were co-transformed into either wild-type (WT, SEY6210) or *atg2*Δ cells (FRY383). Transformants were first plated on SMD medium lacking tryptophan and histidine to select for cells harboring both plasmids, before growing them on test plates (SMD medium lacking histidine, tryptophan, uracil, and supplemented with 250μM methionine) for 3-4 days. No growth on the test plates indicates an interaction between the expressed N_{ui}- and C_{ub}-RUra3-fusion proteins. B. Atg2-Atg9 interaction in different Y2H background strains. Atg9 and Atg2 were fused to the activation domain (AD) and/or the DNA binding domain (BD) of the transcription factor Gal4, respectively. Plasmids were transformed into the wild-type Y2H test strain (WT, PJ69-4A) or the same strain lacking *ATG18* (FRY382), and after growing on a plate selecting for both plasmids (SMD medium without uracil and tryptophan), colonies were spotted on SMD medium-containing plates lacking uracil, tryptophan and histidine. Growth on these plates indicates an interaction between the AD- and BD-fusion proteins. The empty pGBDU-C1 plasmid was used as a control.

ability to interact. An empty pGBDU-C1 vector was used as a negative control. As shown in **Figure 1B** and as expected (Shintani et al., 2001), no growth was observed in the negative control while cells expressing both BD-Atg2 and AD-Atg9 were able to grow, confirming that the two proteins interact. To determine

that the observed interaction between Atg9 and Atg2 occurs independently from Atg18, we repeated the same analysis in a Y2H strain in which *ATG18* was deleted. In this mutant background the cells were still able to grow revealing that the interaction between Atg9 and Atg2 does not require Atg18 (**Figure 1B**).

Together, the split-ubiquitin and the Y2H assay results confirm an Atg18-independent interaction between Atg2 and Atg9.

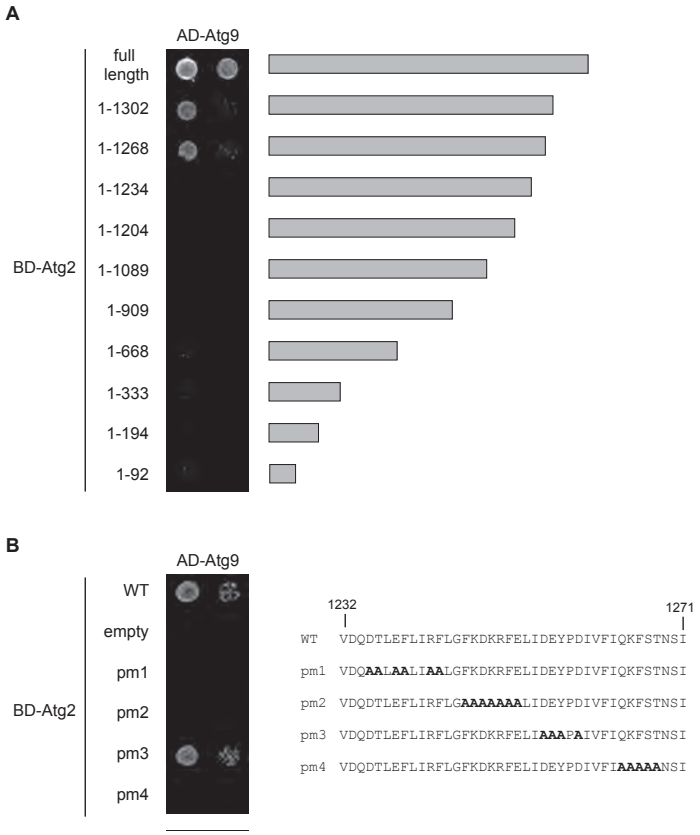

Figure 2. Identification of the Atg9-binding motifs in Atg2. A. Amino acids between the position 1232 and 1268 of Atg2 are essential for the interaction of this protein with Atg9. A number of C-terminal Atg2 truncations were generated and cloned into the pGBDU-C1 plasmid expressing the BD fusion proteins. Their interaction with the AD-Atg9 chimera was tested using the Y2H assay as described in panel A. B. Atg2 point mutants 1, 2 and 4 do not display an interaction with Atg9 by Y2H. The BD-fusions of 4 different Atg2 point mutants were tested for their ability to interact with AD-Atg9 as described in panel A. On the right, the amino acids sequence of Atg2 between residues 1232 and 1271 is shown. For each point mutant, the charged and polar amino acids that were substituted with alanines are indicated in bold.

Identification of the Atg9-binding motifs of Atg2

To map the Atg9-binding region of Atg2 we employed the Y2H system. We generated a number of C-terminal truncations of Atg2 and tested whether they were still able to interact with Atg9. As shown in **Figure 2A**, binding was still observed between Atg9 and the Atg2(1-1268) truncation, but not with the Atg2(1-1234) mutant protein. This observation revealed that a stretch of 34 amino acids present in the C-terminus of Atg2, between the amino acids at positions 1234 and 1268, is essential for the association of this protein with Atg9. To determine which residues within the identified region of Atg2 are important for mediating binding to Atg9, we mutated several charged and polar amino acids by substituting them for non-polar alanines in the full-length Atg2. We generated 4 different point mutants and tested their capacity to interact with Atg9 by Y2H (**Figure 2B**). Only the Atg2(PM3) mutant was still able to bind Atg9, whereas no growth was observed with any of the other 3 point mutants, indicating that the mutated residues in the latter versions of Atg2 are probably involved in mediating the binding to Atg9.

Mapping the Atg2-binding region of Atg9

We also opted to identify the Atg2-binding region in Atg9 because this information will be important to further gain insights into the relevance of the Atg2-Atg9 interaction, but to also determine how Atg2 recruitment to the PAS is regulated. Atg9 is an integral membrane protein with 6 highly conserved transmembrane domains (TMDs) and the two termini are cytosolic (**Figure 3A**) (He et al., 2006). We reasoned that the region of interaction would be located in either one of the termini or one of the cytosolically exposed amino acid loops connecting the TMDs. To determine which region binds Atg2 we generated a number of C-terminal truncations of Atg9 and test their interaction with Atg2 by Y2H assay. Each truncation led to the sequential elimination of parts of the protein exposed on the cytosol, including the C-terminus, and loop1 (L1) and loop2 (L2), which connect some of the transmembrane segments (**Figure 3B**). Growth was observed with cells expressing the Atg9(1-937), Atg9(1-868) and Atg9(1-811) truncations, indicating that this mutant forms of Atg9 are still able to interact with Atg2. In contrast, binding was no longer detected with the Atg9(1-748) truncation and smaller ones revealing that a stretch of approximately 60 amino acids, between residues 748 and 811, is probably mediating binding to Atg2.

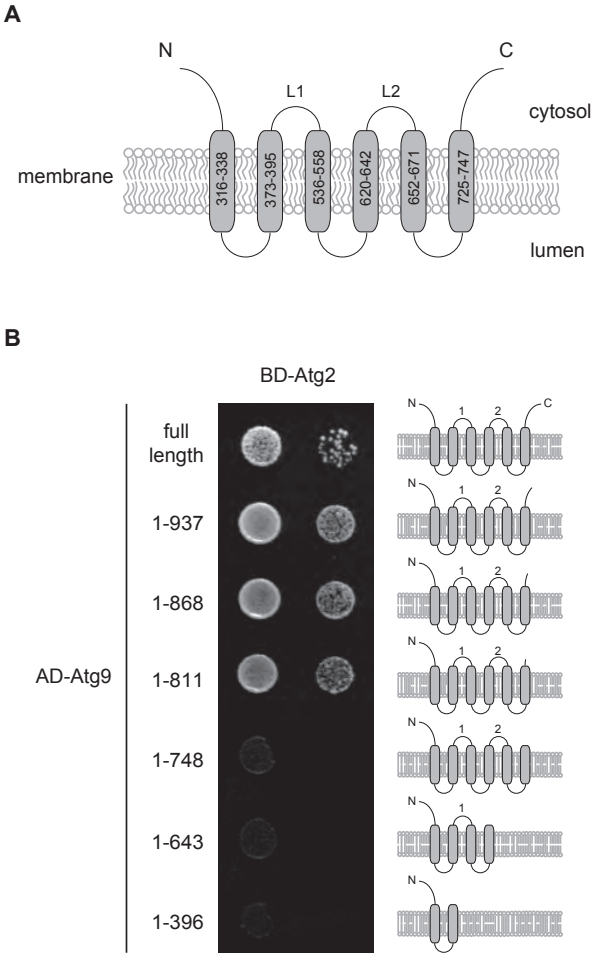

Figure 3. Mapping the Atg2-binding region in Atg9. A. Schematic representation of Atg9 topology. Atg9 is a multi-spanning membrane protein with 6 transmembrane segments and cytosolic termini. The positions of the amino acids present within each transmembrane domain are indicated as well as the 2 connecting cytosolic loops (L1 and L2). B. The amino acids between positions 748 and 811 within the C-terminus of Atg9 are essential for the interaction with Atg2. A number of C-terminal truncations of Atg9 were generated and as shown on the right of the panel, each truncation leads to the specific elimination of a part of the protein exposed on the cytosolic side, e.g. part of its C-terminus or one of the 2 loops. The truncated versions of Atg9 were cloned into the pGAD-C1 plasmid and their interaction with BD-Atg2 was tested by Y2H assay as described in Figure 1B.

Atg2 binding to Atg9 is essential for bulk and selective types of autophagy

To study the relevance of the interaction between Atg9 and Atg2 in autophagy, we generated plasmids expressing untagged Atg2(PM1), Atg2(PM2), Atg2(PM3) and

Atg2(PM4) under the control of the authentic *ATG2* promoter. For this purpose, the different mutations were introduced into the pYCG_YNL242w plasmid carrying the wild-type *ATG2* gene (Barth and Thumm, 2001). These constructs were co-transformed into the *atg2*Δ mutant with a plasmid expressing the GFP-Atg8 fusion protein to perform the GFP-Atg8 processing assay. This is an established method to monitor bulk autophagy (Cheong and Klionsky, 2008). Upon completion of an autophagosome, a pool of GFP-Atg8 remains in the interior of this vesicle and it is delivered into the vacuole, where GFP is proteolytically removed from Atg8. The free GFP moiety is relatively stable in the vacuole lumen and accumulates over time upon induction of autophagy. As a result, the measurement of free GFP appearance is a way to assess autophagosome flux to the vacuole. As expected, when this assay was performed in wild type cells, a band of 25 kDa corresponding to free GFP appeared over time under starvation conditions indicating the normal progression of autophagy (**Figure 4A**). In contrast, no cleavage of GFP-Atg8 was observed in the *atg2*Δ mutant due to a complete autophagy block (Barth et al., 2001; Guan et al., 2001). As shown in **Figure 4A**, Atg2(PM2) and Atg2(PM3) were able to complement this defect very similar to the wild type Atg2, indicating that the mutated amino acid in these two forms of Atg2 are not required for bulk autophagy. In contrast, a complete block of the pathway was observed when expressing the Atg2(PM1) and Atg2(PM4) mutants.

Next, we examined the effects of the Atg2 point mutations on the Cvt pathway, a selective type of autophagy operating under growing conditions in yeast (Lynch-Day and Klionsky, 2010). As expected, the majority of Ape1 was present in its mature form in wild type cells grown in a nutrient-rich medium whereas only prApe1 was detected in the *atg2*Δ mutant because of its Cvt pathway block (**Figure 4B**, (Shintani et al., 2001; Wang et al., 2001)). In agreement with the results obtained with the GFP-Atg8 processing assay, the cells expressing wild type Atg2, Atg2(PM2) or Atg2(PM3) processed prApe1 into mApe1 to an identical extent as the control wild type strain. In contrast, a complete defect of the Cvt pathway was observed in the *atg2*Δ knockout carrying the Atg2(PM1) and Atg2(PM4) mutants.

The results of Atg2(PM2) are unexpected if compared with the data obtained with the Y2H, in which this point mutant no longer bound to Atg9. Further research is needed to elucidate this discrepancy in our data. Nevertheless, we concluded that the mutated residues in Atg2(PM1) and Atg2(PM4) are probably mediating the interaction of Atg2 with Atg9, and are essential for the progression of non-selective and selective types of autophagy.

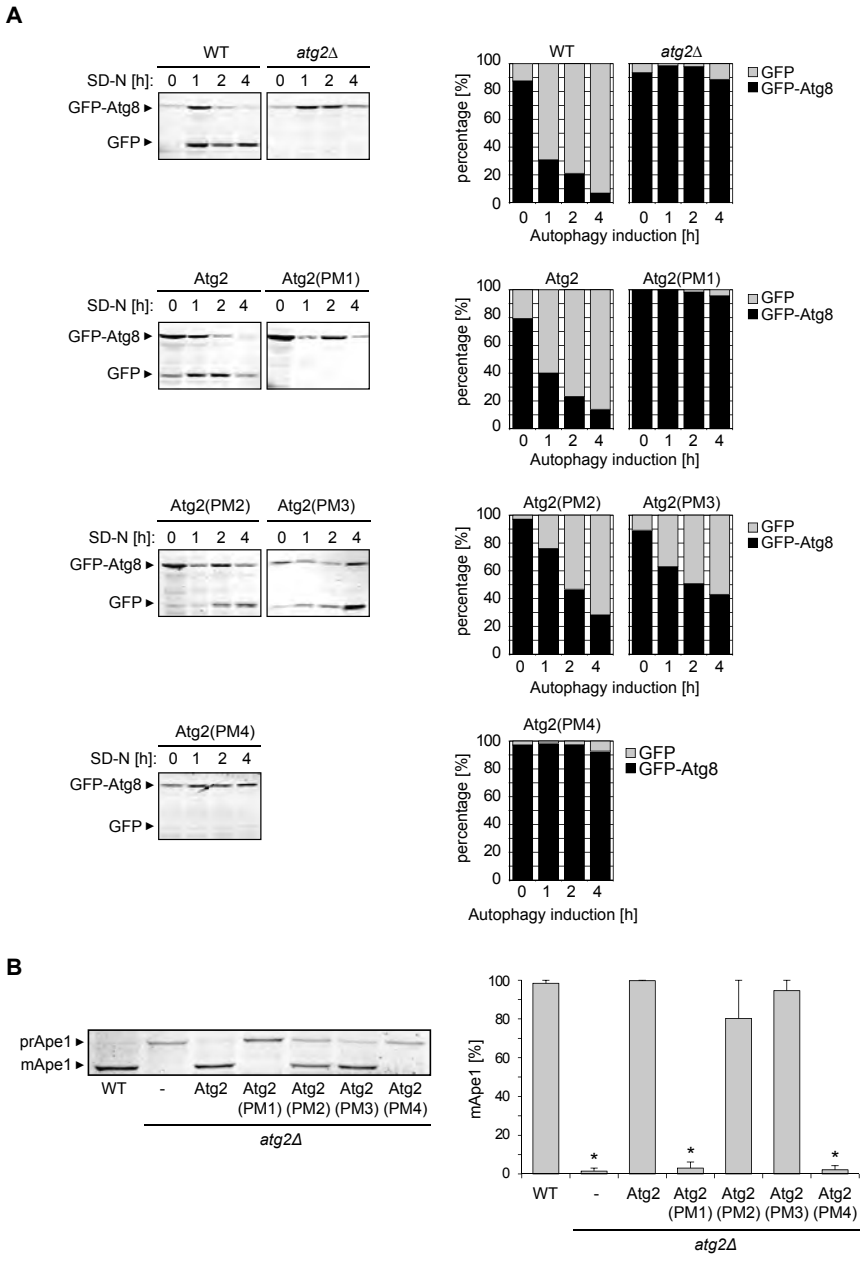

Figure 4. The Atg9-Atg2 interaction is essential for the Cvt pathway and autophagy. A. Mutations in the putative Atg9-binding region of Atg2 lead to an impairment of autophagy. Wild type (SEY6210) and *atg2*Δ (FRY375) cells carrying both the pCuGFPATG8414 construct and, one of the plasmids expressing the different Atg2 point mutants were grown in rich medium to an early log phase and transferred to the starvation medium to induce autophagy.

Cell aliquots were taken at 0, 1, 2 and 4 h, before analyzing the cell extracts by western blot using the antibody against GFP. The detected bands were quantified using the Odyssey software and the percentages of GFP-Atg8 (black) and free GFP (grey) were plotted. Data represent the average of 2 experiments. B. Mutations in the Atg9-binding domain of Atg2 severely affect the Cvt pathway. Strains analyzed in panel A were grown in rich medium to an early log phase. Cell aliquots were then collected and cell extracts analysed by western blot using anti-Ape1 antibodies. The detected bands were quantified as in panel A and the percentages of mApe1 were plotted. The graphs represent the average of 2 experiments ± SEM, and asterisks indicate a significant difference with the WT (two-tailed *t*-test: $P < 0.05$).

DISCUSSION

To gain insights into the mechanism of Atg9 retrieval from the PAS to the peripheral Atg9 reservoirs, we have characterized the interaction between this protein and Atg2. Atg2 together with Atg18 have been implicated in Atg9 recycling, but the function of both proteins remains unknown (Mari and Reggiori, 2007; Reggiori et al., 2005; Reggiori et al., 2004). To get a better understanding of the molecular role of Atg2 and the functional relevance of the interaction between Atg2 and Atg9, we have identified the binding motifs in Atg2 and Atg9 required for their association using the Y2H system.

We have found two proximal amino acids stretches in the C-terminal half of Atg2 that could be involved in its binding to Atg9 (**Figure 2**). This result sets the bases for future in vivo analyses to confirm that these residues indeed mediate the interaction of Atg2 with Atg9. To this end, we plan to generate plasmids expressing endogenous levels of tagged versions of Atg2 carrying mutations in these amino acids. These point-mutated constructs will be used to conduct protein A (PA) affinity isolation experiments using IgG-Sepharose beads and Atg9-PA as the bait. Nonetheless, some initial observations indicate that the identified motifs could be the correct ones. We have observed a severe impairment in the progression of non-selective and selective types of autophagy in cells expressing these Atg9-binding mutants of Atg2 (**Figure 4**). We predict that the block in autophagy is caused by the inability of these two mutants to be recruited to the PAS. This hypothesis, however, has to be accurately investigated by assessing the cellular distribution the Atg9-binding mutants of Atg2 by fluorescence microscopy.

Atg2 is highly conserved among other eukaryotes and two mammalian Atg2 orthologs, Atg2A and Atg2B, have recently been characterized (Velikkakath et al., 2012). Similar to what has been reported for yeast (Shintani et al., 2001;

Wang et al., 2001), silencing of both Atg2A and Atg2B in mammalian cells causes a block in autophagy and affects trafficking of Atg9 (Velikkakath et al., 2012). Amino acid sequence alignments of the identified region between amino acids 1234-1268 in yeast revealed that the mutated residues in Atg2(PM1) and Atg2(PM4) are present in other fungi and that several of them, e.g. D1235, F1239 and F1243, are also conserved among higher eukaryotes (**Figure 5**). In the study from the Mizushima's laboratory, they show that a stretch of approximately 100 amino acids in the C-terminal region of Atg2A is essential for autophagy and required for correct localization of Atg2A to the autophagosomal membranes (Velikkakath et al., 2012). This region, however, does not include the sequence that we have identified as the potential Atg9-binding site. It remains to be determined whether the Atg9-binding site of Atg2A resides in a different region of the protein or whether the identified region by Velikkakath and co-workers affects the function of Atg2A in autophagy without compromising the interaction with mAtg9. In this regard, it will be interesting to investigate the localization of yeast Atg2 lacking the stretch of amino acids identified in Atg2A. Based on our Y2H results, the absence of this stretch of amino acids, which localizes between amino acid residues 1365-1481 in yeast Atg2, should not affect the Atg9-binding capacity of Atg2 (**Figure 2**). In parallel, mutating in Atg2A the conserved residues present in the putative sites mediating yeast Atg2 interaction with Atg9 and test the ability of the resulting mutant protein to interact with mAtg9, will tell us whether the Atg9-binding site is conserved in higher eukaryotes.

```
                     1232                                   1271
                      |   pm1       pm2      pm3      pm4     |
S.cerevisiae         VDQDTLEFLIRFLGFKDKRFELIDEYPDIVFIQKFSTNSI
Pan troglodytes      VDQDALFFLKDFFTSLVAGINPVVPGETSAEARPETRAQP
Canis familiaris     VDQDALFFLKDFFTSLVAGINPMVSAETSAEARPETRVQP
Bos taurus           VDQDALLFLRDFFTTLAASINPMVPAETSAEARPETPVPP
Mus musculus         VDQDALFFLKDFFTSLAASINPMVPGDTSEAPR-ETHSRP
Rattus norvegicus    VDQDALFFLKDFFTSLAASINPMVPGDTFEAHR-ETHSRP
Homo sapiens         VDQDALFFLKDFFTSLVAGINPVVPGETSAEARPETRAQP
```

Figure 5. Alignment of part of the amino acid sequence of Atg2 from various organisms. The potential Atg9-binding region between amino acids 1232-1271 identified in this work was aligned with the same region of Atg2 from other organisms using the ClustalW2 software. The residues that were mutated into alanines in this work are highlighted in bold and the names of point mutants are indicated above the sequence.

In this study we have also identified a region of approximately 60 amino acids within the C-terminus of Atg9 that could be responsible for the binding to Atg2 (**Figure 3**). Atg9 is a conserved transmembrane protein with similar topology, i.e. 7 predicted TMDs and cytosolic N- and C-termini, in all eukaryotes (He et al., 2006; Young et al., 2006). Interestingly, an amino acid sequence alignment analysis revealed that the region that we have identified as the potential Atg2-binding region in the C-terminus of Atg9 is extremely well conserved (**Figure 6A**). For the future, we have planned to substitute several of the conserved and (preferably charged and polar amino acids) within this region for non-polar alanines (**Figure 6B**). The involvement of the mutated amino acids in the binding of Atg9 to Atg2 will be then assessed by Y2H assay before eventually testing them in a more physiological context by pull-down experiments.

While the molecular mechanism of Atg9 retrograde transport and the involvement of Atg2 in this process remain elusive, some hypothesis can be made. In a recent study from our laboratory, we have shown that Atg2 and PtdIns3P are the key determinants responsible for Atg18 recruitment to autophagosomal membranes (Rieter *et al*, in preparation). One possible speculation is that the function of Atg2 is to recruit Atg18 to the PAS, which subsequently promotes Atg9 recycling. Another option is that Atg9 retrieval from the PAS/autophagosomes requires the concerted action of both Atg2 and Atg18, or alternatively, Atg2 has a function in Atg9 retrieval independently from its function in recruiting Atg18 to the PAS. Obviously, all these scenarios are far from being demonstrated and further investigations are needed to fully comprehend the mechanism of Atg9 recycling during autophagosome biogenesis. The Atg9-binding mutants obtained in this study provide a useful tool to achieve this. The continuation of this study will thus overall contribute to our understanding of the molecular mechanism in autophagy.

A

```
                 750                                                          811
                  |                                                            |
S. cerevisiae      GRIVDFFRENSEYVDGLGYVCKYAMFNMKNIDGEDTHSMDEDSLTKKIAVNGSHTLN----------SKRRS
Mus musculus       LEIIDFFRNFTVEVVGVGDTCSFAQMDVRQHGHPQWLSGGQTEASVYQQAED---------------GKTEL
Rattus norvegicus  LEIIDFFRNFTVEVVGVGDTCSFAQMDVRQHGHPQWLSGGQTEASVYQQAED---------------GKTEL
Homo sapiens       LEIIDFFRNFTVEVVGVGDTCSFAQMDVRQHGHPQWLSAGQTEASVYQQAED---------------GKTEL
Gallus gallus      LDIVDFFRNFTVEVVGVGDTCSFAQMDVRQHGHPAWMSAGKTEASIYQQAED---------------GKTEL
Danio rerio        LEIIDFFRNFTVDVVGVGDTCSFAQMDVRQHGHPAWMSAGKTEASIYQQAED---------------GKTEL
D. melanogaster    IELVRFFRTFTVSVRGVGNVCSFAQMDVRKHGNPDWQLTSELEEMTRATAQQPQQEPQQQSL---AGGKTEM
C. elegans         SQLANFFHDYTERVDGLGDVCSFAVMDVGKHGDPKWNHIKELKAIVEDQEDQQQAQSVVTSLNRARDGKTEL
```

B

```
                 750                                                  811
                  |                                                    |
WT                GRIVDFFRENSEYVDGLGYVCKYAMFNMKNIDGEDTHSMDEDSLTKKIAVNGSHTLNSKRRS
pm1               GRIVDFFRENSEYVDGLGYVCKYAMFNMKNIDGEDTHSMDEDSLTKKIAVNGSHTLNS****
pm2               GRIVD***AENSEYVDGLGYVCKYAMFNMKNIDGEDTHSMDEDSLTKKIAVNGSHTLNSKRRS
pm3               GRIVDFFREN*A*EY***ALGYVCKYAMFNMKNIDGEDTHSMDEDSLTKKIAVNGSHTLNSKRRS
pm4               GRIVDFFRENSEYVDG**A*Y****AMFNMKNIDGEDTHSMDEDSLTKKIAVNGSHTLNSKRRS
```

Figure 6. Sequence alignment of Atg9 between amino acid residues 750-811. A. Alignment of the amino acid sequence between residues 750-811 of Atg9 from various organisms. B. Putative point mutants interfering with Atg9 binding to Atg2. The amino acid sequence of Atg9 between residues 750-811 is shown. The charged and polar amino acids that have been substituted with alanines in each Atg9 point mutant are indicated in bold.

ACKNOWLEDGMENTS

The authors thank Daniel Klionsky for reagents. F.R. is supported by ZonMW-VIDI (917.76.329), ECHO (700.59.003), ALW Open Program (821.02.017) and DFG-NOW cooperation (DN82-303) grants.

REFERENCES

1. Barth, H., K. Meiling-Wesse, U.D. Epple, and M. Thumm. 2001. Autophagy and the cytoplasm to vacuole targeting pathway both require Aut10p. *FEBS Lett.* 508:23-28.
2. Barth, H., and M. Thumm. 2001. A genomic screen identifies AUT8 as a novel gene essential for autophagy in the yeast *Saccharomyces cerevisiae*. *Gene*. 274:151-156.
3. Cheong, H., and D.J. Klionsky. 2008. Biochemical methods to monitor autophagy-related processes in yeast. *Methods Enzymol.* 451:1-26.
4. Fengsrud, M., E.S. Erichsen, T.O. Berg, C. Raiborg, and P.O. Seglen. 2000. Ultrastructural characterization of the delimiting membranes of isolated autophagosomes and amphisomes by freeze-fracture electron microscopy. *European journal of cell biology*. 79:871-882.
5. Gietz, R.D., and R.H. Schiestl. 2007. High-efficiency yeast transformation using the LiAc/SS carrier DNA/PEG method. *Nat Protoc*. 2:31-34.
6. Guan, J., P.E. Stromhaug, M.D. George, P. Habibzadegah-Tari, A. Bevan, W.A. Dunn, Jr., and D.J. Klionsky. 2001. Cvt18/Gsa12 is required for cytoplasm-to-vacuole transport, pexophagy, and autophagy in *Saccharomyces cerevisiae* and *Pichia pastoris*. *Mol Biol Cell*. 12:3821-3838.
7. Gueldener, U., J. Heinisch, G.J. Koehler, D. Voss, and J.H. Hegemann. 2002. A second set of loxP marker cassettes for Cre-mediated multiple gene knockouts in budding yeast. *Nucleic Acids Res*. 30:e23.
8. He, C., M. Baba, Y. Cao, and D.J. Klionsky. 2008. Self-interaction is critical for Atg9 transport and function at the phagophore assembly site during autophagy. *Mol Biol Cell*. 19:5506-5516.
9. He, C., H. Song, T. Yorimitsu, I. Monastyrska, W.L. Yen, J.E. Legakis, and D.J. Klionsky. 2006. Recruitment of Atg9 to the preautophagosomal structure by Atg11 is essential for selective autophagy in budding yeast. *J Cell Biol*. 175:925-935.
10. Itakura, E., and N. Mizushima. 2010. Characterization of autophagosome formation site by a hierarchical analysis of mammalian Atg proteins. *Autophagy*. 6:764-776.
11. James, P., J. Halladay, and E.A. Craig. 1996. Genomic libraries and a host strain designed for highly efficient two-hybrid selection in yeast. *Genetics*. 144:1425-1436.
12. Kim, J., W.P. Huang, P.E. Stromhaug, and D.J. Klionsky. 2002. Convergence of multiple autophagy and cytoplasm to vacuole targeting components to a perivacuolar membrane compartment prior to de novo vesicle formation. *J Biol Chem*. 277:763-773.
13. Klionsky, D.J. 2007. Autophagy: from phenomenology to molecular understanding in less than a decade. *Nat Rev Mol Cell Biol*. 8:931-937.
14. Legakis, J.E., W.L. Yen, and D.J. Klionsky. 2007. A cycling protein complex required for selective autophagy. *Autophagy*. 3:422-432.
15. Levine, B., and D.J. Klionsky. 2004. Development by self-digestion: molecular mechanisms and biological functions of autophagy. *Dev Cell*. 6:463-477.
16. Longtine, M.S., A. McKenzie, 3rd, D.J. Demarini, N.G. Shah, A. Wach, A. Brachat, P. Philippsen, and J.R. Pringle. 1998. Additional modules for versatile and economical PCR-based gene deletion and modification in *Saccharomyces cerevisiae*. *Yeast*. 14:953-961.
17. Lynch-Day, M.A., and D.J. Klionsky. 2010. The Cvt pathway as a model for selective autophagy. *FEBS Lett.* 584:1359-1366.
18. Mari, M., J. Griffith, E. Rieter, L. Krishnappa, D.J. Klionsky, and F. Reggiori. 2010. An Atg9-containing compartment that functions in the early steps of autophagosome biogenesis. *J Cell Biol*. 190:1005-1022.

19. Mari, M., and F. Reggiori. 2007. Atg9 trafficking in the yeast *Saccharomyces cerevisiae*. *Autophagy*. 3:145-148.

20. Mari, M., and F. Reggiori. 2010. Atg9 reservoirs, a new organelle of the yeast endomembrane system? *Autophagy*. 6:1221-1223.

21. Mizushima, N., B. Levine, A.M. Cuervo, and D.J. Klionsky. 2008. Autophagy fights disease through cellular self-digestion. *Nature*. 451:1069-1075.

22. Nakatogawa, H., K. Suzuki, Y. Kamada, and Y. Ohsumi. 2009. Dynamics and diversity in autophagy mechanisms: lessons from yeast. *Nat Rev Mol Cell Biol*. 10:458-467.

23. Noda, T., J. Kim, W.P. Huang, M. Baba, C. Tokunaga, Y. Ohsumi, and D.J. Klionsky. 2000. Apg9p/Cvt7p is an integral membrane protein required for transport vesicle formation in the Cvt and autophagy pathways. *J Cell Biol*. 148:465-480.

24. Orsi, A., M. Razi, H.C. Dooley, D. Robinson, A.E. Weston, L.M. Collinson, and S.A. Tooze. 2012. Dynamic and transient interactions of Atg9 with autophagosomes, but not membrane integration, are required for autophagy. *Mol Biol Cell*. 23:1860-1873.

25. Reggiori, F. 2006. 1. Membrane origin for autophagy. *Curr Top Dev Biol*. 74:1-30.

26. Reggiori, F., T. Shintani, U. Nair, and D.J. Klionsky. 2005. Atg9 cycles between mitochondria and the pre-autophagosomal structure in yeasts. *Autophagy*. 1:101-109.

27. Reggiori, F., K.A. Tucker, P.E. Stromhaug, and D.J. Klionsky. 2004. The Atg1-Atg13 complex regulates Atg9 and Atg23 retrieval transport from the pre-autophagosomal structure. *Dev Cell*. 6:79-90.

28. Reggiori, F., C.W. Wang, P.E. Stromhaug, T. Shintani, and D.J. Klionsky. 2003. Vps51 is part of the yeast Vps fifty-three tethering complex essential for retrograde traffic from the early endosome and Cvt vesicle completion. *J Biol Chem*. 278:5009-5020.

29. Robinson, J.S., D.J. Klionsky, L.M. Banta, and S.D. Emr. 1988. Protein sorting in *Saccharomyces cerevisiae*: isolation of mutants defective in the delivery and processing of multiple vacuolar hydrolases. *Mol Cell Biol*. 8:4936-4948.

30. Shintani, T., K. Suzuki, Y. Kamada, T. Noda, and Y. Ohsumi. 2001. Apg2p functions in autophagosome formation on the perivacuolar structure. *J Biol Chem*. 276:30452-30460.

31. Suzuki, K., T. Kirisako, Y. Kamada, N. Mizushima, T. Noda, and Y. Ohsumi. 2001. The pre-autophagosomal structure organized by concerted functions of *APG* genes is essential for autophagosome formation. *EMBO J*. 20:5971-5981.

32. Suzuki, K., Y. Kubota, T. Sekito, and Y. Ohsumi. 2007. Hierarchy of Atg proteins in pre-autophagosomal structure organization. *Genes Cells*. 12:209-218.

33. Velikkakath, A.K., T. Nishimura, E. Oita, N. Ishihara, and N. Mizushima. 2012. Mammalian Atg2 proteins are essential for autophagosome formation and important for regulation of size and distribution of lipid droplets. *Mol Biol Cell*. 23:896-909.

34. Wang, C.W., J. Kim, W.P. Huang, H. Abeliovich, P.E. Stromhaug, W.A. Dunn, Jr., and D.J. Klionsky. 2001. Apg2 is a novel protein required for the cytoplasm to vacuole targeting, autophagy, and pexophagy pathways. *J Biol Chem*. 276:30442-30451.

35. Wittke, S., N. Lewke, S. Muller, and N. Johnsson. 1999. Probing the molecular environment of membrane proteins in vivo. *Mol Biol Cell*. 10:2519-2530.

36. Xie, Z., and D.J. Klionsky. 2007. Autophagosome formation: core machinery and adaptations. *Nat Cell Biol*. 9:1102-1109.

37. Yang, Z., and D.J. Klionsky. 2010. Mammalian autophagy: core molecular machinery and signaling regulation. *Curr Biol*. 22:124-131.

38. Young, A.R.J., E.Y.W. Chan, X.W. Hu, R. Köchl, S.G. Crawshaw, S. High, D.W. Hailey, J. Lippincott-Schwartz, and S.A. Tooze. 2006. Starvation and ULK1-dependent cycling of mammalian Atg9 between the TGN and endosomes. *J Cell Sci*. 119:3888-3900.

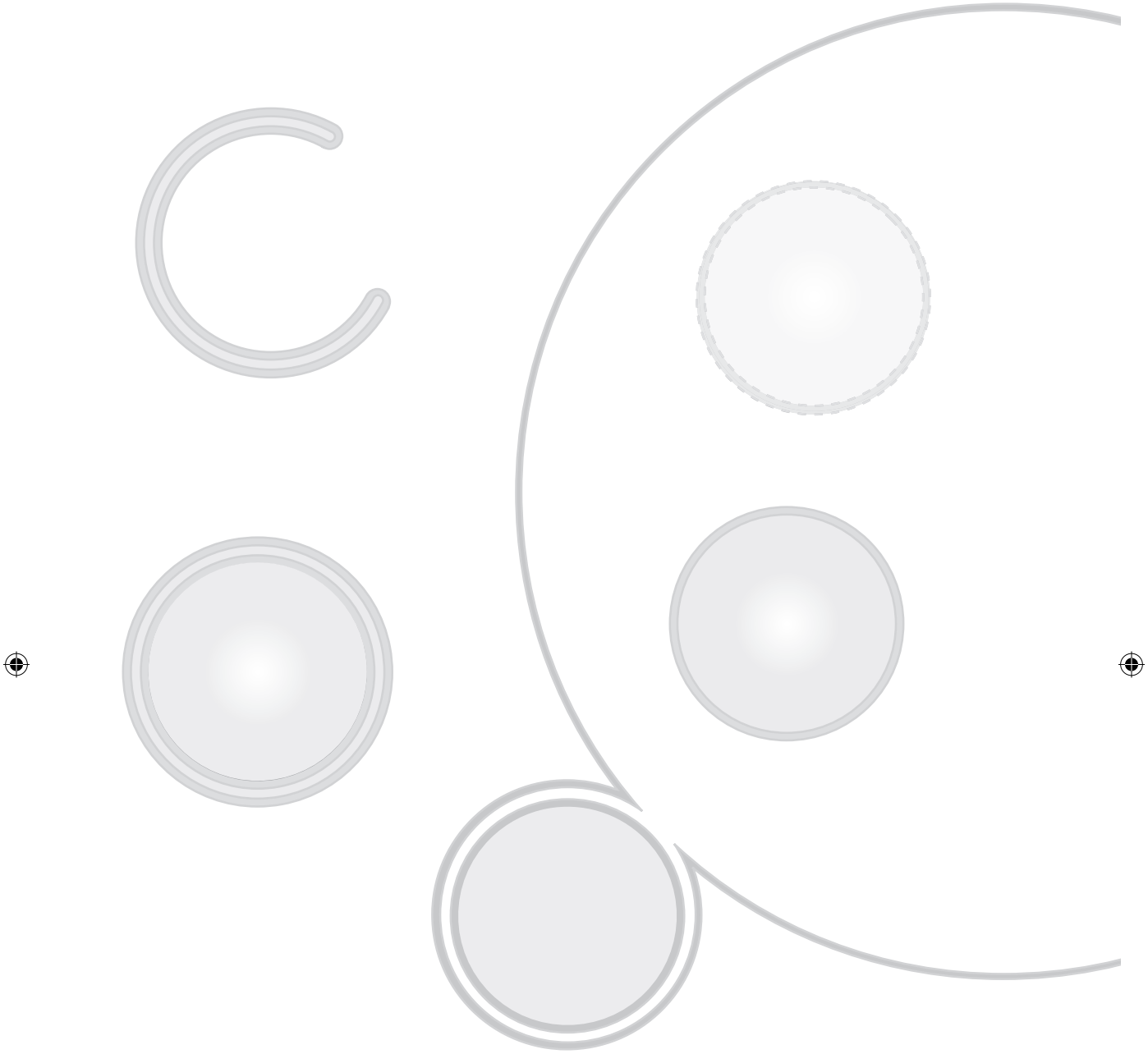

CHAPTER

5

An Atg9-containing compartment that functions in the early steps of autophagosome biogenesis

Muriel Mari,[1,2] Janice Griffith,[1,2] Ester Rieter,[1,2] Lakshmi Krishnappa,[1,2] Daniel J. Klionsky,[3,4,5] and Fulvio Reggiori[1,2]

[1]Department of Cell Biology and [2]Institute of Biomembranes, University Medical Centre Utrecht, Utrecht University, 3584 CX Utrecht, Netherlands; [3]Life Sciences Institute, [4]Department of Molecular, Cellular and Developmental Biology, and [5]Department of Biological Chemistry, University of Michigan, Ann Arbor, MI 48109

The Journal of Cell Biology 2010 190:1005-1022

ABSTRACT

Eukaryotes use the process of autophagy, in which structures targeted for lysosomal/vacuolar degradation are sequestered into double-membrane autophagosomes, in numerous physiological and pathological situations. The key questions in the field relate to the origin of the membranes as well as the precise nature of the rearrangements that lead to the formation of autophagosomes. We found that yeast Atg9 concentrates in a novel compartment comprising clusters of vesicles and tubules, which are derived from the secretory pathway and are often adjacent to mitochondria. We show that these clusters translocate en bloc next to the vacuole to form the phagophore assembly site (PAS), where they become the autophagosome precursor, the phagophore. In addition, genetic analyses indicate that Atg1, Atg13 and phosphatidylinositol-3-phosphate are involved in the further rearrangement of these initial membranes. Thus, our data reveal that the Atg9-positive compartments are important for the de novo formation of the PAS and the sequestering vesicle that are the hallmarks of autophagy.

Key words: autophagy/Cvt pathway/Atg9/autophagosome/PAS

INTRODUCTION

The conserved catabolic pathway of autophagy is essential to generate an internal pool of nutrients that permit cells to survive during prolonged periods of starvation (Mizushima et al., 2008). Recent studies have revealed that because of its ability to eliminate unwanted structures, autophagy also participates in development, cellular differentiation, degradation of aberrant structures, and life span extension, as well as protecting against pathogens and tumors (Levine and Deretic, 2007; Levine and Kroemer, 2008; Mizushima et al., 2008). As a result, this pathway plays a relevant role in the pathophysiology of neurodegenerative, cardiovascular, muscular and autoimmune diseases.

The general mechanism of autophagy involves the sequestration of the cytoplasmic cargo into large double-membrane vesicles called autophagosomes that fuse with lysosomes/vacuoles to provide their contents with access to the hydrolytically active interior of these organelles, thus allowing for the cargo's degradation. The current model of autophagosome biogenesis is that they are formed by expansion and successive sealing of a small membrane cisterna termed the phagophore or isolation membrane (Reggiori and Klionsky, 2005). The phagophore appears to be generated at a specialized site called the phagophore assembly site or the pre-autophagosomal structure (PAS) (Xie and Klionsky, 2007). Most of the studies about the PAS have been done in the yeast *Saccharomyces cerevisiae*, where only one of these structures is present in each cell and it is found in proximity to the vacuole (Xie and Klionsky, 2007). These investigations have revealed that the autophagy-related (Atg) proteins, the components of the conserved machinery mediating autophagosome biogenesis, assemble following a hierarchical order and form this specialized site (Suzuki et al., 2007). Despite the apparent importance of the PAS, very little is known about this site at the molecular level, including the origin of the nucleating membrane and the subsequent rearrangements that allow it to form a sequestering compartment.

Most of the Atg proteins are cytosolic and transiently associate with the PAS by interacting with other Atg components and/or lipids. Atg9 is the only conserved integral membrane protein that is essential for autophagosome formation (Lang et al., 2000; Noda et al., 2000; Young et al., 2006). In yeast, Atg9 localizes to several puncta dispersed throughout the cytoplasm, some of which colocalize with mitochondria markers; however, it remains unclear whether they are part of the outer membrane of this organelle or adjacent to it (Reggiori et

al., 2005; Reggiori et al., 2004a). Atg9 cycles between these peripheral puncta (hereafter referred as the Atg9 reservoirs), that do not contain detectable levels of most other conserved Atg proteins, and the PAS, supporting the notion that Atg9 is involved in the delivery of membrane necessary for the formation of the sequestering vesicles (Reggiori et al., 2004a). In addition, Atg9 is one of the first Atg components to be localized to the PAS (Suzuki et al., 2007). In *atg9*Δ cells, nearly all the other Atg proteins fail to be recruited to the PAS making its role crucial in the assembly of the Atg machinery.

The key organizational function of Atg9 is also exemplified by the fact that Atg9 transport to the PAS is regulated during the yeast cytoplasm-to-vacuole targeting (Cvt) pathway, a biosynthetic selective type of autophagy devoted to the delivery into the vacuole of cytosolic oligomers mostly formed by the precursor vacuolar protease aminopeptidase I (prApe1; Klionsky et al., 1992). After oligomerization, the prApe1 complex binds to its receptor, Atg19, to form the Cvt complex, which is subsequently recruited near the vacuole surface in an Atg11-dependent step (Shintani et al., 2002). Atg11 also binds Atg9 and thus mediates the simultaneous movement of both the Cvt complex and Atg9 (He et al., 2006; Shintani et al., 2002; Shintani and Klionsky, 2004). This regulated relocation triggers the recruitment of the Atg proteins to the PAS and subsequent sequestration of the Cvt complex into a double-membrane Cvt vesicle (Shintani and Klionsky, 2004).

Despite the important progress made in understanding autophagy, the study of the precise function of these factors as well as the mechanism of this pathway has been hampered by the lack of information regarding the membrane dynamics during the autophagosome formation process. To gain insights into this crucial question, we have studied the biogenesis of the yeast PAS by combining a recently developed immuno-electron microscopy (IEM) protocol (Griffith et al., 2008) with yeast genetics. We show that the PAS originates from Atg9-positive clusters of vesicles and tubules that we called Atg9 reservoirs. Translocation of one or more reservoirs in proximity to the vacuole, together with the successive recruitment of other Atg proteins, generates the PAS. Hence, fusion of the tubulovesicular membranes of the Atg9 reservoirs leads to the formation of the phagophore necessary for the subsequent biogenesis of a double-membrane vesicle. Thus, our results suggest the *de novo* formation of the PAS from vesicles and tubules and highlight the crucial role of Atg9 in this process.

MATERIALS AND METHODS

Plasmids

To create the *ATG9-GFP* fusion under the control of a *TPI1* promoter (pATG9GFP416), *ATG9* was amplified by PCR and cloned as a *Hind*III-*Xma*I fragment into the pSNA3416 plasmid digested with *Hind*III-*Age*I (Reggiori and Pelham, 2001). The 3' primer used for this PCR reaction introduced a Gly-Ala-Gly-Ala-Gly-Ala-Gly protein linker between Atg9 and GFP. The integration vector pATG9GFP406 was generated by swapping *TPI1-ATG9-GFP* as a *Xho*I-*Sac*I fragment into a pRS406 plasmid (Sikorski and Hieter, 1989). This construct leads to levels of Atg9-GFP 8 times higher when compared to endogenous Atg9 as assessed by western blot (not shown). The plasmid expressing the Atg9-GFP chimera under the control of the *GAL1* promoter (pGalATG9416) was made by excising the *TPI1* promoter from the pATG9GFP416 vector with *Xho*I-*Hind*III and replacing it with that of *GAL1*, which was obtained by PCR from genomic DNA. The integration vector pATG9mCheV5403, which leads to the expression of Atg9-mChe-V5 under the control of a *TPI1* promoter, was created as follows: First, PCR-amplified *mCHE-V5* was cloned into the pSNA3416 plasmid as an *Age*I-*Kpn*I fragment resulting in the pSNA3mCheV5416 plasmid. The *SNA3* gene was then excised from this plasmid with *Hind*III and *Age*I, and replaced by PCR-amplified *ATG9* digested with *Hind*III and *Xma*I to produce the pATG9mCheV5416 plasmid. The integration vector pATG9mCheV5403 was finally made by swapping *TPI1-ATG9-mCHE-V5* as a *Xho*I-*Sac*I fragment into a pRS403 plasmid (Sikorski and Hieter, 1989). As with the Atg9-GFP chimera (**Fig. 1**), the *TPI1* promoter-driven Atg9-mChe fusion protein is also functional (not shown).

The plasmid expressing monomeric red fluorescent protein (RFP)-Atg8 under the control of the authentic promoter (promRFPATG8415) was created in two steps. First, GFP was excised from the pRS316GFP–AUT7 plasmid (Suzuki et al., 2001) with BamHI and replaced by the gene coding for RFP flanked by BamHI sites. The promoter and gene fusions were then shuttled into the pRS415 vector (Sikorski and Hieter, 1989). The plasmid expressing mChe-V5-Atg8 under the control of the *CUP1* promoter (pCumCheV5ATG8415) was created by excising and replacing *GFP* in the pCuGFPATG8415 vector (Kim et al., 2002; Suzuki et al., 2001; Suzuki et al., 2007) with PCR-generated *mCHE-V5* digested with *Spe*I-*Xma*I.

The plasmid pmitoDsRed415 was generated by digesting the pADHmitoDsRED (Meeusen and Nunnari, 2003) vector with *Not*I-*Hind*III and

cloning the resulting *ADH1* promoter-*mitoDsRED* fragment into the pRS415 vector using the same restriction enzymes.

Template plasmids for the PCR-based integration of the m*Cherry-V5* tag (pFA6a- mCherry-V5-TRP1, pFA6a-mCherry-V5-HIS3 and pFA6a-mCherry-V5-KanMX) at the 3' end of genes were created as follows: The *GFP* gene was excised with *Pac*I and *Asc*I from the pFA6a-GFP-TRP1, pFA6a-GFP-HIS3 and pFA6a-GFP-KanMX vectors (Longtine et al., 1998), respectively, and replaced with the PCR-amplified *mCherry-V5*.

Plasmids pRS416, pJK1-2416 and those used for the genomic integration of Sec7-DsRED, GFP-Atg8 and RFP-Ape1 have been described elsewhere (Losev et al., 2006; Noda et al., 2000; Reggiori et al., 2004a; Sikorski and Hieter, 1989; Suzuki et al., 2001).

Strains

The *S. cerevisiae* strains used in this study are listed in Supplementary Information, **Table 3**. For gene disruptions, the *APE1*, *ATG1*, *ATG9*, *ATG11*, *ATG13* and *ATG14* coding regions were replaced with the *Escherichia coli kan*^{r}, the *S. cerevisiae TRP1* or the *Saccharomyces pombe HIS5* genes using PCR primers containing ~60 bases of identity to the regions flanking the open reading frame.

PCR-based integration of GFP, mCherry-V5 and a triple HA tag at the 3' end of *ATG9*, *IDH1*, *SEC63*, *SEC7* and *VRG4* was used to generate strains expressing C-terminal fusion proteins under the control of the native promoters. The template for integration was pFA6a-3xHA-HIS5, pFA6a-GFP-TRP1, pFA6a-mCherry-V5-TRP1, pFA6a-mCherry-V5-HIS3 and pFA6a-mCherry-V5-HIS3 (Longtine et al., 1998; and see Plasmids). PCR-based integration of *GFP* at the 5' end of *TLG1* and *PEP12* followed by Cre recombinase-mediated excision of the auxotrophic marker was used to generate strains expressing N-terminal fusion proteins under the control of their native promoters (Gauss et al., 2005). The PCR-template for integration was pOM43.

Western blot using specific antibodies recognizing the proteins encoded by the deleted genes, analysis of the Ape1 processing and PCR verification were used to confirm all deletions and integrations, and the functionality of all the genomic fusions.

Table 3. Strains used in this study

Name	Genotype	Reference/Origin
AFM69-1A	*MATa sec7-4 his3,11-15 leu2-3,112 ura3-1*	(Reggiori et al., 2004b)
BY4742	*MATa his3Δ1 leu2Δ0 lys2Δ0 ura3Δ0*	Euroscarf
FBY217	*MATa sec12-4 his3 leu2 ura3 trp1 ade2*	(Reggiori et al., 2004b)
FRY162	SEY6210 *ATG9-GFP::HIS5S.p.*	(Reggiori et al., 2005)
FRY172	SEY6210 *ATG9-PA::TRP1 pep4Δ::LEU2*	(Reggiori et al., 2004a)
FRY196	SEY6210 *ATG9-PA::TRP1 atg1Δ::URA3 pep4Δ::LEU2*	(Reggiori et al., 2004a)
FRY250	SEY6210 *ATG9-PA::TRP1 atg11Δ::URA3 pep4Δ::LEU2*	This study
FRY300	*MATa his3Δ1 leu2Δ0 lys2Δ0 ura3Δ0 pho13Δ::KAN pho8::PHO8Δ60 atg9Δ0*	This study
FRY340	SEY6210 *ATG9-GFP::TRP1 VRG4-mCHE-V5::HIS5 S.p.*	This study
FRY341	SEY6210 *ATG9-GFP::TRP1 SEC7-dsRED::URA3*	This study
FRY342	SEY6210 *GFP-TLG1 ATG9-mCHE-V5::TRP1*	This study
FRY344	SEY6210 *GFP-PEP12 ATG9-mCHE-V5::TRP1*	This study
FRY360	SEY6210 *GFP-TLG1*	This study
JCK007	SEY6210 *atg9Δ::HIS3*	(Noda et al., 2000)
MMY067	SEY6210 *atg9Δ::KAN TPI1-ATG9-GFP::URA3*	This study
MMY068	SEY6210 *atg9Δ::KAN atg1Δ::HIS5 S.p.TPI1-ATG9-GFP::URA3*	This study
MMY069	SEY6210 *atg9Δ::KAN atg11Δ::HIS5 S.p.TPI1-ATG9-GFP::URA3*	This study
MMY070	SEY6210 *atg9Δ::KAN atg13Δ::HIS5 S.p.TPI1-ATG9-GFP::URA3*	This study
MMY071	SEY6210 *atg9Δ::KAN atg14Δ::HIS5 S.p.TPI1-ATG9-GFP::URA3*	This study
MMY072	SEY6210 *atg9Δ::KAN TPI1-ATG9-GFP::URA3 RFP-APE1::LEU2*	This study
MMY073	SEY6210 *atg9Δ::KAN atg1Δ::HIS5 S.p. TPI1-ATG9-GFP::URA3 RFP-APE1::LEU2*	This study
MMY074	SEY6210 *atg9Δ::KAN atg11Δ::HIS5 S.p. TPI1-ATG9-GFP::URA3 RFP-APE1::LEU2*	This study
MMY075	SEY6210 *atg9Δ::KAN atg13Δ::HIS5 S.p. TPI1-ATG9-GFP::URA3 RFP-APE1::LEU2*	This study
MMY076	SEY6210 *atg9Δ::KAN atg14Δ::HIS5 S.p. TPI1-ATG9-GFP::URA3 RFP-APE1::LEU2*	This study
MMY078	SEY6210 *atg9Δ::KAN atg1Δ::HIS5 S.p. ape1Δ::HIS5 S.p. TPI1-ATG9-GFP::URA3*	This study
MMY120	SEY6210 *TPI1-ATG9-mChe-V5::HIS3*	This study
MMY125	BY4742 *SEC7-mChe-V5::KAN*	This study
MMY126	BY4742 *SEC63-mChe-V5::KAN*	This study
MMY127	*MATa sec7-4-mCHE-V5::KAN his3,11-15 leu2-3,112ura3-1*	This study
MMY129	*MATa sec12-4 SEC63-mChe-V5::HIS3 leu2 ura3 trp1 ade2*	This study
MOY003	SEY6210 *atg9Δ::KAN TPI1-ATG9-GFP::URA3 IDH1-3xHA::HIS3*	This study
SEY6210	*MATa ura3-52 leu2-3, 112 his3-Δ200 trp1-Δ901 lys2-801 suc2-Δ9 mel GAL*	(Robinson et al., 1988)

Media

Yeast cells were grown in rich (YPD; 1% yeast extract, 2% peptone, 2% glucose) or synthetic minimal media (SMD; 0.67% yeast nitrogen base, 2% glucose, amino acids and vitamins as needed). Starvation experiments were conducted by adding 200 ng/ml of rapamycin or by transferring cells into a nitrogen starvation medium

(SD-N; 0.17% yeast nitrogen base without amino acids and ammonium sulphate, and 2% glucose).

Fluorescence microscopy

Yeast cells were grown in the appropriate medium before imaging. Endosomes were stained with FM 4-64 as described previously (Sipos et al., 2004). Briefly, 1 ml of log phase cultures was centrifuged and resuspended in 100 μl of ice-cold medium containing 20 μM of FM 4-64 (Invitrogen). After 15 min on ice, cells were washed once with ice-cold medium without FM 4-64 and then resuspended in the same solution before being spotted on a cover slide. Preparations were successively imaged at RT over a 10 min period.

Fluorescence signals were captured with a fluorescence microscope system (DeltaVision RT; (Applied Precision) with a 100× objective lens, equipped with a CoolSNAP HQ camera (Photometrix). Images were generated by collecting a stack of 20 pictures with focal planes 0.20 μm apart in order to cover the entire volume of a yeast cell (4-5 μm) and by successively deconvolving and analyzing them with the softWoRx software (Applied Precision). A single focal plane is shown at each time point.

To perform statistical analyses of the colocalization degree between fluorescence signals, mild conditions were used to fix cells without destroying the fluorescent proteins (Reggiori et al., 2005). The 3-dimensional projection of the picture stacks allows visualizing all the Atg9-positive puncta present in each cell. Subsequently, the number of these puncta colocalizing with the fluorescent organelle protein marker present in the same cells was determined. Percentages represent how many Atg9-positive puncta colocalize with a specific organelle protein marker. In total, approximately 200-350 Atg9-positive puncta were analyzed for each time point and this counting was repeated twice with samples from two independent experiments. Standard deviations between these two countings were calculated. To determine the number of Atg9-positive compartments per cell in strains expressing endogenous or overexpressed Atg9-GFP, the number of green puncta per cell was counted in 100 randomly chosen cells. Estimation of colocalization between endogenous or overexpressed Atg9-GFP puncta and mitochondria labelled with mitochondria-targeted DsRed was also performed in 100 randomly chosen cells. Three different categories of Atg9-GFP puncta were found. Those completely colocalizing with mitochondria were defined as *overlapping*, those adjacent or apposed to mitochondria were defined

as *adjacent*, while those not in proximity to mitochondria were defined as *free*.

The time-lapse experiments were performed by imaging the same cells every 5 s for 4 min and 5 s (50 pictures). At each time point, images were generated by collecting a stack of 3 pictures with focal planes 0.20 µm apart and by successively deconvolving them.

Immuno-electron microscopy

Cells were fixed, embedded in gelatin and cryo-sectioned as described previously (Griffith et al., 2008). Sections were then immuno-labelled using rabbit anti-GFP (Abcam) and anti-Ape1 (a kind gift of I. Sandoval and M. Mazón, Universidad Autonoma de Madrid, Madrid, Spain) antisera, mouse anti-Por1 (Molecular Probes) and anti-HA (a gift of G. Bu, Washington University in St. Louis, St. Louis, MO) antibodies, and goat anti-GFP (Rockland, Gilbertsville, PA) antibody follow by protein A (PA)-gold detection. The specificity of the antigenic reaction has been controlled for each single or double immuno-gold labelling that has been performed (**Fig. S5**). Sections were viewed in an electron microscope (1200 EX; JEOL).

Statistical analysis of IEM data

The presence of gold particles associated with membranes comprising at least 6 vesicular and/or tubular profiles with a distance no greater than 10-15 nm defined an Atg9 cluster while labelled single vesicles at a distance greater than 100 nm from a membranous structure, vesicle or organelle, were defined as isolated vesicles. Membranes comprising 2 to 5 vesicular and/or tubular profiles have not been included in the statistical analyses because they were very rarely observed. A gold particle was assigned to a compartment when no further than 25 nm away from its limiting membrane. The number of Atg9 clusters and Cvt complex per cell section were counted in wild-type, *atg11*Δ and *atg1*Δ strains by randomly analyzing 250 cell profiles per strain over 3 independent experiments. This counting was also used to determine the number of cell sections positive for an Atg9 cluster or a Cvt complex.

The relative distribution of Atg9-GFP tubulo-vesicular clusters was assessed by randomly analyzing 150 sampled profiles from at least 4 distinct grids. These structures (adjacent or not to a Cvt complex) were designated as being associated with a well-defined organelle (nucleus, vacuole or mitochondria) if within 50 nm from its limiting membrane. Structures further away were defined

as cytoplasmic. Estimation of the average surface section of the Atg9 clusters was performed by analyzing 30 micrographs per condition using the point-hit method (Rabouille, 1999).

Subcellular fractionation

Separation of membranes present in a low speed supernatant fractions on sucrose gradients were performed as described previously (Reggiori et al., 2004b). Briefly, 500 OD_{600} equivalents of spheroplasts were lysed in 5 ml of ice-cold hypo-osmotic buffer (50 mM K_2HPO_4, pH 7.5, 200 mM sorbitol, 1 mM EDTA) containing freshly added Complete protease inhibitors (Roche) and 2 mM PMSF by 20 aspirations through a syringe. Cell lysates were centrifuged twice at 500 x *g* for 5 min and 4 ml of the supernatant fractions (T) were subjected to centrifugation at 13,000 x *g* for 15 min to be separated into supernatant (S13) and pellet (P13) fractions. The S13 fractions (2 ml) were subsequently loaded on a top of sucrose step gradients and centrifuged at 170,000 x *g* for 16 h. All fractions were mixed with 4X Sample buffer, heated at 37°C for 5 min and resolved by SDS-PAGE followed by western blot using antibodies or serum against GFP (Roche), V5 (Invitrogen), Tlg1 (a gift from H. Pelham, Medical Research Council Laboratory of Molecular Biology, Cambridge, England, UK), Por1, Pgk1, and Pep12 (all from Invitrogen).

Pho8 activity assay

4 OD_{600} of cells in log phase or nitrogen-starved for 4 h, were harvested by centrifugation, washed with 1 ml of ice-cold water, and resuspended in 400 µl of Lysis buffer (20 mM PIPES, pH 6.8, 0.5% Triton X-100, 50 mM KCl, 100 mM potassium acetate, 10 mM $MgSO_4$, 10 µM $ZnSO_4$, 2 mM PMSF). The same volume of glass beads was added and cells were disrupted by agitation for 5 min. After pelleting of cell debris at 13,000 x g for 5 min, 100 µl of lysate were mixed with 400 µl of Reaction buffer (250 mM Tris-HCl, pH 8.5, 0.4% Triton TX-100, 10 mM $MgSO_4$, 10 µM $ZnSO_4$, 1.25 mM p-nitrophenyl phosphate; Sigma-Aldrich) pre-warmed at 37°C. Incubation was carried out at 37°C for 20 min and stopped by adding 500 µl of 1 M glycine buffer (pH 11.0). Samples were then centrifuged at 13,000 x g for 2 min and 1 ml of supernatant was taken to measure the absorbance at 420. Protein concentration in the lysate was determinate with a D_c Protein Assay kit (Bio-rad Laboratories). Pho8 activity was calculated as (1000 x OD_{420})/(min x [prot]) where min = 20 min and [prot] = protein concentration in the lysate expressed in mg/ml. Results were expressed in a plot as percentage

of the activity measured for the wild type strain starved for nitrogen and error bars represent the standard deviation from 3 experiments.

Ape1 analysis by western blot

2.5 OD_{600} of cells grown in YPD to log phase were collected by centrifugation and proteins were precipitated with 400 µl of ice-cold 10% trichloroacetic acid for 30 min. After spinning the samples for 5 min, pellets were washed with ice-cold acetone. Pellets were subsequently air dried, resuspended in 100 µl of Sample buffer (80 mM Tris-HCl, pH 6.8, 2% SDS, 8.7% glycerol, 2.5% 2-mercaptoethanol and 0.05% bromophenol blue) and boiled for 5 min. Aliquots of 20 µl were loaded on 8% SDS-PAGE gels and after western blot, membranes were probed with the anti-Ape1 antibodies. The anti-Ape1 polyclonal antiserum was generated by injecting the synthetic peptide CKHWRSVYDEFGEL corresponding to amino acid residues 502-514 of Ape1 in New Zealand White rabbits (New England Peptide).

Online supplemental paragraph

Fig. S1 shows the **Fig. 2D** and **2E** without dashed lines as well as additional examples of Atg9 clusters in wild-type cells. **Fig. S2** illustrates that Atg9 overexpression leads to an expansion of the membranes containing this protein without altering their biophysical properties. **Fig. S3** shows the subcellular distribution of Atg9 in various mutant strains. **Fig. S4** presents **Fig. 6C-6F** without dashed lines and ultrastructural views of Atg9 clusters in various mutant strains. **Fig. S5** displays the immuno-gold labeling controls. **Videos 1** and **2** show an Atg9 reservoir becoming the PAS. Online supplemental material is available at http://www.jcb.org/cgi/content/full/jcb.200912089/DC1.

RESULTS

Atg9 localizes to tubulovesicular clusters adjacent to mitochondria

It has been proposed that Atg9 is one of the factors mediating the transport of lipid bilayers to the PAS (Reggiori et al., 2004a). Consequently, the identification of the membranes positive for Atg9 is crucial to understand the nature and biogenesis of the PAS, and its role in autophagosome formation. Fluorescence microscopy has shown that Atg9 resides in numerous puncta, some of them partially colocalizing

with or near mitochondria (Reggiori and Klionsky, 2006; Reggiori et al., 2005). This approach, however, does not make possible to determine the nature of the Atg9 compartments and their structural relationship with mitochondria. To unveil their morphology and acquire mechanistic insights into their contribution to PAS formation, we analyzed the localization and trafficking of Atg9 at the ultrastructural level using a recently developed IEM procedure (Griffith et al., 2008). As the cellular levels of endogenous Atg9 are too low for IEM detection, we created a functional C-terminal green fluorescent protein (GFP)-fusion protein (Atg9-GFP), which behaves like the endogenous one (**Fig. 1**).

Wild-type cells expressing Atg9-GFP were grown in rich medium and prepared for IEM. The vast majority of Atg9-GFP was present in clusters of vesicular (average diameter of 30-40 nm) and tubular structures (**Fig. 2, A-D**; and **Fig. S1**). The Atg9 clusters (defined in *Materials and Methods*) were found in 53% of the cells and their numbers vary from 1 to 3, with occasionally 4, per cell section (**Table 1**). The gold particles corresponding to Atg9-GFP decorated the cytosolic surface of these membranes, in agreement with Atg9 topology that predicts GFP fused to the C terminus to be on the cytosolic face of lipid bilayers (He et al., 2006). Interestingly, the Atg9 clusters were occasionally seen surrounding a circular electron-dense cytoplasmic structure with a diameter of 100-150 nm (**Figs. 2D** and **S1, A** [arrowhead] and **E**). Double immuno-gold labelling for GFP and Ape1 identified it as the Cvt complex (**Figs. 2E** and **S1B**; Baba et al., 1997). When more than one Atg9 cluster was observed in a cell section, only one of them was associated with a Cvt complex (**Tables 1** and **2**; 1% of the cell sections are Cvt complex-positive). In contrast, the Cvt complex was associated with an Atg9 cluster in 80% of the cells where the former was detected, reflecting the close association between these two structures (He et al., 2006).

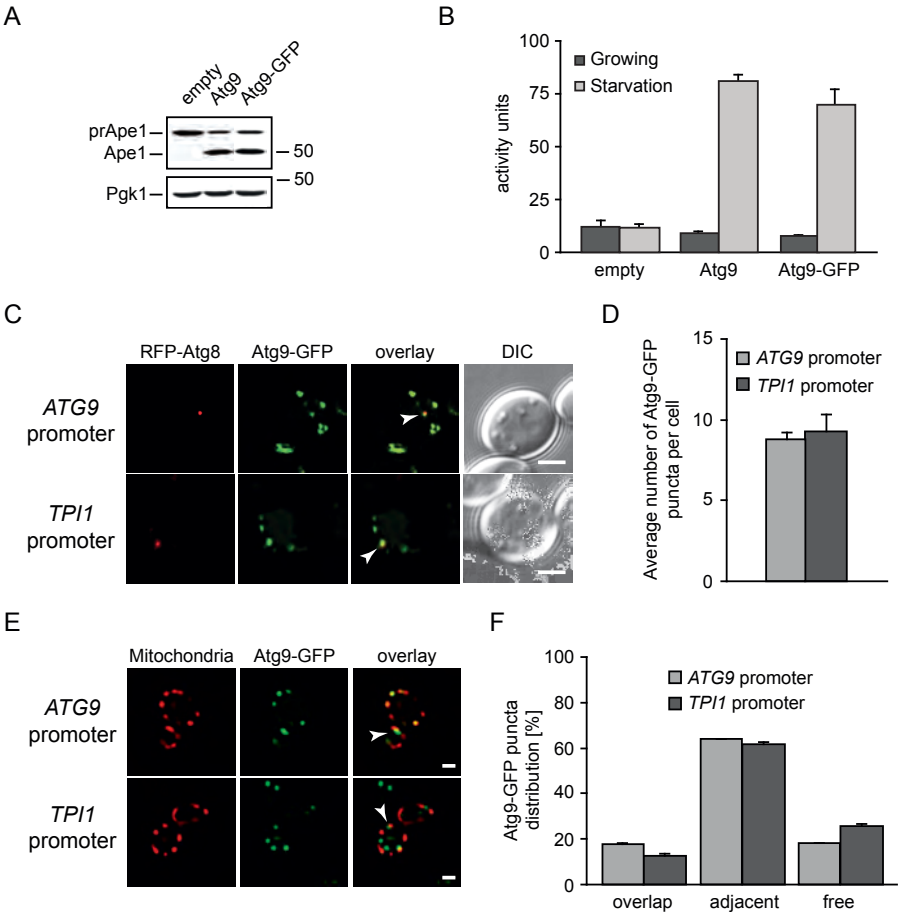

Figure 1. The Atg9-GFP construct for IEM analyses. A. The prApe1 processing is normal in Atg9-GFP-expressing cells. The *atg9Δ* (JCK007) mutant transformed with either an empty vector (pRS416), a plasmid carrying the *ATG9* gene (pJK1-2416) or the ATG9-GFP fusion (pATG9GFP416) was grown in YPD medium to log phase before analyzing prApe1 maturation by immuno-blot. The cytosolic protein Pgk1 was used as a loading control. M_r is indicated in kD. B. Autophagy is normal in presence of Atg9-GFP. The *atg9Δ* (FRY300) cells expressing Pho8Δ60 and transformed with the same plasmids described in panel A, were shifted from YPD medium (dark grey bars) to SD-N medium (light grey bars) for 4 h. Autophagy induction was determined by a Pho8 activity assay. C,D. Atg9-GFP has a normal distribution and one of the Atg9-GFP-containing puncta is the PAS. Strains expressing Atg9-GFP under the control of the *ATG9* promoter (FRY162) or the *TPI1* promoter (MMY067) were transformed with a plasmid (promRFPATG8415) carrying the PAS protein marker RFP-Atg8. Transformants were cultured to log phase and imaged (C). The number of Atg9-GFP puncta per cell was counted (D) and error bars represent the standard deviation of the mean. E,F. Part of Atg9-GFP distributes to mitochondria. The strains analyzed in panel C were transformed with the pmitoDsRed415 plasmid expressing mitochondria-targeted RFP and imaged (E). Arrowheads highlight Atg9 puncta adjacent to mitochondria. Determination of Atg9-GFP puncta distribution on mitochondria (F) was determined as described in *Materials and Methods* and error bars represent the standard deviation of the mean. DIC, differential interference contrast. Bar, 2 μm.

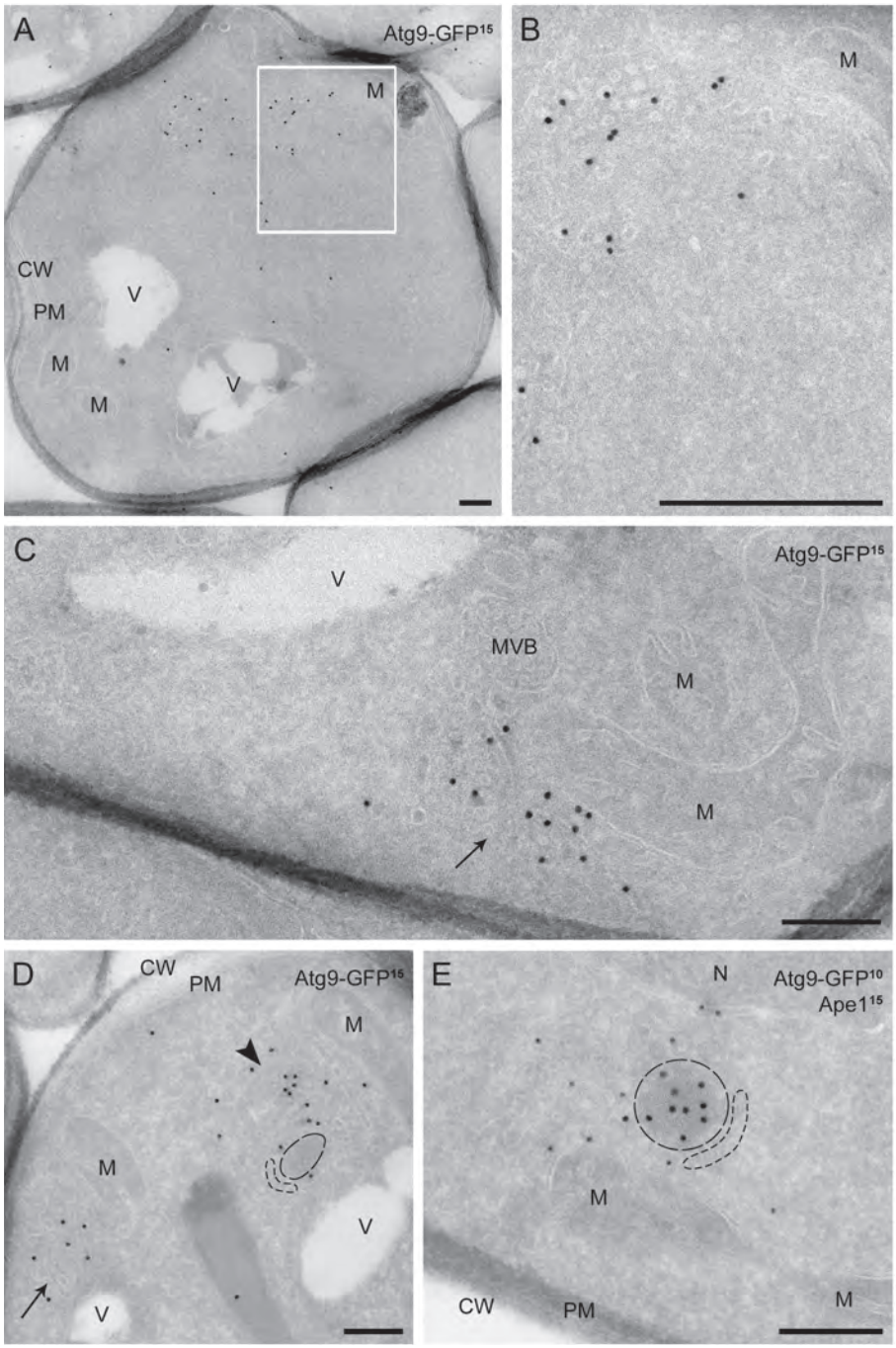

Figure 2. IEM analysis of wild-type cells expressing Atg9-GFP. Atg9-GFP (MMY067) cells were grown to log phase and processed for IEM as described in *Materials and Methods*. Preparations shown in panels A to D were immuno-gold labelled only for GFP while those

presented in panel E were double immuno-gold labelled for GFP and Ape1. A. Overview of a labelled cell section. B. Insets of panel A illustrating an Atg9-positive cluster of vesicles and tubules. C. Atg9-containing membranous arrangements (arrow) adjacent to mitochondria (≤ 50 nm distance). D. Micrograph showing a GFP-labelled cell with 2 Atg9 clusters (marked by an arrow and an arrowhead), one of which (arrowhead) associated with an electron-dense structure with a 100-150 nm diameter (dashed circle). E. The circular electron-dense structures found in close proximity to the Atg9 clusters and labelled for Ape1 are Cvt complexes (dashed circle). The dashed cisterna emphasizes the Cvt complex surface not associated with Atg9-containing membranes. Panels D and E are also shown in Fig. S1A and S1B without dashed lines for clarity while additional examples of Atg9 clusters are presented in Fig. S1C-H. The size of the gold particles is indicated on the top of each picture. Bar, 200 nm. CW, cell wall; M, mitochondria; MVB, multivesicular body; N, Nucleus; PM, plasma membrane; V, vacuole.

Table 1. Frequency of the Atg9-GFP containing structures and the Cvt complex

Criteria	Strain background		
	WT	***atg11Δ***	***atg1Δ***
Atg9-GFP-containing membranous clusters /cell section			
0	47 ± 1.8	57 ± 2.3	84 ± 1.2
1	28 ± 1.3	25 ± 0.8	14 ± 0.7*
2	19 ± 0.9	16 ± 0.8	2 ± 0.2*
3	5 ± 0.8	2 ± 1.1	0
≥4	1 ± 0.2	0	0
Cvt complex/cell section			
0	99 ± 0.1	99.7 ± 0.3	95 ± 0.8
1	1 ± 0.4	0.3 ± 0.1*	5 ± 0.8*
2	0	0	0
3	0	0	0
≥4	0	0	0

Counting and statistical analyses were carried out as described in Materials and methods. All the results are expressed in percentages (%) ± the standard error of the mean.
* $p \leq 0.05$.

In agreement with the fluorescence microscopy data (He et al., 2006; Reggiori and Klionsky, 2006; Reggiori et al., 2005), the Atg9 clusters were predominantly adjacent to mitochondria (57%, **Table 2**) but they were never seen continuous with the outer membrane of this organelle. To reinforce the notion that these clusters are separated from mitochondria we immuno-localized Por1, a component of the mitochondrial outer membrane. The Por1 exclusively found on the surface of mitochondria and absent from the Atg9-containg clusters (**Fig. 3A**). An identical result was also obtained with Idh1, another mitochondrial protein marker (**Fig. 3, B-F**).

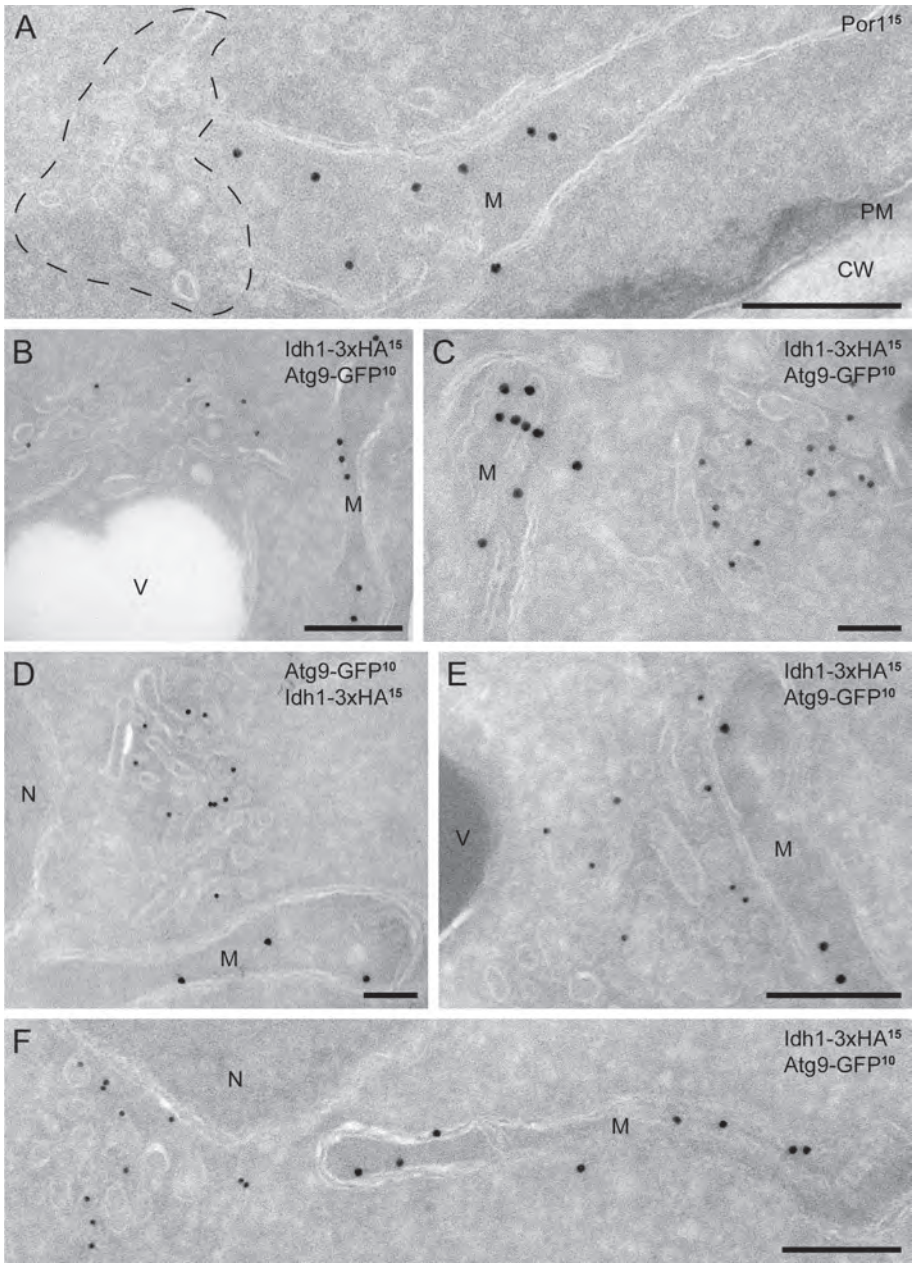

Figure 3. Mitochondrial protein markers do not localize to the Atg9 clusters. A. Ultrathin cryo-sections obtained from a wild-type (MMY067) strain were immuno-gold labelled only for Por1 because the anti-Por1 antibody does not work in double labelling. The dashed contour highlights an Atg9 cluster. B-F. Cells expressing both Atg9-GFP and the mitochondrial marker Idh1-3xHA (MOY003) were processed for IEM and cryo-sections were double immuno-gold labelled for GFP and HA. Bar, 200 nm. CW, cell wall; M, mitochondria; N, nucleus; PM, plasma membrane; V, vacuole.

Table 2. Relative subcellular distribution of the Atg9-GFP containing structures and Cvt complex

Criteria/cell type	Location			
	Adjacent to mitochondria	Perivacuolar	Perinuclear	Other cytoplasmic
Atg9-GFP-containing membranous clusters				
WT	57.0 ± 0.2	3.8 ± 0.05	4.9 ± 0.05	34.3 ± 0.1
atg1 1Δ	50 ± 0.4	4 ± 0.3	2 ± 0.03	44 ± 0.1
atg1Δ	17.5 ± 0.1	37.5 ± 0.1	7.5 ± 0.05	37.5 ± 0.2
Cvt complexes associated with Atg9-GFP-containing membranous clusters				
WT	58.8 ± 0.3	2.0 ± 0.1	3.9 ± 0.2	35.3 ± 0.3
atg1 1Δ	ND	ND	ND	ND
atg1Δ	14.3 ± 0.2	57.1 ± 0.2	12.2 ± 0.5	16.4 ± 0.8
Free Cvt complexes				
WT	2.2 ± 0.2	0	0	97.8 ± 0.3
atg1 1Δ	15.4 ± 1.1	0	1.2 ± 0.8	83.4 ± 1.5
atg1Δ	ND	ND	ND	ND

Counting and statistical analyses were carried out as described in Materials and methods. All the results are expressed in percentages (%) ± the standard error of the mean. ND, not determined because this structure is not present or very rare in the indicated strain.

In parallel, we addressed whether higher levels of Atg9-GFP were altering the Atg9 reservoirs morphology. When we analyzed an untransformed wild-type strain by IEM, we detected identical clusters adjacent to mitochondria, albeit with a reduced size (**Fig. S2A**). To determine if these clusters showed similar biophysical properties in wild-type and Atg9-GFP-overexpressing cells, cell extracts were centrifuged at 13,000 x g. Under these conditions, most of the endogenous Atg9 was found in the low speed supernatant (S13) fraction and only a small amount in the pellet (P13) fraction (**Fig. S2B**; Reggiori et al., 2004b, 2005). The reduction in the amount of Atg9 in the P13 fraction in comparison to previous published data (Reggiori et al., 2005), may represent more efficient spheroplast lysis. Using the same approach for cells overproducing Atg9-GFP, we found this fusion protein in the S13 fraction (**Fig. S2B**). This result indicates that higher levels of Atg9 change the volume of the Atg9 clusters to accommodate more protein but they do not alter their biophysical properties. Similar enlargements have been reported for other organelles like the endoplasmic reticulum (ER), where overproduction of a resident protein leads to ER expansion without altering its physiology (Wright et al., 1988).

We concluded that the Atg9-containing compartments consist of a cluster of vesicles and tubules that are often in the vicinity of mitochondria, but not connected with them.

Atg9 resides in a novel compartment originating from the secretory system

The proximity of the Atg9 clusters adjacent to, but distinct from, mitochondria raised the question of their biogenesis. As Atg9 is a transmembrane protein, it could be inserted into membranes either in the mitochondria or in the ER.

To follow the Atg9 biosynthetic route, Atg9-GFP expression was put under the control of the galactose-inducible *GAL1* promoter. Transfer into a galactose-containing medium for 2 h allowed us to detect Atg9 clusters (**Fig. 4**). No intermediate structures, e.g. mitochondria or ER, were visualized even at earlier time points, probably due to the rapid transport of Atg9 following synthesis. To further explore whether Atg9 is transported through the secretory pathway, we used a strain carrying a thermosensitive allele of *SEC12*, which blocks ER exit (Barlowe and Schekman, 1993). At permissive temperature, the localization pattern of Atg9-GFP was indistinguishable from that observed in wild-type cells (**Fig. 4A**). At restrictive temperature, in contrast, the transport block between the ER and Golgi apparatus resulted in the accumulation of newly synthesized Atg9 in the ER as revealed by colocalization with the specific protein marker Sec63 (**Fig. 4A**; Deshaies et al., 1991). This transport block was reversible indicating that Atg9-GFP was not amassed in a terminal structure but rather accumulated in a transport intermediate (not shown). To examine the role of the Golgi complex in Atg9 transport, we used a thermosensitive *sec7* allele, which blocks protein traffic from this organelle, but does not affect localization of the protein (Franzusoff and Schekman, 1989; Jackson and Casanova, 2000). At 24°C, Atg9-GFP was again normally distributed to several cytoplasmic puncta, and those were only rarely positive for the late Golgi compartment protein marker Sec7 (**Fig. 4B**; Losev et al., 2006). In contrast, at 37°C, newly synthesized Atg9-GFP was present in circular structures, often positive for $Sec7^{ts}$ tagged with **Discosoma *red*** fluorescent protein (dsRed), which occasionally had an elongated conformation (**Fig. 4B**, arrows). These structures are likely Berkeley bodies, aberrant Golgi generated as a result of the *sec7* sorting defect (Novick et al., 1980). Again, the transport block was reversible indicating that Atg9-GFP was not accumulated in a terminal structure (not shown). We concluded that Atg9 is translocated into the ER and reaches its final destination, the Atg9 clusters, probably after passing through the Golgi.

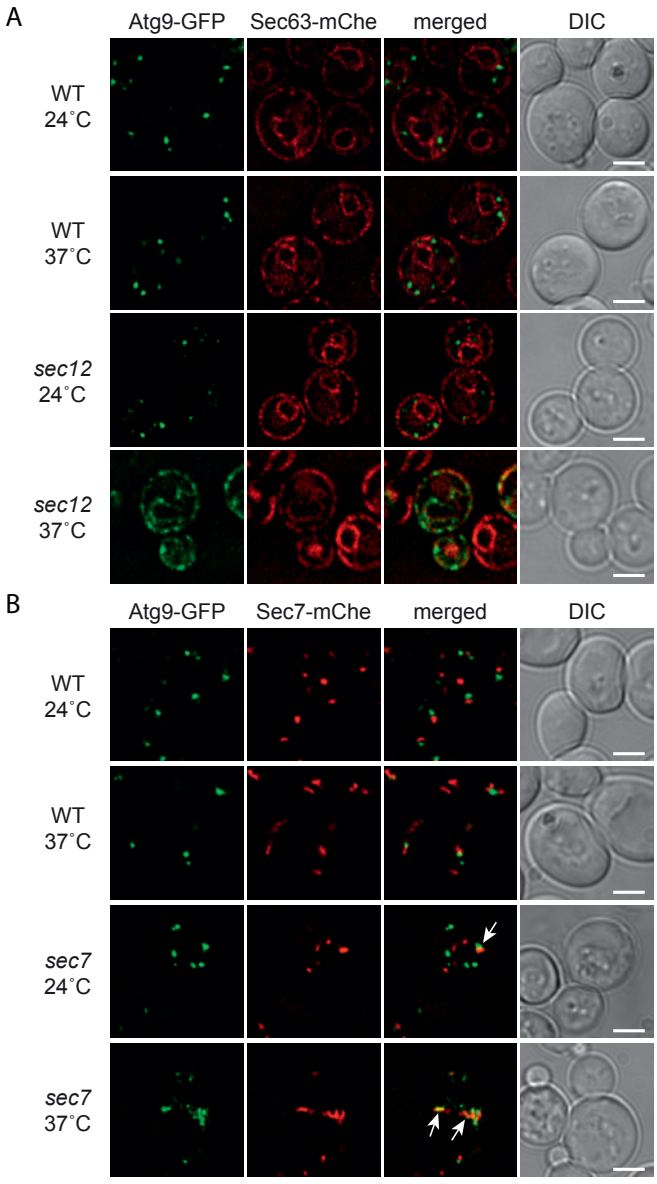

Figure 4. Atg9 is transported through part of the secretory pathway. A. Atg9 is translocated into the ER. The wild-type (MMY126) and *sec12* (MMY129) cells expressing Sec63-mChe-V5 and carrying the pGalATG9GFP416 plasmid were grown in SMD at 24°C before being transferred into a galactose-containing medium. Cultures were subsequently split and separately incubated at either 24°C or 37°C for 2h before imaging. No fluorescence signal was detected when cells were grown in the presence of glucose (not shown). B. Atg9 passes through the Golgi before reaching its final destination. Wild-type (MMY125) and *sec7* (MMY127) cells expressing genomically mChe-V5-tagged Sec7 and Sec7^{ts}, respectively, and transformed with the pGalATG9GFP416 plasmid were analyzed as in panel A. Arrows highlight

the colocalization between Atg9-GFP and Sec7^{ts}-mChe in *sec7*^{ts} cells at 37°C. DIC, differential interference contrast. Bar, 2 μm.

As a post-Golgi organelle, the Atg9 clusters could be endosomes. To test this possibility, we used FM 4-64, a lipophylic dye that, after associating with the plasma membrane (PM), passes through endosomes before reaching the vacuole (Vida and Emr, 1995). At 4°C, endocytosis is inhibited and FM 4-64 exclusively associates with the PM. Transfer of FM 4-64-loaded cells to RT allows the internalization of this dye in a time-dependent manner (Sipos et al., 2004). After 10 min at RT, FM 4-64 reached early endosomes [EE; (Sipos et al., 2004)] as demonstrated by the extensive colocalization with the specific protein marker Tlg1 (**Fig. 5A**; Holthuis et al., 1998). Several Atg9 clusters were faintly positive for FM 4-64 at the same internalization time point (**Fig. 5A**, arrows).

The fact that the Atg9 clusters are connected with the endocytic and secretory systems prompted us to investigate whether known protein markers of these compartments localized on Atg9 clusters. We created strains expressing Atg9-GFP together with dsRed- or Cherry-tagged Tlg1 (EE), Pep12 (late endosomes, LE), Vrg4 (early Golgi), Sec7 (late Golgi) and Atg23 (colocalizes with Atg9) (Holthuis et al., 1998; Losev et al., 2006) under the control of the endogenous promoters. As expected, Atg23 displayed substantial colocalization with Atg9 (**Fig. 5 C**). In contrast, the tagged endosomal and Golgi proteins did not (**Fig. 5, B** and **C**).

Taken together, our results show that the Atg9 clusters represent a novel compartment originating from the secretory pathway and able to exchange at least lipids with the endocytic system.

The Atg9 reservoirs and the PAS have a similar morphological organization

Atg9 is a highly dynamic protein that shuttles between the Atg9 reservoirs and the PAS (Geng et al., 2008; Reggiori et al., 2004a). Therefore, one of the Atg9 clusters described above could represent the PAS. In wild-type cells it is not possible to distinguish the PAS from the Atg9 reservoirs. Therefore we capitalized on certain characteristics of the Cvt pathway for two reasons: i) It uses primarily the same Atg machinery as autophagy, and ii) specific gene deletions can modulate Atg9 trafficking. For instance, Atg11 is essential for both the association between Atg9 and the Cvt complex, and their transport near the vacuole in growing conditions, where they recruits the Atg proteins (**Fig. S3A**; He et al., 2006). As a consequence, no PAS is formed in the *atg11*Δ strain (**Fig. S3B**; Shintani and Klionsky, 2004) and this allows exclusive visualization of the Atg9 reservoirs.

A

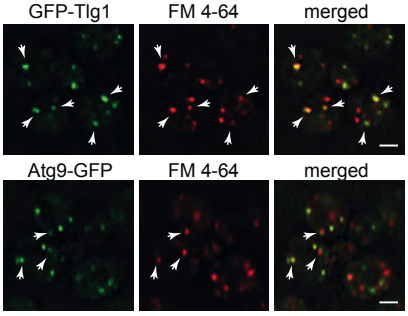

B

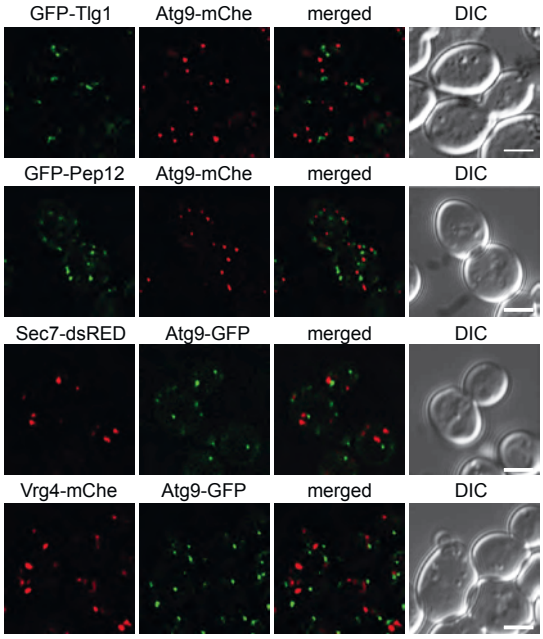

C

Protein marker	Protein marker	Co-localization
Atg23	Atg9 complex	87.9 ± 6.2
Tlg1	EE	12.8 ± 3.5
Pep12	LE	11.0 ± 1.4
Sec7	Late Golgi	8.3 ± 2.0
Vrg4	Early Golgi	11.3 ± 3.8

Figure 5. Atg9 concentrates into a novel organelle. A. Atg9-GFP colocalizes with some FM 4-64-positive puncta shortly after endocytosis. The strains expressing genomically GFP-tagged Tlg1 (FRY360) or Atg9 (FRY162) were grown to log phase and then exposed to FM 4-64 as described in *Materials and Methods*. Arrowheads highlight the colocalization between FM

4-64 and GFP-Tlg1 or Atg9-GFP. B. Atg9 does not colocalize with endosomal and Golgi protein markers. The Atg9-GFP Vrg4-mCHE-V5 (FRY340), Atg9-GFP Sec7-dsRED (FRY341), GFP-Tlg1 Atg9-mCHE-V5 (FRY342) and GFP-Pep12 Atg9-mCHE-V5 (FRY344) strains were grown to log phase before being fixed and imaged. C. The colocalization experiments shown in panel B were statistically evaluated as described in *Materials and Methods*. Atg23 was used as a positive control for colocalization because forming a complex with Atg9 (Reggiori et al., 2004a). DIC, differential interference contrast. Bar, 2 μm.

IEM analysis of the *atg1*Δ cells revealed that the Atg9 clusters adjacent to mitochondria are the Atg9 reservoirs (**Fig. 6, A and B**; **Fig. S4, A-C**; and **Table 2**). The Atg9-positive structures were found in 43% of the cell sections and the subcellular distribution of these compartments was identical to that observed in wild-type cells, showing that the Atg9 reservoirs are the main site of Atg9 concentration (**Table 2**). As expected, the Atg9 reservoirs were no longer associated with Cvt complexes in agreement with the reported phenotype of the *atg1*Δ mutant (**Fig. S3A**; He et al., 2006).

We then used a similar genetic approach to capture the PAS and analyze its ultrastructure. Deletion of *ATG* genes blocks PAS assembly at a precise stage (Suzuki et al., 2007). Under these conditions, this specialized site is identified by fluorescence microscopy as a perivacuolar punctum positive for the Cvt complex and for several Atg proteins, the array of which depends on the knocked out gene (Suzuki et al., 2007). Atg1 is one of the first proteins to be recruited to the PAS and consequently an early formation intermediate accumulates when it is absent (Suzuki et al., 2007). Crucially, Atg9 is exclusively localized at the PAS in *atg1*Δ cells because it cannot recycle to the reservoirs (**Fig. S3**; Reggiori et al., 2004a), providing an excellent tool to capture the forming PAS. Remarkably, the PAS appeared as a single cluster of Atg9-containing vesicles and tubules, very similar to the Atg9 reservoirs observed in wild-type and *atg1*Δ cells (**Fig. 6, C and D**; and **Fig. S4, D-H**). A main difference was that this single cluster was detected in fewer cells (**Table 1**; 16% of the cell sections in comparison with 53% and 43% for wild-type and *atg1*Δ, respectively) and it was no longer in close proximity to the mitochondria but mostly adjacent to the vacuole (**Table 2**; 37% of the time), reinforcing the notion that it corresponds to the PAS (Suzuki et al., 2007). Furthermore, this cluster was associated with the Cvt complex in 94% of the cases, confirming its PAS identity (**Fig. 6, C and D**; and **Fig. S4E-H**).

To corroborate the conclusions drawn from the examination of the *atg1*Δ mutant, we next analyzed the PAS in *atg13*Δ and *atg14*Δ cells where the PAS biogenesis is also blocked at an early assembly stage (Suzuki et al., 2007)

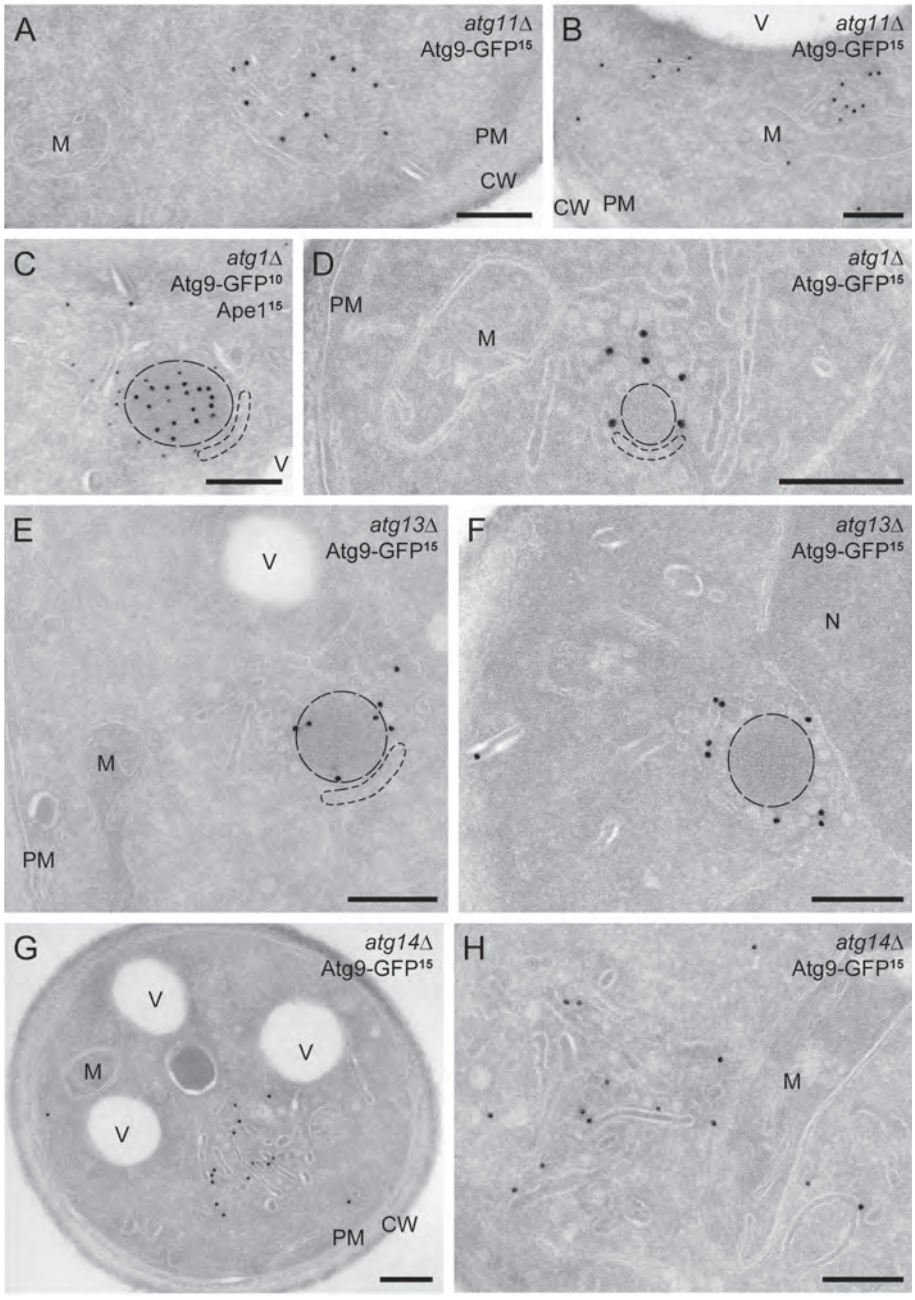

Figure 6. Atg9-GFP distribution in various *atg* mutants. The *atg1*1Δ (MMY069; A and B), *atg1*Δ (MMY068; C and D), *atg13*Δ (MMY070; E and F) and *atg14*Δ (MMY071; G and H) strains were grown and processed as described in Fig. 2. Cryo-sections were immuno-labelled for GFP alone (A, B, D-J) or in combination with Ape1 (C). A,B. The Atg9 reservoirs observed

in *atg11*Δ cells. C,D. The PAS accumulated in the *atg1*Δ knockout. E,F. The PAS present in the *atg13*Δ strain displays a Cvt complex surrounded by numerous small vesicles G,H. Enrichment of tubular membranes at the PAS of the *atg14*Δ mutant. Cvt complexes are highlighted with dashed circles. Panels D to F are also shown in Fig. S4E-F and S4I-J without dashed lines for clarity while additional examples are presented in Fig. S4A-D, S4G-H and S4K-Q. Bar, 200 nm. CW, cell wall; M, mitochondria; N, nucleus; PM, plasma membrane; V, vacuole.

and Atg9 is accumulated at this site (**Fig. S3**; Reggiori et al., 2004a). Similar to *atg1*Δ cells, the number of Atg9 reservoirs was strongly reduced in these mutants and when detected, they were often in association with the Cvt complex and proximal to the vacuole, further suggesting that this is indeed the PAS (**Fig. 6, E-H**; and **Fig. S4, I-Q**). Strikingly, the PAS observed in the absence of *ATG13* and *ATG14* displayed a slightly different morphology from that of *atg1*Δ cells. In the *atg13*Δ knockout (**Fig. 6, E-F**; and **Fig. S4, I-M**), the PAS was comprised almost entirely of small vesicular profiles with a diameter of approximately 25-30 nm, whereas in the *atg14*Δ mutant, more and longer tubular profiles were present in this structure, which in general appeared to be larger (**Fig. 6G-H**; and **Fig. S3, N-Q**).

Together, our data strongly supports the concept that the PAS is a vesicular and tubular cluster with morphology very similar to Atg9 reservoirs. The data also indicate that double-membrane vesicles are formed through a process that initially requires the fusion/remodelling of these membranes through the direct or indirect functions of Atg1, Atg13 and Atg14.

The Atg9 reservoirs participate in the generation of the PAS

The strong morphological similarity between the Atg9 reservoirs and the PAS suggests that the latter originates from the former. If so, these two structures are expected to have similar biochemical properties. To test this, we fractionated intracellular membranes of wild-type, *atg11*Δ and *atg1*Δ strains. Cell extracts were first centrifuged at 13,000 x g. In all three strains, most of the Atg9 was found in the low speed S13 fraction and only a small amount in the pellet P13 fraction (**Figs. 7A** and **S2B**; Reggiori et al., 2004b, 2005). The S13 supernatant fraction was then separated on a sucrose step-density gradient (Reggiori et al., 2004b). From wild-type cells, Atg9 fractionated in a single peak that was for the most part distinct from EE and LE (**Fig. 7, B and C**). Importantly, the Atg9 reservoirs and the PAS that accumulated in the *atg11*Δ and *atg1*Δ mutant, respectively, are also present in the same fractions (**Fig. 7, B and C**). This finding indicates that the Atg9 reservoirs and the PAS have almost identical densities, supporting the notion that the PAS could be derived from the Atg9 reservoirs.

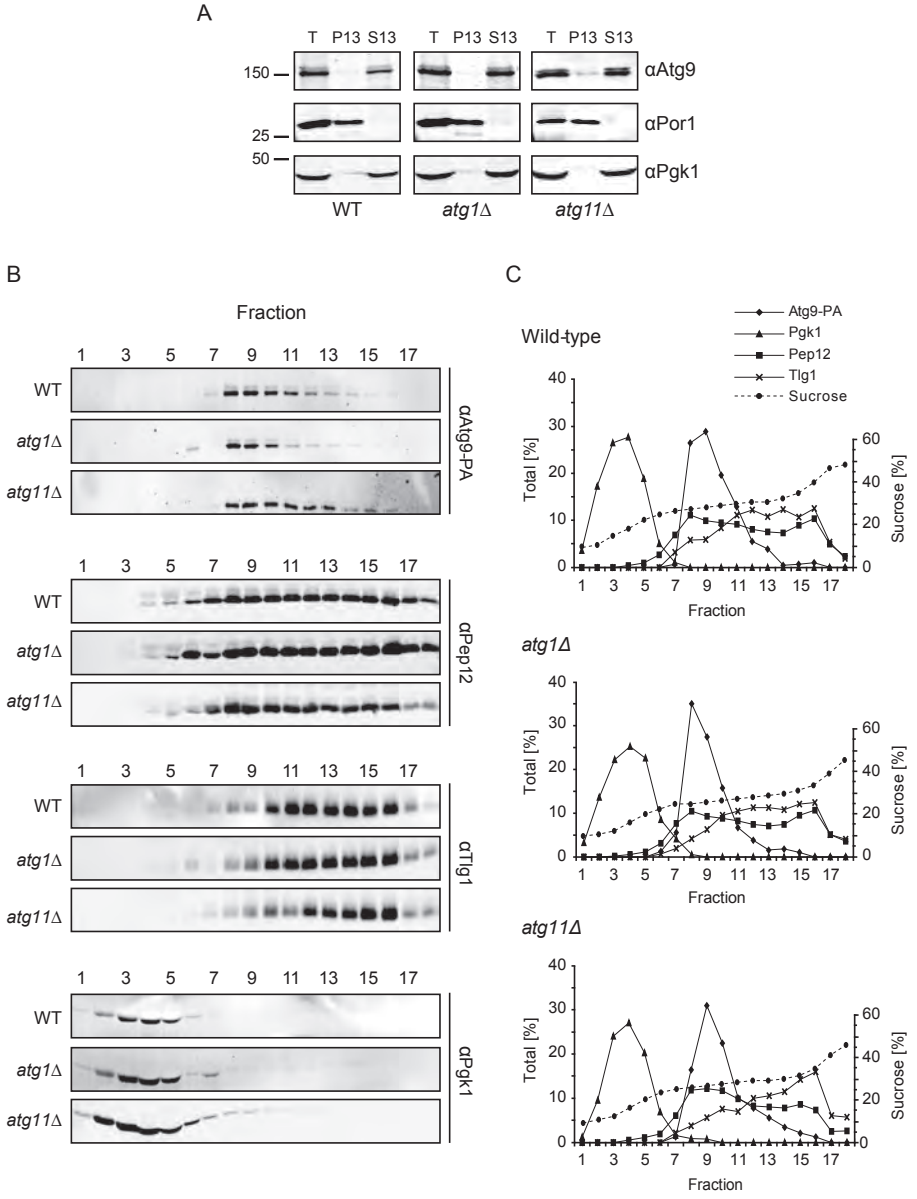

Figure 7. Subcellular fractionation of Atg9 clusters in wild-type, *atg11Δ* and *atg1Δ* backgrounds. A. The Atg9-PA (FRY172), Atg9-PA *atg11Δ pep4Δ* (FRY250) and Atg9-PA *atg1Δ pep4Δ* (FRY196) strains were grown to log phase, converted to spheroplasts and lysed, and cell extracts centrifuged at 13,000 x g for 15 min. The cell extract (T), the supernatant (S13) and the pellet (P13) fractions were then separated by SDS-PAGE and Atg9 distribution analyzed by western blot using anti-PA antibodies. Efficient lysis and correct fractionation were assessed by verifying the partitioning of cytosolic Pgk1 and mitochondrial Por1. M_r is indicated in kD. B.

The S13 supernatants were fractionated on sucrose step-density gradients and the fractions analyzed by western blot using antisera against PA (for Atg9-PA), Pep12, Tlg1 and Pgk1. C. Quantification of the immuno-blots.

Two possible models could explain how the PAS is generated from the Atg9 reservoirs. In the first, reservoirs translocate *en bloc* towards the vacuole, whereas in the second model, single vesicles derived from one or more reservoirs assemble near the vacuole. To determine how the PAS is generated from the Atg9 reservoirs, we took advantage of the fact that Atg9 transport to the PAS requires the Cvt complex in growing conditions, but not when autophagy is induced (Shintani and Klionsky, 2004). In the *ape1*Δ *atg1*Δ double-knockout cells maintained in growing conditions, thus, Atg9 remains locked in the Atg9 reservoirs, whereas it accumulates at the PAS when these cells are starved (Shintani and Klionsky, 2004). To determine how Atg9 is transported from the Atg9 reservoirs to the PAS, we followed the relocalization of Atg9 in the *ape1*Δ *atg1*Δ mutant by IEM over time (up to 1 h) after autophagy induction by nitrogen starvation. At the early time points, the only Atg9-positive structures we identified were clusters of vesicles and tubules; these corresponded to the Atg9 reservoirs, as they were often found, in 47% of the cases, adjacent to the mitochondria (**Fig. 8, A and D**). Before starvation (time 0 min), 40% of the cell profiles were positive for 1 to 3 Atg9 reservoirs. In contrast, 60 min after the induction of autophagy, only 14% of the cell profiles were positive for Atg9 clusters and only one of them was observed per cell section. The Atg9-positive compartments were mostly found close to the vacuole after 60 min (**Fig. 8, B-D**). This observation is in line with the design of the experiment, which predicts an *atg1*Δ-equivalent phenotype (43% of cell profiles positive for 1 to 3 Atg9 clusters) before autophagy induction and an *atg1*Δ phenotype (16% of cell profiles positive for one Atg9 compartment) after starving the cells. The observed phenotypes were not due to a structural reorganization of the Atg9 clusters, e.g. fusion and fission, because the average surface section of the Atg9 clusters is very similar at the 0 and 60 min time points, 0.121 and 0.139 mm^2, respectively (t-test assessment of the individual measurements revealed no significant difference between the values; $p = 0.09$). Importantly, we did not observe a significant increase in the total number of isolated Atg9-positive vesicles in the cytoplasm, supporting the notion that Atg9 reservoirs translocate *en bloc* (**Fig. 8E**).

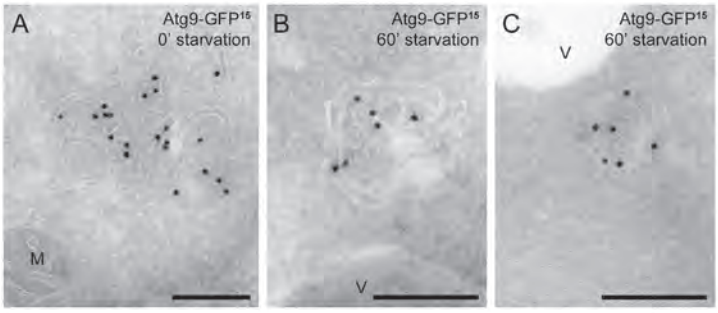

D

	Atg9-GFP-containing membranous clusters [%]			
	mitochondria	vacuole	nucleus	cytoplasm
0' starvation	47 ± 0.1	12 ± 0.1	7 ± 0.05	34 ± 0.1
60' starvation	20.5 ± 0.1	34 ± 0.1	2 ± 0.1	43.5 ± 0.1

E

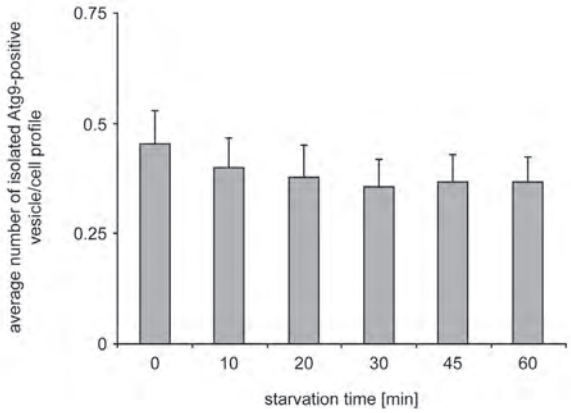

Figure 8. The Atg9 reservoirs move *en bloc* to become the PAS. The *ape1Δ atg1Δ* (MMY078) double mutant was grown to log phase before being nitrogen-starved to induce autophagy. Cell aliquots were collected after 0, 10, 20, 30, 45 and 60 min, processed for IEM and cryo-sections immuno-gold labelled for GFP (A-C). A. An Atg9 reservoir adjacent to a mitochondrion observed at the 0 min time point. B,C. Atg9 clusters close to the vacuole limiting membrane detected after 60 min of starvation. The gold particles size is indicated on the top of each picture. Bar, 200 nm. M, mitochondria; V, vacuole. D. Relative subcellular distribution of the Atg9-GFP clusters in the *ape1Δatg1Δ* cells before and after induction of autophagy for 60 min. Statistical analyses were carried out as described in *Materials and Methods*. E. The number of isolated Atg9-positive vesicles in the cytoplasm does not increase after triggering Atg9 relocalization in the *ape1Δ atg1Δ* mutant by autophagy induction. One hundred cell profiles were randomly selected and the number of isolated Atg9-positive vesicles per cell profile was established. Results in panels D and E are expressed in percentages ± the standard error of the mean.

To further demonstrate that the Atg9 reservoirs are the PAS precursor, we analyzed the evolution of this compartment by time-lapse fluorescence microscopy. At present, the primary distinguishing feature of the PAS is that most of the Atg proteins associate at least transiently with this site. Thus, the idea behind this experiment is that an Atg9 reservoir should acquire the rest of the conserved Atg proteins as it becomes a PAS. To test this hypothesis, we generated a strain expressing higher levels of Atg9-monomeric cherry (mChe) to avoid rapid bleaching of the red fluorescent protein, allowing longer recording intervals. In addition, *ATG8* was genomically tagged with *GFP* in the same cells. We selected Atg8 as a PAS protein marker because this factor is the last Atg protein to be recruited at this site (Suzuki et al., 2007) and consequently, its presence at the PAS reflects the complete assembly of the Atg machinery. The engineered cells were then grown to logarithmic (log) phase before being transferred in SD-N medium for 20 min and imaged. Nitrogen starvation was used to induce autophagy because under these conditions, double-membrane vesicles form at a higher frequency, increasing the chance of capturing PAS biogenesis. As shown in **Fig. 9** and **Video 1**, this approach allowed us to observe Atg9 reservoirs becoming the PAS; GFP-Atg8 was seen to move from a cytosolic location and ultimately colocalized with a reservoir. Importantly, the same result was obtained with cells expressing endogenous Atg9-GFP and carrying a plasmid expressing mChe-Atg8 (**Video 2**). These results demonstrate that the PAS originates from the Atg9 reservoirs, and consequently this latter compartment supplies at least part of the phagophore membrane. They also further support the notion that the Atg9 reservoirs translocate *en bloc* to become the PAS.

DISCUSSION

To shed light on the long-standing issue in autophagy of how autophagosomes are generated, we investigated PAS biogenesis using Atg9 as a protein marker. We discovered that the Atg9 reservoirs are clusters of vesicles and tubules that are often adjacent to mitochondria but not continuous with them (**Fig. 2, S1, Table 1 and 2**). The reason for the intimate connection between these two organelles remains unknown and their proximity could be simply due to both organelles being associated with actin cables. Nevertheless, it is now clear that the Atg9 reservoirs are not directly generated from mitochondria. First, we never observed

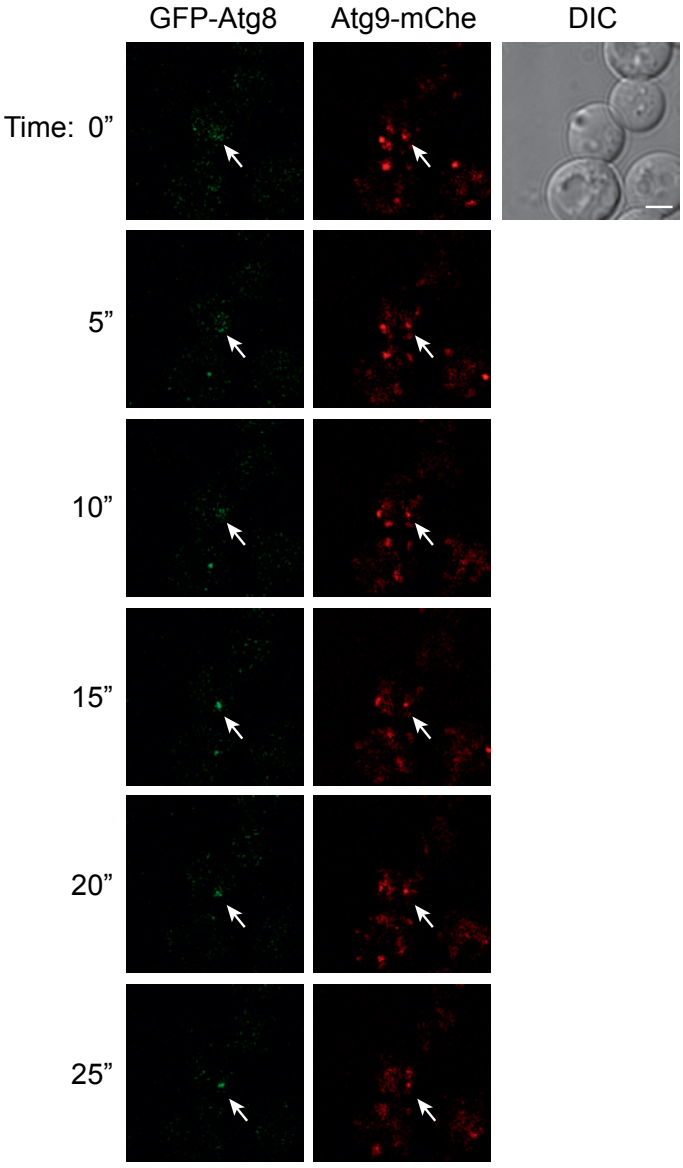

Figure 9. Live cell imaging of an Atg9 reservoir becoming the PAS. Atg9-mCherry GFP-Atg8 (MMY120) cells were grown to log phase and transferred to SD-N medium for 20 min before being imaged as described in *Materials and Methods*. Sequential images acquired with a time-lapse of 5 s are shown. The white arrow highlights the Atg9 reservoirs that ultimately colocalize with Atg8 in the process of becoming the PAS. The complete video reconstruction is presented in Video 1. An identical result was obtained with cells expressing endogenous Atg9-GFP (FRY172) and carrying the pCumCheV5ATG8415 plasmid, which expresses mChe-Atg8 (Video 2). DIC, differential interference contrast. Bar, 2 μm.

the membrane of the vesicles/tubules comprising this compartment in continuity with the mitochondrial outer membrane. Second, Atg9 was not detected on the surface of this organelle, and conversely, the mitochondrial protein markers Por1 and Idh1 were not found localizing to the Atg9 reservoirs (**Fig. 2B-E, 3, S1**). Finally, our studies about Atg9 biosynthesis show that this protein is translocated into the ER and reaches its final location via part of the secretory pathway (**Fig. 4**). Our results could appear to be in contradiction with published studies that suggested Atg9 localized at the mitochondria (He et al., 2006; Reggiori and Klionsky, 2006; Reggiori et al., 2005; Yen et al., 2007). In these studies, the mitochondrial localization of Atg9 was only hypothetical due to the resolution limits of fluorescence microscopy, and thus these previous analyses could not exclude the possibility that Atg9 is in a structure adjacent to mitochondria. Moreover, only a small fraction of Atg9-containing membranes (**Fig. 6A**), are found associated with mitochondria in subcellular fractionation experiments (Reggiori et al., 2005). Consequently, our data are not inconsistent with the literature, but rather explain previous observations and solve the discordance about Atg9 localization. It has been reported that the *sec12* mutation causes an Atg9 redistribution from pre-existing Atg9 reservoirs to the mitochondria surface (Reggiori and Klionsky, 2006). The Atg9 localization to mitochondria, however, was probably artefactual due to this organelle autofluorescence (our unpublished observations).

Based on our data, the Atg9 reservoirs emerge as a new organelle, and newly synthesized Atg9 is delivered to these sites through part of the secretory pathway (**Fig. 4**). Because of the only partial colocalization between newly synthesized Atg9 and the late Golgi protein marker Sec7 in *sec7* cells (**Fig. 4B**), it remains unclear from which Golgi compartment Atg9 is exiting. In addition, it cannot be excluded that Atg9 passes through another organelle and from there it mediates the formation of the Atg9 reservoirs. These issues are currently being investigated in our laboratory. The Atg9 reservoirs are accessible to endocytic material indicating that they are able to exchange materials with the endocytic system (**Fig. 5A**). Atg9, however, shows minimal colocalization, and only modestly fractionates with protein markers of the EE, LE and Golgi, indicating that this protein concentrates in a unique organelle (**Fig. 5B, 5C, 7C**; Noda et al., 2000; Reggiori et al., 2004b; Yen et al., 2007). In support of this, the disruption of the endocytic system with specific deletions such as that of *VPS4* leads to the concentration of endosomal proteins and several late Golgi factors into an abnormal, large LE adjacent to the vacuole (Odorizzi et al., 1998; Odorizzi et al.,

2003) without affecting Atg9 distribution or autophagy efficiency (Epple et al., 2003; Reggiori and Klionsky, 2006; Reggiori et al., 2004b).

It has been postulated that Atg9 is involved in supplying the nascent autophagosomes with lipid bilayers (Reggiori et al., 2004a). Here we show that the PAS originates from at least one of the Atg9 reservoirs (**Fig. 8, 9**). Thus, we argue that the initial membranes of the PAS and by extension of double-membrane vesicles are derived from the Atg9 reservoirs. We cannot exclude the possibility that during the expansion of the phagophore, additional lipid bilayers are obtained from a different source, for example from the ER, mitochondria or Golgi (Geng et al., 2010; Hailey et al., 2010; Hayashi-Nishino et al., 2009; van der Vaart et al., 2010).

In addition to the similar morphology between the Atg9 reservoirs and the PAS (**Fig. 1, 6, S1, S4**), one of our unpredicted discoveries has been the *en bloc* translocation of the reservoirs to form the PAS next to the vacuole. Our time-lapse fluorescence microscopy showed that the Atg machinery can be recruited to a single Atg9 reservoir (**Fig. 9, Videos 1** and **2**). When the Atg9 movement was triggered from the reservoirs to the PAS, we did not observe an increase in the number of isolated Atg9-containing vesicles and tubules in the cytoplasm (**Fig. 8**). These data support the notion that the Atg9 reservoirs move as clusters. This observation fits with our previous studies showing Atg9 present in cytoplasmic clusters (Reggiori et al., 2005; Reggiori et al., 2004a) and the demonstration that Atg9 self-interacts (He et al., 2008; Reggiori et al., 2005). An alternative model is that the PAS is generated by a small cluster of vesicles and/or tubules that results from the fragmentation of an Atg9 reservoir but we do not consider this likely because we have never seen such a scission event during the live-cell imaging experiments and small clusters comprising less than 6 vesicular and/or tubular profiles have only rarely been observed in our IEM preparations (see *Materials and Methods*). Altogether, our data allow us to postulate a model where at least one Atg9 reservoir acts as a pre-PAS and that a change in localization of this compartment determines the biogenesis of the PAS (**Fig. 10**). The movement of an Atg9 reservoir in close proximity to the vacuole triggers the hierarchical recruitment of the remaining Atg proteins that mediate the rearrangement of these vesicles and tubules into what becomes the phagophore. It remains to be determined which factor(s) on the vacuole limiting membrane or adjacent to it induces the Atg machinery assembly. Nonetheless, at this time we cannot conclusively rule out alternative models, and this hypothesis has to be experimentally demonstrated in future.

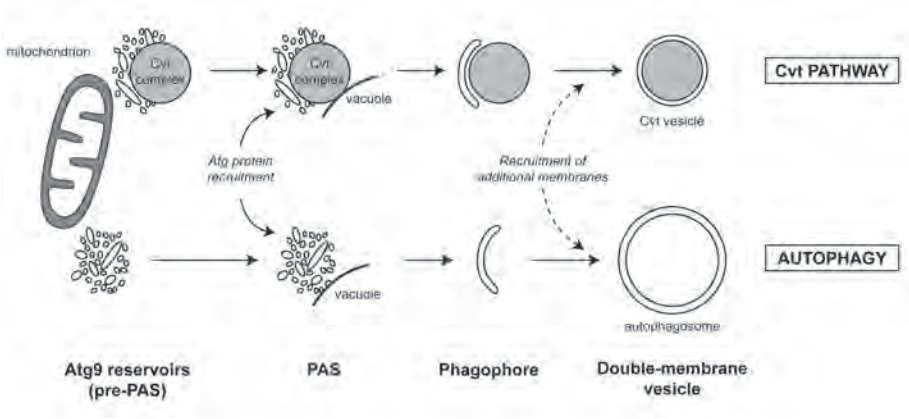

Figure 10. Model for the role of the Atg9 reservoirs in double-membrane vesicle formation. The Atg9 reservoirs, which often are adjacent to mitochondria, act as a pre-PAS. Association with the prApe1 oligomer in nutrient rich conditions (Cvt pathway) and probably cellular signals during starvation (autophagy) induces the translocation of one or more Atg9 reservoirs into close proximity with the vacuole. This relocalization event triggers the recruitment of the rest of the Atg proteins to a reservoir leading to the formation of the PAS. Successive fusion of the tubulo-vesicular membranes composing the PAS and possibly acquisition of additional membrane from other Atg9 reservoirs and/or other sources creates a double-membrane vesicle.

The mammalian orthologue of Atg9 (mAtg9) cycles between the trans-Golgi network (TGN) and LE, and after autophagy stimulation, it relocalizes to autophagosomal membranes (Young et al., 2006). All the proteins encoded by the genes knocked out in our study possess orthologues and some of them have also been implicated in mAtg9 trafficking (Chan et al., 2009; Itakura et al., 2008; Young et al., 2006). Consequently, by extension, our results suggest that the origin of the initial autophagosomal membranes in higher eukaryotes could be the TGN and/or LE, and that the Atg9-positive membranes lead to the formation of the mammalian PAS after relocalization to the cell periphery, but this hypothesis remains to be experimentally tested.

The current hypothesis for double-membrane vesicle formation is that Atg proteins assemble at the PAS and at this site, they mediate the formation of a phagophore that in turn expands into an autophagosome. Two main models have been proposed for the generation of phagophores: First, the generation by emergence from a defined organelle [that is supported by the recent observation according to which mammalian autophagosomes are generated in close proximity to the ER or mitochondria (Hailey et al., 2010; Hayashi-Nishino et al., 2009)], and

second, *de novo* formation by fusion of vesicles. Our results clearly support the model where the initial events of double-membrane vesicle biogenesis in yeast involve the *de novo* fusion of vesicles and tubules. One observation in support of *de novo* formation is that we have detected the Atg9-containing clusters of vesicles and tubules always positioned on one side of the Cvt complex, never completely surrounding this circular structure (**Fig. 2D-E, 6C-F**, dashed cisternae, **S1A-D, S1E, S4E-M**). It is consequently tempting to imagine that the initial fusions generate a small cisterna, e.g., the phagophore. Our data do not exclude the possibility that after these early events, the completion of autophagosomes entails the acquisition of additional membranes through a different mechanism.

What would be the molecular basis for the fusion events? It has recently been shown that lipidated Atg8 mediates the tethering and hemifusion of membranes *in vitro* (Nakatogawa et al., 2007). Our observations indicate that the early fusion events during double-membrane vesicle biogenesis probably do not require these Atg8 functions. In the *atg1*Δ and *atg13*Δ mutants, lipidated Atg8 is present at the PAS (**Fig. S1C-H**, (Suzuki et al., 2007)) but our micrographs clearly illustrate that the Atg9-containing vesicles and tubules are not hemifused (**Fig. 6C-6F, S4E-F, S4H-M**). In *atg14*Δ cells moreover, Atg8 is not associated with the PAS (**Fig. S3C-H**, (Suzuki et al., 2007)) but the Atg9-positive membranes appears to have undergone some fusion and this is exemplified by the presence of larger tubular profiles (**Fig. 6G-H, S4N-Q**). Our data are consistent with the observation that the tethering and hemifusion properties of lipidated Atg8 do not play a role prior to the expansion of the autophagosomal membranes (Nakatogawa et al., 2007; Sou et al., 2008). Because Sec18/NSF and SNARE proteins have so far not been implicated in double-membrane vesicle formation (Ishihara et al., 2001; Reggiori et al., 2004b), future studies will have to address which factors carry out these initial fusion events. The Atg proteins are the most likely candidates because deletion of some of them leads to the formation of a PAS with different membrane rearrangement (**Fig. 6C-6H, S2, S4D-Q**). Our observations show that the protein composition of the PAS dictates the extent of fusion events (**Fig. 6G-H, S4N-Q**) and possibly fission events (**Fig. 6E-F, S4C-D, S4N-Q**) occurring at this site. Atg14 is involved in the recruitment of the kinase complex that generates the PAS pool of phosphatidylinositol-3-phosphate (Obara et al., 2006). Consequently, our results also indicate that the membrane rearrangements occurring at the PAS could be directly influenced by the lipid composition.

In conclusion, our work has revealed that the PAS is formed from a pre-existing cluster of Atg9-containing vesicles and tubules whose composition is unique and from which atypical fusion events generate the double-membrane sequestering vesicles. This discovery provides the knowledge essential to perform further studies on the function of Atg proteins. Understanding the role of Atg proteins in rearranging and fusing membranes will be crucial to unveil the molecular mechanism of autophagy, which in turn will be essential to understand the contribution of this pathway in physiological and pathological situations.

ACKNOWLEDGMENTS

The authors thank G. Bu, A. Conzelmann, B. Glick, H. Pelham, Y. Ohsumi, M. Mazón and I. Sandoval for reagents; C. Rabouille and J.Klumperman for critical reading of the manuscript; R. Scriwanek and M. van Peski for assistance with the figure preparation. F.R. is supported by the Netherlands Organization for Health Research and Development (ZonMW-VIDI) and by the Utrecht University (High Potential grant). D.J.K. is supported by Public Health Service grant GM53396 from the National Institutes of Health.

REFERENCES

1. Baba, M., M. Osumi, S.V. Scott, D.J. Klionsky, and Y. Ohsumi. 1997. Two distinct pathways for targeting proteins from the cytoplasm to the vacuole/lysosome. *J Cell Biol*. 139:1687-95.
2. Barlowe, C., and R. Schekman. 1993. *SEC12* encodes a guanine-nucleotide-exchange factor essential for transport vesicle budding from the ER. *Nature*. 365:347-9.
3. Chan, E.Y.W., A. Longatti, N.C. McKnight, and S.A. Tooze. 2009. Kinase-inactivated ULK proteins inhibit autophagy via their conserved C-terminal domains using an Atg13-independent mechanism. *Mol Cell Biol*. 29:157-71.
4. Deshaies, R.J., S.L. Sanders, D.A. Feldheim, and R. Schekman. 1991. Assembly of yeast Sec proteins involved in translocation into the endoplasmic reticulum into a membrane-bound multisubunit complex. *Nature*. 349:806-8.
5. Epple, U.D., E.-L. Eskelinen, and M. Thumm. 2003. Intravacuolar membrane lysis in *Saccharomyces cerevisiae*. Does vacuolar targeting of Cvt17/Aut5p affect its function? *J Biol Chem*. 278:7810-21.
6. Franzusoff, A., and R. Schekman. 1989. Functional compartments of the yeast Golgi apparatus are defined by the *sec7* mutation. *EMBO J*. 8:2695-702.
7. Gauss, R., M. Trautwein, T. Sommer, and A. Spang. 2005. New modules for the repeated internal and N-terminal epitope tagging of genes in *Saccharomyces cerevisiae*. *Yeast*. 22:1-12.
8. Geng, J., M. Baba, U. Nair, and D.J. Klionsky. 2008. Quantitative analysis of autophagy-related protein stoichiometry by fluorescence microscopy. *J Cell Biol*. 182:129-40.
9. Geng, J., U. Nair, K. Yasumura-Yorimitsu, and D.J. Klionsky. 2010. Post-Golgi Sec proteins are required for autophagy in *Saccharomyces cerevisiae*. *Mol Biol Cell*.
10. Griffith, J., M. Mari, A. De Maziere, and F. Reggiori. 2008. A cryosectioning procedure for the ultrastructural analysis and the immunogold labelling of yeast *Saccharomyces cerevisiae*. *Traffic*. 9:1060-72.
11. Hailey, D.W., A.S. Rambold, P. Satpute-Krishnan, K. Mitra, R. Sougrat, P.K. Kim, and J. Lippincott-Schwartz. 2010. Mitochondria supply membranes for autophagosome biogenesis during starvation. *Cell*. 141:656-67.
12. Hayashi-Nishino, M., N. Fujita, T. Noda, A. Yamaguchi, T. Yoshimori, and A. Yamamoto. 2009. A subdomain of the endoplasmic reticulum forms a cradle for autophagosome formation. *Nat Cell Biol*. 11:1433-7.
13. He, C., M. Baba, Y. Cao, and D.J. Klionsky. 2008. Self-interaction is critical for Atg9 transport and function at the phagophore assembly site during autophagy. *Mol Biol Cell*. 19:5506-16.
14. He, C., H. Song, T. Yorimitsu, I. Monastyrska, W.-L. Yen, J.E. Legakis, and D.J. Klionsky. 2006. Recruitment of Atg9 to the preautophagosomal structure by Atg11 is essential for selective autophagy in budding yeast. *J Cell Biol*. 175:925-35.
15. Holthuis, J.C., B.J. Nichols, S. Dhruvakumar, and H.R.B. Pelham. 1998. Two syntaxin homologues in the TGN/endosomal system of yeast. *EMBO J*. 17:113-26.
16. Ishihara, N., M. Hamasaki, S. Yokota, K. Suzuki, Y. Kamada, A. Kihara, T. Yoshimori, T. Noda, and Y. Ohsumi. 2001. Autophagosome requires specific early Sec proteins for its formation and NSF/SNARE for vacuolar fusion. *Mol Biol Cell*. 12:3690-702.
17. Itakura, E., C. Kishi, K. Inoue, and N. Mizushima. 2008. Beclin 1 forms two distinct phosphatidylinositol 3-kinase complexes with mammalian Atg14 and UVRAG. *Mol Biol Cell*. 19:5360-72.
18. Jackson, C.L., and J.E. Casanova. 2000. Turning on ARF: the Sec7 family of guanine-nucleotide-exchange factors. *Trends Cell Biol*. 10:60-7.

19. Kim, J., W.-P. Huang, P.E. Stromhaug, and D.J. Klionsky. 2002. Convergence of multiple autophagy and cytoplasm to vacuole targeting components to a perivacuolar membrane compartment prior to de novo vesicle formation. *J Biol Chem*. 277:763-73.

20. Klionsky, D.J., R. Cueva, and D.S. Yaver. 1992. Aminopeptidase I of *Saccharomyces cerevisiae* is localized to the vacuole independent of the secretory pathway. *J Cell Biol*. 119:287-99.

21. Lang, T., S. Reiche, M. Straub, M. Bredschneider, and M. Thumm. 2000. Autophagy and the Cvt pathway both depend on *AUT9*. *J Bacteriol*. 182:2125-33.

22. Levine, B., and V. Deretic. 2007. Unveiling the roles of autophagy in innate and adaptive immunity. *Nat Rev Immunol*. 7:767-77.

23. Levine, B., and G. Kroemer. 2008. Autophagy in the pathogenesis of disease. *Cell*. 132:27-42.

24. Longtine, M.S., A. McKenzie, III, D.J. Demarini, N.G. Shah, A. Wach, A. Brachat, P. Philippsen, and J.R. Pringle. 1998. Additional modules for versatile and economical PCR-based gene deletion and modification in *Saccharomyces cerevisiae*. *Yeast*. 14:953-61.

25. Losev, E., C.A. Reinke, J. Jellen, D.E. Strongin, B.J. Bevis, and B.S. Glick. 2006. Golgi maturation visualized in living yeast. *Nature*. 441:1002-6.

26. Meeusen, S., and J. Nunnari. 2003. Evidence for a two membrane-spanning autonomous mitochondrial DNA replisome. *J Cell Biol*. 163:503-10.

27. Mizushima, N., B. Levine, A.M. Cuervo, and D.J. Klionsky. 2008. Autophagy fights disease through cellular self-digestion. *Nature*. 451:1069-75.

28. Nakatogawa, H., Y. Ichimura, and Y. Ohsumi. 2007. Atg8, a ubiquitin-like protein required for autophagosome formation, mediates membrane tethering and hemifusion. *Cell*. 130:165-78.

29. Noda, T., J. Kim, W.-P. Huang, M. Baba, C. Tokunaga, Y. Ohsumi, and D.J. Klionsky. 2000. Apg9p/Cvt7p is an integral membrane protein required for transport vesicle formation in the Cvt and autophagy pathways. *J Cell Biol*. 148:465-80.

30. Novick, P., C. Field, and R. Schekman. 1980. Identification of 23 complementation groups required for post-translational events in the yeast secretory pathway. *Cell*. 21:205-15.

31. Obara, K., T. Sekito, and Y. Ohsumi. 2006. Assortment of phosphatidylinositol 3-kinase complexes--Atg14p directs association of complex I to the pre-autophagosomal structure in *Saccharomyces cerevisiae*. *Mol Biol Cell*. 17:1527-39.

32. Odorizzi, G., M. Babst, and S.D. Emr. 1998. Fab1p PtdIns(3)P 5-kinase function essential for protein sorting in the multivesicular body. *Cell*. 95:847-58.

33. Odorizzi, G., D.J. Katzmann, M. Babst, A. Audhya, and S.D. Emr. 2003. Bro1 is an endosome-associated protein that functions in the MVB pathway in *Saccharomyces cerevisiae*. *J Cell Sci*. 116:1893-903.

34. Rabouille, C. 1999. Quantitative aspects of immunogold labeling in embedded and nonembedded sections. *Methods Mol Biol*. 117:125-44.

35. Reggiori, F., and D.J. Klionsky. 2005. Autophagosomes: Biogenesis from scratch? *Curr Opin Cell Biol*. 17:415-422.

36. Reggiori, F., and D.J. Klionsky. 2006. Atg9 sorting from mitochondria is impaired in early secretion and VFT-complex mutants in *Saccharomyces cerevisiae*. *J Cell Sci*. 119:2903-11.

37. Reggiori, F., and H.R.B. Pelham. 2001. Sorting of proteins into multivesicular bodies: ubiquitin-dependent and -independent targeting. *EMBO J*. 20:5176-86.

38. Reggiori, F., T. Shintani, U. Nair, and D.J. Klionsky. 2005. Atg9 cycles between mitochondria and the pre-autophagosomal structure in yeasts. *Autophagy*. 1:101-9.

39. Reggiori, F., K.A. Tucker, P.E. Stromhaug, and D.J. Klionsky. 2004a. The Atg1-Atg13 complex regulates Atg9 and Atg23 retrieval transport from the pre-autophagosomal structure. *Dev Cell*. 6:79-90.

40. Reggiori, F., C.-W. Wang, U. Nair, T. Shintani, H. Abeliovich, and D.J. Klionsky. 2004b. Early stages of the secretory pathway, but not endosomes, are required for Cvt vesicle and autophagosome assembly in *Saccharomyces cerevisiae*. *Mol Biol Cell*. 15:2189-204.

41. Shintani, T., W.-P. Huang, P.E. Stromhaug, and D.J. Klionsky. 2002. Mechanism of cargo selection in the cytoplasm to vacuole targeting pathway. *Dev Cell*. 3:825-37.

42. Shintani, T., and D.J. Klionsky. 2004. Cargo proteins facilitate the formation of transport vesicles in the cytoplasm to vacuole targeting pathway. *J Biol Chem*. 279:29889-94.

43. Sikorski, R.S., and P. Hieter. 1989. A system of shuttle vectors and yeast host strains designed for efficient manipulation of DNA in *Saccharomyces cerevisiae*. *Genetics*. 122:19-27.

44. Sipos, G., J.H. Brickner, E.J. Brace, L. Chen, A. Rambourg, F. Kepes, and R.S. Fuller. 2004. Soi3p/Rav1p functions at the early endosome to regulate endocytic trafficking to the vacuole and localization of trans-Golgi network transmembrane proteins. *Mol Biol Cell*. 15:3196-209.

45. Sou, Y.S., S. Waguri, J. Iwata, T. Ueno, T. Fujimura, T. Hara, N. Sawada, A. Yamada, N. Mizushima, Y. Uchiyama, E. Kominami, K. Tanaka, and M. Komatsu. 2008. The Atg8 conjugation system is indispensable for proper development of autophagic isolation membranes in mice. *Mol Biol Cell*. 19:4762-75.

46. Suzuki, K., T. Kirisako, Y. Kamada, N. Mizushima, T. Noda, and Y. Ohsumi. 2001. The pre-autophagosomal structure organized by concerted functions of *APG* genes is essential for autophagosome formation. *EMBO J*. 20:5971-81.

47. Suzuki, K., Y. Kubota, T. Sekito, and Y. Ohsumi. 2007. Hierarchy of Atg proteins in pre-autophagosomal structure organization. *Genes Cells*. 12:209-18.

48. van der Vaart, A., J. Griffith, and F. Reggiori. 2010. Exit from the Golgiis required for the expansion of the autophagosomal phagophore in yeast *Saccharomyces cerevisiae*. *Mol Biol Cell*.

49. Vida, T.A., and S.D. Emr. 1995. A new vital stain for visualizing vacuolar membrane dynamics and endocytosis in yeast. *J Cell Biol*. 128:779-92.

50. Wright, R., M. Basson, L. D'Ari, and J. Rine. 1988. Increased amounts of HMG-CoA reductase induce "karmellae": a proliferation of stacked membrane pairs surrounding the yeast nucleus. *J Cell Biol*. 107:101-14.

51. Xie, Z., and D.J. Klionsky. 2007. Autophagosome formation: core machinery and adaptations. *Nat Cell Biol*. 9:1102-9.

52. Yen, W.L., J.E. Legakis, U. Nair, and D.J. Klionsky. 2007. Atg27 is required for autophagy-dependent cycling of Atg9. *Mol Biol Cell*. 18:581-93.

53. Young, A.R.J., E.Y.W. Chan, X.W. Hu, R. Köchl, S.G. Crawshaw, S. High, D.W. Hailey, J. Lippincott-Schwartz, and S.A. Tooze. 2006. Starvation and ULK1-dependent cycling of mammalian Atg9 between the TGN and endosomes. *J Cell Sci* 119:3888-900.

SUPPLEMENTARY FIGURES

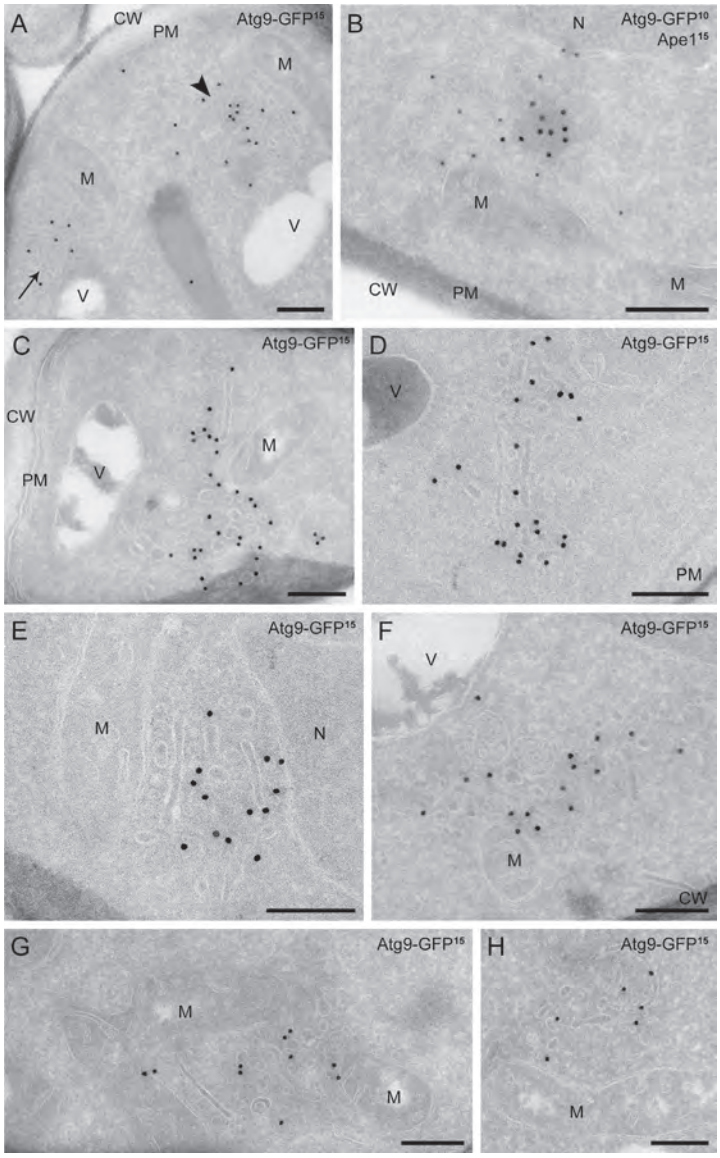

Figure S1. Atg9 clusters in wild type cells. A,B. Figures 2D and 2E are shown without dashed lines for clarity. C-H. Additional micrographs of Atg9 clusters observed in wild type cells expressing Atg9-GFP (MMY067). Bar, 200 nm. CW, cell wall; M, mitochondria; PM, plasma membrane; V, vacuole.

A

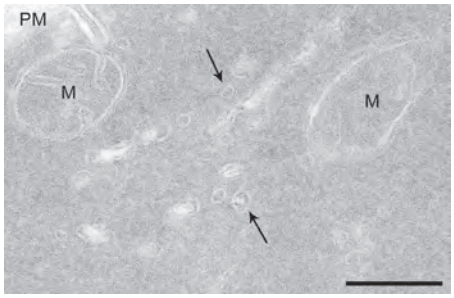

B

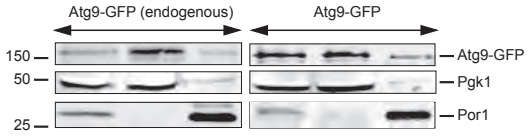

Figure S2. Atg9-containing organelles expand in size upon overexpression of Atg9. A. Clusters of vesicles and tubules (arrows) are found adjacent to mitochondria in untransformed cells. The SEY6210 wild-type strain was grown and processed for IEM before being imaged. B. Larger Atg9 clusters have normal biophysical characteristics. The FRY162 (endogenous ATG9-GFP) and MMY067 (TPI1-driven ATG9-GFP) strains were grown to early logarithmic phase, converted to spheroplasts, lysed and the cell extract (T) was centrifuged at 13,000 x g for 15 min. The supernatant (S13) and the pellet (P13) fractions were then separated by SDS-PAGE and Atg9 distribution analyzed by western blot using anti-GFP antibodies. Efficient lysis and correct fractionation were assessed by verifying the partitioning of cytosolic Pgk1 and mitochondrial Por1. Molecular mass is indicated in kilodaltons. Overexpression of Atg9 does not alter the subcellular distribution of Atg9. Bar, 200 nm. M, mitochondria; PM, plasma membrane.

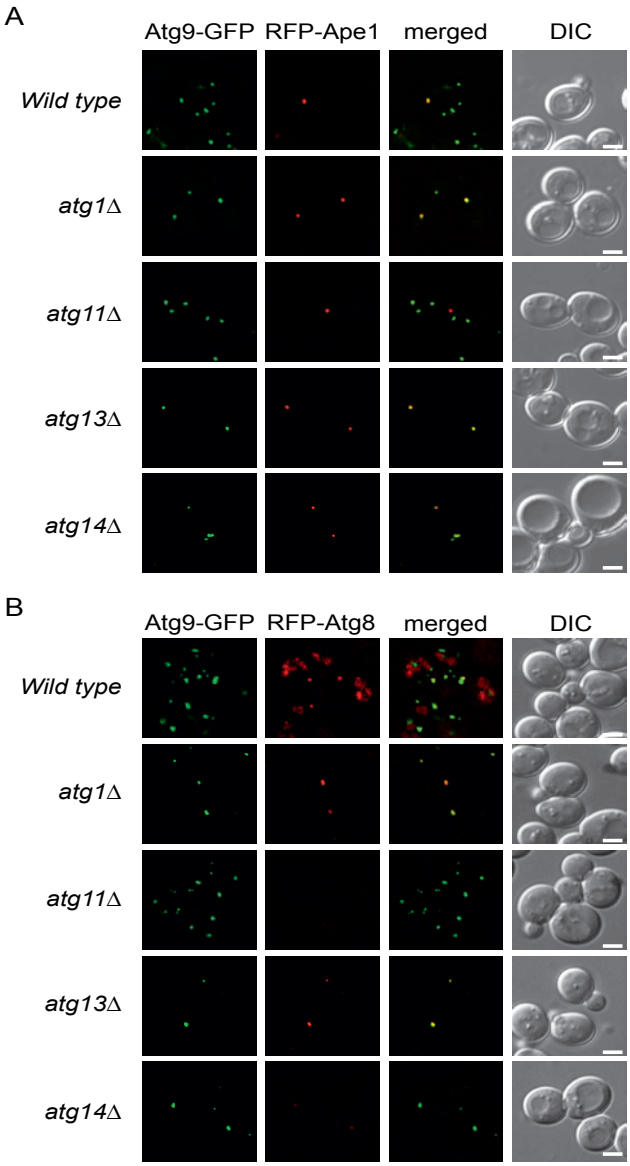

Figure S3. Subcellular distribution of Atg9 and colocalization with Ape1 or Atg8 in various mutants. A. The wild-type (MMY072), atg1Δ (MMY073), atg11Δ (MMY074), atg13Δ (MMY075) and atg14Δ (MMY076) strains were grown to log phase and imaged. Atg9 is distributed in several puncta in wild-type and atg11Δ cells but concentrates to a single location in the absence of ATG1, ATG13 or ATG14. Precursor Ape1 forms an oligomer that always colocalizes with one Atg9-positive dot in all strains except the atg11Δ knockout. B. The wild-type (MMY067), atg1Δ (MMY068), atg11Δ (MMY069), atg13Δ (MMY070) and atg14Δ (MMY071) strains carrying the promRFPATG8415 (RFP-Atg8) plasmid were grown to log phase and imaged. The PAS is present in wild-type, atg1Δ and atg13Δ strains but not in the atg11Δ knockout. In the atg14Δ mutant, Atg8 is not recruited to the PAS. DIC, differential interference contrast. Bar, 2 μm.

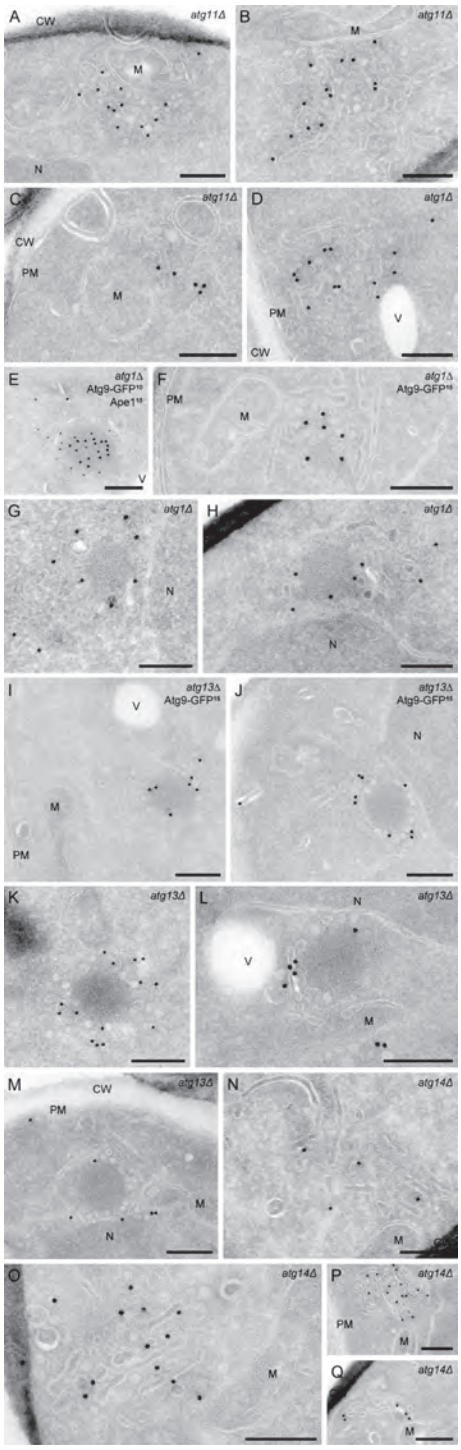

Figure S4. Atg9 clusters in atg mutants. A-C. Extra micrographs of Atg9 reservoirs observed in the atg11Δ (MMY069) cells. D, G, H. Additional profiles of the PAS ultrastructure in the atg1Δ (MMY068) knockout strain. E, F, I, J. Fig. 6C-6F are shown without dashed lines for clarity. K-M. Extra IEM profiles of the PAS observed in the atg13Δ (MMY070) cells. N-Q. Additional micrographs of the PAS in the atg14Δ (MMY071) strain. Ultrathin cryo-sections immuno-gold labelled for GFP were used to identify the Atg9-positive membranes. Bar, 200 nm. CW, cell wall; M, mitochondria; N, nucleus; PM, plasma membrane; V, vacuole.

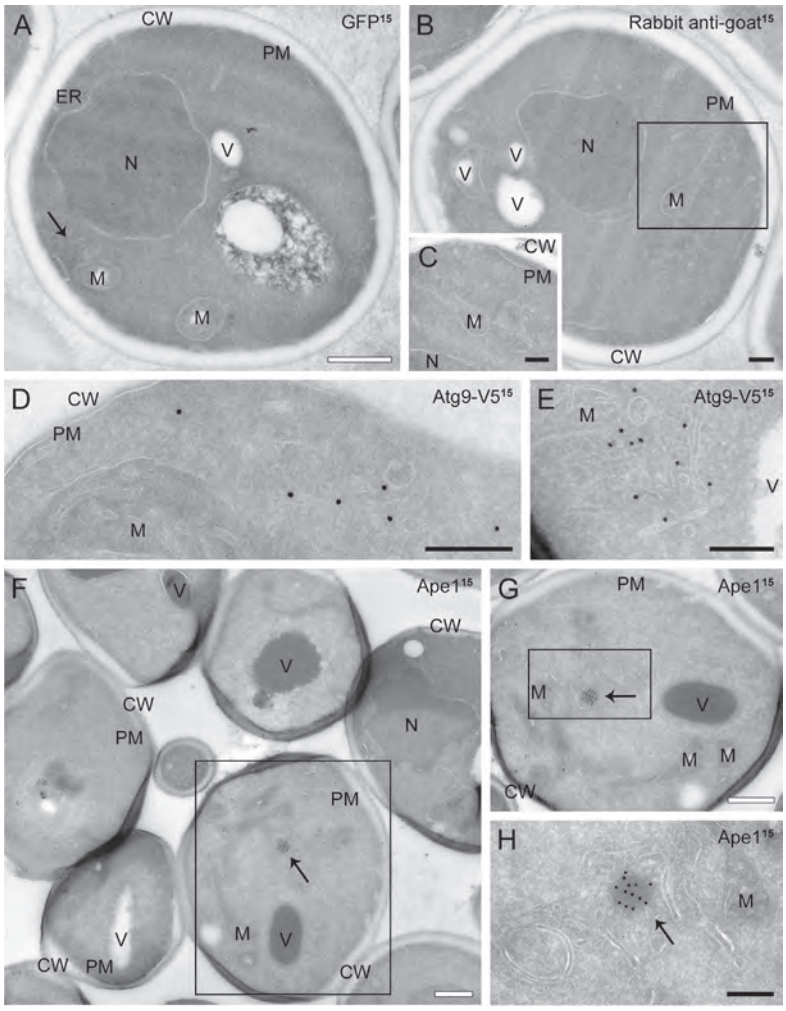

Figure S5. Immuno-gold labelling controls. Wild-type cells expressing Atg9-mCherry-V5 (MMY120, panels A and D-H) or Atg9-GFP (MMY067, panels B and C) under the control of the TPI1 promoter were grown and processed as described in Materials and Methods. Cryo-sections were then immuno-gold labelled for either GFP (A), V5 (D,E), Ape1 (F-G) or only with the secondary antibodies (B,C). A. The anti-GFP antibodies do not label the Atg9 clusters nor other cellular structures in cells not expressing Atg9-GFP. B,C. The secondary antibodies used for the labelings do not decorate either cryo-sections (B) or Atg9-positive compartments (C) in the absence of primary antibodies. D,E. The Atg9 clusters can only be recognized by specific immuno-logical reactions such as with the anti-V5 antibody. F,H. The antiserum against Ape1 exclusively labels the prApe1 oligomer (arrows). Panel G is the inset of panel F and panel H is the inset of panel G. White bar, 500 nm; black bar, 200 nm. CW, cell wall; M, mitochondria; N, nucleus; PM, plasma membrane; V, vacuole.

VIDEO LEGENDS

Video 1. Live-cell imaging of an Atg9 reservoir becoming the PAS (overexpressed Atg9-mChe). Atg9-mCherry GFP-Atg8 (MMY120) cells were grown to a log phase and transferred to SD-N medium for 20 min before being imaged. Images were collected by time-lapse fluorescence microscopy using a DeltaVision RT system (Applied Precision) equipped with a CoolSNAP HQ camera (Photometrix). Frames were taken every 5 s for 4 min and 5 s. At each time point, images were generated by collecting a stack of 3 pictures with focal planes 0.20 µm apart and by successively deconvolving and analyzing them with the softWoRx software (Applied Precision).

Video 2. Live-cell imaging of an Atg9 reservoir becoming the PAS (endogenous Atg9-GFP). Cells expressing endogenous Atg9-GFP (FRY172) and carrying the pCumCheV5ATG8415 plasmid, which expresses mChe-Atg8, were grown to a log phase and transferred to SD-N medium for 20 min before being imaged. Images were collected by time-lapse fluorescence microscopy using a DeltaVision RT system (Applied Precision) equipped with a CoolSNAP HQ camera (Photometrix). Frames were taken every 5 s for 4 min and 5 s. At each time point, images were generated by collecting a stack of 3 pictures with focal planes 0.20 µm apart and by successively deconvolving and analyzing them with the softWoRx software (Applied Precision).

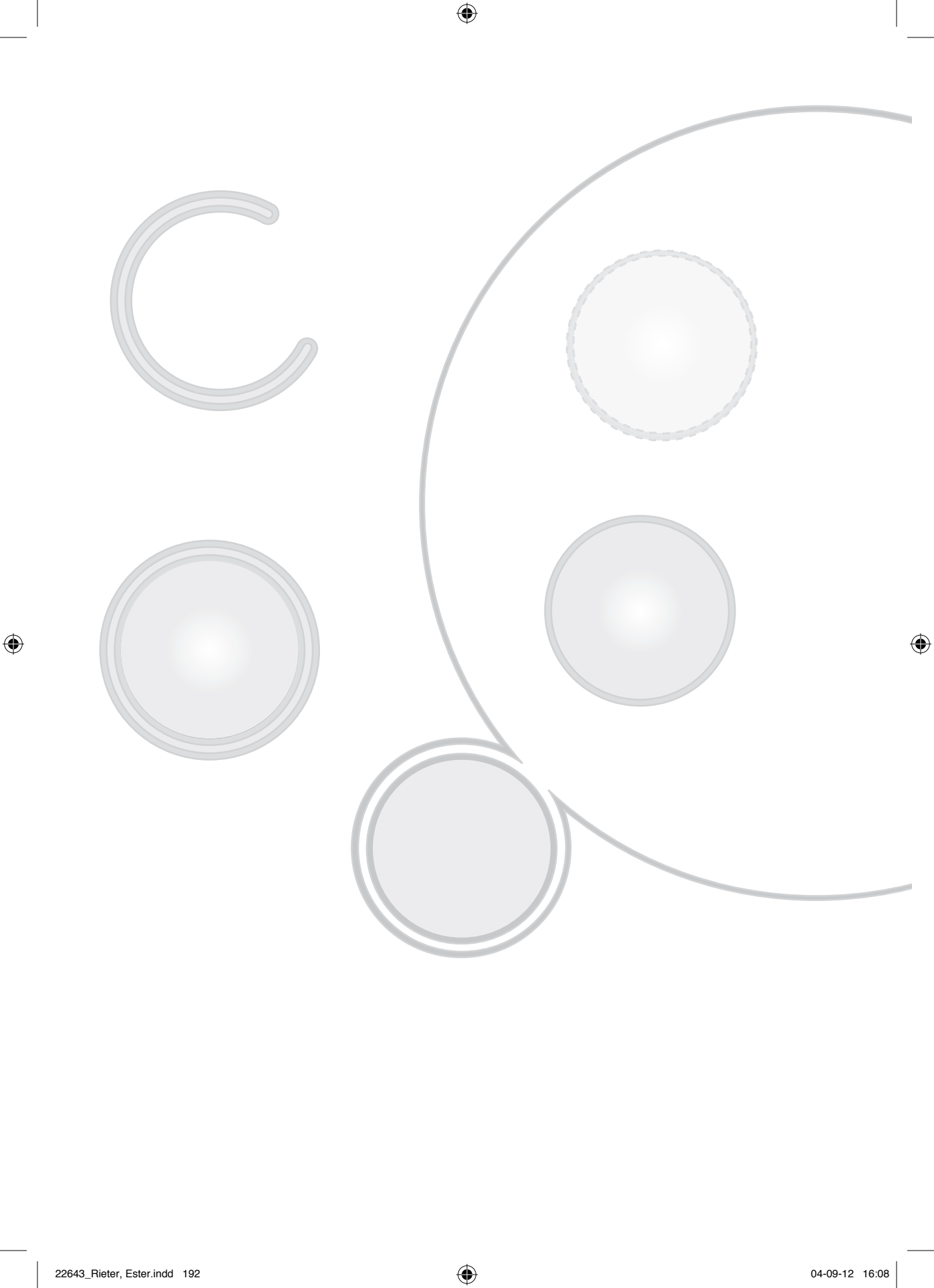

CHAPTER

6

Summarizing discussion

SUMMARIZING DISCUSSION

Despite the great effort that has been made to unravel both the signalling cascades regulating autophagy and the molecular mechanism of autophagosome biogenesis, there are still numerous questions that remain unsolved. Understanding the mechanism underlying this multi-use pathway is of crucial importance not only because it is involved in a multitude of physiological processes, but also because it is implicated in numerous diseases such as neurodegenerative disorders and cancer.

In this thesis we have addressed some fundamental questions regarding the origin of the PAS and the regulated recruitment of Atg18 and Atg2 to this structure using yeast *Saccharomyces cerevisiae* as a model organism. To disclose these unresolved issues we have used a large spectrum of different techniques including the yeast two-hybrid (Y2H) assay, protein A (PA) affinity isolation, immuno-electron microscopy (IEM), fluorescence microscopy, sucrose density/glycerol gradients, the bimolecular fluorescence complementation (BiFC) assays and several well-established biochemical approaches to study the function of the proteins of interest and assessing the progression of autophagy.

In this final chapter the results will be reflected upon, the putative functions of these proteins will be discussed as well as suggestions for future research.

Recruitment of Atg18 to distinct compartments depends on organelle-specific determinants

The WD40 domain-containing protein Atg18 is essential for autophagy but also for vacuole homeostasis and probably endosomal functions (Barth and Thumm, 2001; Efe et al., 2007; Guan et al., 2001; Jin et al., 2008). Very little was known about how Atg18 is specifically targeted to these organelles and what function it executes at these locations. In chapter 3 we reveal the mechanism of Atg18 recruitment to the PAS and provide a model in which the Atg18 β-propeller provides organelle-specificity by binding two determinants on the target membrane. We show that PtdIns3P and Atg2 are the determinants present at the PAS responsible for autophagy-specific recruitment of Atg18 (chapter 3). The ability of the Atg18 β-propeller to simultaneously bind a phosphoinositide and Atg2 suggests that it could act as a scaffold for the assembly of protein-lipid complexes. Based on our current working model, we hypothesize that on the vacuole and endosomes there should be other organelle-specific factors responsible for regulating Atg18 recruitment, besides PtdIns3P and PtdIns(3,5)P being present at these sites (Gillooly et al., 2000; Obara

et al., 2008a). These organelle-specific determinants remain to be identified, as well as the mechanisms involved in Atg18 recruitment to these compartments. Upon identification of these factors, it will be interesting to examine which sequences in Atg18 mediate the binding to them, and whether these include loop 2, other amino acids in the β-propeller or another motif in the protein.

For the specific recruitment to the vacuole, Vac14 was initially considered as the possible binding candidate as it is shown that this protein interacts with Atg18. At the vacuolar membrane Atg18 and Vac14 are part of a complex, which also comprises Fig4, Fab1 and Vac7, regulating PtdIns(3,5)P_2 levels (Efe et al., 2007; Jin et al., 2008). We found that Atg18 interacts with Vac14 through its C-terminus and not its β-propeller (unpublished data). As a result, it seems that in this context the Atg18 β-propeller does not act as the organelle-specific determinant. These preliminary data, however, must be taken cautiously. We have only been able to detect the Atg18-Vac14 interaction by yeast two-hybrid, but we have been unable to confirm this binding by *in vivo* pull-down experiments. In addition the observed interaction could be indirect. Vac7, another member of the PtdIns(3,5)P_2 regulatory complex, is also critical for Atg18 recruitment to the vacuolar membrane (Efe et al., 2007). Efe and co-workers indeed proposed a speculative model in which PtdIns(3,5)P_2 and Vac7 represent the determinants on vacuole membrane for Atg18 recruitment. Currently, there are no evidences that Atg18 and Vac7 interact and consequently it will be important in the future to analyze this potential binding partnership to expand our knowledge about the mechanism underlying Atg18 targeting to different organelles.

The putative role of Atg18 at the PAS

Although our findings presented in chapter 3 highlight the mechanism used to localize Atg18 to the PAS, they do not provide novel insights into the molecular role of this protein in autophagy. A broad range of biological functions have been assigned to β-propeller proteins ranging from signal transduction, transcription regulation, to apoptosis (Paoli, 2001). This makes it difficult to extrapolate from other members of this structural protein family to speculate about the function of Atg18.

Similar to what has been reported in the literature we observed that Atg8 is still recruited to the PAS in absence of Atg18 (Nair et al., 2010) (chapter 3). Because Atg8 is one of the last Atg proteins to be recruited to the PAS, we concluded that Atg18 is probably not involved in the recruitment of the core Atg proteins to the PAS (Nair et al., 2010; Suzuki et al., 2007). Therefore Atg18

most likely functions at a stage subsequent to the recruitment and assembly of the Atg machinery at the PAS (Behrends et al., 2010; Nair et al., 2010). By EM we did not detect autophagosomal intermediates in the cytoplasm of the *atg18Δ* strain expressing the Atg18(L2) mutant unable to bind Atg2 (Chapter 3). This observation suggests that Atg18 plays a role at an early stage during the biogenesis of autophagosomes and not for autophagosome completion or the fusion of these vesicles with the vacuole.

It has been speculated that because the autophagosomal membranes are highly enriched in PtdIns3P, particularly on their interior, Atg18 together with Atg2 may have a function in generating the negative curvature at the inner surface of the phagophore (Obara et al., 2008b). The elongating extremities of the phagophore are occasionally also found to be enriched in PtdIns3P (Obara et al., 2008b), which could promote Atg18 concentration at these sites. Therefore another possibility is that Atg18 is necessary for constructing and maintaining the extremities of the phagophore (Obara et al., 2008b). Upon autophagosome completion, Atg8-PE present on the outer membrane of the autophagosomes is cleaved by Atg4 and released back in the cytoplasm for reuse. It has been suggested that Atg18 prevents the pre-mature cleavage of Atg8-PE by Atg4 thereby regulating efficient autophagosome formation. In fact, recent data have shown that the delipidation of Atg8 is a prerequisite for the release of the Atg machinery from complete autophagosomes prior to their fusion with the vacuole (Nair et al., 2010; Nair et al., 2012). At the vacuole Atg18 acts as a negative regulator of the Fab1 lipid kinase, thereby thus inhibiting the phosphorylation of PtdIns3P into PtdIns(3,5)P_2 (Efe et al., 2007). At present it is very difficult to predict whether Atg18 could perform a similar function at the PAS because Fab1 appears not to be involved in autophagy.

Alternatively, Atg18 is maybe necessary for the dissociation and recycling of Atg proteins from the expanding phagophores and/or autophagosomes. For example, it has been reported that Atg18, together with Atg2, are necessary for the retrieval of Atg9 from the PAS to its cytoplasmic pools. In the absence of Atg2 or Atg18, Atg9 is confined to the PAS (Reggiori et al., 2004). The mechanism of Atg9 retrograde transport and how Atg2 and Atg18 are implicated has not been defined. Initial research to address these questions is presented in chapter 4. One important concept that needs to be considered is that since Atg9 is a transmembrane protein, it needs a carrier to be recycled back from the PAS to the Atg9 reservoirs. The theory that Atg18 is maybe involved in the generation of these carriers is challenging. The idea is supported by a study in which they

postulate that Atg18, together with Vac17 and Myo2, may mediate vesicular budding and transport from the vacuolar membrane (Efe et al., 2007).

All the possible functions of Atg18 proposed here are far from being proved and additional studies are necessary to understand the molecular role of this protein in autophagy.

Insights into the mechanism of Atg9 retrieval from the PAS

The molecular mechanism of Atg9 retrieval from the PAS to the peripheral Atg9 reservoirs is totally unknown. As mentioned, while Atg2 and Atg18 have been implicated in this event (Reggiori et al., 2004), their precise contribution remains to be determined. In chapter 4 we have characterized the interaction between Atg9 and Atg2 to generate experimental tools that could allow gaining more information about both the mechanism of Atg9 retrieval and the molecular function of Atg2 during this process. We have identified a region of 34 amino acids residing in the C-terminal half of Atg2 important for binding Atg9 and found that the Atg2-binding region in Atg9 resides in its C-terminus.

In chapter 4 we have detected an interaction between Atg2 and Atg9 and observed a loss of Atg2 localization to PAS in absence of Atg9 (unpublished observation and (Shintani et al., 2001; Suzuki et al., 2007)). The data from chapter 3 show that on the autophagosomal membranes Atg2 together with PtdIns3P are the key determinants responsible for the autophagy-specific recruitment of Atg18 to these membranes (Rieter *et al.*, submitted). Collectively, these findings allow us to come up with a conceptual model for the sequential recruitment of Atg2 and Atg18 to the autophagosomal membranes (**Figure 1**). In this model and in agreement with the literature (Suzuki et al., 2007), Atg9 is one of the first Atg proteins to arrive at the site where the PAS will be formed. There, it plays a pivotal role in the formation and organization of the PAS by recruiting numerous core Atg proteins (see chapter 5). One of the initial events is probably also the conversion of PtdIns into PtdIns3P by the PtdIns 3-kinase complex I. The simultaneous presence of PtdIns3P and Atg9 provide the determinants that mediate the association of Atg2 to the PAS. Presence of PtdIns3P and Atg2 on the autophagosomal membrane then triggers the recruitment of Atg18 (Rieter *et al.*, submitted). The data in chapter 4 reveal that the Atg9-binding motif of Atg2 is located within the C-terminal half of the protein. Interestingly, unpublished data from our laboratory have shown that the Atg18-binding domain of Atg2 resides in its N-terminus making it structurally possible that Atg2, Atg9 and Atg18 form a complex on the autophagosomal membranes (**Figure 2**).

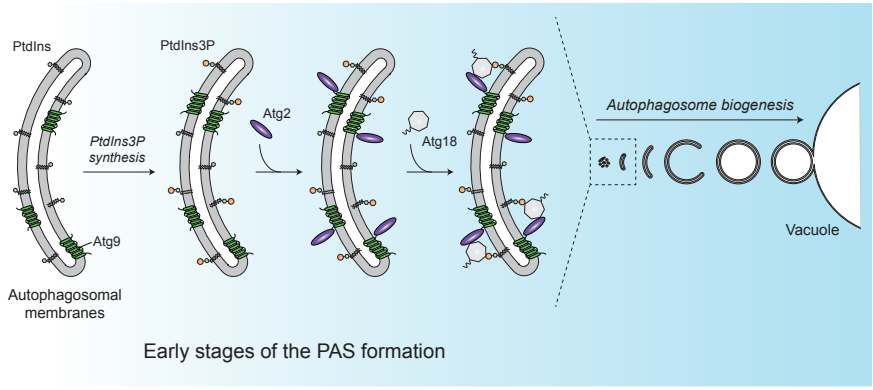

Figure 1. Conceptual model for Atg2 and Atg18 recruitment to the PAS. Atg9, derived from the Atg9 reservoirs, is one of the first Atg proteins present at the newly formed PAS. At an early stage of the organization of this structure, part of PtdIns is converted into PtdIns3P by the PtdIns 3-kinase complex I. PtdIns3P together with Atg9 are essential for the successive association of Atg2 to the PAS. Presence of PtdIns3P and Atg2 on the autophagosomal membrane subsequently triggers the recruitment of Atg18, which is mediated by its β-propeller. It is presently unclear whether these events occur on the phagophore or on another precursor membrane.

The mechanism of Atg9 retrograde transport from the PAS and the role of Atg18 and Atg2 in this event remain elusive (**Figure 2**). It remains to be established for example whether Atg2 is required for all possible Atg18 functions, or whether the role of Atg2 is simply to recruit Atg18 to the PAS. Future research is undoubtedly necessary to test these hypotheses, which are not mutually exclusive. For example it will be very interesting to target Atg18 to the PAS in an Atg2-independent manner and assess Atg9 recycling.

The role and origin of the Atg9 reservoirs in autophagosome biogenesis

Autophagosomes are formed by simultaneous expansion and nucleation of the phagophore. There is an on-going debate in the research field about the origin of both the phagophore and the lipids bilayers required for the expansion of this precursor structure into an autophagosome. Because of its characteristics, the conserved transmembrane protein Atg9 is potentially the ideal protein to answer some of these questions. First, it is associated with lipid bilayers and therefore it is probably involved in the delivery of at least part of the membranes required to form autophagosomes (Legakis et al., 2007; Reggiori et al., 2005). Second, it is one of the first Atg proteins to be recruited to the PAS emphasizing a role for Atg9 in the early stages of autophagosome biogenesis and consequently a probable role in the phagophore formation (Suzuki et al., 2007). The IEM data presented in

chapter 5 show that Atg9 localizes to a novel compartment composed of clusters of vesicles and tubules, which we termed the Atg9 reservoirs. The movement of one of these reservoirs from the periphery of the cell close to the vacuole and the subsequent recruitment of additional Atg proteins leads to the generation of the PAS (Mari et al., 2010) (**Figure 3**). Recently, also mAtg9-containing tubular vesicular compartments have been identified in mammalian cells, which resemble to the yeast Atg9 reservoirs (Orsi et al., 2012).

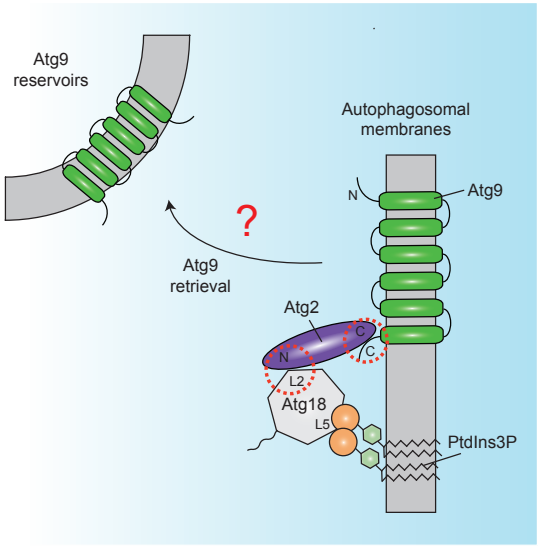

Figure 2. Atg9 retrieval from the PAS. Atg9 is located in the autophagosomal membranes and binds Atg2 via a stretch of amino acids within its C-terminus. Atg2 has two putative Atg9-binding motifs located in the C-terminal half of the protein, allowing the binding to Atg9. Via the Atg18-binding domain that resides in the N-terminus, Atg2 is able to recruit Atg18 to the PAS. Atg18 itself binds Atg2 via residues present in loop 2, a sequence of amino acids that connects blade 1 and 2 of the ß-propeller. Simultaneously, Atg18 binds PtdIns via a conserved FRRG motif present in loop 5. It remains unclear how Atg2 and Atg18 are involved in Atg9 recycling, but probably the formation of the Atg2-Atg18 complex is essential to trigger this event. The putative regions mediating bindings are encircled by red dashed lines.

Initial studies suggest that Atg9 might localize to the mitochondria (Reggiori et al., 2005) making it plausible to conclude that the Atg9 reservoirs are derived from these organelles. Although, we found that the Atg9 reservoirs are often in close proximity of the mitochondria, our IEM data clearly reveal that there is no connection between these compartments. Furthermore, alterations in the morphology of the mitochondria do not seem to affect distribution of

Atg9 (Ohashi and Munro, 2010). In addition and in contrast with what has been observed in mammalian cells, where some Atg proteins were found to localize transiently to the mitochondria and few outer membrane mitochondrial proteins to the autophagosomal membranes (Hailey et al., 2010), we did not detect Atg9 on the mitochondrial surface, or mitochondrial proteins at the Atg9 reservoirs. Another study drew the same conclusions (Sekito et al., 2009). Consequently, we can conclude that at least in yeast the Atg9 reservoirs do not originate from the mitochondria. It thus remains unclear why these two organelles are in close proximity. One possibility is that a putative zone of contact between these two compartments allows direct lipid transfer from the mitochondria to the Atg9-reservoirs. The *de novo* delivery of lipids by lipid transfer proteins or direct lipid transfer from a donor organelle has been proposed as a model for autophagosome biogenesis (Longatti and Tooze, 2009). Moreover, the transfer of mitochondria-derived lipids to the nascent autophagosome has been shown to occur under certain conditions in mammalian cells (Hailey et al., 2010). Although in our studies we show that lipid exchange is possible between the Atg9 reservoirs and the endocytic system (chapter 5) (**Figure 3**), it remains to be determined whether this is also the case with the mitochondria.

Our observations indicate that newly synthesized Atg9 traffics from the ER via the Golgi before reaching the Atg9 reservoirs (chapter 5). This notion has been confirmed by two other reports (Ohashi and Munro, 2010; Yamamoto *et al*., in press). This raises the possibility that the Atg9 carriers and reservoirs are directly derived from this organelle (**Figure 3**). Golgi-derived Atg9 carriers have recently been identified in yeast termed Atg9 vesicles using a high-sensitivity microscopy system (Yamamoto *et al*., in press). In this report they propose a model in which on average three of these Atg9 vesicles contribute to the formation of the PAS. These results are not mutually exclusive with our data; it is possible that after the initial formation of the PAS from one or multiple Atg9 reservoirs, individually Atg9 vesicles further contribute to the expansion of the phagophore. Yamamoto and co-workers found that the majority of the Atg9 vesicles are highly mobile in the cytoplasm whereas only a small portion is in immobile structures (Yamamoto *et al*., in press). This latter population could correspond to the Atg9 reservoirs we identified in chapter 5. It remains, however, unclear which is the relationship between the Atg9 vesicles and reservoirs.

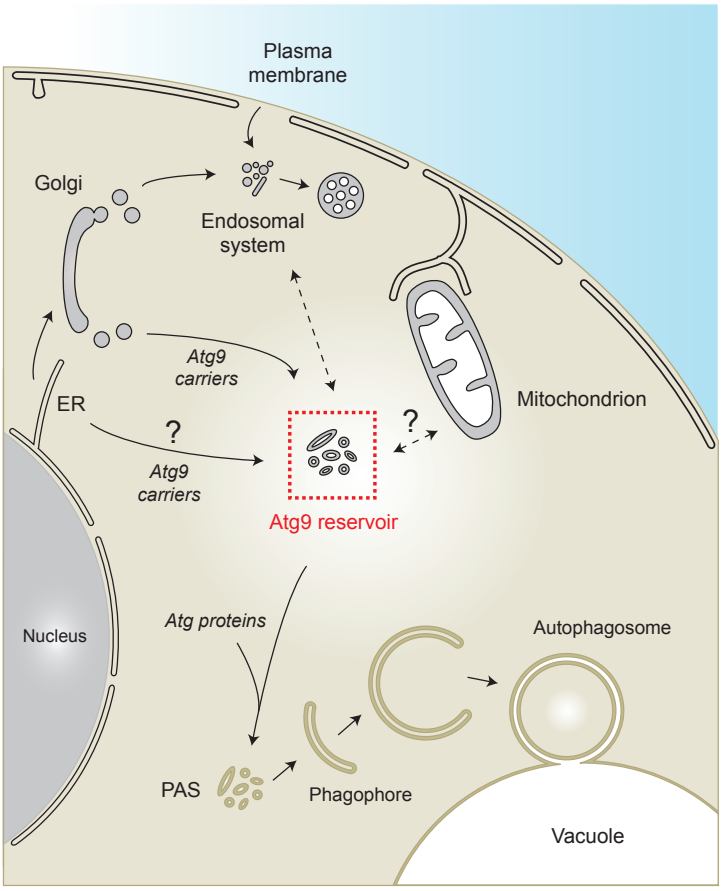

Figure 3. The origin and biogenesis of the Atg9 reservoirs. The Atg9 reservoirs, highlighted by the red dashed square, are generated from the secretory pathway. It remains unclear, however, whether Atg9 carriers exit the Golgi and/or from the ER. Moreover, it is unknown whether multiple Atg9-carriers, potentially originating from different donor compartments, contribute to the formation of a single reservoir and whether distinct Atg9 carriers can fuse with already pre-existing Atg9 reservoirs. The Atg9 reservoirs are often found close to the mitochondria but the functional reason of this proximity is unknown. The Atg9 reservoirs appear to be able to exchange material with the endocytic system (dashed arrows). The movement of at least one of these reservoirs from the periphery of the cell close to the vacuole upon autophagy induction and the subsequent recruitment of additional Atg proteins leads to the generation of the PAS. Adapted from Mari and Reggiori, 2010.

In mammalian cells, Atg9 is mainly located in the TGN and it translocates to peripheral endosomal compartments upon starvation, some of which appear to be autophagosomal intermediates or structure equivalents to the PAS because they are LC3-positive (Webber et al., 2007; Young et al., 2006). Consequently the TGN has been implicated in supplying membrane to the PAS via mAtg9-

containing carrier (Young et al., 2006). A recent study, however, shows that mAtg9 only transiently interacts with autophagosomal precursor structures and that it is not incorporated into the autophagosome membranes in contrast to what has been proposed for yeast (Orsi et al., 2012). While the mechanistic principles of autophagy are not different between organisms, Atg9 appears to have different dynamics in various species. Further research is needed to elucidate the reasons behind these differences. Interestingly, another observation pointing in the direction of the Golgi being one of the sources of membranes for autophagosome biogenesis in mammalian cells come from a paper in which the authors show that fragmentation of the Golgi, regulated by Bif-1, is important for mAtg9 trafficking and autophagy progression (Takahashi et al., 2011).

Many questions still remain and future characterization of the Atg9-carriers and Atg9 reservoirs is necessary to fully comprehend their origin and biogenesis. Although not addressed in this thesis, initial attempts to address the nature and composition of Atg9-containing structures, either Atg9 carriers or reservoirs, have been made by purify Atg9-containing intracellular membranes on sucrose density gradients. Using a mass spectrometry based approach we plan to identify novel proteins present on these membranes and this will provide new information about the players organizing autophagosome biogenesis at the early stages.

REFERENCES

1. Barth, H., and M. Thumm. 2001. A genomic screen identifies AUT8 as a novel gene essential for autophagy in the yeast *Saccharomyces cerevisiae*. *Gene*. 274:151-156.
2. Behrends, C., M.E. Sowa, S.P. Gygi, and J.W. Harper. 2010. Network organization of the human autophagy system. *Nature*. 466:68-76.
3. Efe, J.A., R.J. Botelho, and S.D. Emr. 2007. Atg18 regulates organelle morphology and Fab1 kinase activity independent of its membrane recruitment by phosphatidylinositol 3,5-bisphosphate. *Mol Biol Cell*. 18:4232-4244.
4. Gillooly, D.J., I.C. Morrow, M. Lindsay, R. Gould, N.J. Bryant, J.M. Gaullier, R.G. Parton, and H. Stenmark. 2000. Localization of phosphatidylinositol 3-phosphate in yeast and mammalian cells. *EMBOj*. 19:4577-4588.
5. Guan, J., P.E. Stromhaug, M.D. George, P. Habibzadegah-Tari, A. Bevan, W.A. Dunn, Jr., and D.J. Klionsky. 2001. Cvt18/Gsa12 is required for cytoplasm-to-vacuole transport, pexophagy, and autophagy in *Saccharomyces cerevisiae* and *Pichia pastoris*. *Mol Biol Cell*. 12:3821-3838.
6. Hailey, D.W., A.S. Rambold, P. Satpute-Krishnan, K. Mitra, R. Sougrat, P.K. Kim, and J. Lippincott-Schwartz. 2010. Mitochondria supply membranes for autophagosome biogenesis during starvation. *Cell*. 141:656-667.
7. Jin, N., C.Y. Chow, L. Liu, S.N. Zolov, R. Bronson, M. Davisson, J.L. Petersen, Y. Zhang, S. Park, J.E. Duex, D. Goldowitz, M.H. Meisler, and L.S. Weisman. 2008. Vac14 nucleates a protein complex essential for the acute interconversion of PI3P and PI(3,5)P(2) in yeast and mouse. *EMBOJ*. 27:3221-3234.
8. Legakis, J.E., W.L. Yen, and D.J. Klionsky. 2007. A cycling protein complex required for selective autophagy. *Autophagy*. 3:422-432.
9. Longatti, A., and S.A. Tooze. 2009. Vesicular trafficking and autophagosome formation. *Cell Death Differ*. 16:956-965.
10. Mari, M., J. Griffith, E. Rieter, L. Krishnappa, D.J. Klionsky, and F. Reggiori. 2010. An Atg9-containing compartment that functions in the early steps of autophagosome biogenesis. *J Cell Biol*. 190:1005-1022.
11. Nair, U., Y. Cao, Z. Xie, and D.J. Klionsky. 2010. Roles of the lipid-binding motifs of Atg18 and Atg21 in the cytoplasm to vacuole targeting pathway and autophagy. *J Biol Chem*. 285:11476-11488.
12. Nair, U., W.L. Yen, M. Mari, Y. Cao, Z. Xie, M. Baba, F. Reggiori, and D.J. Klionsky. 2012. A role for Atg8-PE deconjugation in autophagosome biogenesis. *Autophagy*. 8.
13. Obara, K., T. Noda, K. Niimi, and Y. Ohsumi. 2008a. Transport of phosphatidylinositol 3-phosphate into the vacuole via autophagic membranes in *Saccharomyces cerevisiae*. *Genes Cells*. 13:537-547.
14. Obara, K., T. Sekito, K. Niimi, and Y. Ohsumi. 2008b. The Atg18-Atg2 complex is recruited to autophagic membranes via phosphatidylinositol 3-phosphate and exerts an essential function. *J Biol Chem*. 283:23972-23980.
15. Ohashi, Y., and S. Munro. 2010. Membrane delivery to the yeast autophagosome from the Golgi-endosomal system. *Mol Biol Cell*. 21:3998-4008.
16. Orsi, A., M. Razi, H.C. Dooley, D. Robinson, A.E. Weston, L.M. Collinson, and S.A. Tooze. 2012. Dynamic and transient interactions of Atg9 with autophagosomes, but not membrane integration, are required for autophagy. *Mol Biol Cell*. 23:1860-1873.
17. Paoli, M. 2001. Protein folds propelled by diversity. *Prog Biophys Mol Biol*. 76:103-130.
18. Reggiori, F., T. Shintani, U. Nair, and D.J. Klionsky. 2005. Atg9 cycles between mitochondria and the pre-autophagosomal structure in yeasts. *Autophagy*. 1:101-109.

19. Reggiori, F., K.A. Tucker, P.E. Stromhaug, and D.J. Klionsky. 2004. The Atg1-Atg13 complex regulates Atg9 and Atg23 retrieval transport from the pre-autophagosomal structure. *Dev Cell*. 6:79-90.

20. Sekito, T., T. Kawamata, R. Ichikawa, K. Suzuki, and Y. Ohsumi. 2009. Atg17 recruits Atg9 to organize the pre-autophagosomal structure. *Genes Cells*. 14:525-538.

21. Shintani, T., K. Suzuki, Y. Kamada, T. Noda, and Y. Ohsumi. 2001. Apg2p functions in autophagosome formation on the perivacuolar structure. *J Biol Chem*. 276:30452-30460.

22. Suzuki, K., Y. Kubota, T. Sekito, and Y. Ohsumi. 2007. Hierarchy of Atg proteins in pre-autophagosomal structure organization. *Genes Cells*. 12:209-218.

23. Takahashi, Y., C.L. Meyerkord, T. Hori, K. Runkle, T.E. Fox, M. Kester, T.P. Loughran, and H.G. Wang. 2011. Bif-1 regulates Atg9 trafficking by mediating the fission of Golgi membranes during autophagy. *Autophagy*. 7:61-73.

24. Webber, J.L., A.R. Young, and S.A. Tooze. 2007. Atg9 trafficking in Mammalian cells. *Autophagy*. 3:54-56.

25. Young, A.R.J., E.Y.W. Chan, X.W. Hu, R. Köchl, S.G. Crawshaw, S. High, D.W. Hailey, J. Lippincott-Schwartz, and S.A. Tooze. 2006. Starvation and ULK1-dependent cycling of mammalian Atg9 between the TGN and endosomes. *J Cell Sci*. 119:3888-3900.

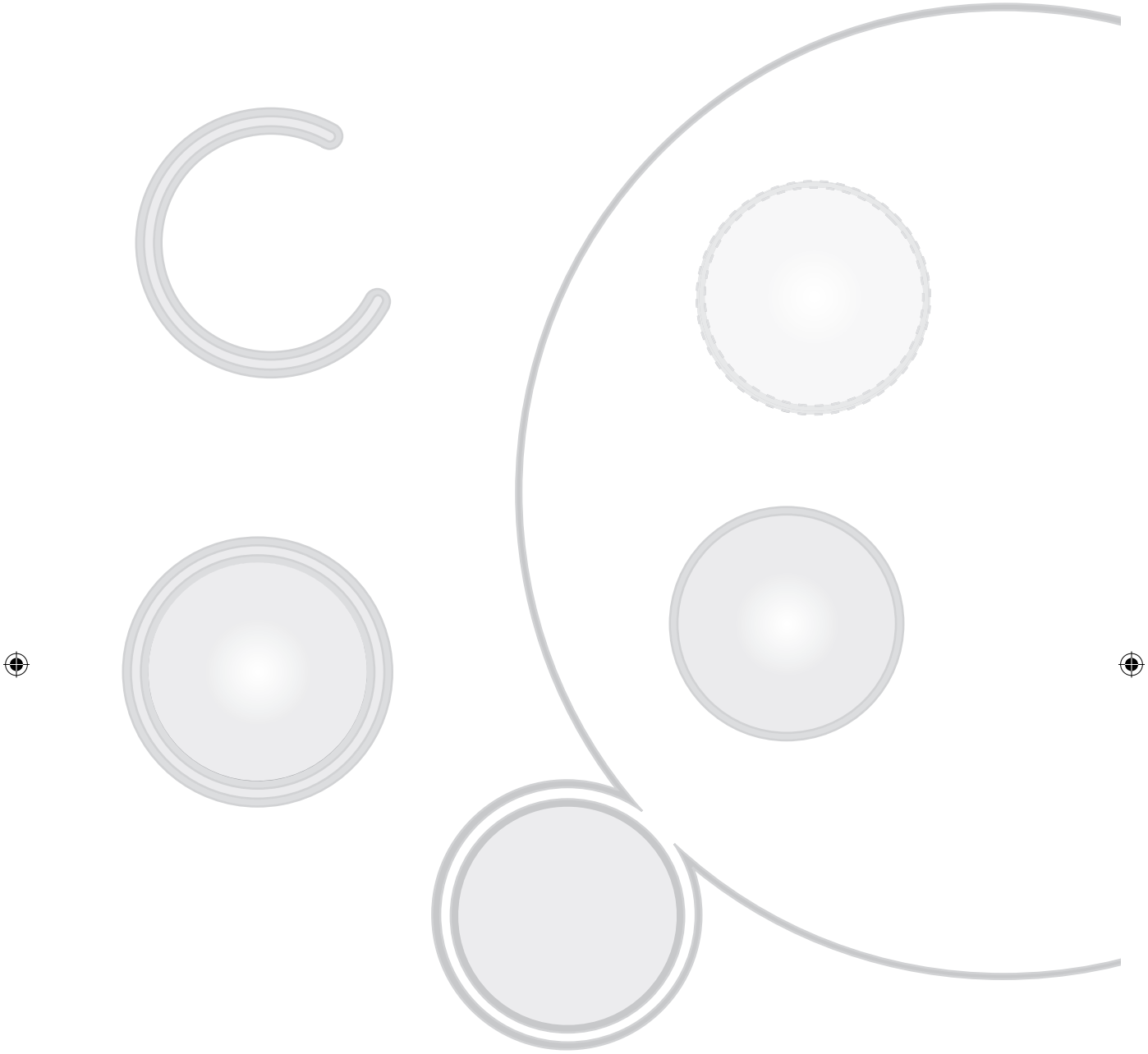

& Addendum

Abbreviation list

Nederlandse samenvatting

Acknowledgements

Curriculum vitae

List of publications

ABBREVIATION LIST

ADP	adenosine diphosphate
AMPK	adenosine monophosphate-activated protein kinase
Ams1	α-mannosidase
Ape1	aminopeptidase I
Arf1/2	ADP-ribosylation factor 1/2
Arp2/3	actin-related protein 2/3
Atg	autophagy related
ATP	adenosine triphosphate
BiFC	bimolecular fluorescence complementation
CFP	cyan fluorescent protein
CMA	chaperone-mediated autophagy
COG	conserved oligomeric Golgi
COP	coat protein
Cvt	cytosol-to-vacuole targeting
DFCP1	double FYVE domain-containing protein
DsRed	*Discosoma* red fluorescent protein
EE	early endosome
EM	electron microscopy
ER	endoplasmic reticulum
GDP	guanosine diphosphate
GFP	green fluorescent protein
GTP	guanosine triphosphate
HOPS	homotypic fusion and vacuole protein sorting
IEM	immuno-electron microscopy
Lamp-2A	lysosome-associated membrane protein type 2A
LatA	latrunculin A
LC3	microtubule-associated protein light chain 3
LE	late endosome
mAtg9	mammalian Atg9
mChe	monomeric Cherry
MHC	major histocompatibility complex
MTOC	microtubule-organizing center
PA	protein A
PAS	phagophore assembly site or pre-autophagosomal structure
PE	phosphatidylethanolamine
PtdIns	phosphatidylinositol
PtdIns3P	phosphatidylionositol-3-phosphate
PtdIns(3,5)P_2	phosphatidylinositol-3,5-biphosphate
SNARE	soluble *N*-ethylmaleimide-sensitive factor (NSF) attachment receptors
TGN	*trans*-Golgi network
TOR	target of rapamycin
TORC1/2	TOR complex 1/2
ULK1	unc-51-like kinase 1
Vps	vacuolar protein sorting
VC	C-terminal fragment of Venus
VN	N-terminal fragment of Venus
WD40	tryptophan-aspartic acid 40
WIPI	WD40 repeat protein Interacting with Phospholnositides
Y2H	yeast two-hybrid

NEDERLANDSE SAMENVATTING

Autofagie is een evolutionair geconserveerd intracellulair afbraakproces dat in alle eukaryotische[1] cellen aanwezig is. Kenmerkend voor dit afbraakproces is de vorming van grote dubbel membraan vesikels[2], genaamd autofagosomen. Tijdens het proces van autofagie worden ongewenste structuren, zoals beschadigde organellen[3], grote eiwitcomplexen en zelfs complete intracellulaire pathogenen, omringd door deze dubbele membranen om zo een autofagosoom te vormen. Autofagosomen fuseren vervolgens met de vacuole[4] in gistcellen of met lysosomen[5] in zoogdiercellen. In deze organellen vindt de afbraak plaats door enzymen die hydrolasen[6] worden genoemd. De resulterende afbraakproducten, zoals aminozuren, nucleotiden, suikers en lipiden, worden teruggetransporteerd naar het cytosol[7] om hergebruikt te worden voor de synthese van nieuwe macromoleculen of als een bron van energie (zie **Hoofdstuk 1, Figuur 1**).

Autofagie is cruciaal voor cellulaire homeostase[8] en het overleven van een cel tijdens extreme omgevingsomstandigheden, zoals uithongering en intracellulaire stress condities, doordat het in staat is om snel overbodige cytoplasmatische[7] componenten te recyclen. Daarnaast is autofagie betrokken bij tal van fysiologische en pathologische situaties zoals celdood, ontwikkeling en differentiatie, bescherming tegen invasieve pathogenen, veroudering, kanker en neurodegeneratieve aandoeningen.

Ondanks grote inspanningen gedurende de afgelopen decennia om de signaalcascades die autofagie reguleren en het moleculaire mechanisme van dit complexe proces te doorgronden zijn er nog tal van vragen onbeantwoord. Bakkersgist *Saccharomyces cerevisiae* is een veel gebruikt model organisme om autofagie te bestuderen. In deze eencellige eukaryoten vindt de formatie van een autofagosoom plaats op één specifieke plaats in de cel vlakbij de vacuole,

[1]Dit zijn cellen die een celkern en een intern membraan bezitten. Naast een celkern hebben de meeste eukaryotische cellen ook andere organellen, zoals mitochondriën of een golgi-apparaat.
[2]Dit zijn membraangebonden blaasjes.
[3]Een organel is een specifiek onderdeel van een eukaryotische cel met een bepaalde functie. Organellen kunnen worden beschouwd als de organen van een cel die de diverse cel processen mogelijk maken.
[4]Een vacuole is een met vocht gevuld blaasje, dat omgeven is door een membraan en zich in het cytoplasma van een cel bevindt. In de vacuole worden onder andere reservestoffen, kleurstoffen, hulpstoffen, afvalstoffen en suikers opgeslagen. Daarnaast worden er in de vacuole stoffen afgebroken.
[5]In dierlijke cellen wordt de functie van de vacuole vervuld door lysosomen.
[6]Hydrolasen; specifiek proteasen in dit geval zijn enzymen die eiwitten en ketens van aminozuren afbreken door de verbinding tussen twee aminozuren te verbreken.
[7]Onder het cytoplasma wordt verstaan alles waar een cel uit bestaat behalve de kern, het celmembraan en de eventuele celwand. Het cytoplasma bestaat uit het cytosol en de organellen en insluitsels die erin drijven. Het cytosol bestaat voor 60-95% uit water evenals eiwitten, RNA, aminozuren, suikers en vele andere stoffen.
[8]Dit is het vermogen van een cel om het interne milieu in een stabiele toestand te houden, terwijl de omstandigheden van het externe milieu, de omgeving waarin de cel leeft, voortdurend veranderen.

de 'Phagophore Assembly Site' genaamd of 'Pre-Autofagosomale Structuur' (PAS). Een van de meest intrigerende vragen is wat de oorsprong is van de PAS, maar ook wat de herkomst is van de lipiden[9] die nodig zijn om de relatief grote autofagosomen te vormen. Onderzoek in gist heeft tot op heden geleid tot de identificatie van 36 *ATG* genen[10] die betrokken zijn bij verschillende vormen van autofagie (zie **Hoofdstuk 1, Figuur 3**). Zestien van deze Atg eiwitten behoren tot de kernmachinerie die nodig is voor de biogenese van de dubbel membraan vesikels; de autofagosomen. Voor veel van deze Atg eiwitten is de precieze moleculaire functie nog onduidelijk.

In de studies beschreven in dit proefschrift komt een aantal van deze onbeantwoorde vraagstukken aan bod met als doel onze kennis te verbreden over het moleculaire mechanisme dat ten grondslag ligt aan de biogenese van een autofagosoom.

Verschillende rollen van het cytoskelet in autofagie

Het cytoskelet[11] van de cel speelt een belangrijke rol in tal van intracellulaire processen. Tijdens veel van deze processen vindt het herschikken van membranen en vesikel-gemedieerd transport[12] plaats. In gistcellen en zoogdiercellen speelt het cytoskelet een belangrijke rol gedurende autofagie. Vooral in zoogdiercellen vervult het een essentiële rol bij het verplaatsen van autofagosomen vanaf meerdere PAS'en naar locaties in de cel waar zich endosomen[13] en lysosomen bevinden. Relatief weinig is bekend over het mechanisme van dit transport en hoe het cytoskelet precies een rol hierin speelt. Recentelijk onderzoek heeft aangetoond dat verschillende onderdelen van het cytoskelet, zoals actine[14] en microtubuli[15], belangrijk zijn voor specifieke aspecten van autofagie. In **Hoofdstuk 2** wordt aan de hand van gepubliceerde literatuur een aantal mogelijke werkmodellen beschreven en worden de verschillen tussen gistcellen en zoogdiercellen besproken.

[9] Lipiden en in het bijzonder fosfolipiden vormen de bouwstenen voor membranen. Een enkel membraan bestaat uit een dubbele laag (bilaag) van fosfolipiden.

[10] *ATG* genen zijn autofagie gerelateerde genen. Genen zijn onderdeel van chromosomen die zich in de celkern bevinden. Een gen bestaat uit stukken DNA, die op hun beurt coderen voor een eiwit. Eiwitten vervullen tal van verschillende functies in de cel.

[11] Het cytoskelet van een cel bestaat uit verschillende soorten ketens van eiwitten die samen zorgen voor stevigheid, vorm en beweeglijkheid van de cel. Daarnaast dient het cytoskelet als geleide voor organellen die vervoerd moeten worden in de cel.

[12] Vesikel-gemedieerd transport houdt in dat via vesikels (kleine membraangebonden blaasjes) allerlei stoffen worden getransporteerd in het cytoplasma van de cel.

[13] Vanaf het celmembraan, het buitenste vlies dat de binnenkant van een cel scheidt van de buitenkant, kunnen extracellulaire macromoleculen geïnternaliseerd worden en komen zo terecht in membraangebonden blaasjes, die endosomen worden genoemd. Deze endosomen kunnen o.a. fuseren met lysosomen.

[14] Actine is een eiwit dat onderdeel is van het cytoskelet. Actinemoleculen polymeriseren tot actine-filamenten (ook wel microfilamenten genoemd) (zie Hoofdstuk 2, Figuur 3).

[15] Dit zijn buisvormige eiwitstructuren opgebouwd uit het eiwit tubuline die onderdeel zijn van het cytoskelet (zie Hoofdstuk 2, Figuur 2).

Functie van Atg18 tijdens autofagie gereguleerd door specifieke plaatsen in de bèta-propeller

Atg18 behoort tot de groep van zestien Atg eiwitten die nodig zijn voor de biogenese van de autofagosomen. Naast een functie in autofagie heeft dit eiwit ook een functie in de homeostase van de vacuole en endosomen. Atg18 heeft een N-terminale bèta-propeller[16] die gevormd wordt door zeven WD40[17] domeinen. Via het geconserveerde aminozuurmotief FRRG, welke zich in de bèta-propeller bevindt en welke specifiek fosfoïnositiden[18] bindt, wordt Atg18 vanuit de cytosol gerekruteerd naar de membranen van zowel de PAS, de vacuole en endosomen. Het is echter niet bekend hoe de associatie van Atg18 met deze organellen is gereguleerd. Aangezien fosfoïnositiden aanwezig zijn op de membranen van zowel de PAS, de vacuole en endosomen, is een aanvullend mechanisme nodig voor de selectieve rekrutering naar specifiek één van deze organellen. In **Hoofdstuk 3** wordt beschreven dat Atg18 wordt gerekruteerd aan de PAS. Dat gebeurt via Atg2 en fosfatidylinositol-3-fosfaat (een bepaalde fosfoïnositide), welke beide aanwezig zijn op de autofagosomale membranen (zie **Hoofdstuk 3, Figuur 9D**). Er wordt een model gepresenteerd waarin de bèta-propeller van Atg18 zorgt voor organel-specificiteit, omdat het in staat is om twee verschillende factoren te binden die aanwezig zijn op het membraan van het gewenste organel. Met dit onderzoek wordt tevens de potentiële capaciteit van bepaalde bèta-propeller eiwitten benadrukt om zowel een eiwit als een lipide te binden om zo eiwit-lipiden complexen te vormen.

Atg18 bindt aan Atg2 via een regio van aminozuren gelokaliseerd in de bèta-propeller, gelegen tegenover het FRRG motief (zie **Hoofdstuk 3, Figuur 9A**). Met behulp van Atg18 mutante eiwitten[19] die niet langer aan het Atg2 eiwit kunnen binden, wordt aangetoond dat als de binding tussen Atg18 en Atg2 is verstoord, de rekrutering van Atg18 naar de PAS niet plaatsvindt, hetgeen leidt tot een blokkade van autofagie. Aan de hand van deze bevindingen wordt geconcludeerd dat Atg18 en Atg2 een functie hebben gedurende een vroeg stadium van autofagie, waarschijnlijk tijdens de biogenese en de organisatie

[16] Afhankelijk van de aminozuren waaruit een eiwit is opgebouwd wordt een eiwit in een bepaalde driedimensionale structuur gevouwen. Bij de vouwing wordt onderscheid gemaakt tussen alfa-helices en bèta-sheets (vlakken). Een bèta-propeller is een structureel eiwit domein bestaande uit vier tot acht schoepvormige bèta-sheets die toroidaal om een centrale as zijn gearrangeerd, wat leidt tot een tertiaire structuur in de vorm van een cilinder (zie Hoofdstuk 3, Figuur 9A).

[17] Een WD40 domein is een klein structureel eiwit motief bestaand uit ongeveer 40 aminozuren, vaak eindigend met de aminozuren tryptofaan (W) en asparaginezuur (D).

[18] Fosfatidylinositol is een fosfolipide en gering onderdeel van de membranen in de cel. Eén of meerdere hydroxyl groepen van de inositol ring van fosfatidylinositol kunnen gefosforyleerd worden, d.w.z. het plaatsen van een fosfaatgroep. De verschillende gefosforyleerde vormen van fosfatidylinositol worden fosfoïnositiden genoemd.

[19] In deze eiwitten zijn enkele aminozuren gemuteerd. D.w.z. dat deze residuen zijn vervangen door het non-polaire aminozuur alanine. Door deze mutaties wordt de bindingscapaciteit voor een ander eiwit verstoord.

van de PAS en dat de wisselwerking tussen beide eiwitten van essentieel belang is.

Moleculaire basis van de interactie tussen Atg2 en Atg9

Het transmembraan eiwit[20] Atg9 is een belangrijke regulator van autophagy omdat het een centrale rol speelt in de vorming van de PAS. In de cel lokaliseert Atg9 zowel op de PAS als op specifieke locaties in het cytoplasma die de 'Atg9 reservoirs' worden genoemd (zie ook **Hoofdstuk 5**). Tijdens autofagosoom biogenese is Atg9 één van de eerste Atg eiwitten die gerekruteerd wordt naar de PAS. Nadat de biogenese van een autofagosoom is voltooid, wordt het eiwit teruggetransporteerd naar de 'Atg9 reservoirs'. Het mechanisme van dit recyclingstransport is niet bekend. Aangetoond is dat zowel Atg18 als Atg2 betrokken zijn bij dit proces, maar de precieze functie van deze eiwitten blijft onduidelijk. Eerdere studies hebben aangetoond dat Atg2 en Atg9 hoogstwaarschijnlijk aan elkaar kunnen binden. Om het mechanisme van Atg9 recycling terug naar het cytoplasma te kunnen bestuderen, hebben we in **Hoofdstuk 4** de wisselwerking tussen Atg9 en Atg2 gekarakteriseerd. Het onderzoek laat zien dat deze twee eiwitten onafhankelijk van Atg18 aan elkaar kunnen binden en dat deze binding essentieel is voor het verloop van autofagie. De bindingsmotieven in beide eiwitten zijn geïdentificeerd met behulp van de 'yeast two-hybrid' techniek[21] en tonen aan dat een stuk van 34 aminozuren in de C-terminus[22] van Atg2 belangrijk is voor de binding aan Atg9. Het muteren van een aantal aminozuren in deze regio van Atg2 leidt tot verstoring van de interactie tussen dit eiwit en Atg9 en tot een blokkade in het autofagie proces. Tevens is een regio van ongeveer 60 aminozuren in de cytosolische C-terminus van Atg9 geïdentificeerd die verantwoordelijk is voor de binding aan Atg2. De tijdens dit onderzoek gegenereerde Atg2 mutante eiwitten verschaft een uniek middel om in de toekomst onderzoek te doen naar het mechanisme van Atg9 transport vanaf de PAS en de functie van de Atg2-Atg9 interactie gedurende dit proces.

[20]Dit is een eiwit dat zich in een membraan bevindt. Vaak gaat het eiwit enkele keren door het membraan heen van de ene kant naar de andere kant van het membraan (zie Hoofdstuk 4, Figuur 3A).
[21]In dit essay zorgt de interactie tussen 2 eiwitten voor de reconstructie van een gist transcriptiefactor, waarna er transcriptie van een selectiemarker plaatsvindt. De aanwezigheid van deze selectiemarker maakt het mogelijk dat de gistcellen kunnen groeien op een speciaal voedingsmedium waarin deze selectiemarker ontbreekt.
[22]Een eiwit is een keten van aminozuren en heeft aan het ene uiteinde van de keten een ongebonden carboxygroep, de C-terminus en aan het andere uiteinde een ongebonden aminogroep, de N-terminus.

Functionering van een Atg9-bevattend compartiment in de vroege stadia van autofagosoom biogenese

In **Hoofdstuk 5** wordt aangetoond dat het transmembraan eiwit Atg9 een essentiële rol speelt in autofagie, omdat het betrokken is bij de vorming van de PAS. Met behulp van immuno-electronen microscopie[23] en fluorescentie microscopie[24] wordt aangetoond dat Atg9 zich concentreert in een nieuw compartiment bestaande uit vesikels en tubuli, die deels afkomstig zijn van de secretoire route[25]. Hoewel deze Atg9-positieve membraan structuren zich vaak bevinden in de buurt van de mitochondriën[26], vormen deze structuren, Atg9 reservoirs genaamd, een nieuw soort organel. Eiwit markers voor andere organellen zoals de mitochondriën lokaliseerden namelijk niet op deze membraanstructuren.

Dit onderzoek toont aan dat de Atg9 reservoirs in het cytoplasma de voorlopers vormen van de PAS en dat na inductie van autofagie één of meerdere van deze structuren zich *en bloc* verplaatsen in de nabijheid van de vacuole om hier de PAS te vormen en vervolgens de phagophore (zie **Hoofdstuk 5**, **Figuur 10**). De phagophore is een komvormige cisterne (membraan structuur) die uiteindelijk door middel van membraan expansie uitgroeit tot een volledige autofagosoom (zie ook **Hoofdstuk 1**, **Figuur 2**). Bovendien wijzen uitgevoerde genetische analyses er op dat de eiwitten Atg1 en Atg13, en fosfatidylinositol-3-fosfaat zijn betrokken bij de membraanherschikkingen van de Atg9 reservoirs, die nodig zijn voor de vorming van de phagophore.

Samengevat levert het onderzoek beschreven in dit proefschrift een belangrijke bijdrage aan de kennis over het moleculaire mechanisme van autofagie. Deze kennis is van essentieel belang om te begrijpen wat de bijdrage van dit proces is in zowel fysiologische en pathologische situaties.

[23]Bij deze techniek wordt gebruik gemaakt van een bundel elektronen om het oppervlak of de inhoud van objecten af te beelden. Doordat versnelde elektronen een veel kleinere golflengte hebben dan fotonen, is de resolutie van een elektronenmicroscoop veel hoger dan die van een lichtmicroscoop.
[24]Is een techniek waarbij fluorescerende kleurstoffen of fluoroforen worden gebruikt die oplichten als ze worden bestraald met licht van een bepaalde golflengte. In veel gevallen wordt de fluorofoor direct gekoppeld aan het eiwit van interesse, waardoor een fluorescerend fusie-eiwit of chimera ontstaat.
[25]Het endoplasmatisch reticulum (ER) speelt een belangrijke rol tijdens eiwit synthese. Vanaf het ER worden eiwitten via kleine vesikels naar het golgi-apparaat getransporteerd. In de golgi worden de eiwitten omgebouwd en opgeslagen om later naar andere bestemmingen in de cel te worden vervoerd, zoals het celmembraan waar de secretie plaatsvindt.
[26]In deze boonvormige organellen wordt de energie uit koolhydraten en vetten overdragen aan het adenosinetrifosfaat (ATP), dat een chemische energiedrager is. De energie die vervolgens weer vrij komt door de hydrolyse van ATP, wordt in de cel gebruikt voor allerlei processen.

DANKWOORD

Tja het enige wat mij nu nog rest is het schrijven van dit dankwoord. Iets wat ik stellig voor me uit heb geschoven uit angst om iemand te vergeten. Hoewel ik veel mensen dankbaar ben om uit één lopende redenen, zou ik graag een aantal personen in het bijzonder willen bedanken.

Allereerst wil ik mijn co-promotor dr. Fulvio Reggiori bedanken. Beste Fulvio, in tegenstelling tot mijn voorgangers richt ik me in het Nederlands tot je, dit aangezien je ondertussen de Nederlandse taal redelijk beheerst. Ik wil je bedanken voor de afgelopen vier jaar, niet alleen voor alles wat ik van je heb geleerd, maar ook voor je vertrouwen en optimisme. Ik bewonder je gedrevenheid voor de wetenschap.

Ook wil ik mijn twee promotoren prof. dr. Judith Klumperman en prof. dr. Paul Coffer bedanken. Beste Judith, heel erg bedankt voor je advies en hulp gedurende de afgelopen vier jaar, vooral tijdens een aantal moeilijke perioden. Beste Paul, ontzettend bedankt voor het afgelopen jaar en de baan die je me hebt aangeboden.

Mijn dank gaat ook uit naar alle mensen van de 'Reggiori groep' en oud-collega's die deel uitmaakten van deze groep: Aniek, Iryna, Mustafa en Eduardo. Niet alleen bedankt voor alle wetenschappelijke discussies, maar ook voor de gezelligheid op het lab. Mijn studenten Ana Maria en Elena wil ik uiteraard ook bedanken, ik heb jullie met veel plezier begeleid, en ook de andere studenten in de groep: Fabian en Remko. Jullie hebben allemaal een bijdrage geleverd aan dit proefschrift.

Ik wil verder iedereen van de afdeling Celbiologie bedanken voor alle suggesties en input gedurende de afgelopen vier jaar. In het bijzonder alle mensen van de 'Coffer' groep. Ontzettend bedankt voor het afgelopen jaar! Stephin, Veerle, Desireé, Catalina, Anita en Ana-Rita bedankt dat jullie een plekje voor me wilden maken in de overvolle, maar vooral gezellige Aio kamer. Ook René, Viola, Wieke, en David wil ik extra bedanken. Beste René, jij bent mijn steun en toeverlaat geweest vanaf dag één. Zonder jouw hulp had ik de figuren in dit boekje nooit kunnen maken. Viola, bedankt voor alle hulp met m'n glycerol gradiënten en super dat je op tijd terug wilde komen uit Australië voor m'n promotie. Wieke en David bedankt voor jullie betrokkenheid, gezelligheid en vooral humor.

Tot slot wil ik ook mijn familie en vrienden bedanken voor alle support. In het bijzonder mijn twee paranimfen Anke en Léon, bedankt voor alle kilo's sushi en liters bier gedurende de afgelopen vier jaar. Ik ben blij dat jullie mijn paranimfen willen zijn. Annemarie, Dieuwertje, Roeland, Alike, Kristy en Soula bedankt voor jullie vriendschap, de interesse die jullie voor mijn werk hebben getoond en het begrip gedurende de laatste maanden. Harold, bedankt voor je adviezen en het zeer kritisch lezen van mijn Nederlandse samenvatting.

Miepi ook jij verdient een bijzondere vermelding in dit dankwoord. Bedankt voor alle wijsheid die je me hebt mee gegeven en je trots. Mijn ouders, mam en pap, en broers Melchior, Casper en Sebastiaan bedankt voor het vertrouwen dat jullie in me hebben.

Tot slot, lieve Marjon ik weet dat het afgelopen jaar niet makkelijk voor je is geweest. Bedankt voor al het geduld dat je met me hebt gehad en alles wat je voor me hebt gedaan om het afronden van mijn promotie iets te verlichten.

Ester

CURRICULUM VITAE

Ester Mirjam Rieter werd geboren op 12 juli1981 te Roermond. In 1999 behaalde zij haar VWO diploma aan het Stedelijk Lyceum in Roermond. In 2002 begon zij aan de HBO studie 'Biologie en Medisch laboratorium Onderzoek' aan de Fontys Hogeschool Toegepaste Natuurwetenschappen in Eindhoven. Tijdens haar studie liep zij stage bij het Swiss Institute of Allergy and Asthma Research (SIAF) in Davos in Zwitserland. Daar deed ze onderzoek naar de IgE-bindingscapaciteit van humane zelf-antigenen onder begeleiding van prof. R. Crameri. Haar tweede stage liep zij bij het Institute for Molecular Bioscience (IMB) in Brisbane in Australië. Onder begeleiding van prof. D. Hume en dr. M. Sweet bestudeerde zij de epigenetische regulatie van murine macrofagen activatie. In 2006 ronde zij haar HBO studie af om datzelfde jaar te beginnen aan de tweejarige master opleiding 'Cancer Genetics and Developmental Biology' van de faculteit Biomedische Wetenschappen aan de Universiteit Utrecht. In het kader van deze master liep zij stage bij het Hubrecht laboratorium in Utrecht. Daar werkte zij onder leiding van prof. F.J. Meijlink mee aan het genetisch in kaart brengen en embryologisch karakteriseren van muis hartmutanten, die geïdentificeerd waren in een forward genetic screen. Vervolgens besloot zij om haar laatste stage te doorlopen bij de afdeling Celbiologie van het Universitair Medisch Centrum Utrecht (UMCU) bij dr. F.M. Reggiori. Het onderwerp van deze stage betrof de identificatie van nieuwe Atg9 bindingspartners in gist *Saccharomyces cerevisiae*. In 2008 behaalde zij haar master diploma, waarna zij aansluitend als promovenda begon bij de afdeling Celbiologie in het Universitair Medisch Centrum Utrecht onder begeleiding van dr. F.M. Reggiori. Het onderzoek met als doel de moleculaire organisatie van de 'phagophore assemblage plaats' te bestuderen is beschreven in dit proefschrift.

LIST OF PUBLICATIONS

Rieter, E., F. Vinke, D. Bakula, E. Cebollero, C. Ungermann, T. Proikas-Cezanne and F. Reggiori. **Atg18 function in autophagy is regulated by specific sites within its ß-propeller.** *In revision (The Journal of cell science)*

Cebollero, E., A. van der Vaart, M. Zhao, E. Rieter, DJ. Klionsky, JB. Helms, and F. Reggiori. 2012. **Phosphatidylinositol-3-phosphate clearance plays a key role in autophagosome completion**. *Current biology. In press*.

Wansleeben, C., L. van Gurp, H. Feitsma, C. Kroon, E. Rieter, M. Verberne, V. Guryev, E. Cuppen, and F. Meijlink. 2011. **An ENU-mutagenesis screen in the mouse: identification of novel developmental gene functions**. *PloS one*. 6:e19357.

Mari, M., J. Griffith, E. Rieter, L. Krishnappa, D.J. Klionsky, and F. Reggiori. 2010. **An Atg9-containing compartment that functions in the early steps of autophagosome biogenesis**. *The Journal of cell biology*. 190:1005-1022.

Rieter*, E., I. Monastyrska*, D.J. Klionsky, and F. Reggiori. 2009. **Multiple roles of the cytoskeleton in autophagy**. *Biological reviews of the Cambridge Philosophical Society*. 84:431-448.